Award Number: W81XWH-07-1-0523

TITLE: Biochemical characterisation of *TSC1* and *TSC2* variants identified in patients with tuberous sclerosis complex

PRINCIPAL INVESTIGATOR:Mark Nellist

CONTRACTING ORGANIZATION:Erasmus MC
The Netherlands

REPORT DATE:July 2010

TYPE OF REPORT:Final

PREPARED FOR: U.S. Army Medical Research and Materiel Command
Fort Detrick, Maryland 21702-5012

REPORT DOCUMENTATION PAGE

Form Approved
OMB No. 0704-0188

1. REPORT DATE
01-07-2010

2. REPORT TYPE Final

3. DATES COVERED
1 Jul 2007 - 30 Jun 2010

4. TITLE AND SUBTITLE

Biochemical characterisation of *TSC1* and *TSC2* variants identified in patients with tuberous sclerosis complex

5a. CONTRACT NUMBER

5b. GRANT NUMBER
W81XWH-07-1-0523

5c. PROGRAM ELEMENT NUMBER

6. AUTHOR(S)

Mark Nellist, Marianne Hoogeveen-Westerveld, Dicky Halley

5d. PROJECT NUMBER

5e. TASK NUMBER

5f. WORK UNIT NUMBER

7. PERFORMING ORGANIZATION NAME(S) AND ADDRESS(ES)

Erasmus MC,

The Netherlands

8. PERFORMING ORGANIZATION REPORT NUMBER

9. SPONSORING / MONITORING AGENCY NAME(S) AND ADDRESS(ES)
U.S. Army Medical Research and Materiel Command,
Fort Detrick,
Maryland 21702-5012

10. SPONSOR/MONITOR'S ACRONYM(S)

11. SPONSOR/MONITOR'S REPORT NUMBER(S)

12. DISTRIBUTION / AVAILABILITY STATEMENT

Approved for public release; distribution unlimited

13. SUPPLEMENTARY NOTES

14. ABSTRACT

The key findings of the project during the research period (1/7/07 - 31/7/10) are as follows:
1. Derivation and functional testing of 107 TSC2 variants: 69 classified as pathogenic; 38 classified as probably neutral..
2. Development of an In-Cell Western assay to measure TSC1-TSC2 activity.
3. Demonstration that *TSC1* missense mutations inactivate the TSC1-TSC2 complex to cause TSC.
4. Derivation and functional testing of 45 unclassified TSC1 variants: 16 classified as pathogenic; 29 classified as probably neutral
5. Identification of TSC1 functional domains.
6. Improvements in assay cost, throughput and reproducibility.

15. SUBJECT TERMS
Tuberous Sclerosis Complex, unclassified variants, TSC1, TSC2

16. SECURITY CLASSIFICATION OF:			**17. LIMITATION OF ABSTRACT**	**18. NUMBER OF PAGES**	**19a. NAME OF RESPONSIBLE PERSON**
a. REPORT	**b. ABSTRACT**	**c. THIS PAGE**	U U	186	USAMRMC
U	U	U			**19b. TELEPHONE NUMBER** *(include area code)*

Table of Contents

Introduction

Subject: Tuberous sclerosis complex (TSC) is a genetic disorder caused by mutations in the *TSC1* and *TSC2* tumour suppressor genes [1 - 3]. The *TSC1* and *TSC2* gene products form a protein complex that inhibits the activity of the mammalian target of rapamycin (mTOR) complex 1 (TORC1). TORC1 coordinates nutritional, hormonal and other cues to regulate the cellular growth machinery. Therefore, inactivation of the TSC1-TSC2 complex results in inappropriate TORC1 activity and cell growth defects [4].

Mutation analysis of the *TSC1* and *TSC2* genes is a useful diagnostic tool for helping individuals and families affected by TSC [5]. In most cases of TSC, a definite pathogenic *TSC1* or *TSC2* mutation is identified. However, in some cases it is difficult to determine whether identified sequence changes are pathogenic or not. These 'unclassified variants', typically missense changes, small in-frame insertions or deletions, or changes that could affect splicing, present a significant problem for diagnostics and genetic counselling.

Purpose: The purpose of this research project was to develop and apply assays of TSC1-TSC2 function to determine whether unclassified *TSC1* and *TSC2* variants are pathogenic or not. In this way, the individuals carrying these variants, as well as their families, could obtain clearer information about their condition and the associated risks. Furthermore, correlation of the biochemical effects of the different variants with the observed patient phenotypes could provide insight into genotype-phenotype correlations in TSC, and the identification of amino acids and/or regions that are important for different aspects of TSC1-TSC2 function could help define the structural and catalytic domains of the TSC1-TSC2 complex.

Scope: The specific aims of the project were to:

1. Apply functional assays to determine whether specific *TSC1* and *TSC2* variants are pathogenic mutations.
2. Determine whether specific *TSC1* and *TSC2* mutations are associated with specific TSC phenotypes.
3. To identify amino acid residues that are essential for TSC1 or TSC2 function.
4. To develop a simple, reliable and rapid test for TSC1-TSC2 function.

Body

1. Application of functional assays to determine whether specific TSC1 and TSC2 variants are pathogenic mutations.

The TSC1-TSC2 complex inhibits the mammalian target of rapamycin (mTOR) complex 1 (TORC1), preventing the phosphorylation of TORC1 substrates, including p70 S6 kinase (S6K) [4]. To investigate the effects of amino acid substitutions and small in-frame insertions or deletions on TSC1 and TSC2 function, we introduced the corresponding nucleotide changes into *TSC1* and *TSC2* expression constructs by site-directed mutagenesis and expressed the variant proteins in mammalian cells in culture. After 24 hours, cell lysates were prepared and subjected to denaturing polyacrylamide gel electrophoresis (SDS-PAGE). After transfer to nitrocellulose membranes, the activity of the TSC1 and TSC2 variants was estimated by immunoblotting. The phosphorylation status of ectopically expressed S6K and the expression levels of the TSC1 and TSC2 variants were determined using an Odyssey infra-red scanner (Li-Cor Biosciences). S6K phosphorylated at the T389 position was detected using a commercially available antibody (1A5, Cell Signaling Technology); TSC1 and total S6K were detected with a rabbit polyclonal antibody against the myc epitope tag (Cell Signaling Technology); TSC2 was detected with a rabbit polyclonal antibody [6]. Unclassified *TSC1* and *TSC2* variants were selected from our own patient cohort, the Leiden Open Variation Database (http://www.lovd.nl/TSC1; http://www.lovd.nl/TSC2), case reports from literature, or were specific requests from genetic counsellors. We performed functional testing on 107 TSC2 variants and 45 TSC1 variants, applying systematic criteria to determine whether TSC1-TSC2 function was affected by the corresponding amino acid changes. A manuscript summarising the results of these experiments is currently in preparation and will be submitted for publication in the near future (see Supplementary Data: Appendix 1).

At the start of the project, it was not known whether missense mutations in the *TSC1* gene could cause TSC. Our work showed that pathogenic TSC1 amino acid changes do occur and that, so far, they are all clustered within a conserved ~250 amino acid region close to the N-terminal of the protein. These substitutions affect the turn-over and stability of TSC1 [7, 8]. Some substitutions had no discernible effect on the activity of the TSC1-TSC2 complex in our assays. However, in some cases there was evidence from predictive computer-based algorithms (NetGene2 Server, www.cbs.dtu.dk/services/NetGene2; BDGP: Splice Site Prediction by Neural Network, www.fruitfly.org/seq_tools/splice.html; Human Splicing Finder, www.umd.be/HSF/HSF.html) that the corresponding nucleotide changes could affect

splicing. We obtained ethical approval to approach patients for skin biopsies and have prepared RNA from fibroblasts cultures derived from patients. In one case, we detected a novel *TSC2* splice isoform with a small in-frame deletion. This change was tested using our functional assay, and we concluded that it was pathogenic [9]. In another case, we idenitified a putative *TSC1* splice site mutation, predicted to cause an in-frame deletion. However, the deletion had no effect in our functional assay. TSC1 was still active. We concluded that this change was unlikely to be pathogenic [8]. Unfortunately we were unable to complete the analysis of any other fibroblast cultures prior to the ending of the funding period. We will apply for new funding to continue and complete this work.

2. Determine whether specific TSC1 and TSC2 mutations are associated with specific TSC phenotypes.

Although they occur mostly in isolation, renal angiomyolipomas (AML) are a frequent symptom in TSC patients. We investigated a case in which an individual was identified with bilateral AMLs, but without other signs suggestive for TSC. We identified 2 UVs in the probands *TSC2* gene, one paternal, one maternal. Our analysis indicates that while neither variant is likely to cause TSC, it is possible that they affected the pathogenesis of the AMLs in this patient, and suggests that *TSC2* variants that do not cause TSC may play a role in the aetiology of AML (see Supplementary Data: Appendix 2).

We identified a TSC2 R1200W variant in multiple, unrelated families exhibiting relatively mild symptoms of TSC. We investigated the effect of the R1200W substitution on TSC2 activity in relation to the observed phenotypes (see Supplementary Data: Appendix 3).

TSC-associated cortical tubers show many histopathologic similarities to the malformations associated with focal cortical dysplasia type IIb (FCD IIb). We demonstrated decreased binding between TSC2 and the TSC1 H732Y variant associated with FCD IIb [10].

3. Effect of truncation on TSC1 and TSC2 function

We studied the effects of truncating *TSC1* and *TSC2* mutations on the activity of the TSC1-TSC2 complex. Truncation of TSC1 revealed regions of the protein involved in stability, aggregation and interaction [11].

To study the effect of truncation on TSC2 in more detail, we removed the amino acid sequences encoded by specific exons using site-directed mutagenesis. The sequences encoded by exons 3, 5, 6, 12, 19, 22, 25 and 41 were removed. Unfortunately, due to the ending of the funding period, we were unable to investigate the effects of these deletions on the TSC1-

TSC2 interaction, or on the activity of the TSC1-TSC2 complex. We will apply for new funding to continue and complete this work.

4. Identification of amino acid residues/domains that are essential for TSC1 or TSC2 function.

Amino acid substitution prediction methods use sequence and/or structural information to predict the effects of amino acid changes on protein function [12, 13]. In the absence of adequate genetic or functional data, prediction methods have been applied to try and resolve whether specific variants are pathogenic or not [14]. The more information there is about a particular protein, the more accurate the prediction is likely to be. We have compared our functional data with predictions using the SIFT algorithm [12, 13]. Some predicted tolerated changes were found to affect TSC1-TSC2 function; while no effect on function could be established for some changes that were predicted not to be tolerated, indicating that predictive methods are not reliable for molecular genetic diagnostics and that functional tests provide important, extra insight into the effects of different amino acid changes (see Supplementary Data: Appendix 1).

Studies using truncated TSC2 proteins [15, 16], indicate that the N-terminal region of TSC2 is important for the interaction with TSC1. Interaction between TSC1 and TSC2 stabilises TSC1 in a soluble, TSC2-bound form, increasing the amount of TSC1 detected by immunoblotting [17]. We quantified the effects of different TSC2 variants on TSC1 expression levels. TSC1 expression levels were reduced in the presence of pathogenic TSC2 variants with amino acid changes to the N-terminal region of the protein (amino acids 1 - 900). In contrast, most changes to the C-terminal region of TSC2 (amino acids 900 - 1807) did not have such a large effect on TSC1 expression levels. Nevertheless, amino acid substitutions within this region still resulted in inactivation of the TSC1-TSC2 complex, as estimated from the T389 phosphorylation of S6K (see Supplementary Data: Appendix 1).

Our studies on a series of truncated TSC1 proteins as well as on a number of pathogenic TSC1 amino acid changes showed that a conserved ~250 amino acid region close to the N-terminal of the TSC1 is required for TSC1 stability [7, 8, 11].

4. Development of a rapid test for TSC1-TSC2 function.

At the start of the project our approach was to perform several different tests to analyse TSC1-TSC2 binding and the effect of TSC1-TSC2 expression on TORC1 activity. We set up an in-cell Western (ICW) assay for analysing TSC2 variants [18]. ICW assays have

the advantage of being reproducible, amenable to automation and simple to perform. However, the ICW required large quantities of antibody, making the test relatively expensive. Therefore, we decided to focus on improving our immunoblot assay. The ability to reproducibly quantify the intensity of the signals obtained by immunoblotting [19] has made it possible to reliably estimate the differences between the variants being tested, wild-type TSC2 and known inactive, pathogenic variants. We have been able to improve the immunoblot assay so that larger numbers of variants can be analysed more easily and accurately, and at a reduced cost per analysed variant (see Supplementary Data: Appendix 1).

Key Research Accomplishments (1/7/07 - 31/7/10)

1. Derived and tested 107 TSC2 variants: 69 pathogenic; 38 probably neutral.
2. Derived and tested 45 TSC1 variants: 16 pathogenic; 29 probably neutral.
3. Improvements in assay cost, throughput and reproducibility.
4. Identification of regions of TSC1 involved in interactions, stability and aggregation.
5. Identification of regions of TSC2 involved in the interaction with TSC1.

Reportable Outcomes (since the start of the project)

1. Manuscripts (see Supplementary Data: Appendix 4):

Nellist M, Sancak O, Goedbloed M, Adriaans, Wessels M, Maat-Kievit A, Baars M, Dommering C, van den Ouweland A and Halley D. "Functional characterisation of the TSC1-TSC2 complex te assess multiple *TSC2* variants identified in single families affected by tuberous sclerosis complex". BMC Med. Genet. (2008) 9:10 doi:10.1186/1471-2350-9-10.

Nellist M, van den Heuvel D, Schluep D, Exalto C, Goedbloed M, Maat-Kievit A, van Essen T, van Spaendonck-Zwarts, Jansen F, Helderman P, Bartalini G, Vierimaa O, Penttinen M, van den Ende J, van den Ouweland A and Halley D. "Missense mutations to the *TSC1* gene cause tuberous sclerosis complex". Eur. J. Hum. Genet. (2009) 17: 319 - 328.

Coevoets R, Arican S, Hoogeveen-Westerveld M, Simons E, van den Ouweland A, Halley D and Nellist M. "A reliable cell-based assay for testing unclassified *TSC2* gene variants." Eur. J. Hum. Genet. (2009) 17: 301 - 310.

Mozaffari M, Hoogeveen-Westerveld M, Kwiatkowski D, Sampson J, Ekong R, Povey S, den Dunnen J, van den Ouweland A, Halley D and Nellist M. "Identification of a region required for TSC1 stability by functional analysis of *TSC1* missense mutations found in individuals with tuberous sclerosis complex". BMC Med. Genet. (2009) 10:88 doi:10.1186/1471-2350-10-88.

Lugnier C, Majores M, Fassunke J, Pernhorst K, Niehusmann P, Simon M, Nellist M, Schoch S and Becker A. "Hamartin variants that are frequent in focal dysplasias and cortical tubers have reduced tuberin binding and aberrant subcellular distribution *in vitro*". J. Neuropathol. Exp. Neurol. (2009) 68:1136-1146.

Hoogeveen-Westerveld M, Exalto C, Maat-Kievit A, van den Ouweland A, Halley D and Nellist M. "Analysis of TSC1 truncations defines regions involved in TSC1 stability, aggregation and interaction. Biochim. Biophys. Acta (2010), doi: 10.1016/j.bbadis.2010.06.004.

2. Abstracts/Presentations:

Nellist M "Functional analysis of TSC1 and TSC2 variants" 9th International Research Conference on Tuberous Sclerosis Complex, 11 - 13th September 2008, University of Sussex, Brighton, U.K. (invited talk).

Mozaffari M, Hoogeveen-Westerveld M and Nellist M "Functional analysis of *TSC1* missense mutations identified in individuals with tuberous sclerosis complex" Poster Session, 6th November 2008, LAM/TSC Seminar series, Harvard Medical School, Boston, Massachusetts, U.S.A. (poster presentation).

Nellist M "Genetic basis of tuberous sclerosis complex" 8th Dutch Endo-Neuro-Psycho Meeting, 3rd - 5th June 2009, Doorwerth, The Netherlands. (invited talk)

Nellist M "Functional analysis of TSC1 and TSC2 variants identified in individuals with tuberous sclerosis complex" 9th July 2009, Department of Neuropathology, University Hospital, Bonn, Germany (invited talk)

3. Degrees awarded (supported by this award):

none

4. Databases:

Data generated by this study will be added to the LOVD *TSC1* and *TSC2* mutation databases [7, 8].

Conclusions

Pathogenic, non-truncating *TSC1* and *TSC2* mutations can be distinguished from non-pathogenic changes by studying the effects of the changes on the TSC1-TSC2 protein complex. Functional characterisation of unclassified *TSC1* and *TSC2* variants complements existing diagnostic tests and enables appropriate clinical care and counselling for more TSC patients and their relatives. According to the results of our functional assessment we classified 69 TSC2 variants and 16 TSC1 variants as pathogenic, and 38 TSC2 variants and 29 TSC1 variants as probably neutral.

Characterisation of multiple TSC1 and TSC2 variants has helped refine the important structural and catalytic regions in TSC1 and TSC2 and should help provide insight into the folding and three-dimensional structure of the TSC1-TSC2 complex, as well as the regulation and mechanism of GAP catalysis. The stability of different variants, the strength of the TSC1-TSC2 interaction and the catalytic GAP activity all influence the biological activity of the TSC1-TSC2 complex.

Innovations:

The functional characterisation of TSC1 and TSC2 variants has extended the diagnostic service that can be offered to TSC patients and their families. Further, it has helped

refine important structural and functional regions in TSC1 and TSC2, and identified specific genotype-phenotype correlations in TSC.

Impact:

Tests to distinguish pathogenic and non-pathogenic *TSC1* and *TSC2* variants are of direct importance to the individuals who carry or may inherit these variants. The data generated by this study should benefit individuals and families in whom the tested variants are identified.

Comparison of the biochemical effects of different pathogenic variants with the corresponding phenotypes in affected individuals has provided insight into possible genotype-phenotype correlations in TSC. Several reports indicate that specific non-truncating *TSC2* mutations are associated with a less severe TSC phenotype.

Finally, the identification of amino acids essential for TSC1-TSC2 function has provided more insight into TSC1-TSC2 function. These data will be useful not only for assessing and testing the accuracy of current predictive methods of amino acid substitution analysis but also in the development of improved predictive algorithms for analysing unclassified *TSC1* and *TSC2* variants.

References

1. Gomez M, Sampson J, Whittemore V, eds. *The tuberous sclerosis complex*. Oxford University Press, Oxford, UK, 1999.

2. The European Chromosome 16 TSC Consortium. Identification and characterisation of the tuberous sclerosis gene on chromosome 16. Cell 75 (1993) 1305-1315.

3. van Slegtenhorst M, de Hoogt R, Hermans C, Nellist M, Janssen LAJ, Verhoef S, Lindhout D, van den Ouweland AMW, Halley DJJ, Young J, Burley M, Jeremiah S, Woodward K, Nahmias J, Fox M, Ekong R, Wolfe J, Povey S, Osborne J, Snell RG, Cheadle JP, Jones AC, Tachataki M, Ravine D, Sampson JR, Reeve MP, Richardson P, Wilmer F, Munro C, Hawkins TL, Sepp T, Ali, JBM, Ward S, Green AJ, Yates JRW, Short MP, Haines JH, Jozwiak S, Kwiatkowska J, Henske EP and Kwiatkowski DJ. Identification of the tuberous sclerosis gene (*TSC1*) on chromosome 9q34. Science (1997) 277 805-808.

4. Huang J and Manning BD: The TSC1-TSC2 complex: a molecular switchboard controlling cell growth. Biochem J. (2008) 412 179-190.

5. Sancak O, Nellist M, Goedbloed M, Elfferich P, Wouters C, Maat-Kievit A, Zonnenberg B, Verhoef S, Halley D and van den Ouweland A. Mutational analysis of the TSC1 and TSC2 genes in a diagnostic setting: Genotype - phenotype correlations and comparison of diagnostic DNA techniques in Tuberous Sclerosis Complex. Eur. J. Hum. Genet. (2005) 13 731-741.

6. Nellist M, Sancak O, Goedbloed MA, Rohe C, van Netten D, Mayer K, Tucker-Williams A, van den Ouweland AMW and Halley DJJ. Distinct effects of single amino acid changes to tuberin on the function of the tuberin-hamartin complex. Eur. J. Hum. Genet. (2005) 13 59-68.

7. Nellist M, van den Heuvel D, Schluep D, Exalto C, Goedbloed M, Maat-Kievit A, van Essen T, van Spaendonck-Zwarts, Jansen F, Helderman P, Bartalini G, Vierimaa O, Penttinen M, van den Ende J, van den Ouweland A and Halley D. Missense mutations to the *TSC1* gene cause tuberous sclerosis complex. Eur. J. Hum. Genet. (2009) 17 319-328.

8. Mozaffari M, Hoogeveen-Westerveld M, Kwiatkowski D, Sampson J, Ekong R, Povey S, den Dunnen J, van den Ouweland A, Halley D and Nellist M. Identification of a region required for TSC1 stability by functional analysis of *TSC1* missense mutations found in individuals with tuberous sclerosis complex. BMC Med. Genet. (2009) 10:88

9. Jansen FE, Braams O, Vincken KL, Algra A, Anbeek P, Jennekens-Schinkel A, Halley D, Zonnenberg BA, van den Ouweland A, van Huffelen AC, van Nieuwenhuizen O and Nellist M. Overlapping neurologic and cognitive phenotypes in patients with *TSC1* or *TSC2* mutations. Neurology (2008) 70 908-915.

10. Lugnier C, Majores M, Fassunke J, Pernhorst K, Niehusmann P, Simon M, Nellist M, Schoch S and Becker A. Hamartin variants that are frequent in focal dysplasias and cortical tubers have reduced tuberin binding and aberrant subcellular distribution *in vitro*. J. Neuropathol. Exp. Neurol. (2009) 68 1136-1146.

11. Hoogeveen-Westerveld M, Exalto C, Maat-Kievit A, van den Ouweland A, Halley D and Nellist M. Analysis of TSC1 truncations defines regions involved in TSC1 stability, aggregation and interaction. Biochim. Biophys. Acta (2010), doi: 10.1016/j.bbadis.2010.06.004.

12. Ng PC and Henikoff S. Predicting the effects of amino acid substitutions on protein function. Annu. Rev. Genomics Hum. Genet. (2006) 7 61-80.

13. Ng PC and Henikoff S. Accounting for human polymorphisms predicted to affect protein function. Genome Res. (2002) 12 436-446.

14. Mathe E, Olivier M, Kato S, Ishioka C, Hainaut P and Tavtigian SV. Computational approaches for predicting the biological effect of p53 missense mutations: a comparison of three sequence analysis based methods. Nuc. Acids. Res. (2006) 34 1317-1325.

15. Nellist M, Verhaaf B, Goedbloed M, Reuser A, van den Ouweland A and Halley D. *TSC2* missense mutations inhibit tuberin phosphorylation and prevent formation of the tuberin-hamartin complex. Hum. Molec. Genet. (2001) 10 2889-2898.

16. Li Y, Inoki K, Guan K-L. Biochemical and functional characterization of small GTPase Rheb and TSC2 GAP activity. Mol. Cell Biol. (2004) 24 7965-7975.

17. Nellist M, van Slegtenhorst M, Goedbloed M, van den Ouweland A, Halley D and van der Sluijs P. Characterization of the cytosolic tuberin-hamartin complex: tuberin is a cytosolic chaperone for hamartin. J. Biol. Chem. (1999) 274 35647-35652.

18. Coevoets R, Arican S, Hoogeveen-Westerveld M, Simons E, van den Ouweland A, Halley D and Nellist M. A reliable cell-based assay for testing unclassified *TSC2* gene variants. Eur. J. Hum. Genet. (2009) 17 301-310.

19. Schutz-Geschwender A, Zhang Y, Holt T, McDermitt D and Olive DM (2004) Quantitative, two-color Western blot detection with infrared fluorescence. http://www.licor.com/bio/PDF/IRquant.pdf (25 Jul.2006).

Supporting Data

Appendix 1: Functional assessment of variants in the *TSC1* and *TSC2* genes identified in individuals with Tuberous Sclerosis Complex (manuscript in preparation)

Appendix 2: Unclassified *TSC2* variants associated with bilateral, sporadic angiomyolipoma (manuscript in preparation)

Appendix 3: The *TSC2* c.3598C>T (p.R1200W) missense mutation co-segregates with tuberous sclerosis complex in multiple mildy affected kindreds (manuscript in preparation)

Appendix 4: publications

Appendix 1:

Title page:

Functional assessment of variants in the *TSC1* and *TSC2* genes identified in individuals with Tuberous Sclerosis Complex

Marianne Hoogeveen-Westerveld[1], Marjolein Wentink[1], Diana van den Heuvel[1], Melika Mozaffari[1], Rosemary Ekong[2], Sue Povey[2], Johan den Dunnen[3], Kay Metcalfe[4], Stephanie Vallee[5], Stefan Krueger[6], JoAnn Bergoffen[7], Vandana Shashi[8], Frances Elmslie[9], David Kwiatkowski[10], Julian Sampson[11], Anneke Maat-Kievit[1], Ans van den Ouweland[1], Dicky Halley[1] and Mark Nellist[1]

[1]Department of Clinical Genetics, Erasmus Medical Centre, 3015 GE Rotterdam, The Netherlands.

[2]Research Department of Genetics, Evolution and Environment, University College London, London NW1 2HE, U.K.

[3]Department of Human and Clinical Genetics, Leiden University Medical Centre, 2333 ZC Leiden, The Netherlands.

[4]Department of Genetic Medicine, Central Manchester University Hospitals NHS Foundation Trust, Manchester M13 9WL, U.K.

[5]Department of Clinical Genetics, Dartmouth-Hitchcock Medical Center, Lebanon, NH 03756, U.S.A.

[6]Center for Human Genetics, Gutenbergstr. 5, D-01307 Dresden, Germany.

[7]Department of Genetics, 5755 Cottle Road, San Jose, CA 95123, U.S.A.

[8]Department of Pediatrics, Duke University Medical Center, Durham, NC, U.S.A.

[9] Department of Medical Genetics, St. George's Hospital, London SW17 0RE, U.K.

[10]Translational Medicine Division, Brigham and Womens Hospital, Boston MA 02115, U.S.A.

[11]Institute of Medical Genetics, University of Wales College of Medicine, Heath Park, Cardiff CF4 4XN, U.K.

To whom correspondence should be addressed: Dr. Mark Nellist, Department of Clinical Genetics, Erasmus Medical Centre, Dr. Molewaterplein 50, 3015 GE Rotterdam, The Netherlands, Tel: +31 10 7044628; Fax: +31 10 7044736; email: m.nellist@erasmusmc.nl

Running title: Functional assessment of TSC1 and TSC2 variants

Abstract

The effects of missense changes and small in-frame deletions and insertions on protein function are not easy to predict. The identification of such unclassified variants (UVs) in individuals at risk of genetic disease can complicate genetic counselling. One solution is to perform functional tests to assess whether UVs affect protein function. We have used this strategy to characterise variants identified in the *TSC1* and *TSC2* genes in individuals with, or suspected of having, Tuberous Sclerosis Complex (TSC). Here we present an overview of our functional studies on 45 TSC1 and 107 TSC2 variants. Using a standardised protocol we classified 16 TSC1 variants and 69 TSC2 variants as pathogenic.

Keywords: tuberous sclerosis complex, TSC1, TSC2, unclassified variants

Introduction

Tuberous Sclerosis Complex (TSC) is an autosomal dominant disorder characterised by the development of hamartomas in a variety of organs and tissues, most notably the brain, skin and kidneys [Gomez et al., 1999]. Most individuals with TSC have epilepsy and many suffer from cognitive impairments and/or autism-spectrum disorders. Mutations in either the *TSC1* gene on chromosome 9q34 [van Slegtenhorst et al., 1997], or the *TSC2* gene on chromosome 16p13.3 [European Chromosome 16 Tuberous Sclerosis Consortium, 1993] cause TSC and comprehensive mutation screens in TSC patients have identified a wide variety of pathogenic mutations [Jones et al., 1999; Niida et al., 1999; Dabora et al., 2001; Sancak et al., 2005; Au et al., 2007]. Most *TSC1* and *TSC2* mutations result in premature termination of the respective open-reading frame and complete inactivation of the mutated allele. However, approximately 20% of the mutations identified in the *TSC2* gene, and a small number of *TSC1* mutations [Hodges et al., 2001; Nellist et al. 2009], are non-terminating missense changes or small in-frame deletions or insertions. The consequences of such non-terminating changes are not easy to predict with certainty, making it difficult to distinguish disease-causing mutations from neutral (non-pathogenic) variants, particularly if clinical and/or genetic data are incomplete. In a cohort of 490 putative TSC cases, we identified 29 variants (6% of the total) that could not be classified as either pathogenic or neutral from the available clinical and genetic data [Sancak et al., 2005]. In such cases, *in vitro* functional comparisons between the wild-type and variant proteins can help assess whether an unclassified variant (UV) is pathogenic or not [Nellist et al. 2008].

The *TSC1* and *TSC2* gene products, TSC1 and TSC2, interact to form a protein complex that integrates multiple growth factor- and energy-dependent signals to help control cell growth [Inoki and Guan, 2009]. The N-terminal region of TSC2 is required for the

binding with TSC1 [Li et al., 2004], while the TSC2 C-terminal region contains the active site of the complex, an "asparagine-thumb" GTPase activating protein (GAP) domain [Daumke et al., 2004]. The TSC1-TSC2 complex stimulates the GTPase activity of RHEB to promote the conversion of active, GTP-bound RHEB to inactive RHEB-GDP and thereby prevent the RHEB-GTP-dependent stimulation of the mammalian target of rapamycin (mTOR) complex 1 (TORC1) [Li et al., 2003]. In cells lacking either *TSC1* or *TSC2*, the downstream targets of TORC1, including elongation factor 4E binding protein 1 (4E-BP1), p70 S6 kinase (S6K) and ribosomal protein S6, are constitutively phosphorylated [Zhang et al., 2003; Kwiatkowski et al., 2001].

The effects of specific amino acid changes on TSC1-TSC2 complex formation, on the activation of RHEB GTPase activity by the complex, and on the phosphorylation status of 4E-BP1, S6K and S6, have been determined [Nellist et al., 2001; Inoki et al. 2002, Tee et al, 2002]. Pathogenic missense changes in the N-terminal region of TSC1 (amino acids 50 - 224) reduce TSC1 stability [Nellist et al. 2009; Mozaffari 2009]. Pathogenic missense changes in TSC2 have distinct effects on the TSC1-TSC2 complex, depending on the region of TSC2 that is affected. Some TSC2 amino acid substitutions prevent TSC1-TSC2 complex formation while others do not affect TSC1-TSC2 binding, but still inactivate the complex [Nellist et al., 2005].

Interestingly, although *TSC2* mutations are generally associated with a more severe TSC phenotype [Dabora et al. 2001], there are several reports of families where specific *TSC2* missense mutations cosegregate with apparently mild forms of the disease [Khare et al., 2001; O'Connor et al., 2003; Mayer et al., 2004; Jansen et al., 2006]. This raises the possibility that specific types of *TSC1* or *TSC2* mutation may help determine the clinical course of the disease, as has been proposed for the neurodevelopmental abnormalities associated with TSC [de Vries and Howe, 2007]. In other genetic diseases, clear correlations

between the effects of specific missense mutations on protein function and the clinical course are recognised [Hermans et al., 2004] and for individuals with specific *TSC1* or *TSC2* variants, it would be useful to be able to predict whether the detected changes are more or less likely to lead to a severe phenotype.

Previously we have used immunoblotting, double-label immunofluorescent microscopy, in-cell Western analysis and GAP assays to study the effects of 47 *TSC2* missense and in-frame insertions/deletions and 26 *TSC1* missense and in-frame insertions/deletions on TSC1-TSC2 activity [Nellist et al., 2005; Jansen et al., 2006, Jansen et al., 2008, Nellist et al., 2008, Nellist et al., 2009; Coevoets et al., 2009; Mozaffari et al., 2009]. Here we compare these 73 variants to 79 new variants (19 *TSC1* and 60 *TSC2*) using a standardised protocol. To assess the effects of the variants on both the formation and activity of the TSC1-TSC2 complex we decided to use immunoblotting followed by infra-red scanner-based detection. In our experience, double-label microscopy and GAP assays were too labour-intensive and/or unreliable for routine use and, although the in-cell Western was a simple and reliable assay [Coevoets et al., 2009], it required large amounts of (expensive) antibodies and did not provide information on the TSC1-TSC2 interaction.

Our aim was to investigate the reliability of the assay, the degree of concordance between the *in vitro* results and computer-based predictive methods and, ultimately, to use the results of the functional assessment to determine whether UVs identified in individuals with, or suspected of having, TSC were pathogenic. Furthermore, we hoped to gain insight into the structural properties of TSC1 and TSC2 by comparing the properties of the different variants.

Materials and Methods

TSC1 and TSC2 variants

The relative positions of the variants selected for functional assessment are shown in Figure 1. Previously untested variants are indicated in Tables 1., 2. and 3. It is important to note that the TSC2 variants were compared to wild-type TSC2 as originally described [European Chromosome 16 Tuberous Sclerosis Consortium, 1993]. This isoform lacks the amino acids encoded by the alternatively spliced exon 31. The amino acid numbering according to the *TSC2* Leiden Open Variation Database (LOVD) (http://www.lovd.nl/TSC2), where this differs from the original numbering due to the inclusion of exon 31, is given in Table 3.

Constructs and antisera

Expression constructs encoding the TSC1 and TSC2 variants were derived from the wild-type expression constructs [Nellist et al., 2005] using the QuikChange site-directed mutagenesis kit (Stratagene, La Jolla, U.S.A.). In each case the complete open reading frame of the mutated construct was verified by sequence analysis. In most cases, multiple clones were isolated, checked and used for the assays described below. Other constructs used in this study have been described previously [Nellist et al., 2005]. Antibodies were purchased from Cell Signaling Technology (Danvers, U.S.A.) (1A5, anti T389 phospho-S6K mouse monoclonal; 9B11, anti-myc tag mouse monoclonal; anti-myc tag rabbit polyclonal), Li-Cor Biosciences (Lincoln, U.S.A.) (goat anti-rabbit 680 nm and goat anti-mouse 800 nm conjugates) or DAKO (Glostrup, Denmark) (cyanine (Cy2)-coupled secondary antibodies against mouse immunoglobulins), or have been described previously [van Slegtenhorst et al., 1998].

Transfection-based immunoblot assay for functional assessment of TSC1 and TSC2 variants

TSC1 and TSC2 variants were assayed using essentially the same protocol. HEK 293T cells were seeded into 24-well plates and grown overnight in Dulbecco's modified Eagle medium (DMEM) (Lonza, Verviers, Belgium) supplemented with 10% foetal bovine serum, 50 U/ml penicillin and 50 μg/ml streptomycin in a 10% carbon dioxide humidified incubator. Cells at 80 - 90% confluency were transfected with 0.2 μg TSC2 expression construct, 0.4 μg TSC1 expression construct and 0.1 μg S6K expression construct using 2.1 μg polyethyleneimine (Polysciences Inc., Warrington, U.S.A.) in DMEM, as described previously [Coevoets et al., 2009]. For control transfections, pcDNA3 vector DNA was added to make a total of 0.7 μg DNA per transfection. In each experiment up to 20 TSC1 or TSC2 variants were tested. Cells expressing the TSC2 variants were compared to cells expressing wild-type TSC1-TSC2, a known pathogenic variant (TSC2-R611Q [Nellist et al., 2005]), TSC1 and S6K only (no TSC2), and cells transfected with vector DNA only (control). Cells expressing the TSC1 variants were compared to wild-type TSC1-TSC2, a known pathogenic variant (TSC1-L117P [Nellist et al., 2009]), TSC2 and S6K only (no TSC1), TSC1 and S6K only (no TSC2) and cells transfected with vector DNA only (control).

After 4 hours the transfection mixtures were replaced with DMEM supplemented with 10% foetal bovine serum, 50 U/ml penicillin and 50 μg/ml streptomycin. Twenty-four hours after transfection the cells were transferred to ice, washed with phosphate-buffered saline (PBS) (4^{o}C) and harvested in 75 μl lysis buffer (50 mM Tris-HCl pH 8.0, 150 mM NaCl, 50 mM NaF and 1% Triton X100, containing a protease inhibitor cocktail (Complete, Roche Molecular Biochemicals, Woerden, The Netherlands)). The soluble, supernatant fractions were recovered by centrifugation (10 000 g for 10 minutes at 4^{o}C), diluted in loading buffer and incubated at 96^{o}C for 5 minutes prior to electrophoresis on Criterion^{TM} 4-12% SDS-PAGE gradient gels (Bio-Rad, Hercules, U.S.A.) and transfer to nitrocellulose membranes, according to the manufacturer's recommendations.

Blots were blocked for 1 hour at room temperature with 5% low-fat milk powder (Campina Melkunie, Eindhoven, The Netherlands) in PBS and incubated overnight at 4^{o}C with the following primary antibodies: 1/15 000 dilution of 1895 (rabbit polyclonal against TSC2 [van Slegtenhorst et al., 1998]), 1/5 000 dilution of 2197 (rabbit polyclonal against TSC1 [van Slegtenhorst et al. 1998]), 1/5 000 dilution of a rabbit polyclonal against the myc epitope tag and 1/2 000 dilution of 1A5 (mouse monoclonal against p70 S6 kinase (S6K) phosphorylated at amino acid T389). Antibodies were diluted in PBS containing 0.1 % Tween 20 (PBST) (Sigma-Aldrich Fine Chemicals, Poole, U.K). After washing 3 times for 5 minutes in PBST, the blots were incubated for 1 hour at room temperature in the dark in PBST containing 1/10 000 dilutions of goat anti-rabbit 680 and goat anti-mouse 800 secondary antibodies. After washing 3 times for 5 minutes in PBST and once in PBS, the blots were scanned using the Odyssey^{TM} Infrared Imager (Li-Cor Biosciences) at default intensity, medium quality, 169 μm resolution with 0 mm focus offset. To estimate the expression levels of the different proteins and the ratio of T389-phosphorylated S6K to total S6K, in the presence of the different TSC1 and TSC2 variants, the scanned blots were analysed using the Odyssey quantification software. The integrated intensities of the protein bands were determined using default settings with the 3 pixel width border mean average background correction method. To correct for the detection of endogenous proteins, we subtracted the signals detected in control cells (transfected with vector DNA only) from the corresponding TSC2, TSC1, S6K and T389-phosphorylated S6K signals for all variants.

Immunofluorescent detection of TSC1 variants

HEK 293T cells were seeded onto glass coverslips coated with poly-L-lysine (Sigma-Aldrich) and transfected with expression constructs encoding the TSC1 variants. Twenty-four hours after transfection the cells were fixed, permeabilised and incubated with a mouse

monoclonal antibody specific for the TSC1 C-terminal myc epitope tag, followed by a Cy2-coupled secondary antibody against mouse immunoglobulins, as described previously [Mozaffari et al. 2009]. Cells were studied using a Leica DM RXA microscope and Image Pro-Plus version 6 image analysis software.

Prediction analysis

To indicate whether the *TSC1* and *TSC2* nucleotide changes might affect RNA splicing, 3 different splice-site prediction programs were used: www.cbs.dtu.dk/services/NetGene2, www.genet.sickkids.on.ca/~ali/ splicesitefinder.html, and www.fruitfly.org/seq_tools/splice.html.

To indicate whether the TSC1 and TSC2 amino acid substitutions were likely to affect TSC1-TSC2 structure and function, the Sorting Intolerant From Tolerant (SIFT) algorithm was used [Ng and Henikoff, 2006]. SIFT scores were calculated using multiple sequence alignments of TSC1 and TSC2 from 16 different species (human, chimpanzee, maccaca, cow, dog, horse, mouse, rat (TSC1 only), chicken, zebrafish (TSC2 only), pufferfish, honey bee (TSC1 only), fruitfly, mosquito, methylotrophic yeast (TSC2 only) and fission yeast).

Results

Immunoblot analysis

We compared 152 variants (45 TSC1 and 107 TSC2), including 79 previously untested variants (19 TSC1 and 60 TSC2). Each variant was tested in at least 4 independent transfection experiments. In each experiment, the integrated intensities of the bands on the immunoblot corresponding to TSC2, TSC1, total S6K and T389-phosphorylated S6K were

determined for each variant relative to the integrated intensities of the bands for wild-type TSC1-TSC2. The variants were then assessed according to 3 criteria.

First, to determine whether the different variants were transfected at comparable efficiencies, the total S6K signals were compared per variant. Next, the activity of TORC1, as indicated by the amount of T389-phosphorylated S6K, was estimated in the presence of the different variants. For each variant, the ratio of the T389-phosphorylated S6K signal to the total S6K signal, relative to wild-type TSC1-TSC2, was determined. We referred to this as the T389/S6K ratio. The higher the T389/S6K ratio, the higher the activity of TORC1, and therefore the lower the activity of the exogenously expressed TSC1 and TSC2. This was the primary criterium for deciding whether a variant was likely to be pathogenic and cause TSC.

Finally, in addition to the T389/S6K ratio, we compared the signals of the TSC1 and TSC2 variants and their wild-type binding partner (TSC1 or TSC2) to the signals for wild-type TSC1-TSC2. If the variant signal itself, or the signal of the wild-type binding partner, was significantly less than the wild-type TSC1-TSC2 complex, this was taken as supporting evidence that the variant was pathogenic.

Representative examples of immunoblots of 13 TSC1 variants and 15 TSC2 variants are shown in Figures 2 and 3 respectively. The mean values for the TSC2, TSC1 and S6K signals and the mean T389/S6K ratios for all the variants tested are shown in Figures 4, 5 and 6.

As shown in Figures 4D, 5D and 6D, the S6K signals were relatively constant for all the variants and controls, indicating that the transfection efficiencies were comparable between the different variants. The mean T389/S6K ratios for the TSC1 and TSC2 variants are shown in Figures 4C, 5C and 6C. To determine whether the T389/S6K ratios for the different variants were significantly different from wild-type TSC1-TSC2, we performed Student's t-tests. We classified the variants with a T389/S6K ratio significantly higher than

wild-type TSC1-TSC2 ($p < 0.05$), as pathogenic (Figures 4C, 5C and 6C and Tables 1, 2 and 3). Sixty-nine TSC2 variants (69/107; 64%) and 16 TSC1 variants (16/45; 36%) fell into this category. For variants where the T389/S6K ratio was not significantly higher than wild-type TSC1-TSC2 ($p > 0.05$), we compared the T389/S6K ratio to the pathogenic variant that was included in each transfection experiment (TSC2 R611Q for TSC2 variants; TSC1 L117P for TSC1 variants). Variants that did not have a significantly higher T389/S6K ratio than wild-type TSC1-TSC2, had a significantly lower T389/S6K ratio than the corresponding pathogenic variant, indicating that the variant was active in our assay. We classified these variants as probably neutral (Tables 1, 2 and 3).

Next, we compared the signal for each variant with the corresponding signal for the wild-type protein (Figures 4B, 5A and 6A). We classified variants with a significantly lower mean signal than the corresponding wild-type protein ($p < 0.05$, paired t-test) as unstable (Tables 1, 2 and 3). We identified 39 unstable TSC2 variants and 16 unstable TSC1 variants. All of the unstable TSC1 variants were classified as pathogenic, according to the comparisons between the variant and wild-type T389/S6K ratios. Furthermore, consistent with a previous study [Mozaffari et al., 2009], all the unstable TSC1 variants gave a diffuse cytoplasmic signal as detected by immunofluorescent microscopy, in contrast to wild-type TSC1 and the stable TSC1 variants that all gave a characteristic punctate localisation pattern (data not shown). Of the unstable TSC2 variants, 36/39 were defined as pathogenic according to the comparisons of the T389/S6K ratios. In the 3 remaining cases (TSC2 R1159L, TSC2 R1159Q and TSC2 R1772C), the variant inhibited S6K T389-phosphorylation as effectively as wild-type TSC2, despite being detected at lower levels (Figure 6A and C).

In a previous study we concluded that the R1772C variant was unlikely to be pathogenic because an individual with this variant and TSC had another *TSC2* mutation [Nellist et al., 2008]. Furthermore, individuals with this variant and no signs of TSC have

been identified (http://www.lovd.nl/TSC2). Therefore, we classified the TSC2 R1772C variant as probably neutral (Table 3). The antiserum used to detect the TSC2 variants binds epitopes encoded by the last exon of *TSC2*, which includes codon 1772 (M. Wentink, M. Nellist; unpublished results). It is possible that the R1772C substitution reduces the affinity of the antiserum for TSC2, resulting in a lower immunoblot signal.

The R1159L and R1159Q variants inhibited S6K-T389 phosphorylation as ceffectively as wild-type TSC2 in our assay and were therefore classified as probably neutral (Table 3) However, the reduced signals for these variants may reflect destabilising effects of the substitutions on TSC2. It is possible that the variants are too unstable to inhibit TORC1 signalling *in vivo* and are consequently pathogenic changes (see Discussion).

Finally, we compared the signals for wild-type TSC1 in the presence of the different TSC2 variants (Figures 5B and 6B), and the signals for wild-type TSC2 in the presence of the different TSC1 variants (Figure 4A). Coexpression of TSC2 helps stabilise TSC1 [Nellist et al., 1999]. Therefore we classified TSC2 variants that were associated with a significantly reduced TSC1 signal ($p < 0.05$, paired t-test) and TSC1 variants that were associated with a significantly reduced TSC2 signal ($p < 0.05$, paired t-test) as destabilising. Three TSC1 variants, L93R, N198F199delinsI and M224R, were associated with a significant reduction in the TSC2 signal (Figure 4A). In each case we had classified the variant as pathogenic due to a significantly increased T389/S6K ratio compared to wild-type TSC1 (Table 1). Thirty-eight TSC2 variants were associated with a significant reduction in the TSC1 signal (Figures 5B and 6B). We divided these variants into 2 groups. One group of 31 variants clustered within the N-terminal half of TSC2 (amino acids 98 - 897), while a small group of 7 variants clustered close to the C-terminus (amino acids 1525 - 1773). In all 38 cases we had classified the variant as pathogenic due to a significantly increased T389/S6K ratio compared to wild-type TSC1-TSC2 (Tables 2 and 3).

Prediction Analysis

We investigated the possibility that the nucleotide changes corresponding to variants that did not affect TSC1-TSC2 function in our assay affected either *TSC1* or *TSC2* splicing. We analysed the *TSC1* and *TSC2* nucleotide changes using 3 different splice-site prediction programs and identified 8 variants (5 *TSC1* and 3 *TSC2*) that were predicted to cause splicing abnormalities (Tables 1 and 2). In one case (*TSC2* c.1235A>T), this was confirmed by functional assessment of the predicted TSC2 splice variant (TSC2 412del8; Figures 3 and 5, Table 2; [Jansen et al., 2008]).

Next, we investigated whether the functional assessments of the TSC1 and TSC2 variants were in agreement with the Sorting Intolerant From Tolerant (SIFT) amino acid substitution prediction method [Ng and Henikoff, 2006]. The SIFT algorithm combines information from the chemical structure of the individual amino acids and the evolutionary conservation of a protein to predict whether specific substitutions can be tolerated by the protein. SIFT analysis of TSC1 indicated that the N-terminal (amino acids 1 - 300) and C-terminal (amino acids 700 - 1164) regions were relatively intolerant to amino acid changes [Mozaffari et al., 2009]. All the TSC1 variants classified as pathogenic according to our functional assessment clustered within the substitution intolerant N-terminal region (Table 1). SIFT predicted that 18/41 (44%) of the TSC1 missense changes would not be tolerated. In 36 cases (88%), the SIFT prediction was consistent with the functional assessment. In 5 cases (R190C, R246K, R246T, H732Y and R1097H), SIFT predicted that the substitution would not be tolerated, while the functional assessment indicated that the amino acid changes were probably neutral. In the case of the R246K and R246T substitutions, splice site prediction analysis indicated that the corresponding nucleotide changes (c.737G>A and c.737G>C) were likely to cause splicing errors. Similarly, although the K121R, G305R and G305W

substitutions were tolerated by the SIFT analysis and were probably neutral according to the functional assessment, splice site prediction analysis indicated that the corresponding nucleotide changes were most likely splice site mutations. The TSC1 H732Y variant has been identified in individuals without TSC (http://www.lovd.nl/TSC1) and is unlikely to cause TSC, consistent with the results of our functional assessment (Figures 2 and 4; Table 1). However, this variant is associated with focal cortical dysplasia type II [Lugnier et al. 2009]. Therefore, the SIFT result may still be accurate, even though the H732Y substitution is not critical for TSC1 function as determined in our assay. Due to reduced amino acid sequence conservation at the C-terminus of TSC1, the SIFT prediction for the TSC1 R1097H substitution was made with a low degree of confidence, and is therefore not reliable (data not shown).

SIFT analysis of TSC2 indicated that amino acids 1 - 900 and 1500 - 1807, corresponding to the TSC1-binding domain and the GAP domain respectively, were intolerant of amino acid substitutions (Supplemental Figure 1). In total, the SIFT prediction and functional assessment were consistent for 78 TSC2 variants (81%)(Tables 2 and 3). SIFT tolerated 42/96 (44%) of the TSC2 amino acid substitutions subjected to functional testing. Of these, 13 (31%) were classified as pathogenic according to the functional assessment. Of the 54 substitutions not tolerated by SIFT, 5 were classified as neutral according to the functional assessment. In one case where the substitution was tolerated by SIFT (c.1118A>C, p.Q373P) and 2 cases where the substitution was not tolerated (c.1235A>T, p.E412V and c.1255C>T, p.P419S), the functional assessment indicated that the amino acid substitution was probably neutral, while splice site analysis predicted that the corresponding nucleotide change would affect splicing.

Overall, there was broad agreement between the SIFT predictions and our functional assessments for both the TSC1 and TSC2 variants. Nevertheless, there were sufficient

exceptions to indicate that the results of SIFT and similar prediction algorithms should be treated with caution.

In summary, using a transfection-based immunoblot assay we classified 16/45 TSC1 variants (36%) and 69/107 TSC2 variants (64%) as pathogenic. Of the 79 previously untested variants, we classified 42 (53%) as pathogenic, including 5/19 TSC1 (26%) and 37/60 TSC2 variants (62%). We classified 24/45 TSC1(53%) and 35/107 TSC2 variants (33%) as probably neutral. In 8 cases (5 TSC1 and 3 TSC2), the variant was neutral according to the functional assessment, but splice site analysis predicted that the corresponding nucleotide change was likely to be a pathogenic splice site mutation.

Discussion

Mutation analysis of individuals with, or suspected of having, a genetic disease facilitates the diagnosis, treatment and genetic counselling of those individuals and their families. However, in some cases it is not possible to determine from the genetic data whether an identified nucleotide change is disease-causing. Functional analysis of predicted protein variants provides an additional method for determining whether specific changes are pathogenic.

We have characterised the effects of 152 TSC1 and TSC2 amino acid substitutions and small in-frame insertions/deletions on the TSC1-TSC2 complex. Based on our functional assessment we classified 85 (56%) of the changes as pathogenic. In 8 (5%) cases where we did not detect an effect on protein function, the corresponding nucleotide change was predicted to cause splicing defects.

We tested 45 TSC1 variants, of which 42 were amino acid substitutions and 3 were in-frame insertion/deletion changes. In 4 cases we analysed multiple changes at the same codon.

Sixteen variants were detected at significantly reduced levels compared to wild-type TSC1. In each case, TORC1 activity, as estimated from the ratio of T389 phosphorylated S6K to total S6K, was increased compared to the wild-type control and we classified these variants as pathogenic. Consistent with previous studies [Nellist et al., 2009, Mozaffari et al., 2009], all the variants that were detected at low levels by immunoblotting mapped to the TSC1 N-terminal region (amino acids 50 - 224) and had a distinct cytoplasmic localisation pattern compared to wild-type TSC1, confirming the importance of this region for TSC1 function, localisation and stability.

We tested 104 TSC2 variants, of which 95 were amino acid substitutions, 3 were small in-frame insertions (1 - 3 amino acids) and 6 were in-frame deletions (1 - 26 amino acids). In 12 cases we analysed multiple changes at the same codon. Fifty-five changes affected the N-terminal half of the protein (amino acids 1 - 900), and 52 affected the C-terminal region (amino acids 901 - 1784). Twenty-one (38%) of the changes in the N-terminal region were unstable, and 31 (56%) were associated with significantly reduced levels of TSC1, consistent with an important role for the TSC2 N-terminal region in binding and stabilising TSC1 [Li et al. 2004]. Eighteen (35%) of the changes in the C-terminal region were unstable and 7 (13%) were associated with significantly reduced levels of TSC1. The 7 C-terminal variants associated with reduced levels of TSC1 mapped between amino acids 1525 and 1729, suggesting that this region may also play a role in maintaining stable TSC1-TSC2 complexes.

We compared our functional assessment with the classifications listed in the *TSC1* and *TSC2* LOVD (http://www.lovd.nl/TSC1; http://www.lovd.nl/TSC2). In general there was good agreement between the LOVD classifications and our functional assessment (Tables 1, 2 and 3). However, we identified one TSC1 variant (F216S) and 4 TSC2 variants (K599M, F615S, R951S and L1771I) for which there was strong disagreement. The TSC1 F216S variant is classified as probably not pathogenic in the LOVD because it was identified in an

apparently unaffected parent, but is a pathogenic change according to our functional assessment. The TSC2 K599M substitution is classified as pathogenic in the LOVD because it was identified as a *de novo* change in a TSC patient [Niida et al. 1999] and because it reduced the TSC2-dependent inhibition of 4E-BP1 phosphorylation *in vitro* [Tee et al. 2002]. However, consistent with our previous studies [Nellist et al. 2001; Nellist et al. 2005], in our assay, the K599M substitution did not affect TSC1-TSC2 binding or stability, and inhibited S6K T389 phosphorylation as effectively as wild-type TSC2. The TSC2 F615S substitution is classified as having no known pathogenicity in the LOVD, but is a pathogenic change according to our functional assessment, consistent with our previous studies [Nellist et al. 2001; Nellist et al. 2005]. The TSC2 R951S substitution is classified as probably pathogenic in the LOVD, but according to our functional assessment is probably neutral. Codon 951 is encoded by the alternatively spliced exon 25 of the *TSC2* gene [Xu et al. 1995]. Very few pathogenic changes have been identified in this exon (http://lovd.nl/TSC2). Furthermore, complete removal of this exon did not affect TSC2 function in our assay (M. Wentink, M. Nellist, unpublished observations). Finally, the LOVD lists the TSC2 L1773I variant as probably pathogenic, but is probably neutral according to our functional assessment. The L1773I substitution is a conservative change in the last exon of *TSC2*. Deletion of the amino acids encoded by this exon did not affect TSC2 function in our assay (M. Wentink, M. Nellist, unpublished observations).

We classified 31 TSC2 and 29 TSC1 variants as probably neutral. In some cases, these variants are very likely to be rare, neutral variants that do not cause TSC. However, all the variants were identified in individuals with, or suspected of having, TSC and must therefore be considered to be potentially pathogenic. We could not exclude the possibility that some variants had sufficient activity in our over-expression system to inhibit TORC1, while *in vivo*

they may be inactive or unstable. Therefore, it would be useful to have additional, more sensitive assays to characterise these variants in more detail.

We classified 152 different TSC1 and TSC2 variants using a transfection-based immunoblot assay. We distinguished pathogenic TSC1 and TSC2 variants from probable neutral variants according to whether there was evidence for increased S6K-T389 phosphorylation. Based on the functional assessment, 85 variants were classified as pathogenic. In addition, we identified 8 putative splice site mutations. Further work is required to exclude the possibility that the 67 variants classified as probably neutral affect TSC1-TSC2 function *in vivo* and are in fact pathogenic.

Acknowledgments

Financial support was provided by the U.S. Department of Defense Congressionally-Directed Medical Research Program (grant #TS060052), the Michelle Foundation and the Tuberous Sclerosis Alliance. The authors report no conflicts of interest.

References

Adachi H, Igawa M, Shiina H, Urakami S, Shigeno K, Hino O. 2003. Human bladder tumors with 2-hit mutations of tumor suppressor gene *TSC1* and decreased expression of p27. J. Urol. 170:601-604.

Au K-S, Williams AT, Roach ES, Batchelor L, Sparagana SP, Delgado MR, Wheless JW, Baumgartner JE, Roa BB, Wilson CM, Smith-Knuppel TK, Cheung MY, Whittemore VH, King TM, Northrup H. 2007. Genotype/phenotype correlation in 325 individuals referred for a diagnosis of tuberous sclerosis complex in the United States. Genet Med 9:88-100.

Benit P, Kara-Mostefa A, Hadj-Rabia S, Munnich A, Bonnefont JP. 1999. Protein truncation test for screening hamartin gene mutations and report of new disease-causing mutations. Hum Mutat 14:428-432.

Choi JE, Chae JH, Hwang YS, Kim KJ. 2006. Mutational analysis of *TSC1* and *TSC2* in Korean patients with tuberous sclerosis complex. Brain Dev 28:440-446.

Coevoets R, Arican S, Hoogeveen-Westerveld M, Simons E, van den Ouweland A, Halley D, Nellist M 2009 A reliable cell-based assay for testing unclassified *TSC2* gene variants. Eur J Hum Genet 17:301-310.

Dabora SL, Jozwiak S, Franz DN, Roberts PS, Nieto A, Chung J, Choy YS, Reeve MP, Thiele E, Egelhoff JC, Kasprzyk-Obara J, Domanska-Pakiela D, Kwiatkowski DJ. 2001.

Mutational analysis in a cohort of 224 tuberous sclerosis patients indicates increased severity of *TSC2*, compared with *TSC1*, disease in multiple organs. Am J Hum Genet 68:64-80.

Daumke O, Weyand M, Chakrabarti PP, Vetter IR, Wittinghofer A. 2004. The GTPase-activating protein Rap1GAP uses a catalytic asparagine. Nature 429:197-201.

European Chromosome 16 Tuberous Sclerosis Consortium. 1993 Identification and characterization of the tuberous sclerosis gene on chromosome 16. Cell 75:1305-1315.

Gomez MG, Sampson JR, Holets-Whittemore V, eds. 1999 The tuberous sclerosis complex. 3rd edn. Developmental Perspectives in Psychiatry, Oxford University Press, New York and Oxford.

Hermans MM, van Leenen D, Kroos MA, Beesley CE, van der Ploeg AT, Sakuraba H, Wevers R, Kleijer W, Michelakakis H, Kirk EP, Fletcher J, Bosshard N, Basel-Vanagaite L, Besley G, Reuser AJ. 2004. Twenty-two novel mutations in the lysosomal alpha-glucosidase gene (*GAA*) underscore the genotype-phenotype correlation in glycogen storage disease type II. Hum Mutat 23:47-56.

Hodges AK, Li S, Maynard J, Parry L, Braverman R, Cheadle JP, DeClue JE, Sampson JR. 2001. Pathological mutations in *TSC1* and *TSC2* disrupt the interaction between hamartin and tuberin. Hum Mol Genet 10:2899-2905.

Huang J, Dibble CC, Matsuzaki M, Manning BD. 2008. The TSC1-TSC2 complex is required for proper activation of mTOR complex 2. Mol Cell Biol 28:4104-4115.

Hung CC, Su YN, Chien SC, Liou HH, Chen CC, Chen PC, Hsieh CJ, Chen CP, Lee WT, Lin WL, Lee CN. 2006. Molecular and clinical analyses of 84 patients with tuberous sclerosis complex. BMC Med Genet 7:72.

Inoki K, Li Y, Zhu T, Wu J, Guan K-L. 2002. TSC2 is phosphorylated and inhibited by Aky and suppresses mTOR signalling. Nat Cell Biol 4:648-657.

Inoki K, Guan K-L. 2009. Tuberous sclerosis complex, implication from a rare genetic disease to common cancer treatment. Hum Mol Genet 18:R94-R100.

Jansen AC, Sancak O, D'Agostino MD, Badhwar A, Roberts P, Gobbi G, Wilkinson R, Melanson D, Tampieri D, Koenekoop R, Gans M, Maat-Kievit A, Goedbloed M, van den Ouweland AMW, Nellist M, Pandolfo M, McQueen M, Sims K, Thiele EA, Dubeau F, Andermann F, Kwiatkowski DJ, Halley DJJ, Andermann E. 2006. Unusually mild tuberous sclerosis phenotype is associated with *TSC2* R905Q mutation. Ann Neurol. 60:528-539.

Jansen FE, Braams O, Vincken KL, Algra A, Anbeek P, Jennekens-Schinkel A, Halley D, Zonnenberg BA, van den Ouweland A, van Huffelen AC, van Nieuwenhuizen O, Nellist M. 2008. Overlapping neurologic and cognitive phenotypes in patients with *TSC1* or *TSC2* mutations. Neurology 70:908-915.

Jones AC, Shyamsundar MM, Thomas MW, Maynard J, Idziaszczyk S, Tomkins S, Sampson JR, Cheadle JP. 1999. Comprehensive mutation analysis of *TSC1* and *TSC2*, and phenotypic correlations in 150 families with tuberous sclerosis. Am J Hum Genet 64:1305-1315.

Khare L, Strizheva GD, Bailey JN, Au K-S, Northrup H, Smith M, Smalley SL, Henske EP. 2001. A novel missense mutation in the GTPase activating protein homology region of *TSC2* in two large families with tuberous sclerosis complex. J Med Genet 38:347-349.

Kwiatkowski DJ, Zhang H, Bandura JL, Heiberger KM, Glogauer M, el-Hashemite N, Onda H. 2001. A mouse model of TSC1 reveals sex-dependent lethality from liver hemangiomas, and up-regulation of p70S6 kinase activity in *Tsc1* null cells. Hum Mol Genet 11:525-534.

Li Y, Corradetti MN, Inoki K, Guan J-L. 2003. TSC2: filling the GAP in the mTOR signaling pathway. Trends Biochem Sci 28:573-576.

Li Y, Inoki K, Guan K-L. 2004. Biochemical and functional characterization of small GTPase Rheb and TSC2 GAP activity. Mol Cell Biol 24:7965-7975.

Lugnier C, Majores M, Fassunke J, Pernhorst K, Niehusmann P, Simon M, Nellist M, Schoch S, Becker A. 2009. Hamartin variants that are frequent in focal dysplasias and cortical tubers have reduced tuberin binding and aberrant subcellular distribution in vitro. J Neuropathol Exp Neurol 68:1136-1146.

Mayer K, Goedbloed M, van Zijl K, Nellist M, Rott HD. 2004. Characterisation of a novel TSC2 missense mutation in the GAP related domain associated with minimal clinical manifestations of tuberous sclerosis. J Med Genet 41:64.

Mozaffari M, Hoogeveen-Westerveld M, Kwiatkowski D, Sampson J, Ekong R, Povey S, den Dunnen JT, van den Ouweland A, Halley D, Nellist M. 2009. Identification of a region required for TSC1 stability by functional analysis of *TSC1* missense mutations found in individuals with tuberous sclerosis complex. BMC Med Genet 10:88.

Nellist M, van Slegtenhorst MA, Goedbloed M, van den Ouweland AMW, Halley DJJ, van der Sluijs P. 1999. Characterization of the cytosolic tuberin-hamartin complex: tuberin is a cytosolic chaperone for hamartin. J Biol Chem 274:35647-35652.

Nellist M, Verhaaf B, Goedbloed MA, Reuser AJJ, van den Ouweland AMW, Halley DJJ. 2001. *TSC2* missense mutations inhibit tuberin phosphorylation and prevent formation of the tuberin-hamartin complex. Hum Molec Genet 10:2889-2898.

Nellist M, Sancak O, Goedbloed MA, Rohe C, van Netten D, Mayer K, Tucker-Williams A., van den Ouweland AMW, Halley DJJ. 2005. Distinct effects of single amino acid changes to tuberin on the function of the tuberin-hamartin complex. Eur J Hum Genet 13:59-68.

Nellist M, Sancak O, Goedbloed M, Adriaans A, Wessels M, Maat-Kievit A, Baars M, Dommering C, van den Ouweland A, Halley D. 2008. Functional characterisation of the TSC1-TSC2 complex to assess multiple TSC2 variants identified in single families affected by tuberous sclerosis complex. BMC Med Genet 9:10.

Nellist M, van den Heuvel D, Schluep D, Exalto C, Goedbloed M, Maat-Kievit A, van Essen T, van Spaendonck-Zwarts K, Jansen F, Helderman P, Bartalini G, Vierimaa O, Penttinen M,

van den Ende J, van den Ouweland A, Halley D. 2009. Missense mutations to the *TSC1* gene cause tuberous sclerosis complex. Eur J Hum Genet 17:319-328.

Ng PC, Henikoff S. 2006. Predicting the effects of amino acid substitutions on protein function. Ann Rev Genomics Hum Genet 7:61-80.

Niida Y, Lawrence-Smith N, Banwell A, Hammer E, Lewis J, Beauchamp RL, Sims K, Ramesh V, Ozelius L. 1999. Analysis of both *TSC1* and *TSC2* for germline mutations in 126 unrelated patients with tuberous sclerosis. Hum Mutat 14:412-422.

O'Connor SE, Kwiatkowski DJ, Roberts PS, Wollmann RL, Huttenlocher PR. 2003. A family with seizures and minor features of tuberous sclerosis and a novel *TSC2* mutation. Neurology 61:409-412.

Qin W, Kozlowski P, Taillon BE, Bouffard P, Holmes AJ, Janne P, Camposano S, Thiele E, Franz D, Kwiatkowski DJ. 2010. Ultra deep sequencing detects a low rate of mosaic mutations in Tuberous Sclerosis Complex. Hum Genet 127:573-582.

Ramantani G, Niggemann P, Hahn G, Nake A, Fahsold R, Lee-Kirsch MA. 2008. Unusual radiological presentation of tuberous sclerosis complex with leptomeningeal angiomatosis associated with a hypomorphic mutation in the *TSC2* gene. J Child Neurol 24:333-337.

Rendtorff ND, Bjerregaard B, Frodin M, Kjaergaard S, Hove H, Skovby F, Brondum-Nielsen K, Schwartz M. 2005. Analysis of 65 tuberous sclerosis complex (TSC) patients by TSC2

DGGE, TSC1/TSC2 MLPA, and TSC1 long-range PCR sequencing, and report of 28 novel mutations. Hum Mutat 26:374-383.

Sancak O, Nellist M, Goedbloed M, Elfferich P, Wouters C, Maat-Kievit A, Zonnenberg B, Verhoef S, Halley D, van den Ouweland A. 2005 Mutational analysis of the *TSC1* and *TSC2* genes in a diagnostic setting: genotype-phenotype correlations and comparison of diagnostic DNA techniques in tuberous sclerosis complex. Eur J Hum Genet 13:731-741.

van Slegtenhorst M, de Hoogt R, Hermans C, Nellist M, Janssen B, Verhoef S, Lindhout D, van den Ouweland A, Halley D, Young J, Burley M, Jeremiah S, Woodward K, Nahmias J, Fox M, Ekong R, Wolfe J, Povey S, Osborne J, Snell RG, Cheadle JP, Jones AC, Tachataki M, Ravine D, Sampson JR, Reeve MP, Richardson P, Wilmer F, Munro C, Hawkins TL, Sepp T, Ali JBM, Ward S, Green AJ, Yates JRW, Short MP, Haines JH, Jozwiak S, Kwiatkowska J, Henske EP, Kwiatkowski DJ. 1997. Identification of the tuberous sclerosis gene *TSC1* on chromosome 9q34. Science 277: 805-808.

van Slegtenhorst M, Nellist M, Nagelkerken B, Cheadle J, Snell R, van den Ouweland A, Reuser A, Sampson J, Halley D, van der Sluijs P. 1998. Interaction between hamartin and tuberin, the *TSC1* and *TSC2* gene products. Hum Mol Genet 7:1053-1057.

Tee AR, Fingar DC, Manning BD, Kwiatkowski DJ, Cantley LC, Blenis J. 2002. Tuberous sclerosis complex-1 and -2 gene products function together to inhibit mammalian target of rapamycin (mTOR)-mediated downstream signaling. Proc Natl Acad Sci USA 99:13571-13576.

de Vries P, Howe CJ. 2007. The tuberous sclerosis complex proteins - a GRIPP on cognition and neurodevelopment. Trends Mol Med 13:319-326.

Xu L, Sterner C, Maheshwar MM, Wilson PJ, Nellist M, Short PM, Haines JL, Sampson JR, Ramesh V. 1995. Alternative splicing of the tuberous sclerosis 2 (*TSC2*) gene in human and mouse tissues. Genomics 27:475-480.

Zhang H, Cicchetti G, Onda H, Koon HB, Asrican K, Bajraszewski N, Vazquez F, Carpenter CL, Kwiatkowski DJ. 2003. Loss of *Tsc1*/*Tsc2* activates mTOR and disrupts PI3K-Akt signaling through downregulation of PDGFR. J Clin Invest 112:1223-1233.

Zhang H, Nanba E, Yamamoto T, Ninomiya H, Ohno K, Mizuguchi M, Takeshita K. 1999. Mutational analysis of *TSC1* and *TSC2* genes in Japanese patients with tuberous sclerosis complex. J Hum Genet 44:391-396.

Titles and legends to figures

Figure 1: Overview of the TSC1 and TSC2 variants analysed as part of this study. Variants are numbered as originally described [van Slegtenhorst et al., 1997; European Chromosome 16 Tuberous Sclerosis Consortium, 1993] and according to the amino acid sequences encoded by the expression constructs used in this study.

(A) TSC1 variants. The positions of the TSC1 variants analysed as part of this study are indicated relative to the coding exons (3 - 23) of the *TSC1* gene.

(B) Variants mapping to the N-terminal half of TSC2 (amino acids 1 - 900). The positions of the variants are indicated relative to exons 1 - 23 of the *TSC2* gene.

(C) Variants mapping to the C-terminal half of TSC2 (amino acids 901 - 1784). The positions of the variants are indicated relative to exons 23 - 41 of the *TSC2* gene. The alternatively spliced exons 25 and 31 are shown in grey and the position of the GAP domain, corresponding to exon 37, is shown in black. The amino acids encoded by exon 31 were not present in the TSC2 expression constructs used in this study.

Figure 2: Immunoblot analysis of TSC1 variants. Cells were transfected with expression constructs encoding TSC2, S6K and wild-type TSC1 (TSC1/TSC2/S6K), TSC2, S6K and the pathogenic L117P variant (L117P), TSC2, S6K and the TSC1 variants, TSC2 and S6K only (TSC2/S6K), TSC1 and S6K only (TSC1/S6K) or with an empty vector (control) and analysed by immunoblotting.

(A) Immunoblot showing signals for wild-type TSC2 (TSC2), wild-type TSC1 and the TSC1 variants (TSC1), total S6K (S6K) and T389-phosphorylated S6K (T389).

(B) Quantification of the TSC2 signals shown in (A), relative to the wild-type control (TSC1/TSC2/S6K).

(C) Quantification of the TSC1 signals shown in (A), relative to the wild-type control (TSC1/TSC2/S6K).

(D) Quantification of the total S6K signals shown in (A), relative to the wild-type control (TSC1/TSC2/S6K).

(E) Ratio of T389-phosphorylated S6K to total S6K in the presence of the TSC1 variants. The ratio of the signal for T389 phosphorylated S6K (T389) to the total S6K protein (S6K) was determined relative to the wild-type control (TSC1/TSC2/S6K; T389/S6K ratio = 1) for each variant shown in (A).

Figure 3: Immunoblot analysis of TSC2 variants. Cells were transfected with expression constructs encoding TSC1, S6K and wild-type TSC2 (TSC2), TSC1, S6K and the pathogenic R611Q variant (R611Q), TSC1, S6K and the TSC2 variants, or with an empty vector (control), and analysed by immunoblotting.

(A) Immunoblot showing signals for wild-type TSC2 and the TSC2 variants (TSC2), wild-type TSC1 (TSC1), total S6K (S6K) and T389-phosphorylated S6K (T389).

(B) Quantification of the TSC2 signals shown in (A), relative to the wild-type control (TSC2).

(C) Quantification of the TSC1 signals shown in (A), relative to the wild-type control (TSC2).

(D) Quantification of the total S6K signals shown in (A), relative to the wild-type control (TSC2).

(E) Ratio of T389-phosphorylated S6K to total S6K in the presence of the TSC2 variants. The ratio of the signal for T389 phosphorylated S6K (T389) to the total S6K protein (S6K) was determined relative to the wild-type control (TSC2; T389/S6K ratio = 1) for each variant shown in (A).

Figure 4.: Functional assessment of the TSC1 variants. The signals for TSC2, TSC1, total S6K (S6K) and T389-phosphorylated S6K (T389) were determined per variant, relative to the wild-type control (TSC1) in at least 4 independent transfection experiments. The mean signals are shown for each variant. Error bars represent the standard error of the mean; variants that were significantly different from the wild-type control (TSC1) are indicated with an asterisk. The signals from cells expressing exogenous TSC2 and S6K only, and no exogenous TSC1, are also shown (TSC2).

(A) Mean TSC2 signals in the presence of the TSC1 variants, relative to wild-type TSC1-TSC2 (TSC1; signal = 1).

(B) Mean signals for the TSC1 variants, relative to wild-type TSC1 (TSC1; signal =1).

(C) Mean T389/S6K ratios for the TSC1 variants, relative to wild-type TSC1-TSC2 (TSC1; ratio = 1).

(D) Mean total S6K signals in the presence of the TSC1 variants, relative to wild-type TSC1-TSC2 (TSC1; signal = 1).

Figure 5.: Functional assessment of the TSC2 variants mapping to the N-terminal half of TSC2 (amino acids 1 - 900). The signals for TSC2, TSC1, total S6K (S6K) and T389-phosphorylated S6K (T389) were determined per variant, relative to the wild-type control (TSC2) in at least 4 independent transfection experiments. The mean signals are shown for each variant. Error bars represent the standard error of the mean; variants that were significantly different from the wild-type control (TSC2) are indicated with an asterisk.

(A) Mean signals for the TSC2 variants, relative to wild-type TSC2 (TSC2; signal =1).

(B) Mean TSC1 signals in the presence of the TSC2 variants, relative to wild-type TSC1-TSC2 (TSC2; signal = 1).

(C) Mean T389/S6K ratios for the TSC2 variants, relative to wild-type TSC1-TSC2 (TSC2; ratio = 1).

(D) Mean total S6K signals in the presence of the TSC2 variants, relative to wild-type TSC1-TSC2 (TSC2; signal = 1).

Figure 6.: Functional assessment of the TSC2 variants mapping to the C-terminal half of TSC2 (amino acids 901 - 1784). The signals for TSC2, TSC1, total S6K (S6K) and T389-phosphorylated S6K (T389) were determined per variant, relative to the wild-type control (TSC2) in at least 4 independent transfection experiments. The mean signals are shown for each variant. Error bars represent the standard error of the mean; variants that were significantly different from the wild-type control (TSC2) are indicated with an asterisk.

(A) Mean signals for the TSC2 variants, relative to wild-type TSC2 (TSC2; signal =1).

(B) Mean TSC1 signals in the presence of the TSC2 variants, relative to wild-type TSC1-TSC2 (TSC2; signal = 1).

(C) Mean T389/S6K ratios for the TSC2 variants, relative to wild-type TSC1-TSC2 (TSC2; ratio = 1).

(D) Mean total S6K signals in the presence of the TSC2 variants, relative to wild-type TSC1-TSC2 (TSC2; signal = 1).

Figure 1

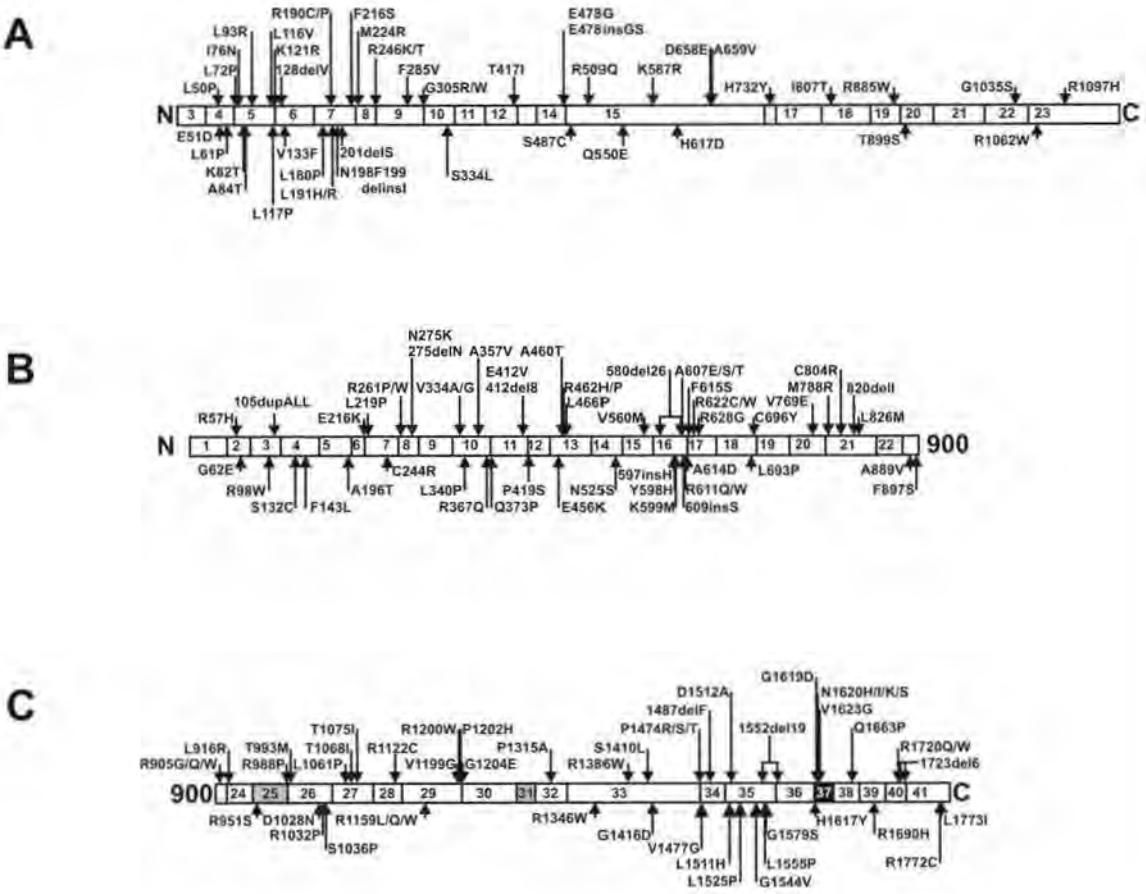

Figure 2

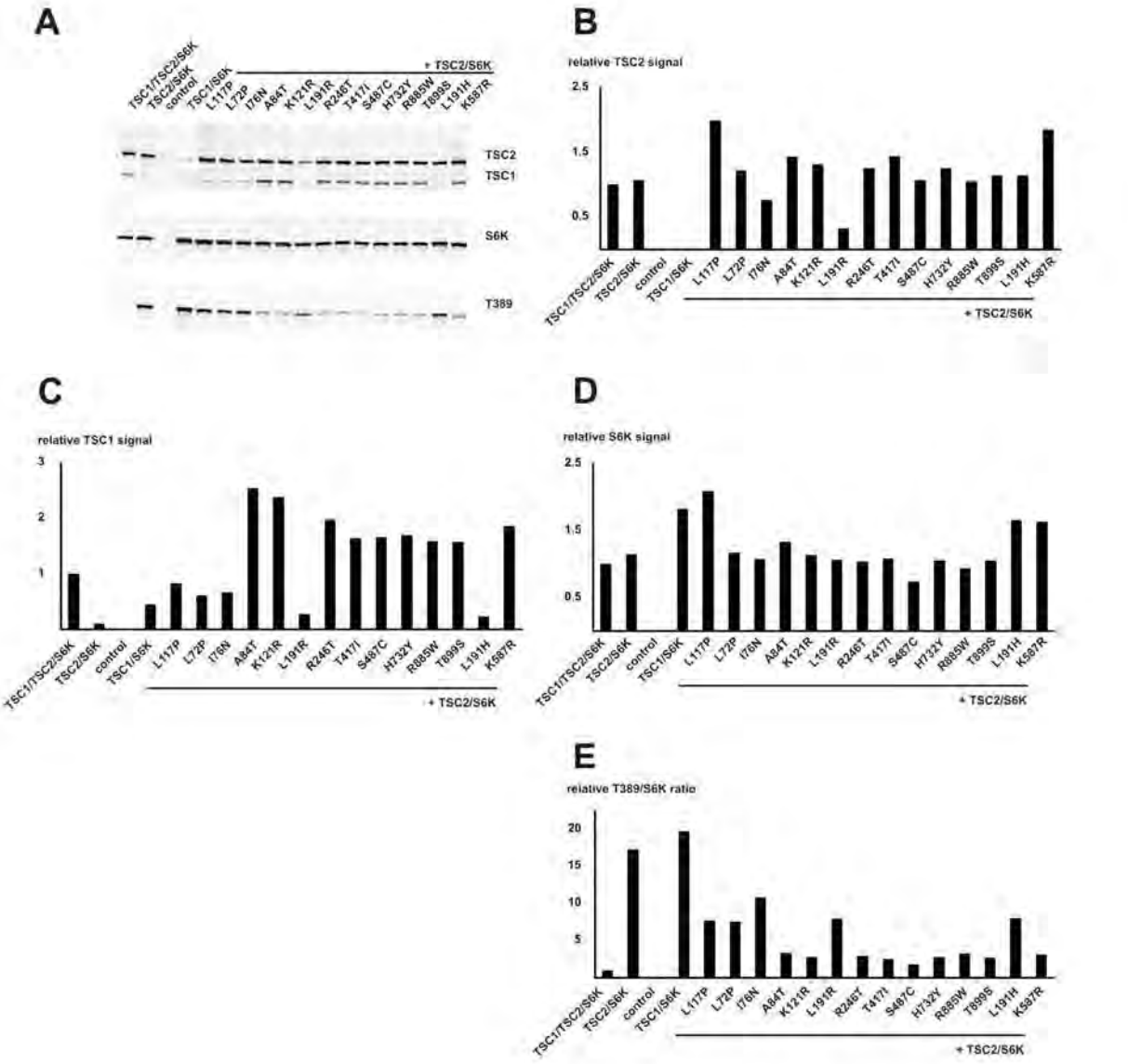
A
TSC1/TSC2/S6K
TSC2/S6K
control
TSC1/S6K
L117P
L72P
I76N
A84T
K121R
L191R
R246T
T417I
S487C
H732Y
R885W
T899S
L191H
K587R
+ TSC2/S6K
TSC2
TSC1
S6K
T389
B
relative TSC2 signal
2.5
1.5
0.5
C
relative TSC1 signal
3
2
1
D
relative S6K signal
2.5
1.5
0.5
E
relative T389/S6K ratio
20
15
10
5

Figure 3

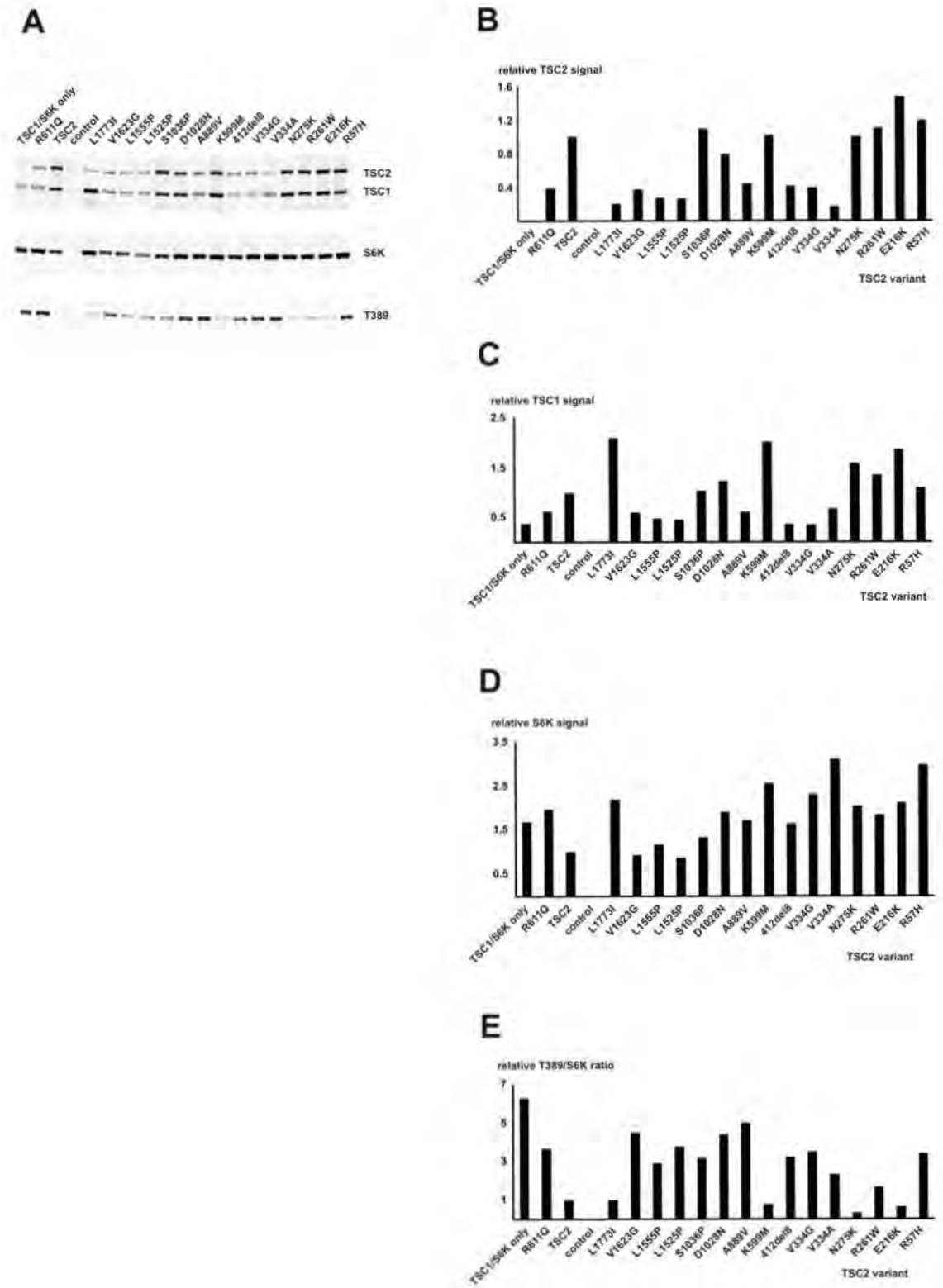
A
TSC1/S6K only
R611Q
TSC2
control
L1773I
V1623G
L1555P
L1525P
S1036P
D1028N
A889V
K599M
412del8
V334G
V334A
N275K
R261W
E216K
R57H
TSC2
TSC1
S6K
T389
B
relative TSC2 signal
1.6
1.2
0.8
0.4
TSC2 variant
C
relative TSC1 signal
2.5
1.5
0.5
TSC2 variant
D
relative S6K signal
3.5
2.5
1.5
0.5
TSC2 variant
E
relative T389/S6K ratio
7
5
3
1
TSC2 variant

Figure 4

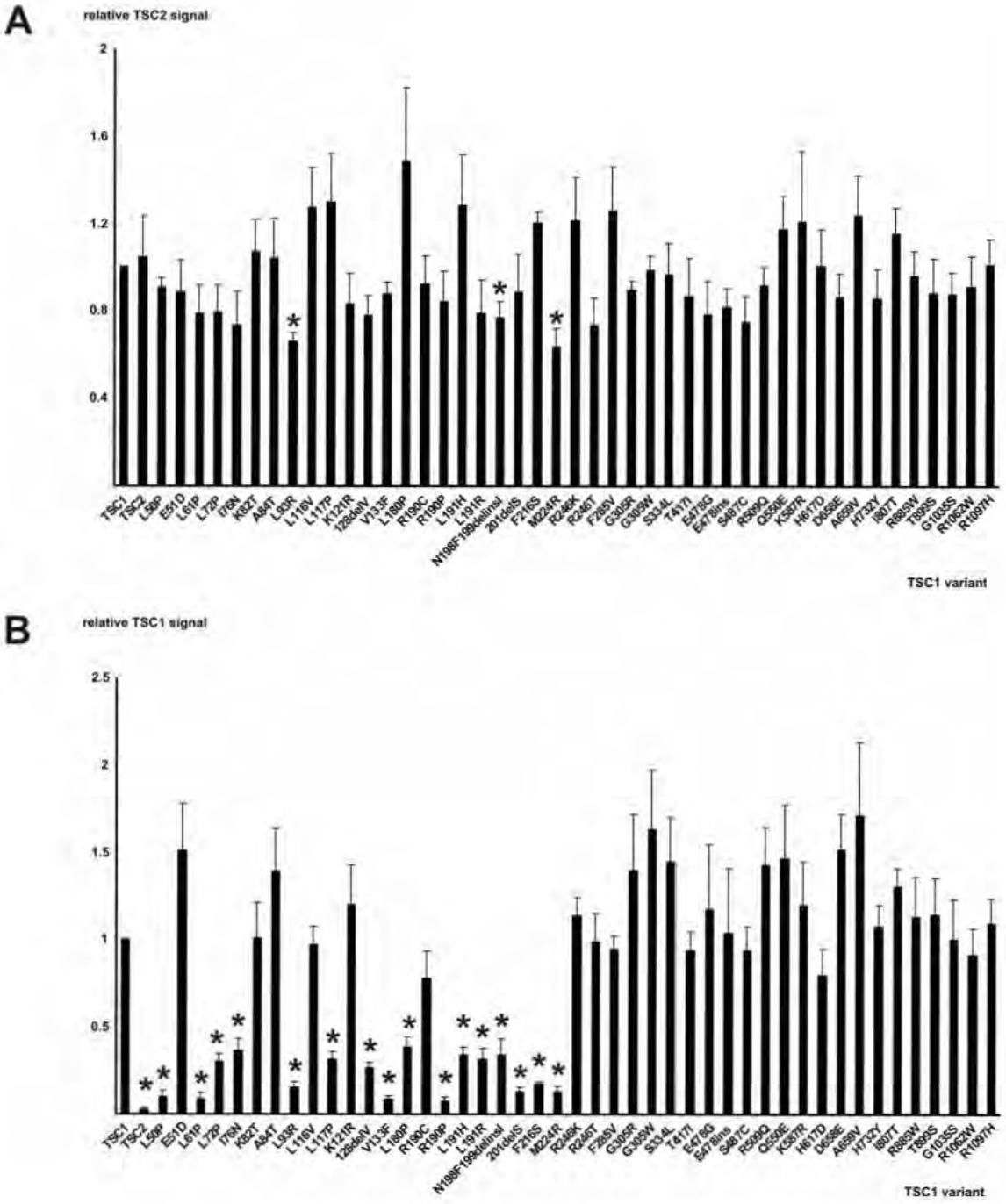
A
relative TSC2 signal
2
1.6
1.2
0.8
0.4
TSC1
TSC2
L36P
E51D
L61P
L72P
I76N
K82T
A84T
L93R
L116V
L117P
K121R
129delV
V133F
L180P
R190C
R190P
L191H
L191R
N198F199delinsI
201delS
F216S
M224R
R246K
R246T
F265V
G305R
G305W
S334L
T417I
E478G
E478ins
S487C
R509Q
Q550E
K587R
H617D
D658E
A659V
H732Y
I807T
R885W
T895S
G1035S
R1062W
R1097H
TSC1 variant
B
relative TSC1 signal
2.5
2
1.5
1
0.5
TSC1
TSC2
L36P
E51D
L61P
L72P
I76N
K82T
A84T
L93R
L116V
L117P
K121R
129delV
V133F
L180P
R190C
R190P
L191H
L191R
N198F199delinsI
201delS
F216S
M224R
R246K
R246T
F265V
G305R
G305W
S334L
T417I
E478G
E478ins
S487C
R509Q
Q550E
K587R
H617D
D658E
A659V
H732Y
I807T
R885W
T895S
G1035S
R1062W
R1097H
TSC1 variant

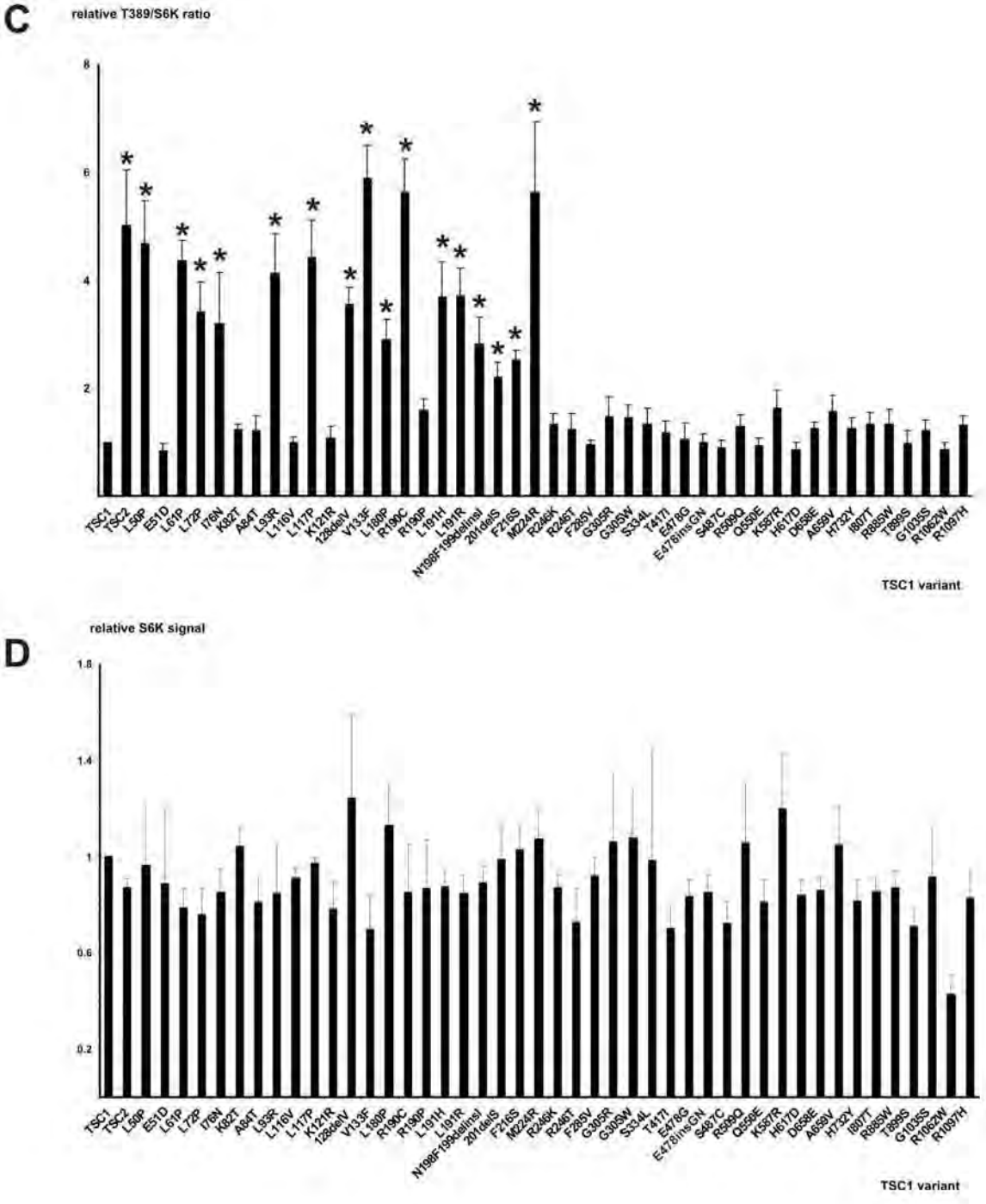
C
relative T389/S6K ratio
8
6
4
2
TSC1
TSC2
L50P
E51D
L61P
L72P
I76N
K82T
A84T
L93R
L116V
L117P
K121R
1284delV
V133F
L180P
R190C
R190P
L191H
L191R
N198F199delinsI
201delS
F216S
M224R
R246K
R246T
F285V
G305R
G305W
S334L
T417I
E478G
E478insGN
S487C
R509Q
Q556E
K587R
H617D
D658E
A659V
H732Y
I807T
R885W
T895S
G1035S
R1062W
R1097H
TSC1 variant
D
relative S6K signal
1.8
1.4
1
0.6
0.2
TSC1
TSC2
L50P
E51D
L61P
L72P
I76N
K82T
A84T
L93R
L116V
L117P
K121R
1284delV
V133F
L180P
R190C
R190P
L191H
L191R
N198F199delinsI
201delS
F216S
M224R
R246K
R246T
F285V
G305R
G305W
S334L
T417I
E478G
E478insGN
S487C
R509Q
Q556E
K587R
H617D
D658E
A659V
H732Y
I807T
R885W
T895S
G1035S
R1062W
R1097H
TSC1 variant

Figure 5

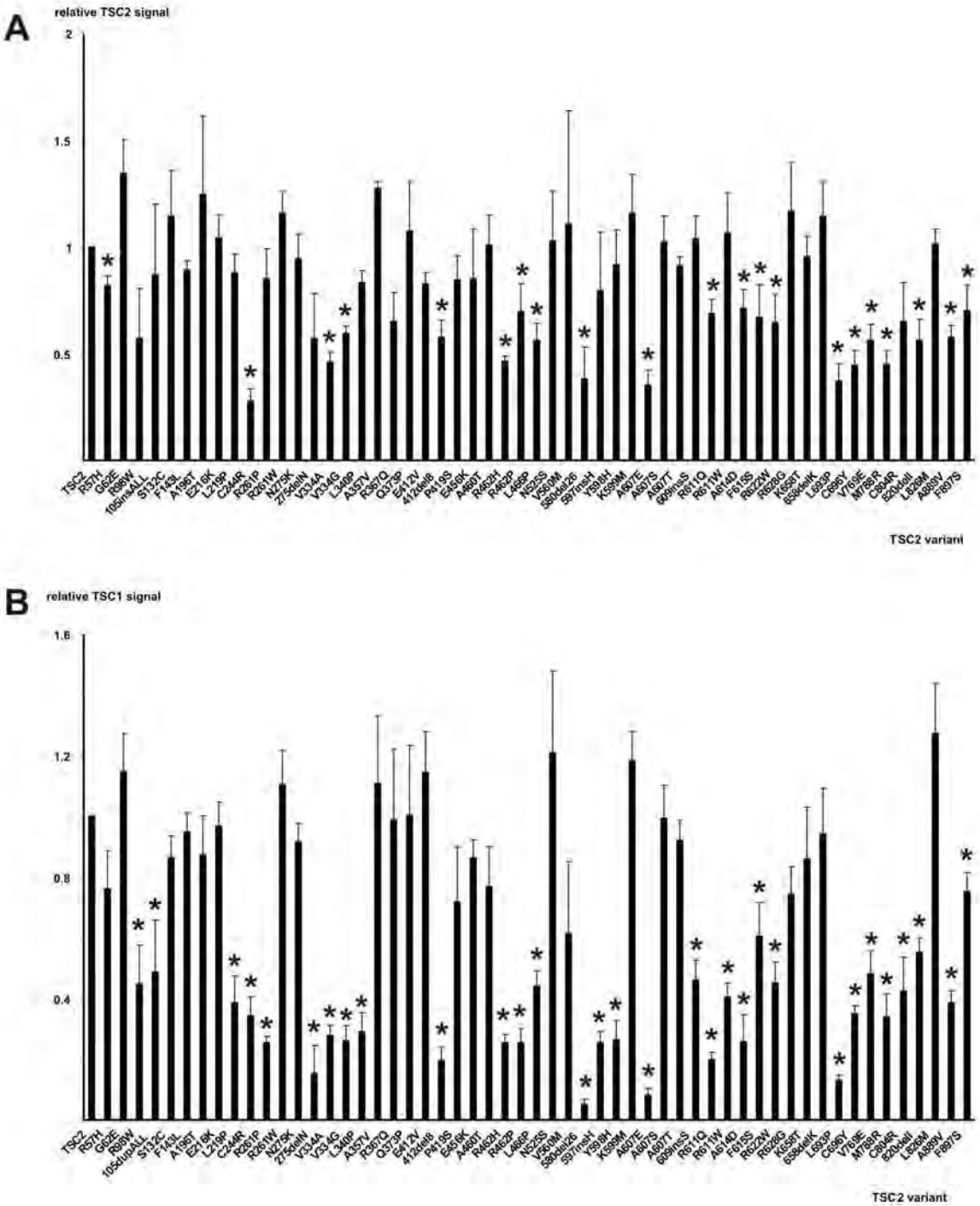
A
relative TSC2 signal
2
1.5
1
0.5
TSC2
R57H
G62E
R98W
105insALL
S132C
F143L
A196T
E216K
L219P
C244R
R261P
R261W
N275K
275delN
V334A
V334G
L340P
A357V
R367Q
Q373P
E412V
412delE
P415S
E456K
A460T
R462H
R462P
L466P
N525S
V560M
560delE26
597insH
Y598H
K599M
A607E
A607S
A607T
609insS
R611Q
R611W
A614D
F615S
R622W
R626G
K656T
656delK
L693P
C696Y
V769E
M788R
C804R
820del
L826M
A889V
F897S
TSC2 variant
B
relative TSC1 signal
1.6
1.2
0.8
0.4
TSC2 variant

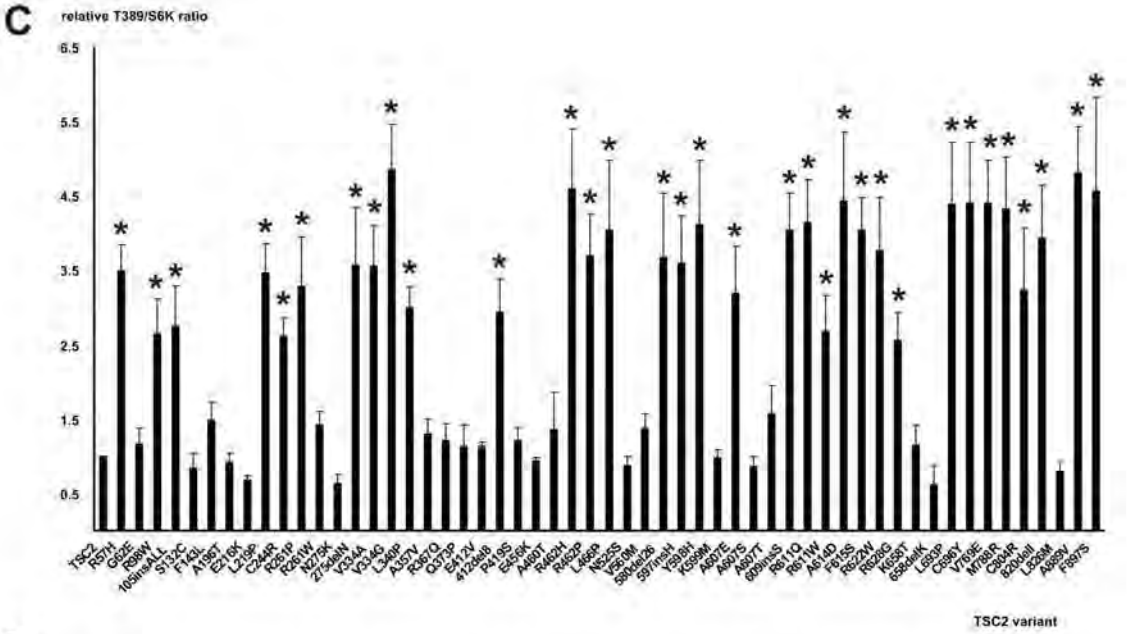
C
relative T389/S6K ratio
6.5
5.5
4.5
3.5
2.5
1.5
0.5
TSC2
R57H
G62E
R98W
105insALL
S132C
F143L
A196T
E216K
L219P
C244R
R261P
R261W
N275K
275delN
V334A
V334G
L346P
A357V
R367Q
Q373P
E412V
412delB
P419S
E456K
A469T
R462H
R462P
L466P
N525S
V560M
598del26
597insH
Y598H
K599M
A607E
A607S
A607T
669insS
R611Q
R611W
A614D
F615S
R622W
R628G
K658T
658delK
L693P
C696Y
V769E
M788R
C804R
820delI
L826M
A869V
F897S
TSC2 variant
D
relative S6K signal
1.8
1.4
1
0.6
0.2
TSC2
R57H
G62E
R98W
105dupALL
S132C
F143L
A196T
E216K
L219P
C244R
R261P
R261W
N275K
275delN
V334A
V334G
L346P
A357V
R367Q
Q373P
E412V
412delB
P419S
E456K
A469T
R462H
R462P
L466P
N525S
V560M
598del26
597insH
Y598H
K599M
A607E
A607S
A607T
669insS
R611Q
R611W
A614D
F615S
R622W
R628G
K658T
658delK
L693P
C696Y
V769E
M788R
C804R
820delI
L826M
A869V
F897S
TSC2 variant

Figure 6

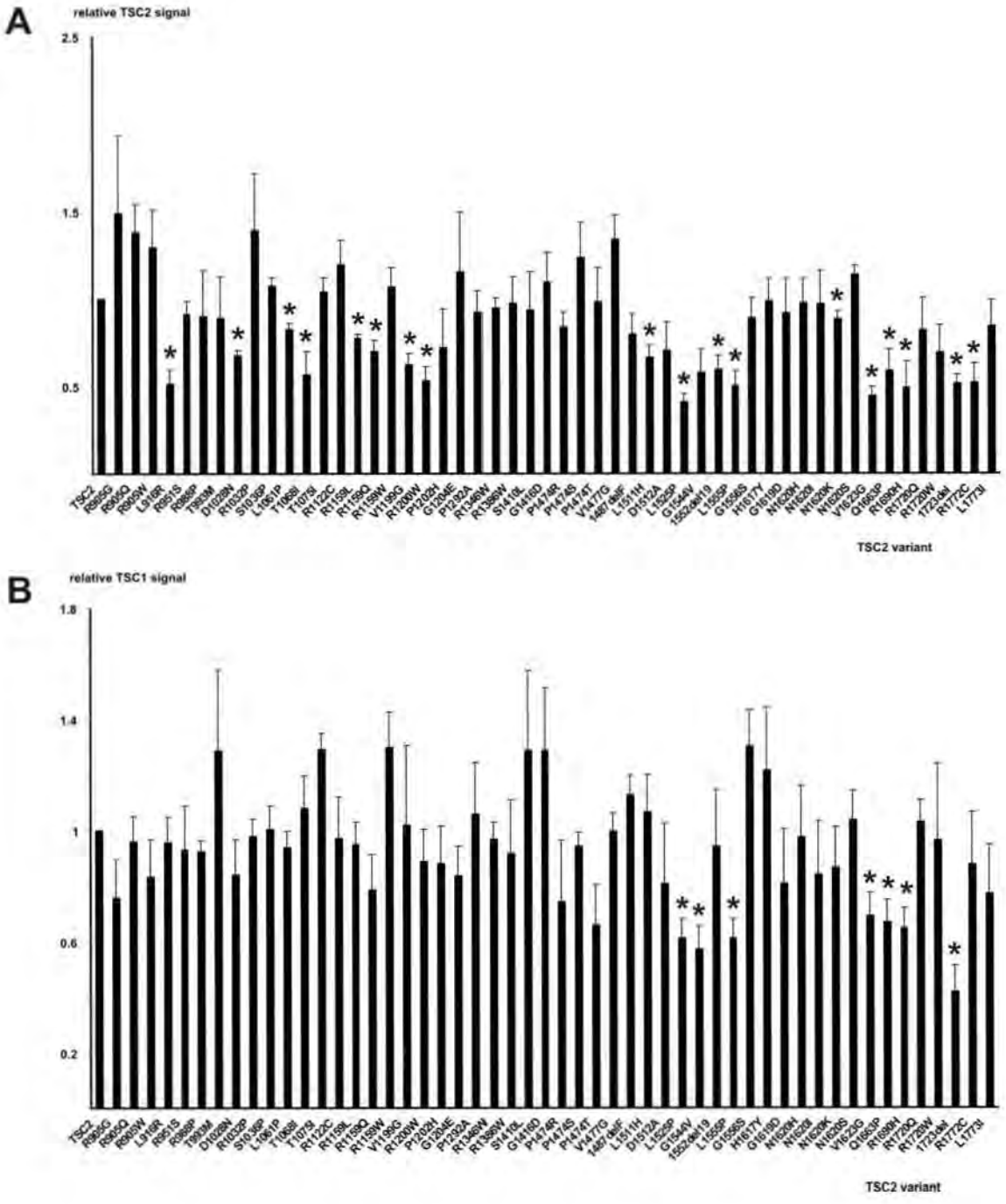
A
relative TSC2 signal
2.5
1.5
0.5
TSC2
R905G
R905Q
R905W
L916R
R951S
R968P
T990M
D1028N
R1032P
S1036P
L1061P
T1065I
T1077I
R1122C
R1159I
R1159Q
R1159W
V1199G
R1200W
P1202H
G1204E
P1232A
R1346W
R1398W
S1410L
G1416D
P1474R
P1474S
P1474T
V1477G
1487delF
L1511H
D1512A
L1522P
G1544V
1552ins19
L1555P
G1556S
H1617Y
G1619D
N1620H
N1620I
N1620K
N1620S
V1623G
Q1663P
R1690H
R1720Q
R1728W
1723delI
R1772C
L1773I
TSC2 variant
B
relative TSC1 signal
1.8
1.4
1
0.6
0.2
TSC2
R905G
R905Q
R905W
L916R
R951S
R968P
T990M
D1028N
R1032P
S1036P
L1061P
T1065I
T1077I
R1122C
R1159I
R1159Q
R1159W
V1199G
R1200W
P1202H
G1204E
P1232A
R1346W
R1398W
S1410L
G1416D
P1474R
P1474S
P1474T
V1477G
1487delF
L1511H
D1512A
L1522P
G1544V
1552ins19
L1555P
G1556S
H1617Y
G1619D
N1620H
N1620I
N1620K
N1620S
V1623G
Q1663P
R1690H
R1720Q
R1728W
1723delI
R1772C
L1773I
TSC2 variant

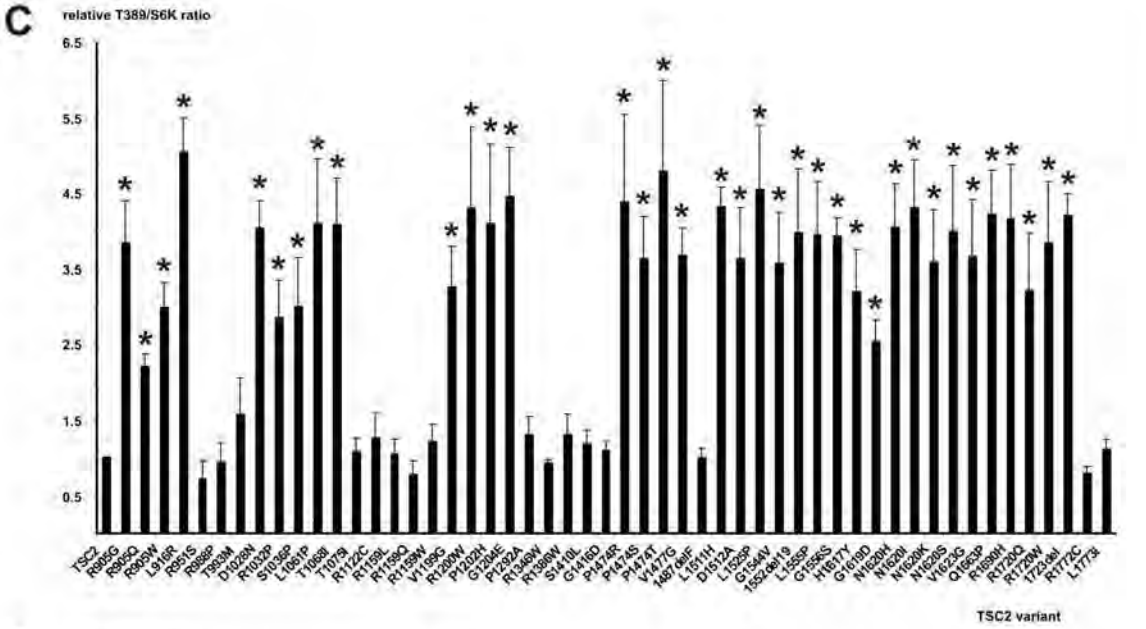
C
relative T389/S6K ratio
6.5
5.5
4.5
3.5
2.5
1.5
0.5
TSC2
R905G
R905Q
R905W
L916R
R951S
R998P
T993M
D1028N
R1032P
S1036P
L1061P
T1068I
T1075I
R1122C
R1159L
R1159Q
R1159W
V1199G
R1200W
P1202H
G1204E
P1232A
R1346W
R1386W
S1410L
G1416D
P1474R
P1474S
P1474T
V1477G
1497 delF
L1511H
D1512A
L1525P
G1544V
1552 delI19
L1555P
G1556S
H1617Y
G1619D
N1620H
N1620I
N1620K
N1620S
V1623G
Q1663P
R1698H
R1720Q
R1720W
1723delI
R1772C
L1773I
TSC2 variant
D
relative S6K signal
2
1.6
1.2
0.8
0.4
TSC2
R905G
R905Q
R905W
L916R
R951S
R998P
T993M
D1028N
R1032P
S1036P
L1061P
T1068I
T1075I
R1122C
R1159L
R1159Q
R1159W
V1199G
R1200W
P1202H
G1204E
P1232A
R1346W
R1386W
S1410L
G1416D
P1474R
P1474S
P1474T
V1477G
1497 delF
L1511H
D1512A
L1525P
G1544V
1552 delI19
L1555P
G1556S
H1617Y
G1619D
N1620H
N1620I
N1620K
N1620S
V1623G
Q1663P
R1698H
R1720Q
R1720W
1723delI
R1772C
L1773I
TSC2 variant

Table 1. *TSC1* variants.

TSC1 nucleotide changes and exon numbers are given according to the *TSC1* Leiden Open Variation Database (http://www.lovd.nl/TSC1). Nucleotide changes predicted to cause splicing defects are marked with an asterisk. Amino acid changes are numbered according to van Slegtenhorst et al., 1997. Amino acid substitutions predicted by SIFT to be tolerated (T) or not tolerated (NT) are indicated. Previously untested variants are indicated in bold.

Exon	Variant	SIFT prediction	LOVD classification	Reference/ source	Functional assessment
4	c.149T>C (p.L50P)	NT	unknown	Mozaffari et al., 2009	unstable, pathogenic
4	c.153A>C (p.E51D)	T	probably no pathogenicity	Mozaffari et al., 2009	probably neutral
4	c.182T>C (p.L61P)	NT	probably pathogenic	Mozaffari et al., 2009	unstable, pathogenic
5	**c.215T>C (p.L72P)**	**NT**	**probably pathogenic**	**Benit et al., 1999**	**unstable, pathogenic**
5	**c.227T>A (p.I76N)**	**NT**	**unknown**	**Au et al., 2007**	**unstable, pathogenic**
5	**c.245A>C (p.K82T)**	**T**	**unknown**	**Adachi et al., 2003**	**probably neutral**
5	**c.250G>A (p.A84T)**	**T**	**probably no pathogenicity**	**LOVD**	**probably neutral**
5	c.278T>G (p.L93R)	NT	probably pathogenic	Mozaffari et al., 2009	unstable, destabilising,

					pathogenic
5	**c.346T>G (p.L116V)**	**T**	**unknown**	**this study**	**probably neutral**
5	c.350T>C (p.L117P)	NT	probably pathogenic	Nellist et al., 2009	unstable, pathogenic
5	**c.362A>G* (p.K121R)**	**T**	**unknown**	**LOVD**	**probably neutral (predicted splice mutation)**
6	c.381_383delTGT* (p.128delV)	-	unknown	Nellist et al., 2009	unstable, pathogenic
6	c.397G>T (p.V133F)	NT	unknown	Mozaffari et al., 2009	unstable, pathogenic
7	c.539T>C (p.L180P)	NT	probably pathogenic	Nellist et al., 2009	unstable, pathogenic
7	c.568C>T (p.R190C)	NT	no known pathogenicity	Mozaffari et al., 2009	probably neutral
7	c.569G>C (p.R190P)	NT	unknown	Mozaffari et al., 2009	unstable, pathogenic
7	c.572T>A (p.L191H)	NT	probably pathogenic	Nellist et al., 2009	unstable, pathogenic
7	**c.572T>G (p.L191R)**	**NT**	**unknown**	**LOVD**	**unstable, pathogenic**
7	c.593_595delACT (p.N198F199delinsI)	-	probably pathogenic	Hodges et al., 2001; Mozaffari et al., 2009	unstable, destabilising, pathogenic

7	**c.602_604delCCT (p.S201del)**	**-**	**unknown**	**Hung et al., 2006**	**unstable, pathogenic**
7	**c.647T>C (p.F216S)**	**NT**	**probably no pathogenicity**	**LOVD**	**unstable, pathogenic**
8	c.671T>G (p.M224R)	NT	probably pathogenic	Nellist et al., 2009	unstable, destabilising, pathogenic
8	c.737G>A* (p.R246K)	NT	probably pathogenic	Nellist et al., 2009	probably neutral (predicted splice mutation)
8	**c.737G>C* (p.R246T)**	**NT**	**probably pathogenic**	**LOVD**	**probably neutral (predicted splice mutation)**
9	**c.853T>G (p.F285V)**	**T**	**unknown**	**this study**	**probably neutral**
9	c.913G>A* (p.G305R)	T	probably pathogenic	Nellist et al., 2009	probably neutral (predicted splice mutation)
9	c.913G>T* p.G305W	T	probably pathogenic	Nellist et al., 2009	probably neutral (predicted splice mutation)
10	c.1001C>T p.S334L	T	probably no pathogenicity	Mozaffari et al., 2009	probably neutral
12	**c.1250C>T**	**T**	**no known**	**Choi et al., 2006**	**probably neutral**

	(p.T417I)		**pathogenicity**		
14	c.1433A>G* (p.E478G)	T	unknown	Mozaffari et al., 2009	probably neutral
14	c.1433A>G* (p.E478GinsGN)	-	unknown	Mozaffari et al., 2009	probably neutral
15	**c.1460C>G (p.S487C)**	**T**	**unknown**	**this study**	**probably neutral**
15	c.1526G>A (p.R509Q)	T	probably no pathogenicity	Nellist et al., 2009	probably neutral
15	c.1648C>G (p.Q550E)	T	unknown	Mozaffari et al., 2009	probably neutral
15	**c.1760A>G (p.K587R)**	**T**	**no known pathogenicity**	**LOVD**	**probably neutral**
15	**c.1849C>G (p.H617D)**	**T**	**unknown**	**this study**	**probably neutral**
15	c.1974C>G (p.D658E)	T	probably no pathogenicity	Mozaffari et al., 2009	probably neutral
15	c.1976C>T (p.A659V)	T	probably no pathogenicity	Mozaffari et al., 2009	probably neutral
17	**c.2194C>T (p.H732Y)**	**NT**	**no known pathogenicity**	**Lugnier et al., 2009**	**probably neutral**
19	c.2420T>C (p.I807T)	T	unknown	Mozaffari et al., 2009	probably neutral
21	**c.2653C>T (p.R885W)**	**T**	**unknown**	**Au et al., 2007**	**probably neutral**

21	**c.2696C>G (p.T899S)**	**T**	**unknown**	**Zhang et al., 1999**	**probably neutral**
23	c.3103G>A (p.G1035S)	T	no known pathogenicity	Nellist et al., 2009	probably neutral
23	**c.3184C>T (p.R1062W)**	**T**	**unknown**	**Qin et al., 2010**	**probably neutral**
23	c.3290G>A (p.R1097H)	NT	probably no pathogenicity	Nellist et al., 2009	probably neutral

Table 2. *TSC2* variants (amino acids 1 - 900).

TSC2 nucleotide changes and exon numbers are given according to the *TSC2* Leiden Open Variation Database (http://www.lovd.nl/TSC2). Nucleotide changes predicted to cause splicing defects are marked with an asterisk. Amino acid changes were numbered according to European Chromosome 16 Tuberous Sclerosis Consortium, 1993. Amino acid substitutions predicted by SIFT to be tolerated (T) or not tolerated (NT) are indicated. Previously untested variants are indicated in bold.

Exon	Variant	SIFT prediction	Reference	Pathogenicity (LOVD database)	Functional assessment
2	**c.170G>A (p.R57H)**	**NT**	**this study**	**unknown**	**unstable, pathogenic**
2	c.185G>A (p.G62E)	T	Coevoets et al., 2009	unknown	probably neutral
3	c.292C>T	NT	Coevoets et	unknown	destabilising,

	(p.R98W)		al., 2009		pathogenic
3	**c.307_315dup (p.105insALL)**	**-**	**LOVD**	**unknown**	**destabilising, pathogenic**
4	c.395C>G (p.S132C)	T	Nellist et al., 2008	probably no pathogenicity	probably neutral
4	c.447C>G (p.F143L)	T	Nellist et al., 2008	probably no pathogenicity	probably neutral
5	c.586G>A (p.A196T)	T	Nellist et al., 2008	probably no pathogenicity	probably neutral
6	**c.646G>A (p.E216K)**	**T**	**this study**	**unknown**	**probably neutral**
7	**c.656T>C (p.L219P)**	**NT**	**this study**	**unknown**	**destabilising, pathogenic**
7	c.730T>C (p.C244R)	NT	Nellist et al., 2008	probably pathogenic	unstable, destabilising, pathogenic
8	**c.782G>C (p.R261P)**	**T**	**LOVD**	**probably pathogenic**	**destabilising, pathogenic**
8	**c.781C>T (p.R261W)**	**NT**	**Hodges et al., 2001**	**probably no pathogenicity**	**probably neutral**
8	**c.825C>G (p.N275K)**	**T**	**this study**	**unknown**	**probably neutral**
8	c.824_826del (p.275delN)	-	Coevoets et al., 2009	unknown	destabilising, pathogenic
10	**c.1001T>C**	**NT**	**this study**	**unknown**	**unstable,**

	(p.V334A)				**destabilising, pathogenic**
10	**c.1001T>G (p.V334G)**	**NT**	**LOVD**	**probably pathogenic**	**unstable, destabilising, pathogenic**
10	**c.1019T>C (p.L340P)**	**NT**	**this study**	**unknown**	**pathogenic**
10	**c.1070C>T (p.A357V)**	**T**	**this study**	**unknown**	**probably neutral**
10	c.1100G>A (p.R367Q)	T	Nellist et al., 2005	no known pathogenicity	probably neutral
10	c.1118A>C* (p.Q373P)	T	Coevoets et al., 2009	unknown	probably neutral (predicted splice mutation)
11	c.1235A>T* (p.E412V)	NT	Jansen et al., 2008	unknown	probably neutral (splice mutation)
11	c.1235A>T* (p.412del8)	-	Jansen et al., 2008	unknown	unstable, destabilising, pathogenic
11	**c.1255C>T* (p.P419S)**	**NT**	**Huang et al., 2008**	**probably pathogenic**	**probably neutral (predicted splice mutation)**
13	**c.1366A>G (p.E456K)**	**T**	**this study**	**unknown**	**probably neutral**
13	**c.1378G>A**	**T**	**Ramantani**	**unknown**	**probably neutral**

	(p.A460T)		**et al., 2008**		
13	**c.1385G>A (p.R462H)**	**NT**	**this study**	**unknown**	**unstable, destabilising, pathogenic**
13	**c.1385_1386delinsCT (p.R462P)**	**NT**	**this study**	**unknown**	**unstable, destabilising, pathogenic**
13	**c.1397T>C (p.L466P)**	**T**	**LOVD**	**unknown**	**unstable, destabilising, pathogenic**
14	c.1574A>G (p.N525S)	T	Nellist et al., 2005	no known pathogenicity	probably neutral
15	**c.1678G>A (p.V560M)**	**T**	**this study**	**unknown**	**probably neutralc**
16	c.1736del78 (p.580del26)	-	Coevoets et al., 2009	unknown	unstable, destabilising, pathogenic
16	c.1790insCAC (p.597insH)	-	Jansen et al., 2008	unknown	destabilising, pathogenic
16	c.1792T>C (p.Y598H)	T	Nellist et al., 2008	probably pathogenic	destabilising, pathogenic
16	c.1796A>T (p.K599M)	T	Tee et al., 2002; Nellist et al., 2005	pathogenic	probably neutral

16	c.1820C>A (p.A607E)	T	Coevoets et al., 2009	unknown	unstable, destabilising, pathogenic
16	**c.1819G>T (p.A607S)**	**T**	**this study**	**unknown**	**probably neutral**
16	**c.1819G>A (p.A607T)**	**T**	**LOVD**	**probably no pathogenicity**	**probably neutral**
16	c.1826_1828dup (p.609insS)	-	Nellist et al., 2005	pathogenic	destabilising, pathogenic
16	c.1832G>A (p.R611Q)	NT	Nellist et al., 2005	pathogenic	unstable, destabilising, pathogenic
16	c.1831C>T (p.R611W)	NT	Nellist et al., 2005	pathogenic	destabilising, pathogenic
17	c.1841C>A* (p.A614D)	T	Nellist et al., 2005	probably pathogenic	unstable, destabilising, pathogenic
17	c.1844T>C (p.F615S)	T	Nellist et al., 2005	no known pathogenicity	destabilising, pathogenic
17	**c.1864C>T (p.R622W)**	**NT**	**this study**	**unknown**	**unstable, destabilising, pathogenic**
17	**c.1882C>G* (p.R628G)**	**T**	**Au et al., 2007**	**unknown**	**destabilising, pathogenic**

18	**c.1973A>C (p.K658T)**	**T**	**this study**	**unknown**	**probably neutral**
18	**c.1972_1974del (p.658delK)**	**-**	**this study**	**no known pathogenicity**	**probably neutral**
18	**c.2078T>C (p.L693P)**	**NT**	**this study**	**unknown**	**unstable, destabilising, pathogenic**
18	c.2087G>A (p.C696Y)	NT	Nellist et al., 2005	unknown	unstable, destabilising, pathogenic
20	c.2306T>A (p.V769E)	T	Nellist et al., 2005	probably pathogenic	unstable, destabilising, pathogenic
21	**c.2363T>G (p.M788R)**	**NT**	**LOVD**	**probably pathogenic**	**unstable, destabilising, pathogenic**
21	**c.2410T>C (p.C804R)**	**NT**	**LOVD**	**probably pathogenic**	**destabilising, pathogenic**
21	c.2458_2460del (p.820delI)	-	Nellist et al., 2008	pathogenic	unstable, destabilising, pathogenic
21	c.2476C>A (p.L826M)	NT	Nellist et al., 2005	no known pathogenicity	probably neutral
23	**c.2666C>T (p.A889V)**	**NT**	**LOVD**	**probably pathogenic**	**unstable, destabilising,**

					pathogenic
23	**c.2690T>C (p.F897S)**	**NT**	**Rendtorff et al., 2005**	**probably pathogenic**	**unstable, destabilising, pathogenic**

Table 3. *TSC2* variants (amino acids 900 - 1807).

TSC2 nucleotide changes and exon numbers are given according to the *TSC2* Leiden Open Variation Database (http://www.lovd.nl/TSC2). Nucleotide changes predicted to cause splicing defects are marked with an asterisk. Amino acid changes were numbered according to the sequence of the wild-type TSC2 expression construct [European Chromosome 16 Tuberous Sclerosis Consortium, 1993]. Amino acid changes according to the *TSC2* Leiden Open Variation Database are also given, where this differs from the original sequence due to the inclusion of 23 amino acids encoded by the alternatively spliced exon 31. Amino acid substitutions predicted by SIFT to be tolerated (T) or not tolerated (NT) are indicated. Previously untested variants are indicated in bold.

Exon	**Variant**	**SIFT prediction**	**Reference**	**Pathogenicity (LOVD database)**	**Functional assessment**
23	c.2713C>G (p.R905G)	NT	Jansen et al. 2006	probably pathogenic	pathogenic
23	c.2714G>A (p.R905Q)	NT	Jansen et al. 2006	pathogenic	pathogenic

23	c.2713C>T (p.R905W)	NT	Jansen et al. 2006	pathogenic	pathogenic
24	c.2765T>G (p.L916R)	NT	Jansen et al., 2008	probably pathogenic	unstable, pathogenic
25	**c.2853A>T (p.R951S)**	**T**	**this study**	**probably pathogenic**	**probably neutral**
25	**c.2963G>C (p.R988P)**	**T**	**this study**	**unknown**	**probably neutral**
26	c.2978C>T (p.T993M)	T	Nellist et al., 2008	probably no pathogenicity	probably neutral
26	**c.3082G>A (p.D1028N)**	**NT**	**this study**	**unknown**	**unstable, pathogenic**
26	**c.3095G>C (p.R1032P)**	**NT**	**this study**	**probably pathogenic**	**pathogenic**
26	**c.3106T>C (p.S1036P)**	**NT**	**O'Connor et al., 2003**	**probably pathogenic**	**pathogenic**
27	**c.3182T>C (p.L1061P)**	**NT**	**this study**	**unknown**	**unstable, pathogenic**
27	c.3203C>A (p.T1068I)	NT	Coevoets et al., 2009	unknown	pathogenic
27	c.3224C>T (p.T1075I)	NT	Coevoets et al., 2009	unknown	probably neutral
28	**c.3382C>T (p.R1122C)**	**T**	**this study**	**unknown**	**probably neutral**
29	**c.3476G>T**	**T**	**LOVD**	**unknown**	**unstable,**

	(p.R1159L)				**probably neutral**
29	**c.3476G>A (p.R1159Q)**	**T**	**LOVD**	**no known pathogenicity**	**unstable, probably neutral**
29	**c.3475C>T (p.R1159W)**	**T**	**LOVD**	**unknown**	**probably neutral**
29	c.3596T>G (p.V1199G)	T	Coevoets et al., 2009	unknown	unstable, pathogenic
29	**c.3598C>T (p.R1200W)**	**NT**	**LOVD**	**pathogenic**	**unstable, pathogenic**
29	**c.3605C>A (p.P1202H)**	**T**	**this study**	**unknown**	**pathogenic**
30	**c.3611G>A* (p.G1204E)**	**NT**	**LOVD**	**probably pathogenic**	**pathogenic**
32	c.3943C>G (p.P1315A/ P1292A)	T	Coevoets et al., 2009	unknown	probably neutral
33	**c.4105C>T (p.R1369W/ R1346W)**	**T**	**LOVD**	**probably no pathogenicity**	**probably neutral**
33	**c.4225C>T (p.R1409W/ R1386W)**	**T**	**LOVD**	**no known pathogenicity**	**probably neutral**
33	c.4298C>T (p.S1433L/ S1410L)	T	Coevoets et al., 2009	unknown	probably neutral
33	c.4316G>A	T	Coevoets et	unknown	probably neutral

	(p.G1439D/G1416D)		al., 2009		
33	**c.4490C>G (p.P1497R/P1474R)**	**NT**	**LOVD**	**pathogenic**	**pathogenic**
33	**c.4489C>T (p.P1497S/P1474S)**	**T**	**this study**	**unknown**	**pathogenic**
33	**c.4489C>A (p.P1497T/P1474T)**	**NT**	**LOVD**	**probably pathogenic**	**pathogenic**
34	**c.4499T>G (p.V1500G/V1477G)**	**T**	**LOVD**	**probably pathogenic**	**pathogenic**
34	**c.4525_4527del (p.1510delF/ 1487delF)**	**-**	**LOVD**	**no known pathogenicity**	**probably neutral**
35	c.4601T>A p.L1534H/L1511H)	NT	Nellist et al., 2008	probably pathogenic	unstable, pathogenic
35	c.4604A>C (p.D1535A/D1512A)	NT	Coevoets et al., 2009	unknown	pathogenic
35	**c.4643T>C (p.L1548P/L1525P)**	**NT**	**this study**	**unknown**	**unstable, destabilising, pathogenic**
36	c.4700G>T (p.G1567V /G1544V)	NT	Coevoets et al., 2009	unknown	destabilising, pathogenic
36	c.4726_4783del (p.1575del19/ 1552del19)	-	Coevoets et al., 2009	unknown	unstable, pathogenic

36	**c.4733T>C (p.L1578P/L1555P)**	**NT**	**LOVD**	**probably pathogenic**	**unstable, destabilising, pathogenic**
36	c.4735G>A (p.G1579S/G1556S)	NT	Nellist et al., 2005	probably pathogenic	pathogenic
37	c.4918C>T (p.H1640Y/H1617Y)	NT	Coevoets et al., 2009	unknown	pathogenic
37	**c.4925G>A (p.G1642D/G1619D)**	**NT**	**this study**	**unknown**	**pathogenic**
37	**c.4927A>C (p.N1643H/N1620H)**	**NT**	**this study**	**unknown**	**pathogenic**
37	**c.4928A>T (p.N1643I/N1620I)**	**NT**	**LOVD**	**probably pathogenic**	**pathogenic**
37	**c.4929C>G (p.N1643K/N1620K)**	**NT**	**LOVD**	**probably pathogenic**	**unstable, pathogenic**
37	**c.4928A>G (p.N1643S/N1620S)**	**NT**	**this study**	**unknown**	**pathogenic**
37	c.4937T>G (p.V1646G/V1623G)	NT	Coevoets et al., 2009	unknown	unstable, destabilising, pathogenic
38	**c.5057A>C (p.Q1686P/Q1663P)**	**T**	**this study**	**unknown**	**unstable, destabilising, pathogenic**
39	**c.5138G>A (p.R1713H/R1690H)**	**NT**	**LOVD**	**unknown**	**unstable, destabilising,**

					pathogenic
40	c.5228G>A (p.R1743Q/R1720Q)	NT	Coevoets et al., 2009	pathogenic	pathogenic
40	c.5227C>T (p.R1743W/ R1720W)	NT	Coevoets et al., 2009	pathogenic	pathogenic
40	**c.5238_5255del (p.1746del6/ 1723del6)**	**-**	**LOVD**	**pathogenic**	**unstable, destabilising, pathogenic**
41	c.5383C>T (p.R1795C/R1772C)	NT	Nellist et al., 2008	no known pathogenicity	probably neutral
41	**c.5386C>A (p.L1796I/L1773I)**	**T**	**LOVD**	**probably pathogenic**	**probably neutral**

Supplemental Figure

SIFT analysis of TSC2. The TSC2 amino acid sequence from the *TSC2* Leiden Open Variation Database was analysed using the SIFT algorithm [Ng and Henikoff, 2006]. The number of tolerated and not tolerated substitutions was determined for each amino acid residue. In the figure each amino acid position is represented by a box. Solid green boxes represent positions that are completely tolerant (all substitutions possible, according to SIFT); open green boxes represent positions where 1 or 2 substitutions are not tolerated. Solid red boxes represent intolerant positions (no substitutions tolerated); open red boxes represent positions where 3 or fewer substitutions are tolerated. Empty boxes represent positions where between 3 and 17 substitutions are tolerated.

TSC2 SIFT analysis

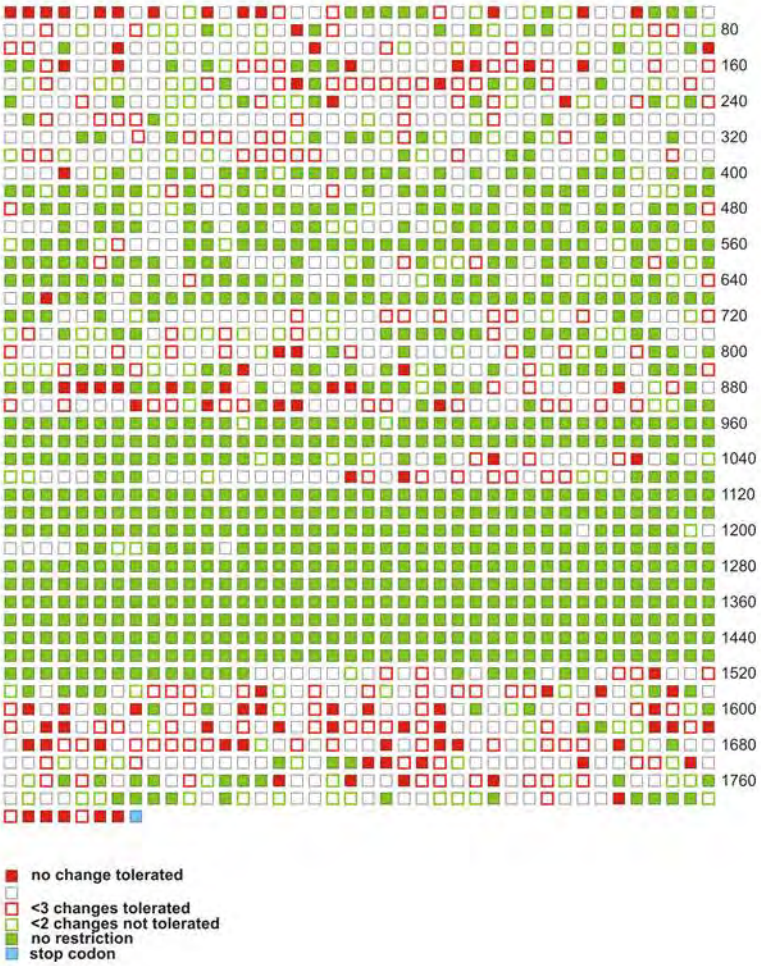

Appendix 2:

Title page:

Unclassified *TSC2* variants associated with bilateral, sporadic angiomyolipoma

Karin Diderich[1,3], Marianne Hoogeveen-Westerveld[1], Ans van den Ouweland[1], Dicky Halley[1], Michael den Bakker[2], Mark Nellist[1] and Anja Wagner[1]

[1] Department of Clinical Genetics, Erasmus Medical Centre, Rotterdam, The Netherlands.

[2] Department of Pathology, Erasmus Medical Centre, Rotterdam, The Netherlands.

[3] To whom correspondence should be addressed: Dr. Karin Diderich, Department of Clinical Genetics, Erasmus Medical Centre, Westzeedijk 112, 3016 AH Rotterdam, The Netherlands, Tel: +31 10 7036915; Fax: +31 10 7043072; email: k.diderich@erasmusmc.nl

Running title: TSC2 variants in angiomyolipoma

Abstract

Angiomyolipomas (AMLs) are classified as PEComas, neoplasms characterised by perivascular epithelioid cell differentiation. AMLs show a marked female predominance, immunoreactivity for melanocytic and smooth muscle markers and occur predominantly in the kidneys, liver and lungs. Renal AML is highly associated with tuberous sclerosis complex (TSC), an autosomal dominant disorder caused by inactivating mutations in either the *TSC1* or *TSC2* gene, and both sporadic and TSC-associated renal AMLs show loss of heterozygosity at the *TSC1* or *TSC2* locus. Here we report on an individual with bilateral, sporadic AMLs, without other clinical signs of TSC, who carries 2 unclassified variants in the *TSC2* gene.

Keywords: angiomyolipoma, loss of heterozygosity, TSC2

Introduction

Angiomyolipoma (AML) consists of various mesenchymal components, including blood vessels, smooth muscle, epithelioid cells and adipose tissue. AMLs show a marked female predominance, immunoreactivity for melanocytic and smooth muscle markers and, along with lymphangiomyomatosis and clear cell 'sugar' tumour of the lung, are classified as PEComas, tumours that show perivascular epithelioid cell differentiation [Hornick and Fletcher, 2006]. Most AML are single, sporadic lesions; multiple AML are rare and can be associated with several different diseases including Klippel-Trenauney-Weber syndrome, multiple endocrine neoplasia (MEN) type 1, Cowden's disease and tuberous sclerosis complex (TSC) [Carter et al., 1995; Dong et al., 1997; Eng, 2000].

TSC is an autosomal dominant disorder characterised by the development of hamartomas in a variety of organs and tissues [Gomez et al., 1999] TSC is caused by inactivating mutations in either the *TSC1* gene on chromosome 9q34 [van Slegtenhorst et al., 1997], or the *TSC2* gene on chromosome 16p13.3 [European Consortium, 1993]. The *TSC1* and *TSC2* gene products, TSC1 and TSC2, interact to form a stable protein complex that inhibits the target of rapamycin complex 1 (TORC1) [Inoki and Guan 2009]. Inactivation of the TSC1-TSC2 complex results in increased TORC1 activity, increased phosphorylation of TORC1 targets including p70 S6 kinase (S6K) and 4E-BP1, and increased protein synthesis and cell growth.

Renal AMLs occur frequently in the TSC patient population [Rakowski et al., 2006]. TSC-associated AMLs often show activated TORC1 signalling [Kenerson et al., 2007] as well as loss of heterozygosity (LOH) at either the *TSC1* or *TSC2* locus [Niida et al., 2001]. LOH at the *TSC2* locus has also been demonstrated in sporadic renal AMLs [Henske et al., 1995], suggesting that genetic alterations in *TSC1* and *TSC2* may play a more general role in the pathogenesis of these lesions. One possibility is that specific *TSC1* and *TSC2* variants,

functionally distinct from the inactivating mutations found in TSC patients, may be sufficient to predispose individuals to developing AMLs. *TSC2* variants that affect *TSC2* gene expression, but are insufficient to cause TSC have been described [Roberts et al., 2003].

Here we describe the genetic and immunohistochemical investigation of a female without signs of TSC but with bilateral renal AMLs, renal cysts and AML and focal nodular hyperplasia of the liver. Two rare *TSC2* variants were identified in the proband. The possible roles of these variants in AML pathogenesis are discussed.

Materials and Methods

Tissue samples

Formalin-fixed, paraffin-embedded samples of the AML were prepared according to standard procedures. DNA was isolated from both a buccal swab and peripheral blood using standard techniques.

Chemicals and reagents

Antibodies were purchased from Cell Signaling Technology (Beverly, U.S.A.) unless stated otherwise. Secondary antibodies for Western blot experiments were obtained from Li-Cor Biosciences (Lincoln, U.S.A.). Other chemicals were from Sigma-Aldrich (St. Louis, U.S.A.), unless stated otherwise.

Immunohistochemistry

Five micrometer tissue sections on glass slides were deparaffinized and rehydrated prior to antigen retrieval and quenching of endogenous peroxidase activity, as described previously [Bakker et al., 2000]. Sections were incubated with primary antibodies overnight at 4^{o}C, followed by a 3-step streptavidin-biotin based detection kit (Zymed Laboratories, San

Fransisco, U.S.A.). Slides were counterstained with haemotoxylin, dehydrated and mounted using Entellan (Electron Microscopy Sciences, Hatfield, U.S.A.), prior to examination under an Olympus BX40 microscope.

Loss of heterozygosity analysis

Genomic DNA was isolated from serial 20 micrometer sections of the paraffin-embedded tumour material as described [van Beers et al. 2006]. DNA concentration and quality were determined by spectrophotometry and agarose gel electrophoresis. Exon-specific PCR amplification, followed by sequencing was performed as previously described [Sancak et al., 2005] using 20 ng template DNA.

Functional analysis of TSC2 variants

Expression constructs encoding TSC2 variants were derived by site-directed mutagenesis (QuikChange, Stratagene, La Jolla, U.S.A.), or have been described previously [Nellist et al., 2005]. In each case, the complete open reading frame of the new construct was verified by sequence analysis.

To investigate the ability of the variants to inhibit TORC1 signalling, HEK 293T cells were transfected with a 4:2:1 mixture of TSC1, TSC2 and S6K expression constructs, as described previously [Coevoets et al., 2009]. The following day the cells were harvested and analysed by immunoblotting.

To analyse the ability of the TSC2 variants to form a stable TSC1-TSC2 complex, coimmunoprecipitation was performed. HEK 293T cells were transfected with a 1:1 mixture of TSC2 and myc-tagged TSC1 expression constructs and lysed, 24 hours later, in 50 mM HEPES pH 7.5, 10% glycerol, 1 mM DTT, 100 mM NaCl, 10 mM NaF, 50 mM β-glycerophosphate and 0.1% Triton X-100 plus Complete protease inhibitor cocktail (Roche

Molecular Biochemicals, Woerden, The Netherlands). After centrifugation (10 000 g, 10 minutes, 4^{o}C), TSC1-TSC2 complexes were immunoprecipitated from the supernatant fraction by gentle mixing with anti-myc immunoaffinity beads (Sigma-Aldrich) for 90 minutes at 4^{o}C. After 3 washes with a 20-fold excess of lysis buffer, the immunoprecipitates were analysed by Western blotting, as described previously [Coevoets et al., 2009].

Results

Patient clincal and genetic investigations

The 34-year old proband presented with abdominal pain and was referred for classification of a liver tumour seen on an abdominal CT scan. Further imaging revealed an AML (maximal diameter 40 mm) and two focal nodal hyperplasias in the liver, a small AML (maximal diameter 9 mm) in the right kidney and a large AML (maximal diameter 81 mm) in the left kidney. A partial left nephrectomy was performed and tumour pathology confirmed the diagnosis AML. The proband had a normal head circumference meaning Cowden's disease was unlikely [ref] and no signs suggestive of Klippel-Trenauney-Weber syndrome were found.

There was no family history of TSC and no signs of the disease in the proband, apart from the AMLs. Dermatological, neurological, opthalmological, cardiac and dental investigations revealed no signs of TSC. In addition, imaging showed no lymphangioleiomyomatosis in the lungs nor focal lesions in the brain. Nevertheless, mutation screening of the *TSC1* and *TSC2* genes was performed. Two *TSC2* variants of uncertain clinical significance were identified in the proband, a *TSC2* 1088C-T (A357V) missense variant in exon 10 and an insertion in intron 38, *TSC2* 5069-47ins34. As shown in Figure 1, the proband inherited the 1088T allele from her father, and the 5069-47ins34 allele from her mother. No other variants were identified in either *TSC2* or *TSC1*. To exclude MEN type 1,

mutation analysis was performed on the *CDKN1B* gene [Georgitsi et al., 2007]. No variants were identified.

Immunohistochemistry

Haemotoxylin-eosin staining revealed abundant fat cells, and characteristic areas of smooth muscle-like cells. Very little normal appearing tissue was visible in the sections examined. Sections of the kidney AML showed regions of HMB-45 positivity, confirming the classification of the tumour as a PEComa (data not shown).

Most cells were robustly positive for S6 and AKT (Figure 2), and were also clearly positive for S6 phosphorylated at the S235/236 position, AKT phosphorylated at either T308 or S473, and S6K phosphorylated at the T389 hydrophobic motif (Figure 2). It was not possible to determine whether the observed staining was increased relative to the normal kidney tissue in this individual as there was no normal kidney tissue in the available paraffin-embedded material. Nevertheless, the strong staining for phosphorylated S6K and S6 indicated that TORC1 signalling was active in the resected AML tissue. Consistent with previous results [Kenerson et al., 2007], we detected phosphorylated AKT in the resected tumour. However, we were unable to determine whether this was reduced compared to the surrounding normal kidney tissue.

Loss of heterozygosity (LOH)

LOH at the *TSC2* locus has been demonstrated in sporadic and TSC-associated AMLs [Niida et al., 2001]. The presence of 2 genetic variants in the probands' *TSC2* gene allowed us to test directly whether LOH had occurred at the *TSC2* locus in the resected, paraffin-embedded AML tissue. We compared sequence reads of *TSC2* exon 10 and exons 38/39 from genomic DNA isolated from leukocytes, with the reads derived from the tumour DNA. In all

cases, comparison of the heterozygous peaks indicated that in the tumour DNA there was a comparative loss of the 1088C (wild-type) - 5069-47ins34 haplotype, inherited from the proband's mother, compared to the 1088T - 5069 (wild-type) haplotype inherited from the father (Figures 1 and 3). The demonstration of LOH in the tumour DNA was consistent with the inactivation of the *TSC2* gene playing an important role in the pathogenesis of the proband's AML. Furthermore, the loss of the mother's allele indicated that the copy of chromosome 16 inherited from the father harboured the variant predisoposing to AML. One possibility was that the *TSC2* 1088C-T (A3576V) missense change was the predisposing allele. Therefore, we investigated whether the ability of the TSC2 A357V missense variant to inhibit TORC1 activity was impaired, as has been demonstrated for TSC2 variants associated with TSC [Nellist et al., 2005]. We used the SIFT algorithm [Ng and Henikoff, 2006] to determine whether the A357V substitution was likely to affect TSC2 function, and performed coimmunoprecipitation and Western blotting to investigate whether the A357V variant was able to bind TSC1 and to inhibit TORC1 signalling. The results of this analysis are shown in Figure 4. SIFT predicted that the A - V substitution would be tolerated by TSC2, and was therefore unlikely to affect the protein's function. Furthermore, using 3 different splice prediction programs (NetGene2 Server, www.cbs.dtu.dk/services/NetGene2; BDGP: Splice Site Prediction by Neural Network, www.fruitfly.org/seq_tools/splice.html; and Splice Site Finder, www.genet.sickkids.on.ca/~ali/ splicesitefinder.html], no effect of the nucleotide change on *TSC2* mRNA splicing was predicted (data not shown). Expression of the TSC2 A357V variant in HEK 293T cells inhibited S6K-T389 phosphorylation (as a read-out for TORC1 activity) as effectively as wild-type TSC2, and significantly better than a known TSC2 pathogenic variant, R611Q (Figure 4). No differences in TSC1-TSC2 binding were observed between wild-type TSC2 and the A357V variant (Figure 4).

Consistent with the lack of TSC-associated lesions in both the proband (except for the AMLs) and her father, the TSC2 A357V variant was still able to inhibit TORC1 activity. Therefore, although we could find no evidence that the A357V substitution affected TSC2 activity, the possibility that the A357V variant is associated with AML could not be excluded.

Discussion

The close association between AMLs and TSC is well-established. Genetic alterations at the *TSC1* and *TSC2* loci and up-regulation of TORC1 signalling in AML tumour tissue indicates that the active TSC1-TSC2 complex plays an important role in preventing the pathogenesis of these lesions.

Here we describe a patient with bilateral AMLs. HMB-45 positivity in the tumour tissue confirmed that the lesions were AMLs, and the detection of activated components of the TORC1 signalling cascade in the tumour tissue was consistent with the dysregulation of this pathway contributing to the pathogenesis of the lesions [Kenerson et al., 2007]. Because bilateral AMLs are associated with TSC [Rakowski et al., 2006], TSC was considered as a diagnosis for the patient. However, no other clinical signs of TSC were identified and no clear inactivating mutation was identified in either the *TSC1* or *TSC2* gene. Interestingly however, 2 rare *TSC2* variants were identified in the probands' DNA and in DNA from her parents.

The *TSC2* 5069-47ins34 variant was inherited by the proband from her mother. In most individuals, the last 18 nucleotides of exon 38 and the beginning of intron 38 consist of 2.3 copies of a 34 base pair repeat sequence (Figure 3). In some individuals one copy of the repeat is deleted (*TSC2* 5051+16del34; Tuberous sclerosis database - Leiden Open Variation Database, http://www.lovd.nl/TSC2), resulting in reduced *TSC2* mRNA expression [Roberts et al., 2003]. An extra copy of the repeat, as found here, has also been described previously

[Roberts et al., 2003](Tuberous sclerosis database - Leiden Open Variation Database, http://www.lovd.nl/TSC2). However, it is not known whether the insertion of an extra copy of the repeat affects *TSC2* mRNA expression. Unfortunately, no RNA from the proband or her mother was available for testing. LOH analysis of the proband's tumour DNA showed that this allele was lost in the AML tissue, suggesting that it is unlikely to predispose to AML.

The *TSC2*1088C-T (A357V) missense change was inherited from the proband's father and was retained in the tumour DNA. It is therefore possible that this variant is either the predisposing allele, or is in close proximity to it. The fact that the father carries the allele, but has not (yet) developed AML can be explained by the observation that sporadic AMLs show a strong female bias [Hornick and Fletcher, 2006] and that sex hormones play an important role in the initiation and/or progression of these lesions. Any effect of the A357V substitution on the activity of the TSC1-TSC2 complex is likely to be mild, since the proband had no signs of TSC apart from the AMLs and renal cysts, and no effect on TSC1-TSC2 function was detected *in vitro*. We could not exclude the possibility that the AMLs are caused by another, undetected *TSC2* variant, or a variant within another gene close to the *TSC2* locus.

Summary

Here we describe the genetic and immunohistochemical investigation of a female with bilateral renal AMLs and AML of the liver, but without a history of TSC. HMB-45 positivity in the tumour tissue, as detected by immunohistochemistry, confirmed that the tumours were AMLs. Furthermore, the demonstration of activated components of the AKT-TORC1 signalling cascade in the tumour cells was consistent with the dysregulation of this pathway contributing to the pathogenesis of these lesions.

Genetic analysis revealed 2 rare *TSC2* variants, *TSC2* 5069-47ins34 and *TSC2*1088C-T (A357V). The *TSC2* 5069-47ins34 variant was inherited from the proband's mother and was

lost from the genomic DNA isolated from the AML. In contrast, the *TSC2*1088C-T (A357V) variant was retained in the tumour DNA, suggesting that the A357V substitution may predispose to the development of AMLs. Consistent with the lack of any further clinical signs of TSC in either the proband or her father, no differences in activity between the TSC2 A357V variant and wild-type TSC2 could be detected.

Acknowledgments

Financial support was provided by the U.S. Department of Defense Congressionally-Directed Medical Research Program (grant #TS060052). The authors report no conflicts of interest.

References

Bakker CE, de Diego Otero Y, Bontekoe C, Raghoe P, Luteijn T, Hoogeveen AT, Oostra BA, Willemsen R. 2000. Immunocytochemical and biochemical characterization of FMRP, FXR1P, and FXR2P in the mouse. Exp Cell Res 258:162-170.

van Beers EH, Joosse SA, Ligtenberg MJ, Fles R, Hogervorst FB, Verhoef S, Nederlof PM. 2006. A multiplex PCR predictor for aCGH success of FFPE samples. Br J Cancer 94:333-337.

Carter DA, Kim K, Brinker RA and Raffel C. 1995. Extradural tumor causing spinal cord compression in Klippel-Trenaunay-Weber syndrome. Surg Neurol 43:257-260.

Coevoets R, Arican S, Hoogeveen-Westerveld M, Simons E, van den Ouweland A, Halley D, Nellist M 2009 A reliable cell-based assay for testing unclassified *TSC2* gene variants. Eur J Hum Genet 17:301-310.

Dong Q, Debelenko LV, Chandrasekharappa SC, Emmert-Buck MR, Zhuang Z, Guru SC, Manickam P, Skarulis M, Lubensky IA, Liotta LA, Collins FS, Marx SJ and Spiegel AM. 1997. Loss of heterozygosity at 11q13: Analysis of pituitary tumors, lung carcinoids, lipomas and other uncommon tumors in subjects with familial multiple endocrine neoplasia type 1. J Clin Endocrinol Metab 82:1416-1420.

Eng C. 2000. Will the real Cowden syndrome please stand up: revised diagnostic criteria. J Med Genet 37:828-830.

European Chromosome 16 Tuberous Sclerosis Consortium. 1993 Identification and characterization of the tuberous sclerosis gene on chromosome 16. Cell 75:1305-1315.

Georgitsi M, Raitila A, Karhu A, van der Luijt RB, Aalfs CM, Sane T, Vierimaa O, Makinen MJ, Tuppurainen K, Paschke R, Gimm O, Koch CA, Gundogdu S, Lucassen A, Tischkowitz M, Izatt L, Aylwin S, Bano G, Hodgson S, DeMenis E, Launonen V, Vahteristo P, Aaltonen LA. 2007. Germline CDKN1B/p27Kip1 mutation in multiple endocrine neoplasia. J Clin Endocrinol Metab 92:3321-3325.

Gomez MG, Sampson JR, Holets-Whittemore V, eds. 1999 The tuberous sclerosis complex. 3rd edn. Developmental Perspectives in Psychiatry, Oxford University Press, New York and Oxford.

Hornick JL, Fletcher CDM. 2006. PEComa: what do we know so far? Histopathol 48:75-82.

Inoki K, Guan K-L. 2009. Tuberous sclerosis complex, implication from a rare genetic disease to common cancer treatment. Hum Mol Genet 18:R94-R100.

Kenerson H, Folpe AL, Takayama TK, Yeung RS. 2007. Activation of the mTOR pathway in sporadic angiomyolipomas and other perivascular epithelioid cell neoplasms. Hum Pathol 38:1361-1371.

Nellist M, Sancak O, Goedbloed MA, Rohe C, van Netten D, Mayer K, Tucker-Williams A., van den Ouweland AMW, Halley DJJ. 2005. Distinct effects of single amino acid changes to tuberin on the function of the tuberin-hamartin complex. Eur J Hum Genet 13:59-68.

Ng PC, Henikoff S. 2006. Predicting the effects of amino acid substitutions on protein function. Ann Rev Genomics Hum Genet 7:61-80.

Niida Y, Stemmer-Rachamimov AO, Logrip M, Tapon D, Perez R, Kwiatkowski DJ, Sims K, MacCollin M, Louis DN, Ramesh V. 2001. Survey of somatic mutations in tuberous sclerosis complex (TSC) hamartomas suggests different genetic mechanisms for pathogenesis of TSC lesions. Am J Hum Genet 69:493-503.

Rakowski SK, Winterkorn EB, Paul E, Steele DJ, Halpern EF, Thiele EA. 2006. Renal manifestations of tuberous sclerosis complex: incidence, prognosis and predictive factors. Kidney Int 70:1777-1782.

Roberts PS, Ramesh V, Dabora S, Kwiatkowski DJ. 2003. A 34 bp deletion within *TSC2* is a rare polymorphism, not a pathogenic mutation. Ann Hum Genet 67:495-503.

Sancak O, Nellist M, Goedbloed M, Elfferich P, Wouters C, Maat-Kievit A, Zonnenberg B, Verhoef S, Halley D, van den Ouweland A. 2005 Mutational analysis of the *TSC1* and *TSC2* genes in a diagnostic setting: genotype-phenotype correlations and comparison of diagnostic DNA techniques in tuberous sclerosis complex. Eur J Hum Genet 13:731-741.

van Slegtenhorst M, de Hoogt R, Hermans C, Nellist M, Janssen B, Verhoef S, Lindhout D, van den Ouweland A, Halley D, Young J, Burley M, Jeremiah S, Woodward K, Nahmias J, Fox M, Ekong R, Wolfe J, Povey S, Osborne J, Snell RG, Cheadle JP, Jones AC, Tachataki M, Ravine D, Sampson JR, Reeve MP, Richardson P, Wilmer F, Munro C, Hawkins TL, Sepp T, Ali JBM, Ward S, Green AJ, Yates JRW, Short MP, Haines JH, Jozwiak S, Kwiatkowska J, Henske EP, Kwiatkowski DJ. 1997. Identification of the tuberous sclerosis gene *TSC1* on chromosome 9q34. Science 277: 805-808.

van Slegtenhorst M, Nellist M, Nagelkerken B, Cheadle J, Snell R, van den Ouweland A, Reuser A, Sampson J, Halley D, van der Sluijs P. 1998. Interaction between hamartin and tuberin, the *TSC1* and *TSC2* gene products. Hum Mol Genet 7:1053-1057.

Figures

Figure 1: Pedigree of the investigated family. The *TSC2* haplotypes are shown for the 1088C-T variant in exon 10 (alleles C or T), and the insertion of an extra copy of the 34 basepair repeat in intron 38 (alleles - or ins34). The haplotypes inherited by the proband (filled circle) are shown in the open boxes.

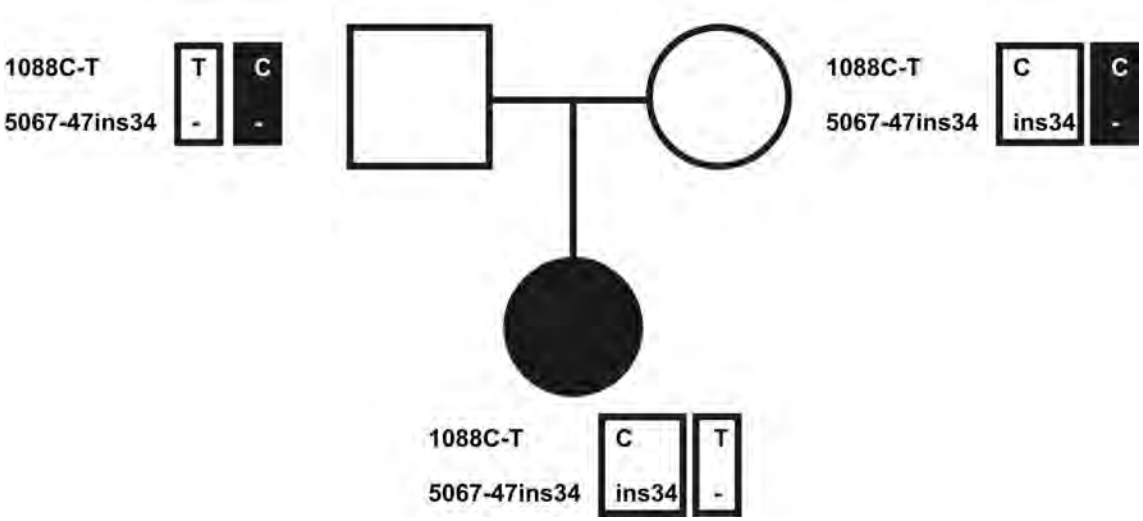

Figure 2 : Immunohistochemical analysis of the AML.

(A) Immunoreactivity for AKT, and S473- and T308- phosphorylated AKT (B) Immunoreactivity for S6K and T389-phosphorylated S6K. (C) Immunoreactivity for S6 and S235/S236-phosphorylated S6. Robust immunoreactivity for the above markers was observed in most tumour cells.

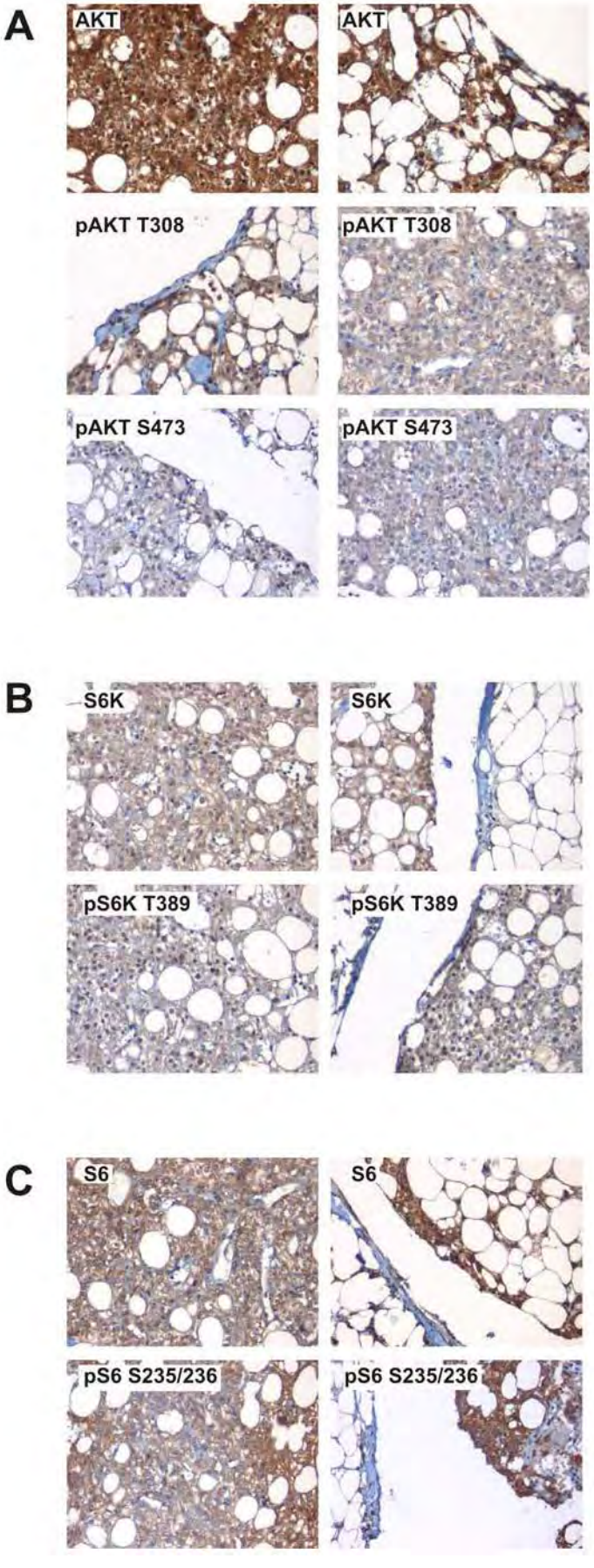
A
AKT
AKT
pAKT T308
pAKT T308
pAKT S473
pAKT S473
B
S6K
S6K
pS6K T389
pS6K T389
C
S6
S6
pS6 S235/236
pS6 S235/236

Figure 3: Loss of heterozygosity analysis. Genomic DNA isolated from blood and from the paraffin-embedded tumour material was amplified by PCR and sequenced. The individual sequencing peaks were compared.

(A) Sequence analysis of the *TSC2* 1088C-T (A357V) variant in the proband. Height of the blue electropherogram peak (arrow; C allele) is comparable to the height of the red peak (arrow; T allele) in the blood DNA (box, top). In contrast, in the tumour DNA, the blue (C allele) peak is reduced relative to the red (T allele) peak.

(B) *TSC2* 5069-47ins34 variant. Sequence (forward strand only) of the repeat region in *TSC2* exon 38 and intron 38. Exonic nucleotides are represented by capital letters, intronic nucleotides are in lower case. The 2.3 copies of the repeat sequence are indicated in purple, orange and blue. The position of the extra copy of the 34 nucleotide repeat detected in the proband (green) is indicated.

(C) Sequence analysis of the *TSC2* 5069-47ins34 variant.

Top: The forward strand sequences of both of the proband's *TSC2* alleles are shown. The allele containing the 34 nucleotide insertion (green) is shown in italics.

Bottom: The heights of the electropherogram peaks in the blood DNA were compared to the peak heights in the tumor samples. The peak heights of the underlined nucleotides, all from the allele containing the insertion, were reduced compared to the corresponding peak from the other allele.

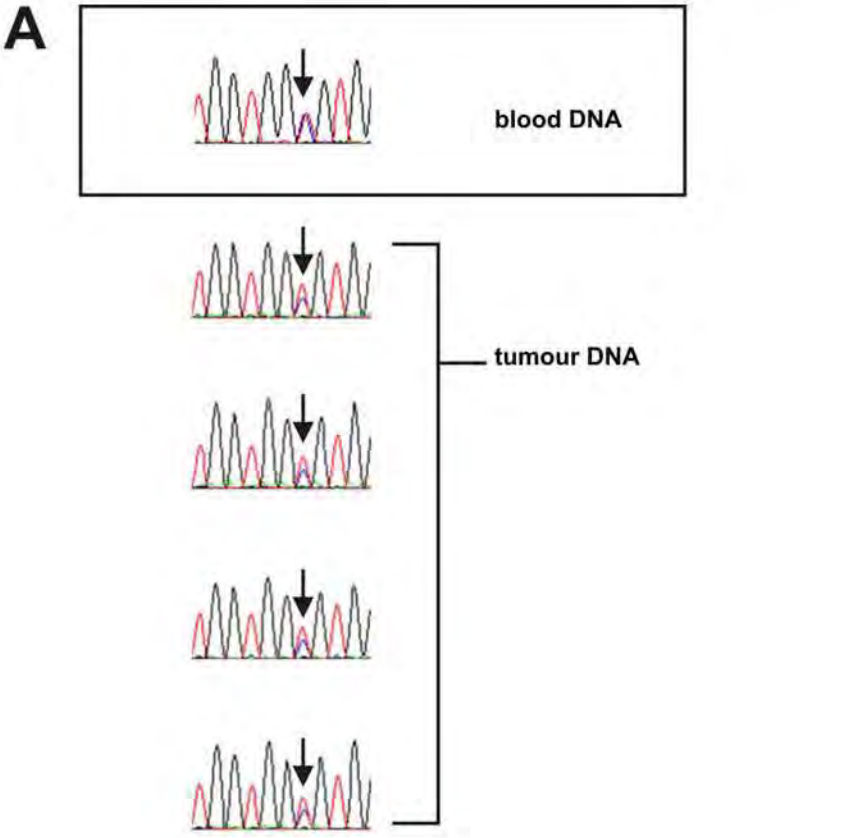
A
blood DNA
tumour DNA

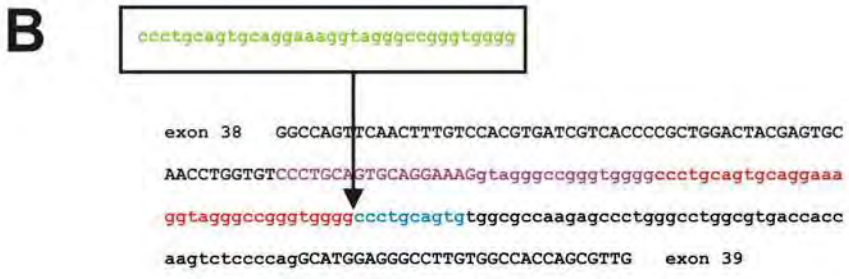
B
ccctgcagtgcaggaaaggtagggccgggtgggg
exon 38 GGCCAGTTCAACTTTGTCCACGTGATCGTCACCCCGCTGGACTACGAGTGC
AACCTGGTGTCCCTGCAGTGCAGGAAAGgtagggccgggtgggggccctgcagtgcaggaaa
ggtagggccgggtgggg ccctgcagtg tggcgccaagagccctgggcctggcgtgaccacc
aagtctccccagGCATGGAGGGCCTTGTGGCCACCAGCGTTG exon 39

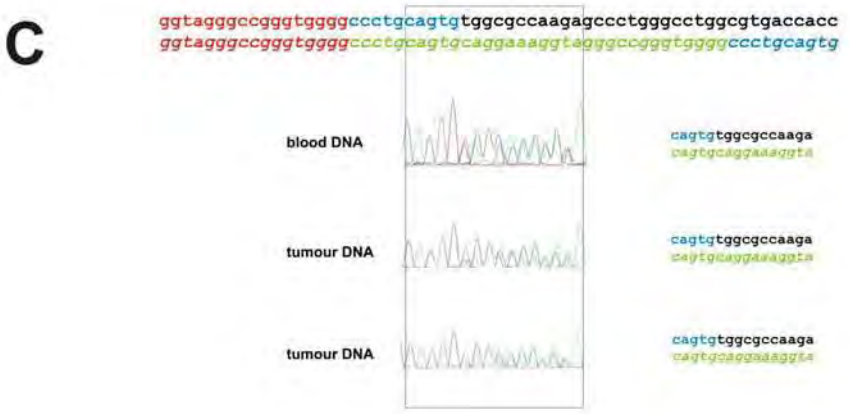
C
ggtagggccgggtgggg ccctgcagtg tggcgccaagagccctgggcctggcgtgaccacc
ggtagggccgggtgggg ccctgcagtgcaggaaaggtagggccgggtgggg ccctgcagtg
blood DNA
tumour DNA
tumour DNA
cagtg tggcgccaaga
cagtgcaggaaaggta
cagtg tggcgccaaga
cagtgcaggaaaggta
cagtg tggcgccaaga
cagtgcaggaaaggta

Figure 4: Functional analysis of the TSC2 A357V variant (A) Cells expressing TSC1, S6K and the TSC2 A357V variant, and control cells expressing TSC1, S6K and either wild-type TSC2 or the pathogenic TSC2 R611Q variant, were analysed by immunoblotting. The signals for TSC2, TSC1, S6K and T389-phosphorylated S6K (T389) are shown.
(B) Quantification of the immunoblot signals to show the inhibition of S6K T389 phosphorylation in the presence of the TSC2 variants. The ratio of the S6K T389 phosphorylation signal to the total S6K signal (T389/S6K) was determined relative to wild-type TSC2 (wild-type TSC2 T389/S6K ratio = 1). Standard deviations are indicated. Variants with a significantly increased T389/S6K ratio (p values < 0.05; paired Student's t-test) compared to wild-type TSC2 are indicated with an asterisk.

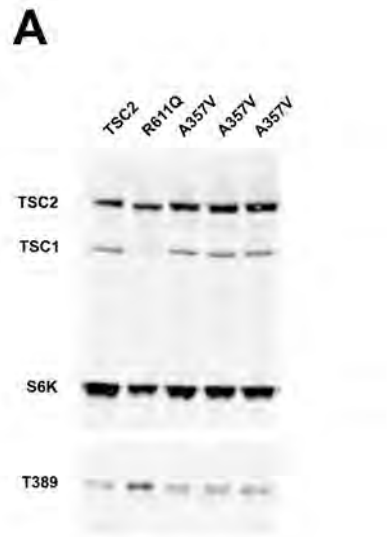
A
TSC2
R611Q
A357V
A357V
A357V
TSC2
TSC1
S6K
T389
B
rel. T389/S6K
6
5
4
3
2
1
0
*
TSC2
R611Q
A357V
C
control
TSC2
R611Q
A357V
TSC2
TSC1
input
TSC2
TSC1
TSC1 IP

Appendix 3:

Title page:

The *TSC2* c.3598C>T (p.R1200W) missense mutation co-segregates with tuberous sclerosis complex in multiple mildy affected kindreds

Marjolein Wentink[1.], Mark Nellist[1.], Marianne Hoogeveen-Westerveld[1.], Bernard Zonnenberg[2.], Dorinne van der Kolk[3.], Soo-Mi Park[4.], Dicky Halley[1.], Ans van den Ouweland[1.] and Anneke Maat-Kievit[1.]

[1.] Department of Clinical Genetics, Erasmus MC, 3015 GE Rotterdam, The Netherlands.

[2.] Department of Oncology, University of Utrecht Medical Centre, Utrecht, The Netherlands.

[3.] Department of Clinical Genetics, University Medical Centre Groningen, Groningen, The Netherlands.

[4.] Department of Clinical Genetics, Addenbrooke's Hospital, Cambridge, U.K.

Corresponding author: Anneke Maat-Kievit (j.a.maat@erasmusmc.nl), Department of Clinical Genetics, Erasmus MC, 3015 GE Rotterdam, The Netherlands.

running title: TSC2 R1200W missense mutation

Abstract

Tuberous sclerosis complex (TSC) is an autosomal dominant disorder characterised by a combination of neurological symptoms and hamartomatous growths in various organ systems. The disease is caused by mutations in the *TSC1* and *TSC2* genes. Overall, *TSC2* mutations are associated with a more severe disease phenotype. We identified the c.3598C>T nucleotide change in the *TSC2* gene in 6 different families with TSC. In each case, the TSC phenotype was mild, characterised by a lack of disfiguring skin lesions, severe mental retardation or major organ involvement.

Our findings support other studies showing that some *TSC2* missense mutations are associated with less severe TSC phenotypes.

keywords: Tuberous sclerosis complex, *TSC2*, TSC2, mild phenotype

Introduction

Tuberous sclerosis complex (TSC) is an autosomal dominant disorder characterized by the development of hamartomas in a variety of tissues, including the brain, skin and kidneys [Gomez et al., 1999]. TSC is caused by mutations in either the TSC1 gene on chromosome 9p34 [van Slegtenhorst et al., 1997] or the TSC2 gene on chromosome 16p13.3 [European Consortium, 1993]. Penetrance is considered to be complete and the disease is estimated to occur in 1/6000 - 1/10000 live births [Gomez et al., 1999]. Approximately 60%-70% of cases are caused by *de novo* mutations, indicating a high spontaneous mutation rate [Cheadle et al., 2000].

The *TSC1* and *TSC2* gene products, TSC1 and TSC2, interact to form a protein complex. TSC2 contains a catalytic GTPase activating protein (GAP) domain and acts on the GTPase RHEB to inhibit RHEB-GTP-dependent stimulation of the target of rapamycin complex 1 (TORC1) [Inoki and Guan, 2009]. Inactivation of the TSC1-TSC2 complex results in the phosphorylation of TORC1 targets, including p70 S6 kinase (S6K), the ribosomal protein S6 and the elongation factor 4 binding protein 1 (4E-BP1).

Although the clinical phenotypes of TSC patients are highly variable, individuals with a *TSC2* mutation are more likely to have more clinical features and more severe symptoms than those with a *TSC1* mutation [Dabora et al., 2001]. Interestingly however, several families with a *TSC2* missense mutation and a mild TSC phenotype have been described [Khare et al., 2001; O' Connor et al., 2003; Mayer et al., 2004; Jansen et al., 2006], suggesting that some *TSC2* mutations may be associated with less severe forms of TSC. Here we report five unrelated families and one sporadic patient, carrying the c.3598 C-T (p.R1200W) missense mutation in the *TSC2* gene. In general, the mutation carriers were

relatively mildly affected, and many carriers did not fulfil the diagnostic criteria for definite TSC. We compared the *in vitro* activity of the TSC2 R1200W mutant protein to wild-type TSC2 and other TSC2 variants. Our analysis indicates that although the R1200W substitution does not prevent TSC1-TSC2 binding, the subcellular distribution of the mutant complex is altered and it is unable to inhibit TORC1 signalling. The effects of the R1200W substitution on *in vitro* assays of TSC1-TSC2 function are discussed in relation to the mild phenotypes observed in the families described here.

Materials and methods

Collection of clinical data

A standardized evaluation form/questionnaire was completed for each family member by the clinician involved.

DNA mutation analysis

Mutation analysis was performed as described previously [Sancak et al., 2005] or by sequence analysis of all coding exons and exon/intron boundaries (primers available on request). The mutation is described according to HGVS nomenclature (Accession number NM_000548.3).

Haplotype analysis

Six microsatellite markers, cgr484 (rs3222244), cgr485 (rs60461442), cgr527, cgr531 (KG8), cgr533 (rs3138606) and cgr534 (rs3138601), were typed in all the available family

members. All the markers mapped within 0.5 Mb of the *TSC2* genomic locus. Primer sequences are available on request.

Prediction analysis

To investigate whether the *TSC2* c.3598C>T change affected RNA splicing, ALAMUT software (Mutation Interpretation Software; version 1.5, May 2009; Interactive Biosoftware, Rouen, France) was used.

The effect of the R1200W substitution on TSC2 structure and function were predicted using SIFT [Ng and Henikoff, 2006]. SIFT scores were calculated using a multiple sequence alignment of TSC2 from 14 different species (human, chimpanzee, maccaca, cow, dog, horse, mouse, chicken, zebrafish, pufferfish, fruitfly, mosquito, methylotrophic yeast and fission yeast).

Constructs and antisera

Expression constructs were derived by site-directed mutagenesis using the Stratagene QuickChange kit, or have been described previously [Nellist et al., 2005]. All constructs were sequenced completely.

Antibodies were purchased from Cell Signaling Technology (Danvers, MA, U.S.A.), except for a mouse monoclonal antibody against TSC2 which was purchased from Zymed Laboratories (San Francisco, CA, U.S.A.), or were described previously [van Slegtenhorst, 1998].

Coimmunoprecipitation

HEK 293T cells in 6 cm dishes were transfected with expression constructs encoding different TSC2 variants and C-terminal myc-tagged TSC1 using polyethyleneimine

(Polysciences Inc., Warrington, PA, U.S.A.)[Coevoets et al., 2009]. Twenty-four hours after transfection the cells were washed with cold PBS and lysed in 0.4 ml lysis buffer (50 mM Tris-HCl pH 7.5, 100 mM NaCl, 50 mM NaF, 1 % Triton X100 and a protease inhibitor cocktail (Complete, Roche Molecular Biochemicals)) for 10 minutes on ice. The lysates were cleared by centrifugation (10 000 g for 10 minutes at 4^{o}C) and the supernatant fractions transfered to EZ Red anti-myc affinity beads (Sigma-Aldrich) pre-equilibrated in lysis buffer. After gentle rotation for 3 hours at 4^{o}C, the beads were recovered by gentle centrifugation (1000 g for 15 seconds at 4^{o}C), washed 3 times with >20-fold excess of lysis buffer, and resuspended in sample buffer prior to immunoblot analysis (Criterion SDS-PAGE system; BioRad, Hercules, CA, U.S.A.). Protein expression levels were estimated by near infra-red detection and quantification of the blotted proteins on an Odyssey^{TM} scanner (Li-Cor Biosciences, Lincoln, NE, U.S.A.).

Immunoblot analysis of S6K T389 and TSC2 T1439 phosphorylation

HEK 293T cells in 3.5 cm dishes were transfected with expression constructs encoding TSC2 variants and myc-tagged TSC1 and S6K and harvested in 0.3 ml lysis buffer, as described above. After centrifugation (10 000 g for 10 minutes at 4^{o}C), the supernatant fractions were recovered and the pellets resuspended by sonication in 0.3 ml lysis buffer. Supernatant and pellet fractions were analysed by immunoblotting, as above.

To investigate the effect of AKT activity on TSC2 T1439 phosphorylation, transfected cells were treated with 10nM wortmannin (Sigma-Aldrich) for 0 - 30 minutes prior to harvesting.

Immunofluorescent microscopy

Tsc2 -/- mouse embryo fibroblasts (MEFs) were seeded onto glass coverslips, transfected and processed for immunofluorescent microscopy as described previously [Nellist et al., 2005]. Fixed, permeabilised cells were incubated with a primary mouse monoclonal antibody specific for TSC2 (Zymed) and a primary rabbit monoclonal antibody specific for S235/236 phosphorylated S6 (Cell Signaling Technology), followed by Cy2- and Cy3-coupled secondary antibodies (DAKO, Carpinteria, CA, U.S.A.). Cells were mounted in Mowiol (Calbiochem, La Jolla, CA, U.S.A.) and studied using a Leica DM RXA microscope and Image Pro-Plus version 6 image analysis software. The S6 S235/236 phosphorylation status of TSC2-expressing cells was compared to non-expressing (untransfected) cells. The numbers of TSC2 positive cells in which S235/236 phosphorylated S6 was visible were counted independently by three observers in two separate experiments.

Results

Clinical and genetic findings

Six families, 5 from The Netherlands and one from the United Kingdom, were identified with the *TSC2* c.3598C>T (p.R1200W) variant. The pedigrees are shown in Figure 1 and the clinical findings are summarised in Tables 1 - 3. Six microsatellite markers mapping close to the *TSC2* locus were typed in all the available family members from the five Dutch families. In each case, the disease haplotype was different (data not shown), indicating that the *TSC2* c.3598C>T change was more likely to have occurred multiple times, than to be derived from a common founder.

Family 1488

Family 1488 is shown in Figure 1A and the clinical findings in the mutation carriers are summarised in Table 2. Six individuals (I.2, II.1, III.3, III.4, IV.1 and IV.2) had signs and/or symptoms of TSC, including 2 (III.3, IV.2) with a history of epilepsy in childhood. All 6 had skin lesions consistent with TSC, but no ophtalmological lesions were found. IV.1 had a single renal cyst, and in IV.2 a possible angiomyolipoma (AML) was detected. III.3 showed signs of cardiomegaly, but no rhabdomyoma were detected. Dental pits (DP) were observed in III.4. Brain magnetic resonance imaging (MRI) or computed tomography (CT) was performed in 6 individuals. A single cortical tuber was detected in IV.1, the only family member to fulfill the diagnostic criteria for definite TSC. Clinical exams did not reveal any signs of TSC in III.2 or IV.3. The *TSC2* c.3598C>T variant was detected in II.1, III.3 and III.4, and was absent from III.2. DNA testing was not possible in the other family members.

Family 15396

Family 15396 is shown in Figure 1B and the clinical findings in the mutation carriers are summarised in Table 2. Five individuals had signs or symptoms of TSC. III.2 had seizures and behavioral disturbances and was diagnosed with definite TSC on the basis of skin lesions, cardiac rhabdomyoma and brain lesions. II.2 and III.1 had skin lesions only. No renal abnormalities were detected. Hydrocephalus was anamnestically reported for III.3 and I.2 was reported to have had epilepsy. However, no other clinical or genetic information were available for these individuals. II.2 and III.2 carried the *TSC2* c.3598C>T variant; II.3 did not.

Family 28874

Family 28874 is shown in Figure 1C and the clinical findings in the mutation carriers are summarised in Table 2. Three individuals were reported to fulfil the criteria for definite TSC, although the results of the clinical investigations were unavailable. Skin lesions were reported in 5 individuals. However, no other abnormalities were found and no epilepsy, mental retardation or behavioral problems were reported. DNA mutation analysis was performed in 13 individuals, 8 of whom carried the *TSC2* c.3598C>T variant.

Family 29614

Family 29614 is shown in Figure 1D and the clinical findings in the mutation carriers are summarised in Table 2. Seven individuals showed at least one sign of TSC. The *TSC2* c.3598C>T variant was identified in 5 individuals, all of whom had skin lesions. Cortical tubers were detected in III.4, IV.2 and IV.3, and IV.3 had a cardiac rhabdomyoma. All thoracic X-ray, dental and ophtalmological examinations were normal. Seven individuals were reported to have had epilepsy. In 4 cases this remitted during childhood. IV.2 and IV.3 were reported as having behavioral disturbances. II.1 did not carry the *TSC2* c.3598C>T variant and was not reported to have any signs of the disease.

Family 22931

The *TSC2* c.3598C>T variant was identified in an individual with seizures, mild mental retardation, skin lesions, cortical tubers and subependymal nodules, but no lesions in kidneys, heart, mouth or eyes (Table 2). No data on other family members was available.

Family 24493

Family 24493 is shown in Figure 1E. III.1 had seizures that remitted at 17 years, brain imaging suggestive of TSC and skin lesions but no renal findings (Table 2). I.1, II.1 and III.2 were all reported to have had epilepsy, however no other data was available for these individuals..

Functional characterisation of the TSC2 R1200W variant

The TSC2 R1200W variant interacts with TSC1 and is phosphorylated by AKT

We compared TSC1-TSC2 complex formation in HEK 293T cells expressing the TSC2 R1200W variant with cells expressing wild-type TSC2 and cells expressing the pathogenic TSC2 R611Q variant [Nellist et al., 2001]. The variants were coexpressed with a TSC1 fusion protein containing a C-terminal myc epitope tag and TSC1-TSC2 complexes were immunoprecipitated using myc-affinity beads. Coimmunoprecipitated TSC2 variants were detected by immunoblotting. As shown in Figure 2A, the TSC2 R1200W variant was coimmunoprecitated with TSC1 as effectively as wild-type TSC2. Next, we compared the AKT-dependent phosphorylation of wild-type TSC2 and the R1200W variant at the T1439 position. As shown in Figure 2B, we did not observe any differences, indicating that TSC2 phosphorylation is unlikely to be affected by the R1200W substitution.

The TSC2 R1200W variant is unable to inhibit TORC1 signalling

To determine whether the TSC2 R1200W variant could inhibit TORC1 signalling, S6 S235/236 phosphorylation was assessed in transfected Tsc2 -/- MEFs by immunofluorescent microscopy (Figure 3) and S6K T389 phosphorylation was estimated in the transfected HEK293T cells by immunoblotting (Figure 4). S6 S235/236 phosphorylation was inhibited in less than 12% of the in *Tsc2* -/- MEFs expressing the

R1200W or R611Q variants, compared to more than 95% of the cells expressing wild-type TSC2 (Figure 4C) and S6K T389-phosphorylation was not inhibited in the presence of the TSC2 R1200W variant (Figure 3A and D). Therefore we concluded that the R1200W substitution is a pathogenic change, that restricts the TSC1-TSC2-dependent inhibition of TORC1 activity, without preventing TSC1-TSC2 binding.

We noticed that the signal for the R1200W variant on the immunoblot was reduced relative to wild-type TSC2 (Figure 4A and B) and that the localisation pattern of this variant in the *Tsc2* -/- MEFs was different to the wild-type protein (Figure 3A). The R1200W variant localised predominantly in a perinuclear aggregate- or inclusion-like pattern.

We determined the proportions of the R1200W variant and co-expressed TSC1 in Triton X100-soluble and -insoluble fractions. As shown in Figure 4F, compared to wild-type TSC2, less of the R1200W variant and more TSC1 was detected in the Triton X100-insoluble fraction, suggesting that the TSC1-TSC2 R1200W complexes are less stable than the wild-type TSC1-TSC2 complex, and more prone to aggregation and/or degradation.

Discussion

The majority of TSC patients are sporadic, and carry a *de novo TSC1* or *TSC2* mutation [Sancak et al., 2005]. In familial cases, approximately half of the mutations identified are in the *TSC2* gene [Sancak et al., 2005], and most families are small and have a unique mutation. Large, multi-generation kindreds are not common. Nevertheless, a few large families have been described where a *TSC2* missense mutation cosegregates with

less severe symptoms of TSC, generally skin lesions and mild neurological symptoms without severe hamartomatous lesions in other organs [Khare et al., 2001; O' Connor et al., 2003; Mayer et al., 2004; Jansen et al., 2006]. Here we describe multiple, unrelated families with predominantly mildly affected individuals carrying a *TSC2* c.3598C>T (p.R1200W) mutation. The clinical diagnoses in the mutation carriers are summarised in Table 1, and the clinical findings are shown in Table 2. We compared the clinical findings in the mutation carriers to a large cohort of TSC patients with *TSC2* mutations [Sancak et al., 2005]. As shown in Table 3, with the exception of hypomelanotic macules, the incidence of the signs and symptoms associated with TSC were lower in the *TSC2* c.3598C>T (p.R1200W) mutation carriers, compared to the general *TSC2* mutation population. Notably, only one *TSC2* c.3598C>T (p.R1200W) mutation carrier was mildly mentally retarded, the rest were of normal intelligence; no renal lesions were detected and the incidence of facial angiofibroma was approximately 4-fold lower than in the total *TSC2* population.

We studied the effect of the R1200W substitution on the TSC1-TSC2 complex *in vitro*, and demonstrated that the change inactivated the TSC1-TSC2 complex, without disrupting TSC1-TSC2 binding. Interestingly, functional studies on the S1036P, R905Q and G1556S substitutions, identified in mildly affected families with TSC, showed that these substitutions also inactivate the TSC1-TSC2 complex without disrupting TSC1-TSC2 binding [unpublished observations; Jansen et al., 2006; Mayer et al., 2004]. It is possible that *in vivo* these variants retain some activity, and therefore provide (partial) protection from the more severe symptoms of TSC. It will be interesting to determine whether other *TSC2* missense mutations that do not affect TSC1-TSC2 binding are associated with less severe TSC phenotypes.

We investigated the possibility that the *TSC2* c.3598C>T (p.R1200W) mutation was a single mutational event by haplotype analysis. We identified a different disease haplotype in each family, and concluded that the *TSC2* c.3598C>T (p.R1200W) change is a recurrent mutation. According to the *TSC2* Leiden Open Variation Database (http://lovd.nl/TSC2), the *TSC2* c.3598C>T (p.R1200W) mutation has been identified in at least 4 other cases of TSC, including 2 *de novo* and 2 familial cases [Wilson et al., 1996; Au et al., 1998; Au et al., 2007]. Wilson et al. described a parent and 2 affected children with skin features and seizures. One family member was mentally retarded, and another had behavioural problems [Wilson et al., 1996]. Au et al. described a large family with mild skin features, epilepsy and cerebral MRI abnormalities, but no retardation or other TSC-associated symptoms [Au et al., 1998].

In summary, we identified the c.3598C>T (p.R1200W) mutation in the *TSC2* gene in 6 unrelated families with TSC. In each family the TSC phenotype was relatively mild. We demonstrated that the TSC2 R1200W substitution inactivated the TSC1-TSC2 complex, without preventing TSC1-TSC2 binding. Interestingly, functional analysis of the R905Q, S1036P and R1200W variants, that all cosegregate with mild symptoms of TSC in extended families, suggests that some *TSC2* variants that inactivate the TSC1-TSC2 complex without affecting TSC1-TSC2 binding may be associated with a milder TSC phenotype.

References

Au KS, Rodriguez JA, Finch JL, Volcik KA, Roach ES, Delgado MR, Rodriguez E Jr, Northrup H. 1998. Germ-line mutational analysis of the *TSC2* gene in 90 tuberous sclerosis patients. Am J Hum Genet 62:286-294.

Au K-S, Williams AT, Roach ES, Batchelor L, Sparagana SP, Delgado MR, Wheless JW, Baumgartner JE, Roa BB, Wilson CM, Smith-Knuppel TK, Cheung MY, Whittemore VH, King TM, Northrup H. 2007. Genotype/phenotype correlation in 325 individuals referred for a diagnosis of tuberous sclerosis complex in the United States. Genet Med 9:88-100.

Cheadle JP, Reeve MP, Sampson JR, Kwiatkowski DJ. 2000. Molecular genetic advances in tuberous sclerosis. Hum Genet 107:97-114.

Coevoets R, Arican S, Hoogeveen-Westerveld M, Simons E, van den Ouweland A, Halley D, Nellist M 2009 A reliable cell-based assay for testing unclassified *TSC2* gene variants. Eur J Hum Genet 17:301-310.

Dabora SL, Jozwiak S, Franz DN, Roberts PS, Nieto A, Chung J, Choy YS, Reeve MP, Thiele E, Egelhoff JC, Kasprzyk-Obara J, Domanska-Pakiela D, Kwiatkowski DJ. 2001. Mutational analysis in a cohort of 224 tuberous sclerosis patients indicates increased severity of *TSC2*, compared with *TSC1*, disease in multiple organs. Am J Hum Genet 68:64-80.

European Chromosome 16 Tuberous Sclerosis Consortium. 1993 Identification and characterization of the tuberous sclerosis gene on chromosome 16. Cell 75:1305-1315.

Gomez MG, Sampson JR, Holets-Whittemore V, eds. 1999 The tuberous sclerosis complex. 3rd edn. Developmental Perspectives in Psychiatry, Oxford University Press, New York and Oxford.

Inoki K, Guan K-L. 2009. Tuberous sclerosis complex, implication from a rare genetic disease to common cancer treatment. Hum Mol Genet 18:R94-R100.

Jansen AC, Sancak O, D'Agostino MD, Badhwar A, Roberts P, Gobbi G, Wilkinson R, Melanson D, Tampieri D, Koenekoop R, Gans M, Maat-Kievit A, Goedbloed M, van den Ouweland AMW, Nellist M, Pandolfo M, McQueen M, Sims K, Thiele EA, Dubeau F, Andermann F, Kwiatkowski DJ, Halley DJJ, Andermann E. 2006. Unusually mild tuberous sclerosis phenotype is associated with *TSC2* R905Q mutation. Ann Neurol. 60:528-539.

Khare L, Strizheva GD, Bailey JN, Au K-S, Northrup H, Smith M, Smalley SL, Petri Henske E. 2001. A novel missense mutation in the GTPase activating protein homology region of *TSC2* in two large families with tuberous sclerosis complex. J Med Genet 38:347-349.

Mayer K, Goedbloed M, van Zijl K, Nellist M, Rott HD. 2004. Characterisation of a novel TSC2 missense mutation in the GAP related domain associated with minimal clinical manifestations of tuberous sclerosis. J Med Genet 41 e64.

Nellist M, Verhaaf B, Goedbloed MA, Reuser AJJ, van den Ouweland AMW, Halley DJJ. 2001. *TSC2* missense mutations inhibit tuberin phosphorylation and prevent formation of the tuberin-hamartin complex. Hum. Molec. Genet. 10:2889 - 2898.

Nellist M, Sancak O, Goedbloed MA, Rohe C, van Netten D, Mayer K, Tucker-Williams A., van den Ouweland AMW, Halley DJJ. 2005. Distinct effects of single amino acid changes to tuberin on the function of the tuberin-hamartin complex. Eur J Hum Genet 13:59-68.

Ng PC, Henikoff S. 2006. Predicting the effects of amino acid substitutions on protein function. Ann Rev Genomics Hum Genet 7:61-80.

O'Connor SE, Kwiatkowski DJ, Roberts PS, Wollmann RL, Huttenlocher PR. 2003. A family with seizures and minor features of tuberous sclerosis and a novel *TSC2* mutation. Neurology 61:409-412.

Roach ES, Gomez MR, Northrup H. 1998. Tuberous sclerosis complex consensus conference: revised clinical diagnostic criteria. J Child Neurol 13:624-628.

Sancak O, Nellist M, Goedbloed M, Elfferich P, Wouters C, Maat-Kievit A, Zonnenberg B, Verhoef S, Halley D, van den Ouweland A. 2005 Mutational analysis of the *TSC1* and *TSC2* genes in a diagnostic setting: genotype-phenotype correlations and comparison of diagnostic DNA techniques in tuberous sclerosis complex. Eur J Hum Genet 13:731-741.

van Slegtenhorst M, de Hoogt R, Hermans C, Nellist M, Janssen B, Verhoef S, Lindhout D, van den Ouweland A, Halley D, Young J, Burley M, Jeremiah S, Woodward K, Nahmias J, Fox M, Ekong R, Wolfe J, Povey S, Osborne J, Snell RG, Cheadle JP, Jones AC, Tachataki M, Ravine D, Sampson JR, Reeve MP, Richardson P, Wilmer F, Munro C, Hawkins TL, Sepp T, Ali JBM, Ward S, Green AJ, Yates JRW, Short MP, Haines JH, Jozwiak S, Kwiatkowska J,

Henske EP, Kwiatkowski DJ. 1997. Identification of the tuberous sclerosis gene *TSC1* on chromosome 9q34. Science 277: 805-808.

van Slegtenhorst M, Nellist M, Nagelkerken B, Cheadle J, Snell R, van den Ouweland A, Reuser A, Sampson J, Halley D, van der Sluijs P. 1998. Interaction between hamartin and tuberin, the *TSC1* and *TSC2* gene products. Hum Mol Genet 7:1053-1057.

Wilson PJ, Ramesh V, Kristiansen A, Bove C, Jozwiak S, Kwiatkowski DJ, Short MP, Haines JL. 1996. Novel mutations detected in the *TSC2* gene from both sporadic and familial TSC patients. Hum Mol Genet 5:249-256.

Figures

Figure 1. Pedigrees of the families with the *TSC2* c.3598 C-T (p.R1200W) mutation. Clear symbols indicate no signs or symptoms of TSC; 1/4-filled symbols indicate possible TSC; half-filled symbols indicate probable TSC; filled symbols indicate definite TSC. Individuals reported as having TSC, but without clinical data are shown in grey. Individuals with epilepsy (E) are indicated. Genotypes are indicated for the individuals for whom DNA testing was performed. + indicates the presence of the *TSC2* c.3598 C-T (p.R1200W) allele.
(A) Family 1488; (B) Family 15396; (C) Family 28874; (D) Family 29614; (E) Family 24993.

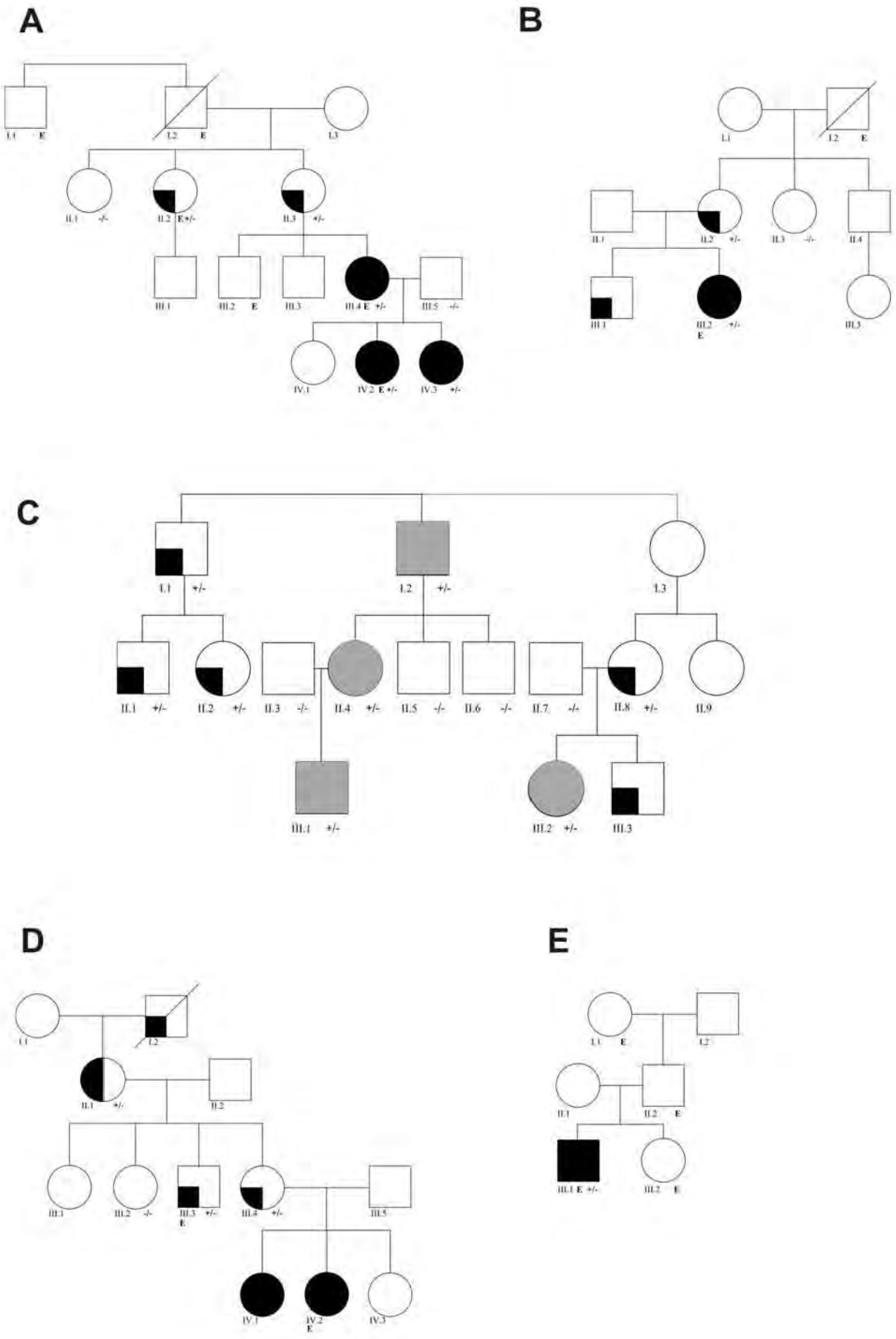
A
I.1 E
I.2 E
I.3
II.1 -/-
II.2 E +/-
II.3 +/-
III.1
III.2 E
III.3
III.4 E +/-
III.5 -/-
IV.1
IV.2 E +/-
IV.3 +/-
B
I.1
I.2 E
II.1
II.2 +/-
II.3 -/-
II.4
III.1
III.2 +/- E
III.3
C
I.1 +/-
I.2 +/-
I.3
II.1 +/-
II.2 +/-
II.3 -/-
II.4 +/-
II.5 -/-
II.6 -/-
II.7 -/-
II.8 +/-
II.9
III.1 +/-
III.2 +/-
III.3
D
I.1
I.2
II.1 +/-
II.2
III.1
III.2 -/-
III.3 +/- E
III.4 +/-
III.5
IV.1
IV.2 E
IV.3
E
I.1 E
I.2
II.1
II.2 E
III.1 E +/-
III.2 E

Figure 2. The TSC2 R1200W variant interacts with TSC1 and is phosphorylated by AKT.

(A) Interaction between TSC1 and the TSC2 R1200W variant. TSC1-TSC2 complexes were immunoprecipitated with a TSC1-specific antibody from cells overexpressing wild-type TSC2 (TSC2), the R611Q or R1200W variants, or TSC1 only (control).

(B) Effect of wortmannin treatment on TSC2-T1439 phosphorylation (T1439) in cells expressing wild-type (TSC2) or the R611Q or R1200W variants.

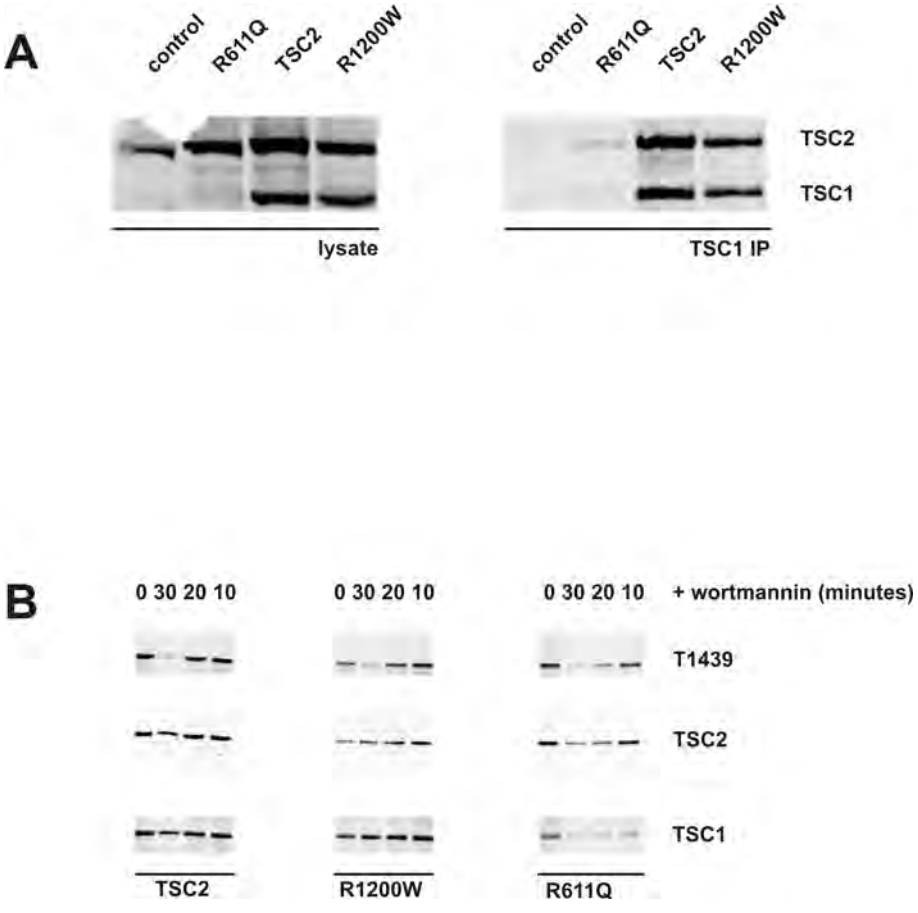

Figure 3. The TSC2 R1200W variant is unable to inhibit S6-S235/236 phosphorylation in *Tsc2* -/- MEFs. S6-S235/236 phosphorylation in *Tsc2* -/- MEFs expressing wild-type TSC2 (TSC2), the R611Q or R1200W variants was estimated by immunofluorescent microscopy.

(A) Expression of wild-type TSC2, or the TSC2 variants. Arrows indicate the transfected cells.

(B) S6-S235/236 phosphorylation in the cells shown in (A). Arrows indicate the transfected cells expressing the TSC2 variants, as shown in (A).

(C) S6-S235/236 phosphorylation in cells expressing wild-type TSC2 (TSC2), the R611Q or R1200W variants was assessed independently by 3 observers in 2 separate experiments. Cells showing clear inhibition of S6-S235/236 phosphorylation were counted.

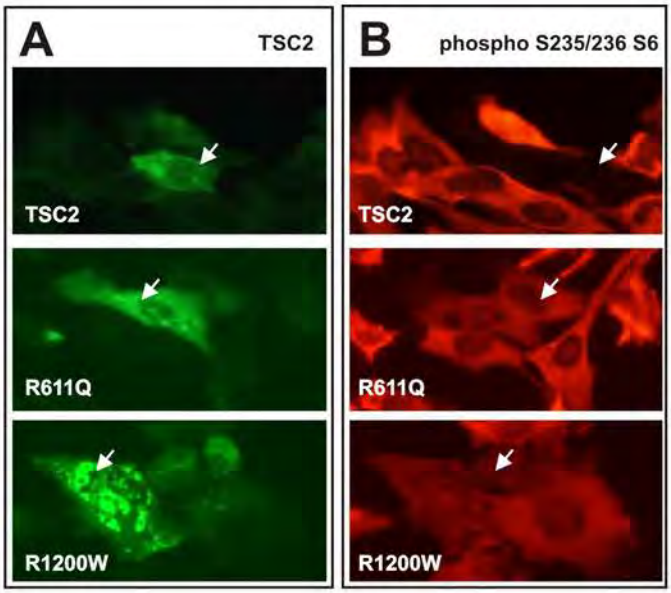
A
TSC2
B
phospho S235/236 S6
TSC2
R611Q
R1200W
TSC2
R611Q
R1200W

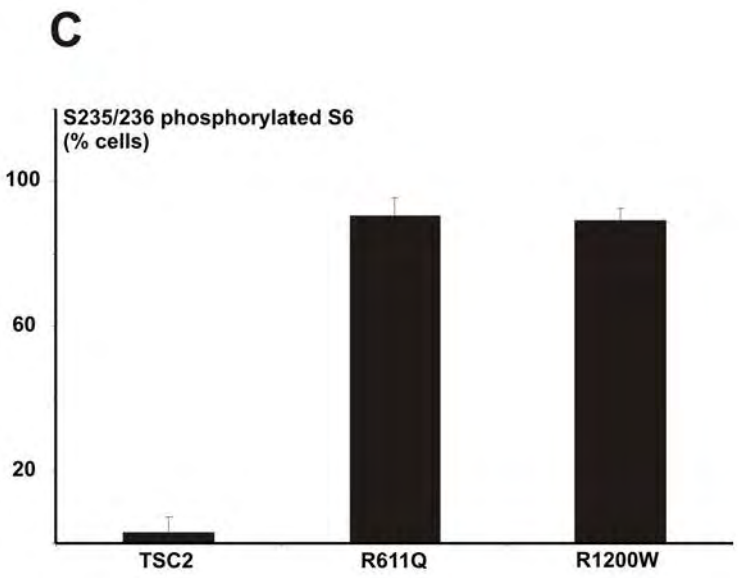
C
S235/236 phosphorylated S6
(% cells)
100
60
20
TSC2
R611Q
R1200W

Figure 4. The TSC2 R1200W variant is unable to inhibit S6K-T389 phosphorylation. S6K-T389 phosphorylation in cells expressing wild-type TSC2 (TSC2), the R611Q or R1200W variants, or no TSC2 (TSC1/S6K) was estimated by immunoblotting in 4 separate experiments. The signals on the blots were quantified, relative to the wild-type (TSC2 ; = 1).

(A) Immunoblot; (B) TSC2 signal; (C) TSC1 signal; (D) T389/S6K ratio; (E) Total S6K signal.

(F) Triton X100 solubility of the TSC2-R1200W variant. Triton X100-soluble and -insoluble cell lysate fractions were analysed by immunoblotting.

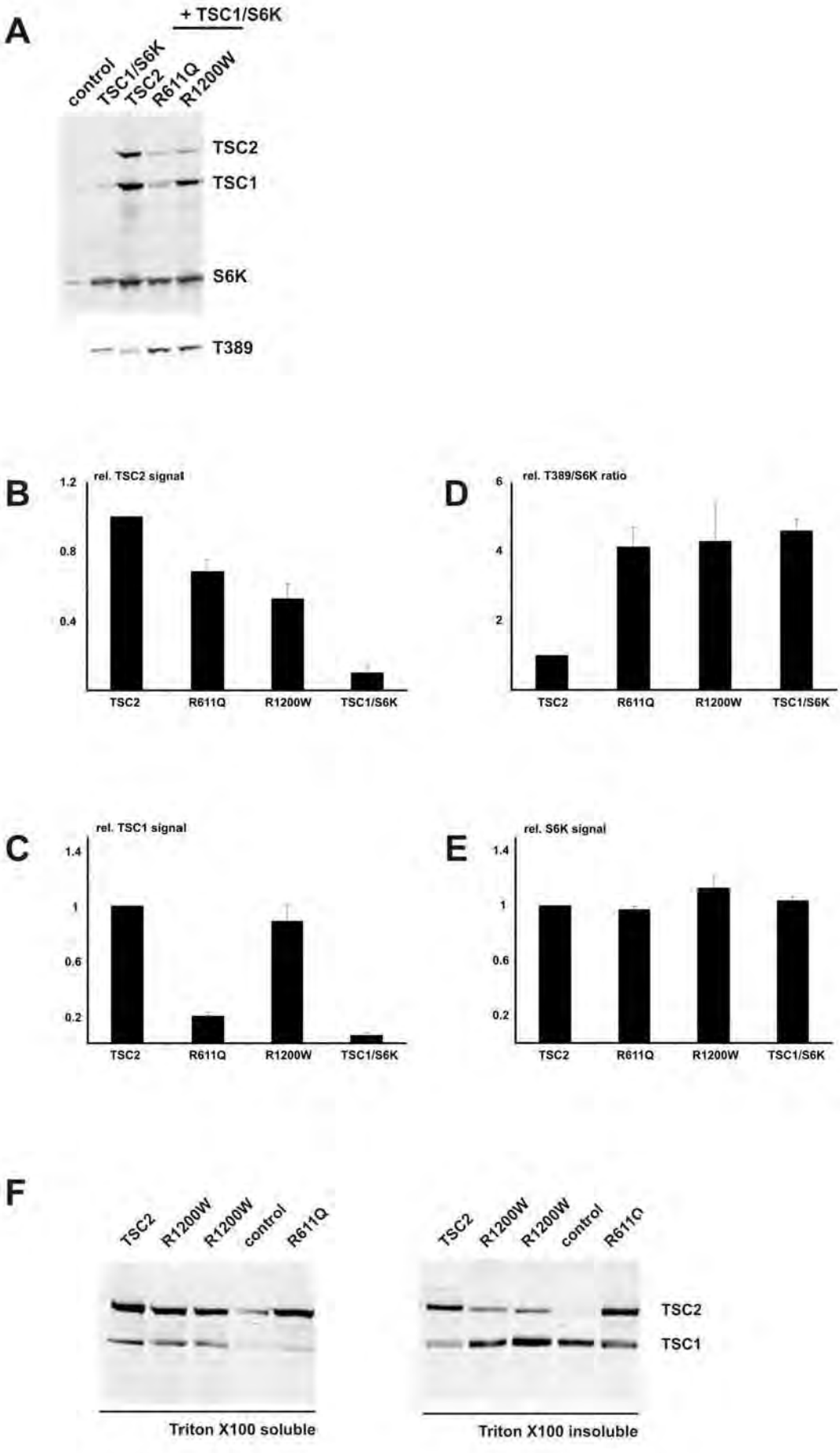
A
+ TSC1/S6K
control
TSC1/S6K
TSC2
R611Q
R1200W
TSC2
TSC1
S6K
T389
B
rel. TSC2 signal
1.2
0.8
0.4
TSC2
R611Q
R1200W
TSC1/S6K
D
rel. T389/S6K ratio
6
4
2
TSC2
R611Q
R1200W
TSC1/S6K
C
rel. TSC1 signal
1.4
1
0.6
0.2
TSC2
R611Q
R1200W
TSC1/S6K
E
rel. S6K signal
1.4
1
0.6
0.2
TSC2
R611Q
R1200W
TSC1/S6K
F
TSC2
R1200W
R1200W
control
R611Q
TSC2
R1200W
R1200W
control
R611Q
TSC2
TSC1
Triton X100 soluble
Triton X100 insoluble

Tables

Table 1. Summary of the clinical diagnoses according to the diagnostic criteria of Roach et al. [Roach et al., 1998] in the *TSC2* c.3598C>T (p.R1200W) mutation carriers.

clinical data	16
no clinical data	4
possible TSC	10/16 (63%)
probable TSC	2/16 (13%)
definite TSC	4/16 (25%)

Table 2. Overview of the clinical findings in the mutation carriers. Key: MR, mental retardation; BD, behavioural disturbance; + indicates the presence of a single major or minor diagnostic criteria; ++ indicates the presence of multiple major or minor diagnostic criteria; - indicates the absence of any signs of TSC.

Individual	**MR/BD**	**Seizures?**	**Diagnosis**	**Skin**	**Kidney**	**Heart**	**Mouth**	**Eyes**	**Brain imaging**
1488 II.1			probable TSC	++					
1488 III.3	BD	yes	possible TSC	+		-		-	-
1488 III.4	-	no	probable TSC	+	-	-	+	-	-
15396 II.2			possible TSC	++	-				-
15396 III.2	BD	yes	definite TSC	++	-	+		-	++

28874 I.1	-	no	possible TSC	+	-	-			-
28874 II.1	-	no	possible TSC	+	-		-		
28874 II.2	-	no	possible TSC	+			-		
28874 II.8			possible TSC	+					
29614 II.2		yes	possible TSC	+					
29614 II.3			possible TSC	+					
29614 III.4	-	yes	definite TSC	+	-		-	-	+
29614 IV.2	BD	yes	definite TSC	++	-	-		-	+
29614 IV.3	BD	yes	definite TSC	+	-	+			+

22931 II.2	MR	yes	definite TSC	++	-	-	-	-	++
24493		yes	probable TSC	+	-				+

Table 3. Comparison of the clinical findings in the *TSC2* c.3598C>T (p.R1200W) mutation carriers to TSC patients with a *TSC2* mutation described by Sancak et al. [Sancak et al., 2005]. Key: HMM, hypomelanotic macule; SP, shagreen patch; FA, facial angiofibroma; AML, renal angiomyolipoma. P indicates the number of individuals positive for the clinical feature and N the total number of patients examined.

Symptoms	***TSC2* c.3598C>T (p.R1200W) mutation carriers P/N (%)**	**Total cohort [Sancak et al., 2005] %**
HMM	16/16 (100%)	92%
SP	5/16 (31%)	49%
FA	3/16 (19%)	82%
CNS lesions	7/10 (62%)	89%
AML	0/10 (0%)	50%
rhabdomyoma	2/7 (29%)	42%
dental pits	1/5 (20%)	50%
eyes (retinal phakoma)	0/6 (0%)	37%
mental retardation	2/10 (20%)	83%
epilepsy	8/13 (62%)	91%

Appendix 4: Publications

BMC Medical Genetics

BioMed Central

Research article

Open Access

Functional characterisation of the TSC1–TSC2 complex to assess multiple *TSC2* variants identified in single families affected by tuberous sclerosis complex

Mark Nellist*[1], Özgür Sancak[1], Miriam Goedbloed[1], Alwin Adriaans[1], Marja Wessels[1], Anneke Maat-Kievit[1], Marieke Baars[2], Charlotte Dommering[2], Ans van den Ouweland[1] and Dicky Halley[1]

Address: [1]Department of Clinical Genetics, Erasmus Medical Centre, Rotterdam, The Netherlands and [2]Department of Clinical and Human Genetics, Free University Medical Centre, Amsterdam, The Netherlands

Email: Mark Nellist* - m.nellist@erasmusmc.nl; Özgür Sancak - Ozgur.Sancak@dsm.com; Miriam Goedbloed - m.goedbloed@erasmusmc.nl; Alwin Adriaans - a.adriaans@erasmusmc.nl; Marja Wessels - m.w.wessels@erasmusmc.nl; Anneke Maat-Kievit - j.a.maat@erasmusmc.nl; Marieke Baars - m.j.baars@amc.uva.nl; Charlotte Dommering - cj.dommering@vumc.nl; Ans van den Ouweland - a.vandenouweland@erasmusmc.nl; Dicky Halley - d.halley@erasmusmc.nl

* Corresponding author

Published: 26 February 2008

BMC Medical Genetics 2008, **9**:10 doi:10.1186/1471-2350-9-10

Received: 9 October 2007

Accepted: 26 February 2008

This article is available from: http://www.biomedcentral.com/1471-2350/9/10

Abstract

Background: Tuberous sclerosis complex (TSC) is an autosomal dominant disorder characterised by seizures, mental retardation and the development of hamartomas in a variety of organs and tissues. The disease is caused by mutations in either the *TSC1* gene on chromosome 9q34, or the *TSC2* gene on chromosome 16p13.3. The *TSC1* and *TSC2* gene products, TSC1 and TSC2, interact to form a protein complex that inhibits signal transduction to the downstream effectors of the mammalian target of rapamycin (mTOR).

Methods: We have used a combination of different assays to characterise the effects of a number of pathogenic TSC2 amino acid substitutions on TSC1–TSC2 complex formation and mTOR signalling.

Results: We used these assays to compare the effects of 9 different TSC2 variants (S132C, F143L, A196T, C244R, Y598H, I820del, T993M, L1511H and R1772C) identified in individuals with symptoms of TSC from 4 different families. In each case we were able to identify the pathogenic mutation.

Conclusion: Functional characterisation of TSC2 variants can help identify pathogenic changes in individuals with TSC, and assist in the diagnosis and genetic counselling of the index cases and/or other family members.

Background

Tuberous sclerosis complex (TSC) is an autosomal dominant disorder characterised by seizures, mental retardation and the development of hamartomas in a variety of organs and tissues [1]. The disease is caused by mutations in either the *TSC1* gene on chromosome 9q34 [2], or the

TSC2 gene on chromosome 16p13.3 [3]. Loss of heterozygosity studies at the *TSC1* and *TSC2* loci in TSC-associated lesions indicate that *TSC1* and *TSC2* are tumour suppressor genes [1]. Comprehensive screens for mutations at both the *TSC1* and *TSC2* loci have been performed in several large cohorts of TSC patients and a wide variety of different pathogenic mutations have been described [4-10]. In most studies approximately 20% of the identified mutations are either missense changes or small, non-truncating insertions/deletions, predominantly in the *TSC2* gene.

The phenotypic expression of TSC is highly variable and in some cases it can be difficult to establish a definitive clinical diagnosis. Generally the diagnosis is made based on multiple clinical criteria that are categorized into major and minor features [11]. The presence of 2 major features, or one major and 2 minor features, is sufficient for a definite diagnosis. In recent years, mutation analysis has become an additional diagnostic tool in familial as well as sporadic TSC. However, it is sometimes difficult to establish whether an identified nucleotide change, particularly a missense change, is a genuine pathogenic mutation, or a (rare) polymorphism. In familial cases where a missense change cosegregates with TSC, or in cases where key relatives are not available for testing, a distinction cannot be made on genetic grounds alone. Furthermore, many tools for the analysis of amino acid substitutions [12-14], may not predict the effect of a particular substitution reliably.

The *TSC1* and *TSC2* gene products, TSC1 and TSC2, interact to form a protein complex which acts as a GTPase activating protein (GAP) for the rheb GTPase, preventing the rheb-GTP-dependent stimulation of cell growth through the mammalian target of rapamycin (mTOR) [15]. In cells lacking either *TSC1* or *TSC2*, the downstream targets of mTOR, p70 S6 kinase (S6K) and ribosomal protein S6, are constitutively phosphorylated [16,17]. The identification of the role of the TSC1–TSC2 complex in regulating signal transduction through mTOR has made it possible to assess the activity of different TSC1 and TSC2 variants. The effects of amino acid changes on TSC1–TSC2 complex formation, on the activation of rheb GTPase activity by the complex, and on the phosphorylation status of S6K and S6, the downstream effectors of mTOR, can be determined [18,19].

Here, we apply assays of TSC1–TSC2 function to assist in the identification, diagnosis and counselling of 4 families with TSC. In each index case at least 2 changes in the *TSC2* gene were detected. To identify the disease-causing mutation in each family we characterised the effects of the changes on the activity of the TSC1–TSC2 complex. In each case we were able to identify the pathogenic *TSC2* variant. Our analysis demonstrates that biochemical assays can help resolve otherwise intractable problems in clinical genetic diagnostics.

Methods

Mutation analysis

DNA was extracted from peripheral blood using standard techniques. Mutation analysis was performed using a combination of single-strand conformational polymorphism analysis, denaturing gradient gel electrophoresis, direct sequencing, Southern blotting and fluorescence *in situ* hybridisation, as previously described [8]. In addition, the multiplex ligation-dependent probe amplification assay was performed (MRC Holland, The Netherlands). *TSC2* sequence changes were numbered according to the original cloning paper [3].

To investigate whether the changes had an effect on RNA splicing, 3 different splice-site prediction programs [12-14]. were used. Amino acid substitutions were evaluated using the PAM 250 [15], BLOSUM 62 [16] and Grantham [17] matrices and SCANSITE [23].

Generation of constructs and antisera

Expression constructs encoding the identified variants were derived using the Stratagene QuikChange site-directed mutagenesis kit and in each case verified by sequencing the complete open reading frame. All the other constructs used in this study have been described previously [21,24,25]. Polyclonal rabbit antisera specific for human TSC1 and TSC2 have been described previously [25]. Other antibodies were purchased from Cell Signaling Technology.

Transfections, immunocytochemistry, immunoblotting, immunoprecipitation assays and the *in vitro* assay of rheb GTPase activity were performed as described previously [21].

Results

Patient characteristics

Family 1

(Figure 1A) The index case (II:2) died shortly after birth due to a solitary rhabdomyoma in the right ventricle of the heart. Post-mortem examination did not reveal any other findings indicative of TSC. Both parents underwent a full clinical evaluation. Dermatological, cardiological, ophthalmological, neurological and radiological examinations were negative for signs of TSC except for one nail groove and one hypomelanotic macule in individual I:1. The sibling of the index case (II:1) was healthy, but was not investigated further. At the first trimester of the third pregnancy, mutation analysis of the index case had not been completed and prenatal DNA testing could not be offered. Fetal echocardiography did not reveal any heart

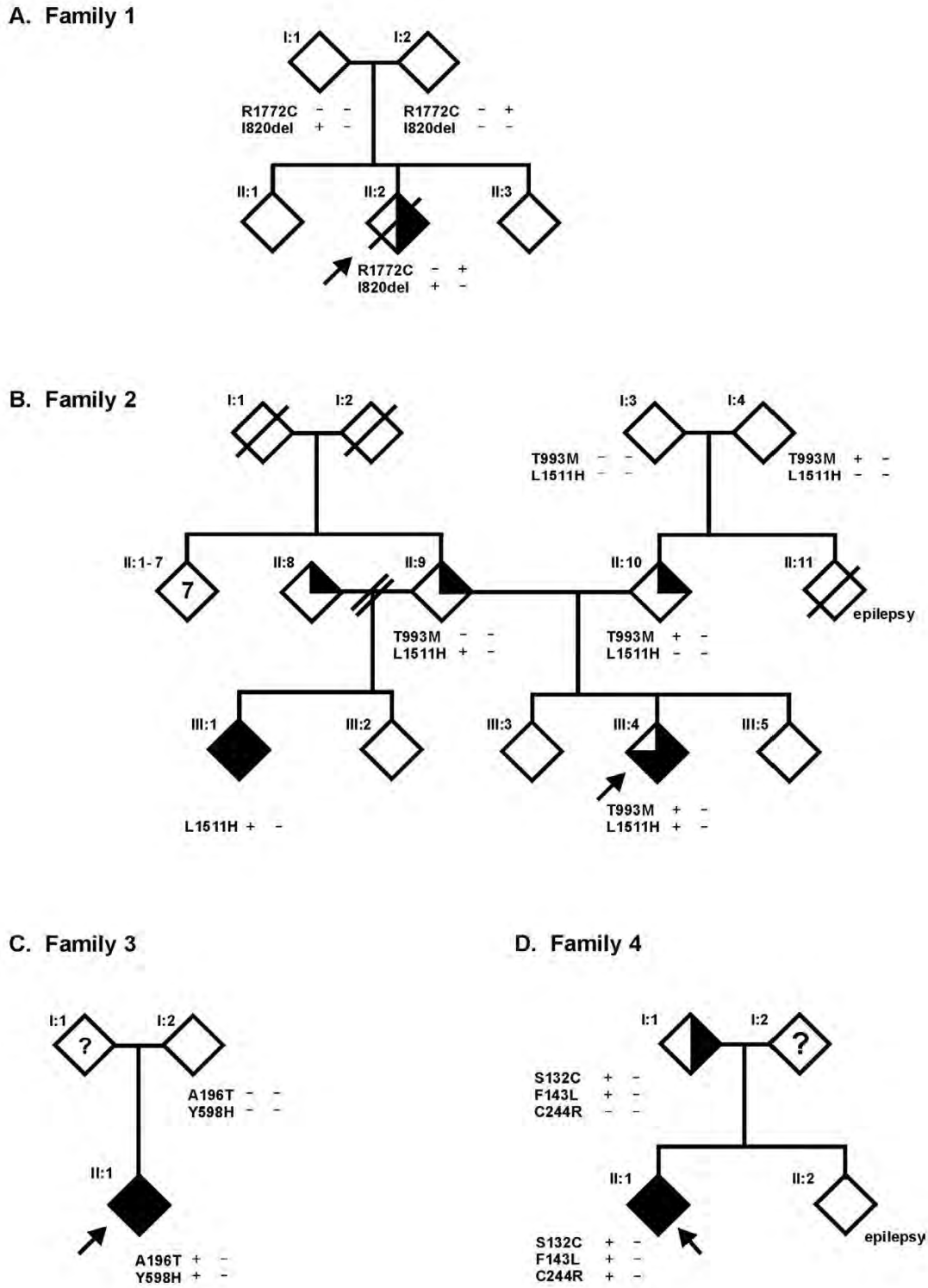

Figure 1

Pedigrees of the investigated families. (A) Family 1, (B) Family 2, (C) Family 3 and (D) Family 4. Arrows indicate the index cases. Clear symbols indicate no signs or symptoms of TSC; 1/4-filled symbols indicate one minor feature of TSC; 1/2-filled symbols indicate possible TSC; 3/4-filled symbols indicate probable TSC, filled symbols indicate definite TSC, and individuals with epilepsy only are indicated. A question mark indicates individuals where no clinical data was available. Genotypes are shown for the individuals where DNA was available for testing.

defects and the pregnancy resulted in the birth of a healthy child (II:3).

Family 2

(Figure 1B) The index case (III:4) had multiple hypomelanotic macules and dental pits, epilepsy and electroencephalographic abnormalities, and was diagnosed with 'probable TSC'. One of the parents of the index case (II:10) had multiple dental pits and a computer tomography scan revealed 2 small calcifications in the nucleus caudatus which were not typical for TSC. Magnetic resonance imaging was performed and showed no additional abnormalities. Individual II:9, the other parent of the index case, had a single 2 centimetre cyst in the left kidney and a single ash leaf-shaped area of hypopigmentation, insufficient for a diagnosis of TSC. Individual II:11, the sibling of II:10, had neurological and ophthalmological problems and died at the age of 13 due to status epilepticus. Individual III:1, the half-sibling of the index case and the child of individual II:9, had a history of possible epilepsy at the age of 3 years and was again diagnosed with epilepsy at 12 years of age. A subsequent full diagnostic work-up identified cortical tubers and 7 hypomelanotic macules, fulfilling the diagnostic criteria for definite TSC. Individual II:8 had multiple dental pits and 10 irregular hypopigmentations, atypical for TSC.

Family 3

(Figure 1C) The index case (II:1) was diagnosed with definite TSC. One parent (I:2) did not show any clinical signs of TSC, and there was no information on the other parent (I:1).

Family 4

(Figure 1D) The index case (II:1) was diagnosed with definite TSC. Individual I:1, the parent of the index case, had angiomyolipoma but no other reported signs of TSC, and individual II:2, the sibling of the index case had epilepsy, but no other signs of TSC.

Mutation analysis

Family 1

The index case (II:2) was heterozygous for 2 changes in the *TSC2* gene: *TSC2* 2476delATC (deletion of isoleucine at codon 820, I820del) and *TSC2* 5332C>T (arginine to cysteine substitution at codon 1772, R1772C). Analysis of the parents indicated that the index case had inherited one change from each parent. No DNA was available from other relatives.

Family 2

The index case (III:4) was heterozygous for 2 missense changes: *TSC2* 2996C>T (threonine to methionine substitution at codon 993, T993M) and *TSC2* 4550T>A (leucine to histidine amino acid substitution at position 1511, L1511H). Analysis of additional family members (individuals I:3, I:4, II:9, II:10 and III:3) confirmed that one substitution was paternal in origin and the other maternal.

Family 3

The index case (II:1) was heterozygous for 2 missense changes: *TSC2* 604G>A (alanine to threonine substitution at codon 196, A196T) and *TSC2* 1810T>C (tyrosine to histidine substitution at codon 598, Y598H). Neither substitution was detected in parent I:2, and DNA from parent I:1 was not available for testing.

Family 4

The index case (II:1) was heterozygous for 3 missense changes in the *TSC2* gene: *TSC2* 413C>G (serine to cysteine substitution at codon 132, S132C), *TSC2* 447C>G (phenylalanine to leucine substitution at codon 143, F143L) and *TSC2* 748T>C (cysteine to arginine substitution at codon 244, C244R). The S132C and F143L substitutions were inherited from parent I:1. No DNA was available from the other parent.

Comparison of the allele ratios of the index cases and parents did not reveal any evidence for somatic mosaicism in the leukocyte DNA from any of the families studied. None of the changes showed an effect on splicing according to the 3 splice-site prediction programs used.

As shown in Table 1, the identified amino acid changes were compared using the PAM 250 [15], BLOSUM 62 [16] and Grantham matrices [17]. In addition, the degree of conservation of the amino acid residues in different metazoan species was compared, as shown in Table 2.

Functional analysis

Families 1 and 2

The genetic data from families 1 and 2 indicated that in both families the index case had inherited a different, rare *TSC2* variant from each parent. To determine whether the I820del, R1772C, T993M and L1511H variants corresponded to pathogenic mutations, the biochemical activity of each variant was compared to wild-type TSC2 and a known, pathogenic TSC2 missense variant (R611Q) using a variety of functional assays.

To investigate the ability of the TSC2 I820del, R1772C, T993M and L1511H variants to interact with TSC1, coimmunoprecipitation experiments were performed using antibodies specific for TSC1. As shown in Figures 2A and 2B, coimmunoprecipitation of the TSC2 I820del variant was reduced compared to wild-type TSC2, but was not prevented completely (compare the I820del variant to the R611Q variant). The R1772C, T993M and L1511H amino

Table 1: Scores of the BLOSUM 62, PAM 250 and Grantham matrices. BLOSUM 62 scores range between -4 and 11, PAM 250 scores between -8 and 17, and Grantham scores between 5 and 215. For the BLOSUM 62 and PAM 250 matrices, a more negative score corresponds to a less conservative amino acid change. For the Grantham matrix, a higher number reflects a less conservative change.

Amino Acid Substitution	Family	BLOSUM 62	PAM 250	Grantham
TSC2 R1772C	1	-3	-4	180
TSC2 T993M	2	-1	-1	81
TSC2 L1511H	2	-3	-2	99
TSC2 A196T	3	0	1	58
TSC2 Y598H	3	2	0	83
TSC2 S132C	4	-1	0	112
TSC2 F143L	4	0	2	22
TSC2 C244R	4	-3	-4	180

acid substitutions did not reduce TSC1–TSC2 coimmunoprecipitation.

Next, the activation of rheb GTPase activity by the immunoprecipitated variant TSC1–TSC2 complexes was assayed. As shown in Figure 2C, in the presence of the wild-type TSC1–TSC2 complex the ratio of rheb-bound GDP to GTP was 3-fold higher than in the presence of TSC1 alone (control GDP/GTP = 0.4; wild-type GDP/GTP = 1.4). Coimmunoprecipitation of the TSC2 I820del variant was reduced compared to wild-type TSC2, and consequently the activation of rheb GTPase activity was also reduced (wild-type GDP/GTP = 1.4; I820del GDP/GTP = 0.9).

Table 2: Evolutionary conservation of the variant TSC2 amino acids. Inter-species conservation of the TSC2 S132, F143, A196, C244, Y598 I820, T993, L1511 and R1772 amino acids is shown.

Family 1			
	I820	R1772	
human	PDII**I**KALP	GQRK**R**LISS	
mouse	PDII**I**KALP	GQRK**R**LISS	
rat	PDII**I**KALP	GQRK**R**LISS	
pufferfish	PDIM**I**KLLP	GQRK**R**LVST	
fruitfly	PEALMRKLP	no homology	
Family 2			
	T993	L1511	
human	SRIQ**T**SLTS	SVQL**L**DQIP	
mouse	SRIQ**T**SLTS	SVQL**L**DQIP	
rat	SRIQ**T**SLTS	SVQL**L**DQIP	
pufferfish	RRMH**T**STTT	AVKV**L**DQMP	
fruitfly	no homology	AVSLIDLVP	
Family 3			
	A196	Y598	
human	DEYI**A**RM V	IQLH**Y**KHSY	
mouse	DEYI**A**SM V	IQLH**Y**KHGY	
rat	DEYI**A**PM V	IQLH**Y**KHGY	
pufferfish	DQNV**A**SM V	LQLH**Y**KNKY	
fruitfly	DKDILVGIV	LELH**Y**ERPK	
Family 4			
	S132	F143	C244
human	KDYP**S** NED	RLEV**F**KALT	IVTL**C**RTIN
mouse	KDYP**S** NED	RLEV**F**KALT	IITL**C**RTIN
rat	KDYP**S** NED	RLEV**F**KALT	IITL**C**RTVN
pufferfish	RDYQPCNED	RLEV**F**KALT	IITL**C**RTVN
fruitfly	IQNHEARED	LLELLDTLT	ITTL**C**RTVN

The immunoprecipitated R1772C and T993M variant complexes increased the GDP/GTP ratio more than 4-fold above the control value, and were therefore both at least as active as wild-type TSC2 (wild-type GDP/GTP = 1.4; R1772C and T993M GDP/GTP = 1.9). In contrast, although TSC1–TSC2 coimmunoprecipitation was unaffected by the L1511H substitution, the activation of rheb GTPase activity was reduced 3-fold compared to wild-type (wild-type GDP/GTP = 1.4; L1511H GDP/GTP = 0.5).

To determine whether the TSC2 I820del, R1772C, T993M and L1511H variants affected mTOR activity, the variants were overexpressed together with TSC1 and S6K in human embryonal kidney 293 cells. Phosphorylation of the exogenous S6K linker domain (T389), as detected by immunoblotting, was used as a read-out for mTOR activity. As shown in Figure 2E and 2F, S6K T389 phosphorylation was increased in the presence of the TSC2 I820del, L1511H and R611Q variants, compared to wild-type TSC2 and the R1772C and T993M variants. To confirm these findings, TSC1 and the TSC2 variants were overexpressed in *Tsc2* -/- mouse embryo fibroblasts (MEFs) [16]. The S235/S236 phosphorylation of S6 in the MEFs expressing the TSC2 variants was determined by double-label immunofluorescent microscopy, as described previously [21]. As shown in Figure 2D, expression of the TSC2 R1772C and T993M variants suppressed S6 phosphorylation in more than 90% of the transfected cells, similar to wild-type TSC2. In contrast, less than 20% of the MEFs expressing the TSC2 I820del, L1511H or R611Q variants showed inhibition of S6 phosphorylation. Therefore, in both assays, the TSC2 I820del and L1511H variants were unable to inhibit mTOR, indicating that both these variants are pathogenic, while the TSC2 R1772C and T993M

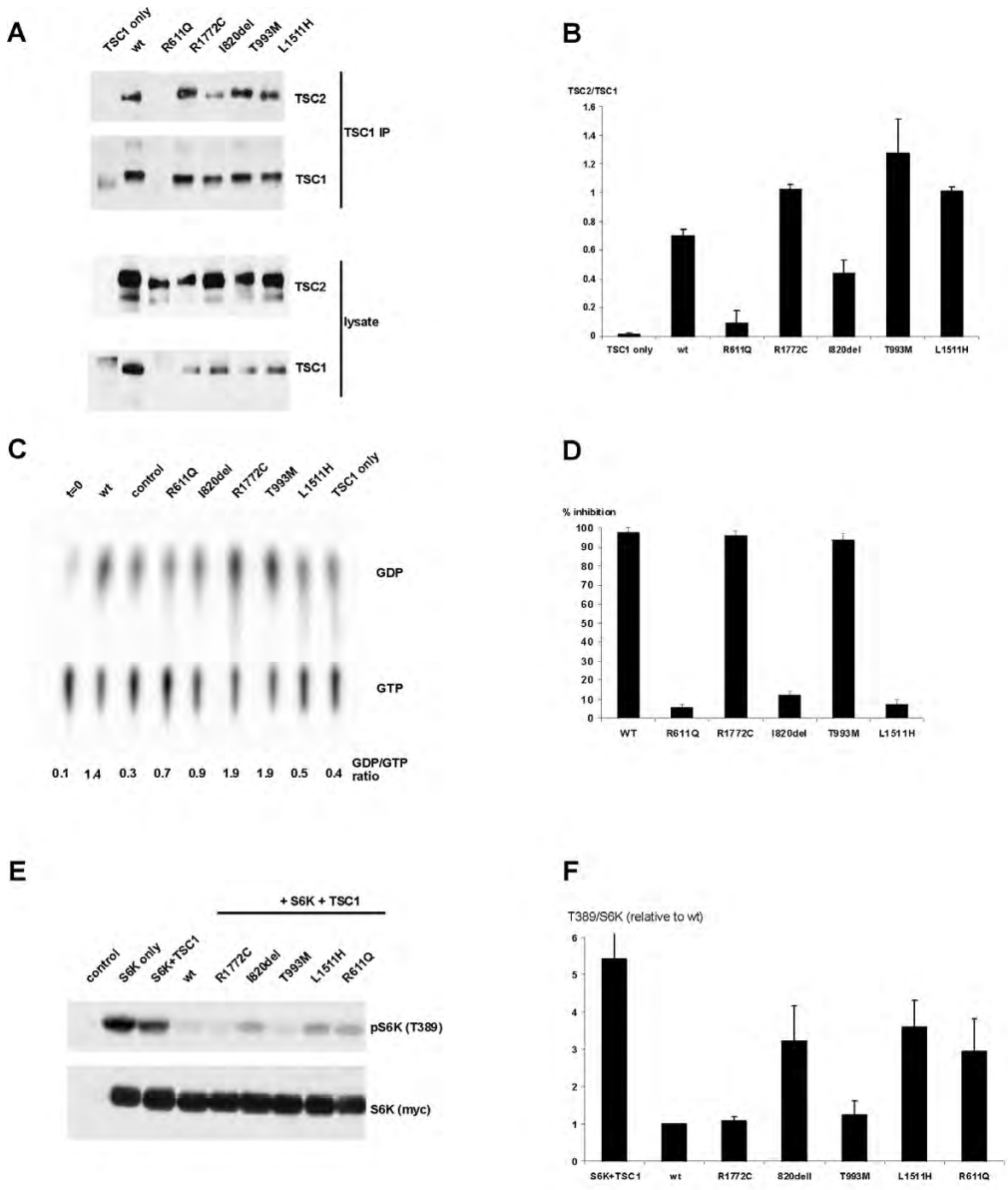

Figure 2

Results of the functional assays on the TSC2 variants identified in family 1 (variants I820del and R1772C) and family 2 (variants T993M and L1511H). (A) Interaction between TSC1 and TSC2 variants. TSC1–TSC2 complexes were immunoprecipitated with antibodies specific for exogenous TSC1 from HEK 293 cells over-expressing TSC1 and wild-type TSC2 (wt) or TSC1 and the TSC2 variants. (B) Interaction between TSC1 and TSC2 variants. Ratio of coimmunoprecipitated TSC2:TSC1, as detected by immunoblotting, was estimated by densitometry scanning (Total Scan). (C) *In vitro* rheb GAP activity of immunoprecipitated TSC1–TSC2 complexes. Rheb-bound GDP/GTP ratios were determined after 90 minutes incubation with the immunoprecipitated wild-type TSC1–TSC2 complex (wt), protein A beads only (control), TSC1 only, or TSC1–TSC2 variant complexes. Rheb-bound GDP/GTP prior to addition of the TSC1–TSC2 complexes is shown (t = 0). (D) Inhibition of S6 phosphorylation in Tsc2 -/- MEFs. Percentage of *Tsc2* -/- MEFs transfected with expression constructs encoding TSC1 and wild-type TSC2, or TSC1 and the TSC2 variants, and showing inhibition of S6 phosphorylation. Data from at least 3 separate experiments are shown. (E) TSC2-dependent inhibition of S6K-T389 phosphorylation. S6K, TSC1 and wild-type TSC2 (wt), or S6K, TSC1 and the TSC2 variants, were coexpressed in HEK 293 cells. Phosphorylation of S6K at the T389 position was determined by immunoblotting. A representative example of at least 3 separate experiments is shown. (E) TSC2-dependent inhibition of S6K-T389 phosphorylation. Ratio of total S6K:T389-phosphorylated S6K, as detected by immunoblotting, was estimated by densitometry scanning (Total Scan). Mean ratios relative to TSC2 wild-type (wt) are shown.

variants were just as active as wild-type TSC2 and are therefore not pathogenic amino acid substitutions.

Families 3 and 4

In families 3 and 4, the clinical and genetic data was incomplete. Multiple *TSC2* variants were identified in the index cases, but it was not clear if they were *de novo*, or had been inherited from an untested parent. It was also unclear whether the changes were confined to the same allele. Therefore, to investigate the effects of the changes on the ability of the TSC1–TSC2 complex to antagonise mTOR signalling, TSC2 variants containing the different combinations of amino acid substitutions were characterised.

As shown in Figure 3A and 3B, S6K T389 phosphorylation was inhibited by expression of the TSC2 S132C, F143L and A196T single variants, and by the S132C/F143L double variant. In contrast, expression of the C244R and Y598H single variants did not inhibit S6K phosphorylation, and expression of TSC1 was reduced in the presence of these variants. Consistent with these observations, the S132C/F143L/C244R triple variant and A196T/Y598H double variant were unable to inhibit S6K phosphorylation and TSC1 expression was reduced in the presence of these variants, compared to in the presence of wild-type TSC2. To provide confirmation for these data, double-label immunofluorescent microscopy was performed to determine whether S6 phosphorylation was down-regulated in *Tsc2* -/- MEFs expressing the different variants. As shown in Figure 3C, expression of the TSC2 C244R, S132C/F143L/C244R, Y598H and A196T/Y598H variants was unable to inhibit S6 phosphorylation in the *Tsc2* -/- MEFs. Therefore, in both assays, the Y598H and C244R variants correspond to the pathogenic mutations in families 3 and 4 respectively.

Discussion

Mutation analysis of the *TSC1* and *TSC2* genes in individuals with TSC, and in those suspected of having the disease, facilitates the diagnosis of TSC, and can help genetic counselling. In most cases, analysis of the patient's DNA results in the identification of a pathogenic mutation. However, in some cases it is impossible to determine from the genetic data alone whether specific, identified changes are pathogenic or not. This can be a particular problem when a change co-segregates with signs of TSC in a single family. To address such cases, we have performed functional analysis of the predicted protein products of the *TSC2* variants identified in 4 families with TSC.

In families 1 and 2 the index case did not fulfil the diagnostic criteria for TSC and had inherited 2 non-truncating *TSC2* nucleotide changes, one from each parent. It was not possible to determine from the clinical and genetic data alone whether the families were affected by TSC and, if that was the case, which nucleotide change was the disease-causing mutation.

In families 3 and 4, in which the index case did fulfil the diagnostic criteria for TSC, it was impossible to determine whether the identified TSC2 variant was pathogenic because essential genetic and/or clinical data was not available. In all the above cases we analysed the effect of the identified changes on the activity of the TSC1–TSC2 complex in order to establish which of the changes were pathogenic mutations.

Families 1 and 2

The *in vitro* GTPase activity of rheb was not stimulated in the presence of the TSC2 I820del and L1511H variants, and neither variant was able to inhibit S6K and S6 phosphorylation as effectively as wild-type TSC2, or the R1772C and T993M variants. In addition, the I820del variant formed a complex with TSC1 less efficiently than wild-type TSC2. The I820del and L1511H changes therefore had similar effects to other pathogenic TSC2 missense mutations, disrupting the function of the TSC1–TSC2 complex *in vitro*. We classified the I820del and L1511H variants as pathogenic mutants. The R1772C and T993M substitutions had no effect on TSC1–TSC2 activity in the assays used and were therefore classified as rare polymorphisms.

In utero cardiac rhabdomyoma was the only sign of TSC in the index patient of family 1 (individual II:2). Rhabdomyoma is the most common foetal and neonatal cardiac tumour and although it can be associated with several different genetic disorders, TSC is implicated in as many as two-thirds of the cases [26]. Confirmation of the inactivating nature of the TSC2 I820del mutation identified in family 1 meant that a diagnosis of TSC could be assigned to individuals I:1 and II:2 with more certainty. Previously, the very mild presentation of the disease in individual I:1 had made diagnosis difficult. Mutation analysis, complemented by functional assays, was required to establish whether this individual carried a pathogenic *TSC2* mutation, and the identification of a mutation in this individual has implications for the family in regard to decisions about having additional children and to the risk of other relatives of the parent. Somatic mosaicism in individual I:1 could not be rigorously excluded, since only leukocyte DNA was available for analysis. Therefore, the recurrence risk for this couple is up to 50%.

Analysis of the TSC2 I820del mutant indicated that the isoleucine residue helps to stabilise TSC1–TSC2 binding. However, since some TSC1–TSC2 binding was detected, and some rheb GAP activity could also be measured, it is possible that the TSC2 I820del variant retains some activ-

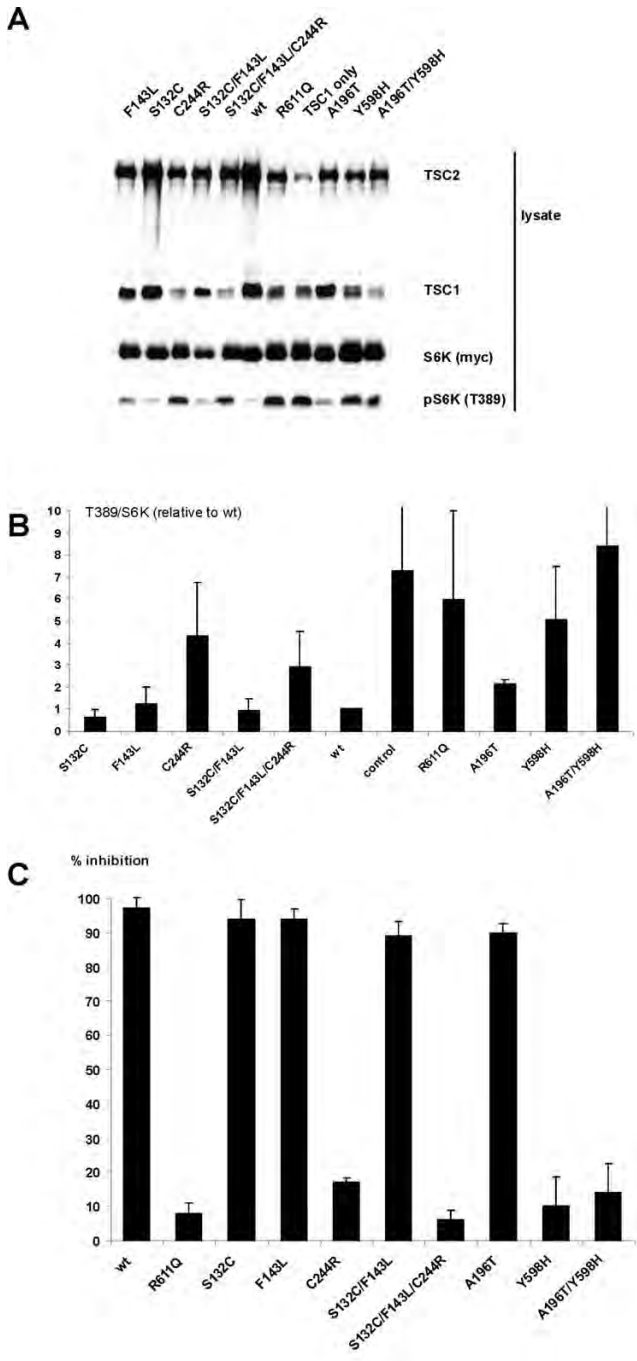

Figure 3
Results of the functional assays on the TSC2 variants identified in family 3 (variants A196T and Y598H) and family 4 (variants S132C, F143L and C244R). (A) TSC2-dependent inhibition of S6K-T389 phosphorylation. S6K, TSC1 and wild-type TSC2 (wt), or S6K, TSC1 and the TSC2 variants, were overexpressed in HEK 293 cells. Phosphorylation of S6K at the T389 position was determined by immunoblotting. A representative example of at least 3 separate experiments is shown. (B) TSC2-dependent inhibition of S6K-T389 phosphorylation. Ratio of total S6K:T389-phosphorylated S6K, as detected by immunoblotting, was estimated by densitometry scanning (Total Scan). Mean ratios relative to TSC2 wild-type (wt) are shown.(C) Inhibition of S6 phosphorylation in *Tsc2* -/- MEFs. Percentage of *Tsc2* -/- MEFs transfected with expression constructs encoding TSC1 and wild-type TSC2, or TSC1 and the TSC2 variants, and showing inhibition of S6 phosphorylation. Data from at least 3 separate experiments are shown.

ity *in vivo*. This provides a possible explanation for the mild symptoms in individual I:1. The second variant identified in family 1, TSC2 R1772C, did not have a deleterious effect on the activity of the TSC1–TSC2 complex. This was somewhat surprising as the R1772 residue is part of the consensus extracellular signal-regulated kinase (ERK) phosphorylation site that has been shown to be involved in regulating the activity of the complex [27,28]. Indeed, SCANSITE [23] indicated that the R1772C substitution destroys the putative ERK phosphorylation site. Furthermore, both the BLOSUM 62 and PAM 250 matrices indicated that the R1772C substitution is likely to have a deleterious effect on TSC2 structure. One possibility is that under certain conditions, the R1772C substitution may have a modifying effect on the TSC1–TSC2 complex, enhancing TSC1–TSC2 activity by preventing the Erk-dependent down-regulation of the complex [28]. This may explain the increased rheb GTPase activity measured in the presence of the TSC2 R1772C variant, compared to wild-type TSC2 (wild-type TSC2 GDP/GTP ratio = 1.4; R1772C GDP/GTP ratio = 1.9; Figure 2B).

Both the 2476delATC (I820del) and 5332C>T (R1772C) variants have been identified in TSC patients by other researchers [29-31]. Strizheva *et al*. [30] suggested that the R1772C substitution could be a pathogenic change while Langkau *et al*. [31] concluded that it was a polymorphism. The status of the I820del change was not certain [29]. Our analysis is consistent with the findings of Langkau *et al*. and, in addition, indicates that the TSC2 I820del variant is pathogenic. Furthermore, this example demonstrates that predictions about the pathogenicity of missense changes based on the results of the BLOSUM 62, PAM 250 and Grantham matrices are not always reliable.

In family 2, mutation analysis resulted in the identification of 2 novel *TSC2* missense changes, 2996C>T (T993M) and 4550T>A (L1511H), in the index case (individual III:4). Individual III:1, the half-sibling of the index case was later diagnosed with TSC on the basis of the accepted clinical criteria and was found to carry the *TSC2* 4550T>A (L1511H) substitution only. No other nucleotide changes were identified in the *TSC1* or *TSC2* genes in either individual. The identification of the TSC2 L1511H change in individual III:1 excluded the T993M change as the common cause of TSC in this family. However, it did not confirm the pathogenicity of the TSC2 L1511H change. The presence of multiple dental pits in both individual II:8 and individual II:10 suggested that the signs of TSC in individuals III:1 and III:4 could be caused by two different mutations, inherited from individuals II:8 and II:12 respectively. However, the functional tests confirmed the pathogenic nature of the TSC2 L1511H substitution, indicating that this was the disease-causing mutation in both cases. The substitution of a basic histidine residue for a nonpolar leucine residue at position 1511 did not affect the TSC1–TSC2 interaction, but did abrogate the rheb GAP activity of the TSC1–TSC2 complex. Although L1511 is outside the predicted TSC2 GAP domain [3], it is clearly necessary for activity. The substitution of a polar threonine for nonpolar methione at position 993 had no deleterious effect on the TSC1–TSC2 interaction or on the activity of the complex. The T993M substitution occurs at a possible site of protein kinase B (PKB)-dependent phosphorylation [27], and may therefore inhibit PKB-mediated inactivation of the TSC1–TSC2 complex. This may explain why the TSC2 T993M variant, like the R1772C variant, had a higher *in vitro* rheb GAP activity than wild-type TSC2 (wild-type TSC2 GDP/GTP ratio = 1.4; T993M GDP/GTP ratio = 1.9; Figure 2B). The T993M polymorphism may therefore also act as a positive modifier of TSC1–TSC2 activity.

In family 3, 2 missense changes (*TSC2* 604G>A (A196T) and *TSC2* 1810T>C (Y598H)) were identified in the index case (individual II:1). Since there was no genetic or clinical data on one of the parents, it was not possible to determine whether either of the changes was responsible for TSC in this individual. Both variants had been identified previously in other TSC patients [29], however in these patients it was also not clear whether the changes were pathogenic. Functional analysis indicated that the TSC2 Y598H substitution reduced TSC1–TSC2 binding and the TSC1–TSC2 dependent inhibition of mTOR activity. In contrast, the A196T substitution did not affect TSC2 activity. Therefore, the Y598H substitution was responsible for TSC in individual II:1, as well as in other TSC patients [29], and the A196T substitution is a rare polymorphism.

In family 4, 3 missense changes were identified in the *TSC2* gene. The 413C>G (S132C) and 447C>G (F143L) substitutions were inherited from a parent with symptoms suggesting TSC. The third substitution, 748T>C (C244R), was either a *de novo* mutation, or was inherited from the other parent, on whom there was no clinical or genetic data. None of these changes have been described previously [29]. One possibility in this family was that the combination of missense changes was responsible for the TSC phenotype. Therefore we tested all the individual TSC2 single amino acid variants (S132C, F143L and C244R) as well as the TSC2 S132C/F143L double variant and TSC2 S132C/F143L/C244R triple amino acid variant. Neither the S132C nor the F143L changes had a significant effect on TSC1–TSC2 function. In some assays the F143L variant appeared less active than wild-type TSC2, but still had the ability to significantly inhibit mTOR activity. In contrast, the C244R amino acid substitution reduced TSC1–TSC2 binding and was unable to inhibit mTOR activity, either alone or in combination with the S132C and F143L variants. We concluded that the C244R

substitution was the pathogenic mutation in the index case. Individual I:1 tested negative for the *TSC2* 748T>C (C244R) substitution, but was diagnosed with angiomyolipomas. Although insufficient for a definite diagnosis of TSC, the incidence of angiomyolipomas is high in the TSC patient population. One possibility is that this individual is a mosaic for the *TSC2* 748T>C (C244R) susbstitution, and that the angiomyolipoma originates from these mosaic cells. An alternative explanation is that the *TSC2* 447C>G (F143L) substitution does have an effect on TSC2 function, sufficient to allow the formation of angiolipoma. The F143L amino acid substitution may therefore be a negative modifier of TSC1–TSC2 activity, in contrast to the R1772C and T993M substitutions identified in families 1 and 2, that, in some assays, appeared to increase TSC1–TSC2 activity. Although there was no evidence in family 1 or family 2 for the non-pathogenic TSC2 variant acting in trans to neutralise the pathogenic variant, it will be interesting to determine whether there are 'hyperactive' TSC1 and TSC2 variants that can (partially) compensate for the presence of pathogenic TSC1 and TSC2 variants. Improving the sensitivity and reliability of the assays of TSC1–TSC2 activity will allow us to more accurately define the activity of different TSC1 and TSC2 variants.

We did not investigate the other putative functions of TSC2 since, in each family, we were able to differentiate between the TSC2 variants on the basis of their inhibition of mTOR signalling. However, it may also be informative to investigate the effects of pathogenic and non-pathogenic amino acid substitutions on the other proposed functions of TSC2, such as the regulation of p27 [32].

Care must always be taken in the interpretation of nucleotide or amino acid changes identified during molecular genetic investigations. As the examples described here demonstrate, both the affection status of individuals in a family and the nature of the nucleotide changes identified in those individuals are not always clear. To distinguish between pathogenic mutations and harmless polymorphisms, we have analysed the effects of different amino acid changes on the activity of the TSC1–TSC2 complex. In each case we have been able to distinguish pathogenic TSC2 variants from rare polymorphic variants, and thereby identify the mutation in each family. We have shown that functional assays can be a useful tool to complement traditional DNA-based mutation analysis in TSC. Identification of the pathogenic mutations in the TSC families described here enabled not only genetic counselling and prenatal testing for future pregnancies but also improved the diagnosis of affected family members to facilitate their critical clinical care. The use of functional assays to differentiate between polymorphisms and pathogenic mutations, in TSC and other diseases, will facilitate not only the identification of pathogenic mutations but will also help establish how different amino acid residues contribute to protein function.

Conclusion

Deletion of isoleucine at amino acid residue 820 of TSC2 and the TSC2 L1511H, C244R and Y598H amino acid substitutions are sufficient to cause TSC. The TSC2 R1772C, T993M, S132C, F143L and A196T substitutions are rare polymorphisms that do not inhibit TSC1–TSC2 function, and do not cause TSC.

Abbreviations

DNA, deoxyribonucleic acid; ERK, extracellular regulated kinase; GAP, GTPase activating protein; GDP, guanosine diphosphate; GTP, guanosine triphosphate; HEK 293, human embryonal kidney cells; MEFs, mouse embryo fibroblasts; mTOR, mammalian target of rapamycin; PKB, protein kinase B; rheb, ras homolog expressed in brain; RNA, ribonucleic acid; S6K, p70 S6 kinase; TSC, tuberous sclerosis complex.

Competing interests

The author(s) declare that they have no competing interests.

Authors' contributions

MN, OS, MG and AA performed the practical work; MW, AM-K, MB and CD co-ordinated the clinical investigations of the patients; AvdO and DH led the research. The manuscript was drafted by OS, MN, AvdO and DH, and read and approved by all authors.

Acknowledgements

Financial support was provided by the U.S. Department of Defense Congressionally-Directed Medical Research Program (grant #TS060052), the Nederlandse Organisatie voor Wetenschappelijk Onderzoek (NWO), the Nationaal Epilepsie Fonds, the Michellestichting and the Department of Clinical Genetics (Erasmus MC). Dr. H. Onda (Brigham and Women's Hospital, USA) is thanked for supplying the *Tsc1* -/- and *Tsc2* -/- MEFs. Dr. M. van Slegtenhorst (Fox Chase Cancer Center, USA) and Dr. T. Nobukini (Friedrich Miescher Institute, Switzerland) are thanked for supplying rheb and S6K expression constructs respectively. We thank the family members who contributed to this study.

References

1. Gomez M, Sampson J, Whittemore V, eds: *The tuberous sclerosis complex* Oxford, UK: Oxford University Press; 1999.
2. van Slegtenhorst M, de Hoogt R, Hermans C: **Identification of the tuberous sclerosis gene *TSC1* on chromosome 9q34.** *Science* 1997, **277(5327):**805-808.
3. The European Chromosome 16 Tuberous Sclerosis Consortium: **Identification and characterization of the tuberous sclerosis gene on chromosome 16.** *Cell* 1993, **75(7):**1305-1315.
4. Jones AC, Shyamsundar MM, Thomas MW: **Comprehensive mutation analysis of *TSC1* and *TSC2*, and phenotypic correlations in 150 families with tuberous sclerosis.** *Am J Hum Genet* 1999, **64(5):**1305-1315.
5. van Slegtenhorst M, Verhoef S, Tempelaars A: **Mutational spectrum of the *TSC1* gene in a cohort of 225 tuberous sclerosis complex patients: no evidence for genotype-phenotype correlation.** *J Med Genet* 1999, **36(4):**285-289.

6. Au KS, Rodriguez JA, Finch JL: **Germ-line mutational analysis of the *TSC2* gene in 90 tuberous sclerosis patients.** *Am J Hum Genet* 1998, **62(2):**286-294.
7. Dabora SL, Jozwiak S, Franz DN: **Mutational analysis in a cohort of 224 tuberous sclerosis patients indicates increased severity of *TSC2*, compared with *TSC1*, disease in multiple organs.** *Am J Hum Genet* 2001, **68(1):**64-80.
8. Sancak O, Nellist M, Goedbloed M: **Mutational analysis of the *TSC1* and *TSC2* genes in a diagnostic setting: genotype-phenotype correlations and comparison of diagnostic DNA techniques in tuberous sclerosis complex.** *Eur J Hum Genet* 2005, **13(6):**731-741.
9. Niida Y, Lawrence-Smith N, Banwell A: **Analysis of both *TSC1* and *TSC2* for germline mutations in 126 unrelated patients with tuberous sclerosis.** *Hum Mutat* 1999, **14(5):**412-422.
10. Au K-S, Williams AT, Roach ES: **Genotype/phenotype correlation in 325 individuals referred for a diagnosis of tuberous sclerosis complex in the United States.** *Genet Med* 2007, **9(2):**88-100.
11. Roach ES, DiMario FJ, Kandt RS: **Tuberous sclerosis consensus conference: recommendations for diagnostic evaluation. National Tuberous Sclerosis Association.** *J Child Neurol* 1999, **14(6):**401-407.
12. **NetGene2 Server** [http://www.cbs.dtu.dk/services/NetGene2]
13. **SpliceSiteFinder** [http://www.genet.sickkids.on.ca/~ali/splicesitefinder.html]
14. **BDGP: Splice Site Prediction by Neural Network** [http://www.fruitfly.org/seq_tools/splice.html]
15. Dayhoff MO, Schwartz RM, Orcutt BC: **A model of evolutionary change in proteins.** "*Atlas of Protein Sequence and Structure*" 1978, **5(3):**345-352.
16. Henikoff S, Henikoff J: **Amino acid substitution matrices from protein blocks.** *Proc Natl Acad Sci USA* 1992, **89:**10915-10919.
17. Grantham R: **Amino acid difference formula to help explain protein evolution.** *Science* 1974, **185(4154):**862-864.
18. Li Y, Corradetti MN, Inoki K: **TSC2: filling the GAP in the mTOR signaling pathway.** *Trends Biochem Sci* 2004, **29:**32-38.
19. Zhang H, Cicchetti G, Onda H: **Loss of Tsc1/Tsc2 activates mTOR and disrupts PI3K-Akt signaling through downregulation of PDGFR.** *J Clin Invest* 2003, **112:**1223-1233.
20. Kwiatkowski DJ, Zhang H, Bandura JL: **A mouse model of TSC1 reveals sex-dependent lethality from liver hemangiomas, and up-regulation of p70S6 kinase activity in Tsc1 null cells.** *Hum Mol Genet* 2002, **11(5):**525-534.
21. Nellist M, Sancak O, Goedbloed MA: **Distinct effects of single amino acid changes to tuberin on the function of the tuberin-hamartin complex.** *Eur J Hum Genet* 2005, **13(1):**59-68.
22. Inoki K, Li Y, Zu T: **TSC2 is phosphorylated and inhibited by Akt and suppresses mTOR signalling.** *Nat Cell Biol* 2002, **4(9):**648-657.
23. Obenauer JC, Cantley LC, Yaffe MB: **Scansite 2.0: Proteome-wide prediction of cell signaling interactions using short sequence motifs.** *Nucleic Acids Res* 2003, **31(13):**3635-3641.
24. Nellist M, Verhaaf B, Goedbloed MA: ***TSC2* missense mutations inhibit tuberin phosphorylation and prevent formation of the tuberin-hamartin complex.** *Hum Mol Genet* 2001, **10(25):**2889-2898.
25. van Slegtenhorst M, Nellist M, Nagelkerken B: **Interaction between hamartin and tuberin, the *TSC1* and *TSC2* gene products.** *Hum Mol Genet* 1998, **7(6):**1053-1057.
26. Isaacs H Jr: **Fetal and neonatal cardiac tumors.** *Pediatr Cardiol* 2004, **25(3):**252-273.
27. Ballif B, Roux PP, Gerber SA: **Quantitative phosphorylation profiling of the ERK/p90 ribosomal S6 kinase-signaling cassette and its targets, the tuberous sclerosis tumor suppressors.** *PNAS* 2005, **102(3):**667-672.
28. Ma L, Chen Z, Erdjument-Bromage H, Tempst P, Pandolfi PP: **Phosphorylation and functional inactivation of TSC2 by Erk implications for tuberous sclerosis and cancer pathogenesis.** *Cell* 2005, **121(2):**179-193.
29. **Tuberous sclerosis database – Leiden Open Variation Database** [http://chromium.liacs.nl/LOVD2/TSC/home.php]
30. Strizheva GD, Carsillo T, Kruger WD: **The spectrum of mutations in *TSC1* and *TSC2* in women with tuberous sclerosis and lymphangiomyomatosis.** *Am J Respir Crit Care Med* 2001, **163(1):**253-258.
31. Langkau N, Martin N, Brandt R: ***TSC1* and *TSC2* mutations in tuberous sclerosis, the associated phenotypes and a model to explain observed *TSC1*/*TSC2* frequency ratios.** *Eur J Pediatr* 2002, **161(7):**393-402.
32. Rosner M, Freilinger A, Hanneder M: **p27Kip1 localization depends on the tumor suppressor protein tuberin.** *Hum Mol Genet* 2007, **16(13):**1541-1546.

Pre-publication history

The pre-publication history for this paper can be accessed here:

http://www.biomedcentral.com/1471-2350/9/10/prepub

European Journal of Human Genetics (2009) 17, 319 – 328

www.nature.com/ejhg

ARTICLE

Missense mutations to the *TSC1* gene cause tuberous sclerosis complex

Mark Nellist*[,1], Diana van den Heuvel[1], Diane Schluep[1], Carla Exalto[1], Miriam Goedbloed[1], Anneke Maat-Kievit[1], Ton van Essen[2], Karin van Spaendonck-Zwarts[2], Floor Jansen[3], Paula Helderman[4], Gabriella Bartalini[5], Outi Vierimaa[6], Maila Penttinen[7], Jenneke van den Ende[8], Ans van den Ouweland[1] and Dicky Halley[1]

[1]*Department of Clinical Genetics, Erasmus Medical Centre, Rotterdam, The Netherlands;* [2]*Department of Genetics, University Medical Center Groningen, University of Groningen, Groningen, The Netherlands;* [3]*Department of Child Neurology, Rudolf Magnus Institute for Neuroscience, University Medical Centre Utrecht, Utrecht, The Netherlands;* [4]*Department of Clinical Genetics, Maastricht University Medical Centre, Maastricht, The Netherlands;* [5]*Department of Clinical Pediatrics, University of Siena, Siena, Italy;* [6]*Department of Clinical Genetics, Oulu University Hospital, Oulu, Finland;* [7]*Clinical Genetics Unit, Department of Pediatrics, Turku University Central Hospital, Turku, Finland;* [8]*Centre of Medical Genetics, University of Antwerp, Antwerp, Belgium*

Tuberous sclerosis complex (TSC) is an autosomal dominant disorder characterised by the development of hamartomas in a variety of organs and tissues. The disease is caused by mutations in either the *TSC1* gene on chromosome 9q34 or the *TSC2* gene on chromosome 16p13.3. The *TSC1* and *TSC2* gene products, TSC1 and TSC2, interact to form a protein complex that inhibits signal transduction to the downstream effectors of the mammalian target of rapamycin (mTOR). Here we investigate the effects of putative *TSC1* missense mutations identified in individuals with signs and/or symptoms of TSC on TSC1–TSC2 complex formation and mTOR signalling. We show that specific amino-acid substitutions close to the N-terminal of TSC1 reduce steady-state levels of TSC1, resulting in the activation of mTOR signalling and leading to the symptoms of TSC.
European Journal of Human Genetics (2009) **17,** 319–328; doi:10.1038/ejhg.2008.170; published online 1 October 2008

Keywords: tuberous sclerosis complex; TSC1; TSC2

Introduction

Tuberous sclerosis complex (TSC) is an autosomal dominant disorder characterised by the development of hamartomas in a variety of organs and tissues, including the brain, skin and kidneys.[1,2]

Mutations in either the *TSC1* gene on chromosome 9q34[3] or the *TSC2* gene on chromosome 16p13.3[4] cause TSC. The *TSC1* and *TSC2* gene products, TSC1 and TSC2, interact to form a protein complex. TSC2 contains a GTPase-activating protein domain and the TSC1–TSC2 complex acts on the rheb GTPase to prevent the rheb-GTP-dependent stimulation of cell growth through the mammalian target of rapamycin (mTOR).[5] In cells lacking either *TSC1* or *TSC2*, the downstream targets of mTOR, including p70 S6 kinase (S6K) and ribosomal protein S6, are constitutively phosphorylated.[6,7] The identification of the role of the TSC1–TSC2 complex in regulating mTOR activity has made it possible to compare TSC1 and TSC2 variants found in the normal population with variants identified in individuals with symptoms of TSC. The effects of amino-acid changes on TSC1–TSC2 complex formation, on the activation of rheb GTPase activity by the complex

*Correspondence: Dr M Nellist, Department of Clinical Genetics, Erasmus Medical Centre, Dr. Molewaterplein 50, 3015 GE Rotterdam, The Netherlands.
Tel: +31 10 7043357; Fax: +31 10 7044736;
E-mail: m.nellist@erasmusmc.nl
Received 2 May 2008; revised 16 July 2008; accepted 27 August 2008; published online 1 October 2008

and on the phosphorylation status of S6K and S6 can be determined.[8]

Comprehensive screens for mutations at both the *TSC1* and *TSC2* loci have been performed in several large cohorts of TSC patients, and a wide variety of different pathogenic mutations have been described.[9–15] Although ~20% of the mutations identified in the *TSC2* gene are missense changes, missense mutations in the *TSC1* gene appear much less frequently. One simple explanation for this observation is that *TSC1* missense mutations are rare because the majority of TSC patients have a mutation in the *TSC2* gene. According to the *TSC1* mutation database,[16] 22 putative missense mutations have been identified in TSC patients. However, only one of these is a confirmed *de novo* mutation. Here, we investigate the effects of 10 *TSC1* missense changes (c.350T>C (p.L117P), c.539T>C (p.L180P), c.572T>A (p.L191H), c.671T>G (p.M224R), c.737G>A (p.R246K), c.913G>A (p.G305R), c.913G>T (p.G305W), c.1526G>A (p.R509Q), c.3103G>A (p.G1035S) and c.3290G>A (p.R1097H)) on TSC1–TSC2 function. We compared these TSC1 variants with wild-type TSC1 and three truncation variants: c.379_381delTGT (p.128delV), c.593_595delACT (p.N198F199delinsI) and c.2075C>T (p.R692X). Our analysis demonstrates that *TSC1* missense mutations reduce steady-state levels of TSC1, resulting in increased mTOR activity and leading to the symptoms of TSC.

Materials and methods

Patient characteristics

Samples from patients with either a putative or definite diagnosis of TSC were received for mutation analysis. Details on clinical symptoms were obtained from the treating physicians who were sent a standardised clinical evaluation form (see Supplementary Table 1).

Mutation analysis

DNA was extracted from peripheral blood using standard techniques. Mutation analysis was performed as described earlier,[13] or by direct sequence analysis of all *TSC1* and *TSC2* coding exons and exon/intron boundaries. In addition, both genes were analysed using the multiplex ligation-dependent probe amplification assay (MRC Holland, Amsterdam, The Netherlands).

To investigate whether the identified changes had an effect on splicing, three different splice-site prediction programs were used,[17–19] as described earlier.[13]

Generation of constructs and antisera

Expression constructs encoding C-terminal YFP- and myc-tagged TSC1 variants were derived using the QuikChange site-directed mutagenesis kit (Stratagene, La Jolla, CA, USA). In each case, the complete open reading frame of the mutated construct was verified by sequence analysis. The other constructs used in this study have been described earlier.[8,20,21] Polyclonal rabbit antisera specific for human TSC1 and TSC2 have been described earlier.[21] Other antibodies were purchased from Cell Signaling Technology (Danvers, MA, USA).

Functional analysis of TSC1 variants

Expression of TSC1 variants in transfected cells Human embryonal kidney (HEK) 293T cells seeded into 6-cm diameter dishes were transfected with a 1:1 mixture of the TSC1 and TSC2 expression constructs using Lipofectamine Plus (Invitrogen, Carlsbad, CA, USA), following the manufacturer's instructions. Two days after transfection, the cells were lysed in 50 mM Tris-HCl (pH 8.0), 100 mM NaCl, 50 mM NaF, 0.5 mM EDTA and 1% Triton X-100 plus protease inhibitors (Roche, Basel, Switzerland) and separated into supernatant and pellet fractions by centrifugation at 10 000 *g* for 10 min at 4°C as described earlier.[22] Wild-type TSC1 and the TSC1 variants were immunoprecipitated from the supernatant fractions by incubation with a monoclonal antibody against the C-terminal myc epitope tag for 90 min at 4°C before incubation with Protein G beads (GE Healthcare, Uppsala, Sweden). After gentle agitation for 90 min at 4°C, the beads were washed three times with a >50-fold excess of lysis buffer. The immunoprecipitated proteins were detected by immunoblotting. Blots were developed using enhanced chemiluminescent detection (GE Healthcare).[8]

Immunoblot analysis of S6K T389 phosphorylation in cells overexpressing TSC1 variants HEK 293T cells were transfected with a 4:2:1 mixture of the TSC1, TSC2 and S6K expression constructs. A total of 1.75 μg DNA was diluted in 200 μl Dulbecco's modified Eagle's medium (DMEM) containing 7 μg polyethyleneimine (Polysciences, Warrington, PA, USA). Where necessary, an empty expression vector (pcDNA3; Invitrogen) was added to make up the total amount of DNA. After 15 min at room temperature, the DNA/polyethyleneimine complexes were added to 80% confluent cells in 3.5-cm diameter dishes. After 4 h at 37°C, the transfection mixture was replaced with DMEM containing 10% foetal calf serum. Twenty-four hours after transfection, the cells were harvested and analysed by immunoblotting as before or by near infrared fluorescent detection on an Odyssey™ Infrared Imager (169 μm resolution, medium quality with 0 mm focus offset) (Li-Cor Biosciences, Lincoln, NE, USA). The integrated intensities of the protein bands were determined using the Odyssey software (default settings with background correction; 3-pixel width border average method). The mean ratios of the T389-phosphorylated S6K signal to the total S6K signal (T389/S6K) and the total TSC2 signal to the total TSC1 signal (TSC2/TSC1) were determined relative to wild-type TSC1 from at least three independent experiments (wild-type T389/S6K and TSC2/TSC1 ratios = 1).

Immunofluorescent detection of S235/236 phosphorylation of ribosomal protein S6 in TSC1-deficient cells *Tsc1*−/− mouse embryo fibroblasts (MEFs)[7] were transfected with expression constructs encoding wild-type TSC1 or the TSC1 variants, using Lipofectamine Plus (Invitrogen), following the manufacturer's instructions. Twenty-four hours after transfection, S6 (S235/236) phosphorylation in the transfected cells was detected by immunofluorescent microscopy using a rabbit polyclonal antibody specific for S235/236-phosphorylated S6.[23] TSC1 variants were identified either directly (for C-terminal-tagged TSC1-YFP variants) or with a mouse monoclonal antibody against the myc epitope tag (for C-terminal-tagged TSC1-myc variants). If possible, at least 50 cells expressing each TSC1 variant were counted per experiment and the number of cells showing a clear reduction in S6 (S235/236) phosphorylation was noted. The mean proportions of expressing cells with reduced S6 phosphorylation were calculated from at least three independent experiments.

Results

Patient characteristics and mutation analysis

The *TSC1* c.350T>C (p.L117P) change was detected in two generations of a family with TSC (Figure 1a). The index patient (I:1) had epilepsy since the age of 22 years and fulfilled the diagnostic criteria for definite TSC, with facial angiofibroma, ungual fibroma, hypomelanotic macules, a shagreen patch and cerebral white matter migration lines. No mental disability was reported. The youngest child

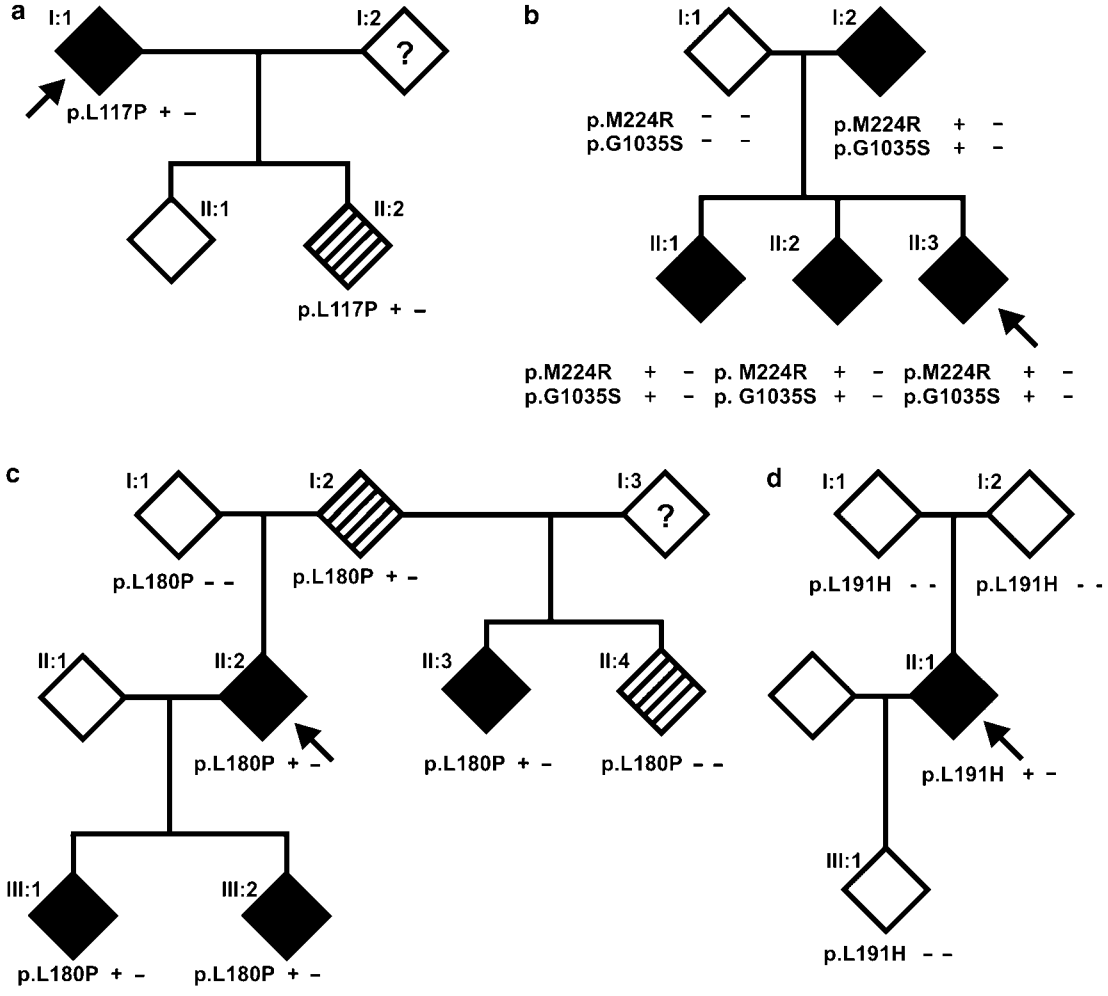

Figure 1 Pedigrees of the investigated families with TSC. Arrows indicate the index cases. Open symbols indicate no signs or symptoms of TSC; black symbols indicate individuals with definite TSC; hatched symbols indicate individuals with possible TSC. A question mark indicates individuals where no clinical data were available. Genotypes are indicated for the individuals where DNA was available for testing. (**a**) Family with TSC and the *TSC1* c.350T>C (p.L117P) variants. (**b**) Family with TSC and cosegregation of the *TSC1* c.671T>G (p.M224R) and c.3103G>A (p.G1035S) variants. (**c**) Family with cosegregation of TSC and the *TSC1* c.539T>C (p.L180P) variants. (**d**) Family with a *de novo TSC1* c.572T>A (p.L191H) mutation.

(II:2) had the c.350T>C change. Despite being somewhat hyperactive, this child developed normally until 4 years of age when epileptic seizures occurred and development stagnated. The child is now severely mentally retarded. No information was available about other signs of TSC. The eldest child (II:1), who could not yet be tested for the c.350T>C change, suffered severe anoxia at birth and has severe infantile encephalopathy with spastic tetraplegia and epilepsy.

The *TSC1* c.671T>G (p.M224R) and *TSC1* c.3103G>A (p.G1035S) changes were identified in two generations of a family with TSC[24] (Figure 1b). The index case (II:3) had definite TSC with multiple shagreen patches, hypomelanotic macules, ungual fibromas, dental pits, epilepsy and severe mental disability. One parent (I:2) and both siblings (II:1 and II:2) of the index case also fulfilled the diagnostic criteria for definite TSC. Individual I:2, who was seizure-free and of below-average intelligence (IQ 73), had skin lesions pathognomonic for TSC. Individual II:1, who was of normal intelligence (IQ 94), had seizures, cortical tubers and multiple TSC skin lesions. Individual II:2 had epilepsy, below-average intelligence (IQ 67) and multiple TSC skin lesions. All the affected individuals in this family were heterozygous for the c.671T>G and c.3103G>A changes. Three affected individuals (I:2, II:1 and II:2) were heterozygous for a polymorphism in the *TSC2* gene (*TSC2* c.1276-32C>G). The index case was homozygous for the wild-type *TSC2* 1276-32C allele, consistent with TSC segregating with a mutation at the *TSC1* locus in this family.

The *TSC1* c.539T>C (p.L180P) change was detected in three generations of a family with TSC (Figure 1c). Individual I:2 had an ungual fibroma as the only reported sign of TSC. Individual II:2 had epilepsy, no mental disability, skin signs typical for TSC and a subependymal giant cell astrocytoma as well as other brain lesions consistent with a definite diagnosis of TSC. Individual II:3, the half-sibling of II:2, had typical TSC-associated skin lesions and possible mild mental retardation. Individual II:4, the other half-sibling of II:2, had a history of seizures during puberty and some skin tags, not typical of TSC. Individual III:1, the child of II:2, had epilepsy, and typical TSC-associated skin and brain lesions. Individual III:2, the sibling of III:1, had multiple cardiac rhabdomyoma and Wolff–Parkinson–White syndrome. No mental disability was reported for either individual III:1 or III:2. TSC did not cosegregate with markers mapping close to the *TSC2* locus on chromosome 16p13.3, and no candidate *TSC2* mutation was identified in the index case.

The *TSC1* c.572T>A (p.L191H) change was identified in an individual who met the clinical criteria for definite TSC, including typical skin, heart and brain lesions. The individual had a history of seizures but no mental disability was reported. The c.572T>A change was absent in the individual's parents and child (Figure 1d). None of these individuals showed any signs of TSC.

Two TSC patients, one Finnish and one Dutch, were identified with the *TSC1* c.737G>A (p.R246K) change. No information was available on the parents of either of these two individuals. The Finnish individual had typical TSC-associated skin, brain and kidney lesions. No mental disability or history of seizures was reported. The Dutch individual was also reported to have definite TSC. The sibling of this individual did not have any signs of TSC and did not carry the c.737G>A change.

The *TSC1* c.1526G>A (p.R509Q) change was identified in a child of African origin, suspected of having TSC due to an echodensity that was detected prenatally in the septum of the heart. After birth, physical examination of the child did not reveal any signs of TSC but multiple congenital malformations that fitted with VACTERL (vertebral anomalies, atresia, cardiac malformations, tracheoesophageal fistula, renal anomalies and limb anomalies) association were identified. The same c.1526G>A change was identified in one of the parents. Neither parent reported any signs of TSC.

The *TSC1* c.3290G>A (p.R1097H) change was identified in a child with cardiac rhabdomyoma who subsequently developed epilepsy at the age of 3 months. An MRI scan of the brain showed multiple subependymal nodules, cortical tubers and white matter abnormalities. This individual fulfilled the diagnostic criteria for definite TSC, with angiomyolipoma and multiple skin lesions. The c.3290G>A change was also identified in one of the parents; neither parent showed any signs of TSC.

The *TSC1* c.379_381delTGT (p.128delV) change was detected in a child with epilepsy and a definite diagnosis of TSC (multiple skin signs, subependymal nodules and angiomyolipoma). No mental disability was reported and no information was available on the phenotypic or genetic status of the parents. The same change has been reported in another unrelated TSC patient.[25] The *TSC1* c.593_595delACT (p.N198F199delinsI), c.913G>A (p.G305R) and c.913G>T (p.G305W) missense changes have been reported earlier to cosegregate with TSC in three independent families.[15,26]

In all the above cases, no other putative pathogenic mutations were identified and comparison of the allele ratios of the index cases and parents (where possible) did not reveal any evidence for somatic mosaicism in the leukocyte DNA.

Comparative analysis of TSC1 amino-acid substitutions

During our initial mutation screening, the L117P change was the only putative pathogenic TSC1 amino-acid substitution identified. We compared the L117P variant with wild-type TSC1, an earlier characterised TSC1 in-frame deletion (N198F199delinsI)[27] and to a common TSC1 truncation mutation, R692X[3,10] (Figure 2). Wild-type TSC1 was detected predominantly in the post 10 000 *g*

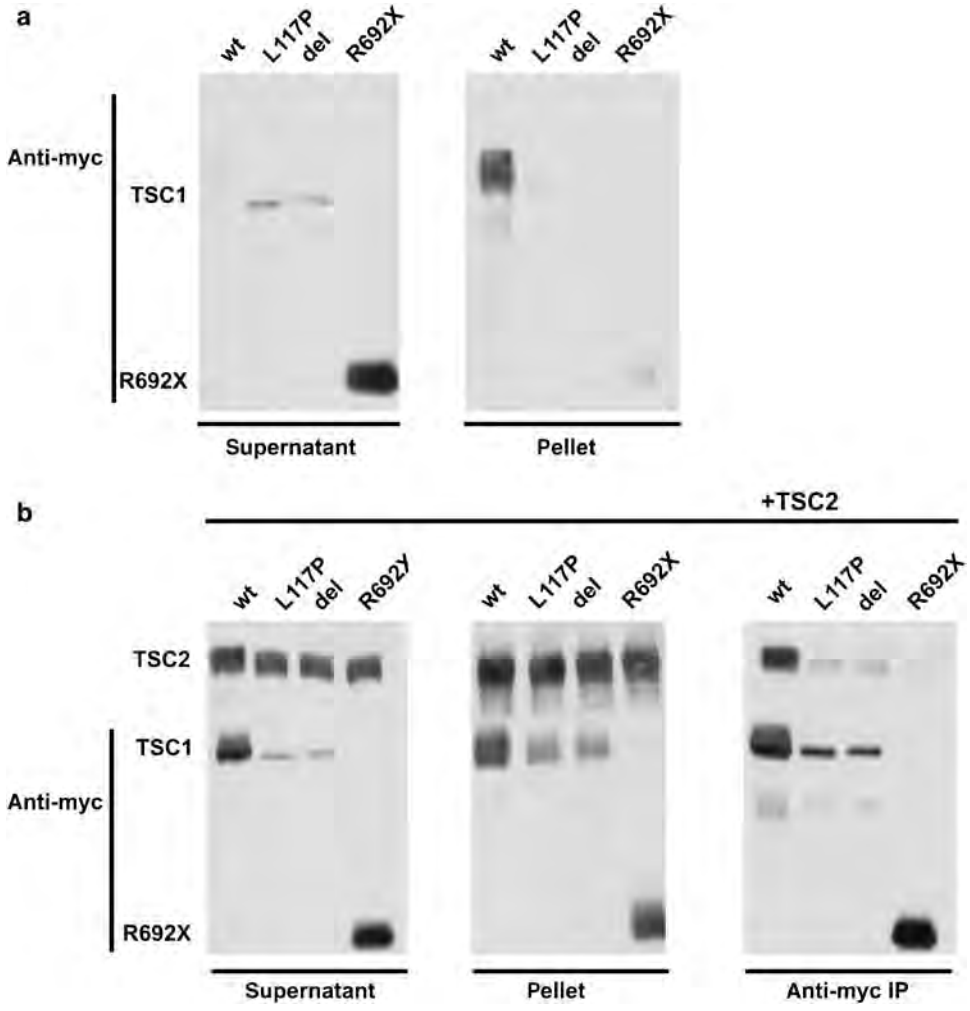

Figure 2 Analysis of the TSC1 L117P variant. Wild-type TSC1 (wt) or the L117P, N198F199delinsI (del) or R692X variants (all containing a C-terminal myc epitope tag) were overexpressed in HEK 293T cells alone (**a**) or in the presence of coexpressed TSC2 (**b**). Cell lysates were separated into post 10 000 *g* centrifugation pellet and supernatant fractions. The TSC1 variants were detected with a monoclonal mouse antibody against the myc epitope tag (9B11; Cell Signaling Technology). TSC1–TSC2 complexes were immunoprecipitated from the supernatant fractions using the same antibody. TSC2 was detected with a polyclonal rabbit antiserum.[8] (**a**) Expression of the TSC1 variants in the absence of TSC2. Wild-type TSC1 (wt) was detected predominantly in the pellet fraction. In contrast, the variants were detected predominantly in the supernatant fraction. The signals for the L117P and N198F199delinsI (del) variants are clearly less than wild-type TSC1 and the R692X variants (as detected with the 9B11 antibody). (**b**) Coexpression of TSC2 and the TSC1 variants. In the presence of TSC2, wild-type TSC1 and the variants were detected in both subcellular fractions. Coexpression of TSC2 resulted in a shift of wild-type TSC1 to the supernatant fraction and a shift of the variants to the pellet fraction. TSC1 and the TSC1 variants were immunoprecipitated with an antibody against the myc epitope tag. TSC2 was coimmunoprecipitated with all three variants. However, in each case, the TSC2 signal in the immunoprecipitate was clearly less than with the wild-type TSC1.

pellet fraction, whereas the three variants were detected in the supernatant fraction (Figure 2a). Upon coexpression of TSC2, the variants as well as wild-type TSC1 were detected in both subcellular fractions (Figure 2b). TSC2 was coimmunoprecipitated from the supernatant fraction with all three variants, although clearly less effectively than with wild-type TSC1.

Next, we investigated whether the variants could inhibit mTOR signalling. Expression of wild-type TSC1 alone is insufficient to inhibit mTOR activity.[28] Therefore, the variants were coexpressed with TSC2 and S6K in HEK 293T cells, and S6K T389 phosphorylation was analysed by immunoblotting (Figure 3a). To try and achieve comparable expression levels of the different variants, we used different quantities of the corresponding expression constructs. Coexpression of wild-type TSC1 and TSC2 resulted in a reduction in S6K T389 phosphorylation, even with low levels of the TSC1 expression construct. In contrast, coexpression of TSC2 with the variants did not reduce S6K T389 phosphorylation, indicating that they were unable to inhibit mTOR effectively. Compared with wild-type TSC1, the L117P

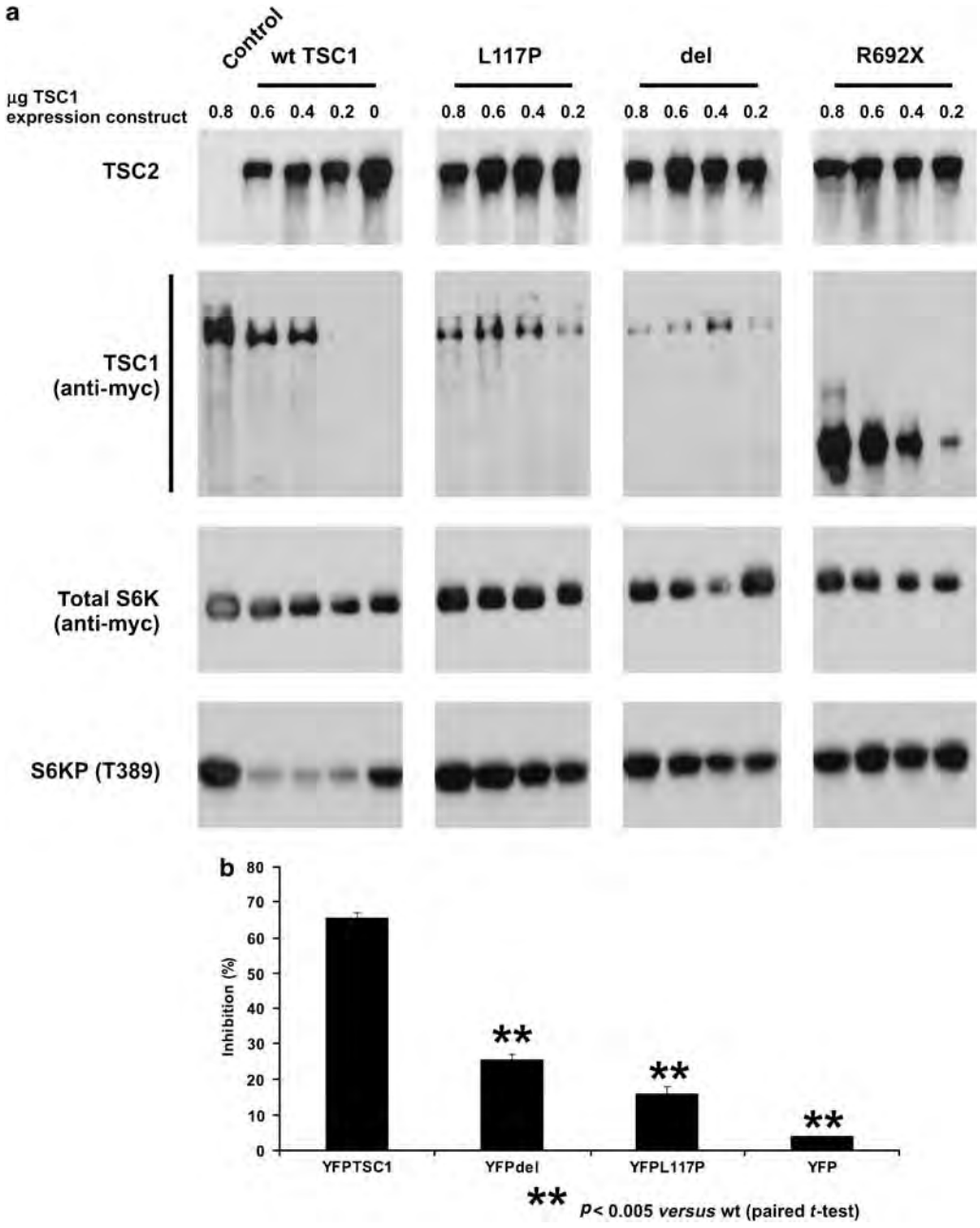

Figure 3 TSC1–TSC2-dependent inhibition of mTOR signalling by the TSC1 L117P variant. (**a**) T389 phosphorylation of S6K in HEK 293T cells coexpressing TSC2, myc-tagged S6K and myc-tagged wild-type TSC1 (wt) or the TSC1 L117P, N198F199delinsI (del) or R692X variants was determined by immunoblotting. Cells transfected with differing amounts of wild-type or variant expression constructs, as indicated, were analysed. The first lane on the left (control) corresponds to cells transfected with S6K and wild-type TSC1 expression constructs only (no TSC2 expression construct). The coexpression of only TSC2 and wild-type TSC1 inhibited S6K phosphorylation. (**b**) TSC1-dependent inhibition of S6 phosphorylation. YFP-tagged wild-type TSC1 (YFPTSC1) and the YFP-tagged N198F199delinsI (YFPdel) and L117P (YFPL117P) variants were expressed in *Tsc1*−/− MEFs. S6 S235/236 phosphorylation in the YFP-positive cells was detected by immunofluorescent microscopy using an antibody specific for S235/236-phosphorylated S6 (Cell Signaling Technology). As a control, S6 phosphorylation in cells expressing YFP only was also determined. At least 50 cells were counted per variant per experiment. Mean percentage scores of three separate experiments are shown. Values significantly different from the wild type are indicated.

and N198F199delinsI variants were detected at low levels, even when the quantity of transfected expression construct DNA was increased.

To confirm that the L117P and N198F199delinsI variants were unable to inhibit mTOR, they were expressed in *Tsc1*−/− MEFs. These cells exhibit constitutive S6 (S235/

236) phosphorylation.[7] As shown in Figure 3b, wild-type YFP-tagged TSC1 reduced S6 phosphorylation in >60% of the YFP-positive *Tsc1*−/− MEFs, consistent with earlier results.[8] In contrast, S6 phosphorylation was reduced in <30% of cells expressing the L117P or N198F199delinsI variants (paired *t*-test $P<0.001$). Nevertheless, a reduction in S6 phosphorylation was observed in a higher proportion of variant-expressing cells than in cells expressing YFP only (paired *t*-test $P<0.02$). Therefore, although both variants were clearly less effective than wild-type TSC, we could not exclude the possibility that the variants can antagonise mTOR activity.

As a result of on-going *TSC1* and *TSC2* mutation screening, we identified eight additional TSC1 single amino-acid changes: p.128delV, p.L180P, p.L191H, p.M224R, p.R246K, p.R509Q, p.G1035S and p.R1097H. The p.M224R and p.G1035S changes cosegregated with TSC in a single family (Figure 1b). To investigate the effects of these two amino-acid substitutions on TSC1 function, the corresponding single and double variants were compared with wild-type TSC1 and the R692X truncation. As shown in Figure 4a, the M224R variant and the M224R/G1035S double variant were detected at lower levels than wild-type TSC1 and the G1035S variant. Furthermore, the expression of wild-type TSC1 or the G1035S variant reduced S6 phosphorylation in >50% of transfected *Tsc1*−/− MEFs whereas <20% of the MEFs expressing the M224R, M224R/G1035S or R692X variants showed a reduction in S6 phosphorylation (Figure 4b), indicating that the M224R substitution is the pathogenic mutation in this family and that the G1035S substitution is a cosegregating neutral variant.[24] We did not observe any differences between the M224R single mutant and the M224R/G1035S double mutant.

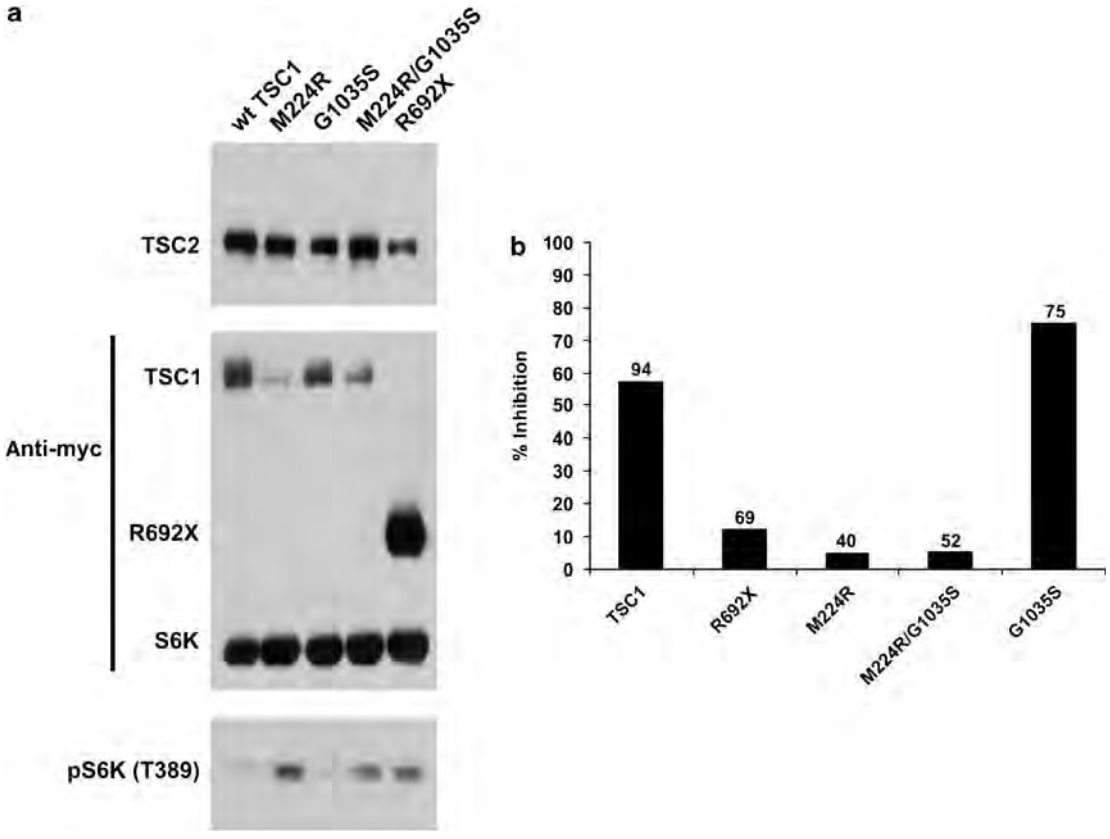

Figure 4 Results of the functional assays on the M224R, G1035S and M224R/G1035S variants. (**a**) TSC1–TSC2-dependent inhibition of S6K-T389 phosphorylation. TSC2, S6K and wild-type TSC1 (wt TSC1), or the TSC1 variants, were expressed in HEK 293T cells. T389 phosphorylation of S6K was determined by immunoblotting and was reduced in the presence of wild-type TSC1 and the G1035S variants only. S6K, wild-type TSC1 and the TSC1 variants were detected with an antibody against the myc epitope tag. The signal for the M224R and M224R/G1035S variants is reduced compared with wild-type TSC1 and the G1035S and R692X variants. A representative example of at least three separate experiments is shown. (**b**) Inhibition of S6 phosphorylation in *Tsc1*−/− MEFs. Wild-type myc-tagged TSC1 (TSC1) and the myc-tagged variants were expressed in *Tsc1*−/− MEFs. S6 S235/236 phosphorylation in the myc-positive cells was determined by double-label immunofluorescent microscopy using a rabbit polyclonal antibody specific for S235/236-phosphorylated S6 and a mouse monoclonal antibody specific for the myc tag. The percentage of *Tsc1*−/− MEFs expressing the TSC1 variants and showing a clear reduction in S6 phosphorylation is indicated. Because the signals for the M224R and M224R/G1035S variants were very low, it was difficult to unequivocally differentiate >50 expressing cells. Therefore, the total number of counted cells after two experiments is indicated above each bar.

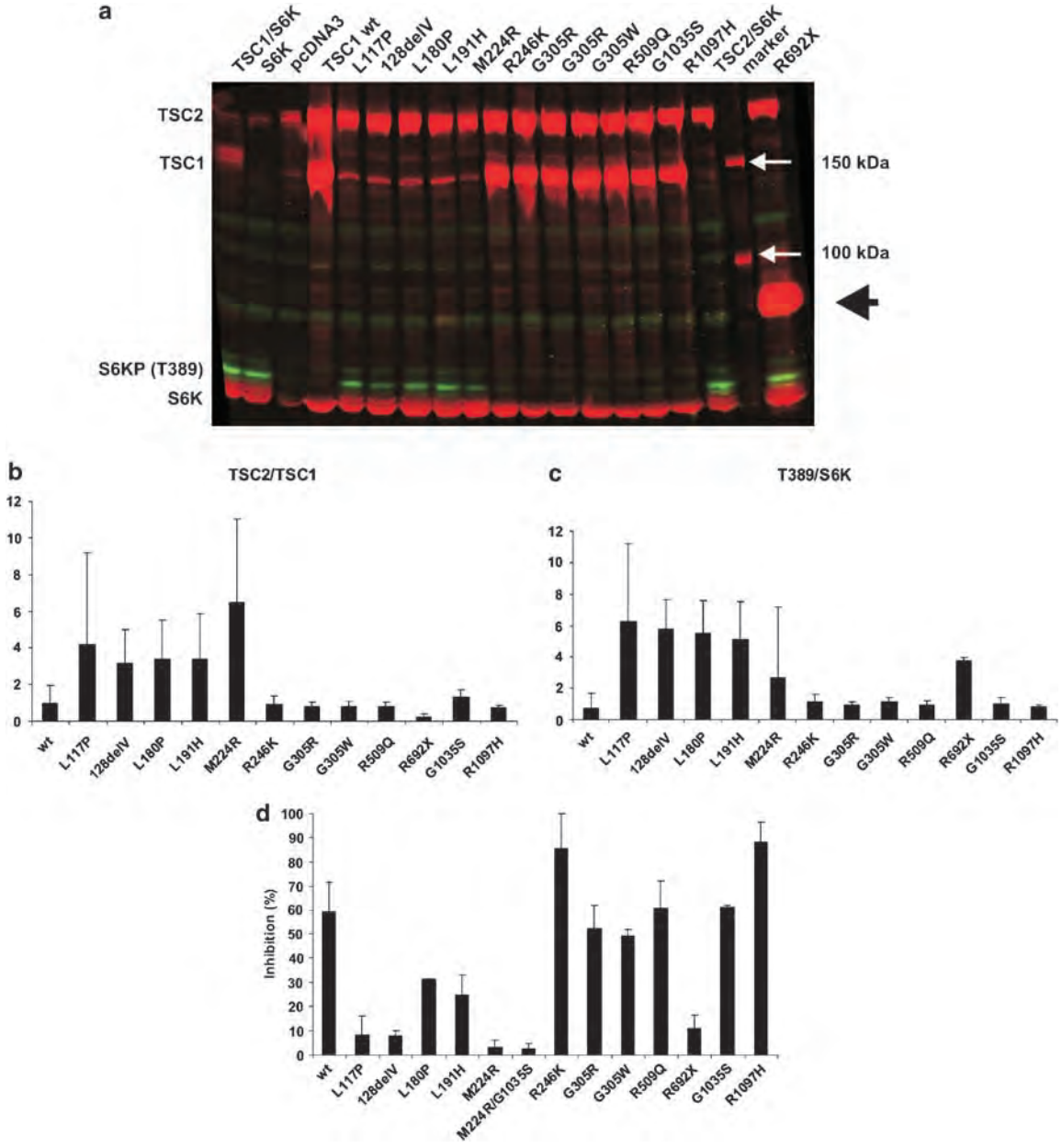

Figure 5 Analysis of the 128delV, L180P, L191H, R246K, G305R, G305W, R509Q and R1097H variants. (**a**) TSC1-dependent inhibition of S6K T389 phosphorylation. S6K T389 phosphorylation was determined by immunoblotting as before except that the blots were developed using Odyssey near infrared detection (Li-Cor Biosciences). Cells expressing S6K, TSC2 and wild-type TSC1 (wt) or the TSC1 variants were analysed. As controls, cells transfected with expression constructs for wild-type TSC1 and S6K only (TSC1/S6K), TSC2 and S6K only (TSC2/S6K), S6K only (S6K) or empty vector only (pcDNA3) were also analysed. S6K and the TSC1 variants were detected with an antibody specific for the myc epitope tag. The R692X truncation variant is indicated with a large arrowhead; molecular weight markers are indicated with small arrows. Expression of wild-type TSC1 or the R246K, G305R, G305W, R509Q, G1035S and R1097H variants clearly inhibited S6K phosphorylation. The signals for the L117P, 128delV, L180P, L191H and M224R variants were clearly reduced compared with wild-type TSC1 (see also panel b), and S6K T389 phosphorylation was increased (see also panel c). A representative example of three separate experiments is shown. (**b**) Relative expression of the TSC1 variants. The integrated intensities of the TSC1 and TSC2 signals for each variant were determined in three independent experiments using the Odyssey scanning software. The mean TSC2/TSC1 ratios, relative to the wild-type TSC1 (wt) (wild-type TSC1 TSC2/TSC1 ratio = 1), were determined. Standard deviations are indicated. (**c**) TSC1-dependent inhibition of S6K T389 phosphorylation. The ratio of the T389 S6K phosphorylation signal intensity to the total S6K signal intensity (T389/S6K) was measured in three independent experiments. The integrated intensity of each band was determined using the Odyssey scanning software and the mean T389/S6K ratios, relative to the wild-type TSC1 (wt) (wild-type TSC1 T389/S6K ratio = 1), were determined. Standard deviations are indicated. (**d**) Inhibition of S6 phosphorylation in *Tsc1*−/− MEFs. Wild-type myc-tagged TSC1 (wt) or the myc-tagged variants were expressed in *Tsc1*−/− MEFs. S6 S235/236 phosphorylation in the myc-positive cells was determined by immunofluorescent microscopy as before. At least 50 cells were counted per variant per experiment. Each variant was tested in at least two separate experiments. Mean percentages of *Tsc1*−/− MEFs expressing the TSC1 variants and showing reduced phosphorylation of S6 are shown. Standard deviations are indicated.

To determine whether the 128delV, L180P, L191H, R246K, R509Q and R1097H amino-acid changes were pathogenic, we compared these variants with the previously characterised L117P and R692X variants, and with two additional putative missense variants, G305R and G305W[15] (Figure 5). The R246K, G305R, G305W, R509Q and R1097H variants were detected at comparable levels with wild-type TSC1 (Figure 5a and b) and were just as effective at inhibiting S6K T389 phosphorylation (Figure 5a and c). In contrast, the 128delV, L180P and L191H variants were detected at low levels, similar to the L117P and M224R variants (Figure 5a and b). Furthermore, S6K T389 phosphorylation was not inhibited by the expression of these variants (Figure 5a and c). Consistent with the immunoblot data, the expression of the L117P, 128delV, L180P, L191H, M224R, M224R/G1035S and R692X variants in *Tsc1*−/− MEFs reduced S6 phosphorylation in <40% of cells, whereas wild-type TSC1 and the R246K, G305R, G305W, R509Q, G1035S and R1097H variants reduced S6 phosphorylation in >50% of the expressing cells (Figure 5d).

We concluded that the 128delV, L180P and L191H changes destabilise TSC1, resulting in increased mTOR activity. The R246K, G305R, G305W, R509Q, G1035S and R1097H amino-acid substitutions did not affect TSC1 function in our assays.

Splice-site prediction analysis

Splice-site prediction analysis of the identified variants was performed according to a standard protocol[13] using three independent splice-site prediction programs.[17–19] Effects were predicted for four of the variants: *TSC1* c.379_381delTGT (p.128delV), c.737G>A (p.R246K) c.913G>A (p.G305R) and c.913G>T (p.G305W).

According to two of the prediction programs, the c.379_381delTGT mutation created a potential new acceptor site within exon 6. However, the values of the new site (0.48 and 0.33 in Fruitfly and NetGene2, respectively) were lower than the values of the wild-type acceptor site (0.98 and 0.97, respectively). It is therefore unlikely that this sequence change affects splicing.

The R246K, G305R and G305W amino-acid substitutions did not affect TSC1 function. However, the c.737G>A (p.R246K) nucleotide substitution altered the last nucleotide of exon 8 and all three programs indicated that this change disrupted the intron 8 splice donor site, leaving a new potential donor site 90 nucleotides downstream. Similarly, the c.913G>A (p.G305R) and c.913G>T (p.G305W) substitutions affect the last nucleotide of exon 9 and were predicted by all three programs to disrupt splicing to the intron 9 donor site. We concluded that these three variants are most likely pathogenic splice-site mutations, not missense mutations. Unfortunately, the effect of these sequence changes on *TSC1* RNA splicing could not be confirmed experimentally because no new samples could be obtained.

An overview of the functional assays and splice-site analysis is presented in Supplementary Table 2.

Discussion

Mutation analysis of the *TSC1* and *TSC2* genes in individuals with TSC, and in those suspected of having the disease is important for diagnosis and genetic counselling. During our screening of a cohort of approximately 900 index cases with TSC, or possible TSC, we identified eight putative pathogenic *TSC1* missense changes, c.350T>C (p.L117P), c.539T>C (p.L180P), c.572T>A (p.L191H), c.671T>G (p.M224R), c.737G>A (p.R246K), c.1526G>A (p.R509Q), c.3103G>A (p.G1035S) and c.3290G>A (p.R1097H), as well as a putative pathogenic in-frame deletion mutant, *TSC1* c.379_381delTGT (p.128delV). We compared these variants with the earlier reported c.913G>A (p.G305R), c.913G>T (p.G305W), c.593_595delACT (p.N198F199delinsI) and c.2074C>T (p.R692X) mutants.[2,15,26]

The TSC1 L117P, 128delV, L180P, L191H, N198F199-delinsI and M224R changes resulted in reduced levels of TSC1 and a reduction in TSC1-dependent inhibition of mTOR activity, as detected by immunoblotting. In each case, the functional characterisation was consistent with the genetic and phenotypic findings and we concluded that the changes were pathogenic.

The R246K, G305R, G305W, R509Q, G1035S and R1097H amino-acid substitutions did not affect TSC1 function in our assays. However, we concluded that the *TSC1* c.737G>A (p.R246K), c.913G>A (p.G305R) and c.913G>T (p.G305W) changes were most likely pathogenic splice-site mutations. The c.737G>A transition was predicted to destroy the splice donor site at the 3′ end of exon 8 and the c.913G>A and c.913G>T substitutions affect the last nucleotide of exon 9, also disrupting the normal splice donor site. The c.1526G>A (p.R509Q), c.3103G>A (p.G1035S) and c.3290G>A (p.R1097H) variants did not appear to affect either *TSC1* RNA splicing or TSC1 function. The c.1526G>A change was identified in a foetus suspected of having TSC. However, after birth, the child showed multiple congenital malformations that fitted with VACTERL association, and a normal physical examination of the child did not reveal any signs of TSC. We concluded that this variant is unlikely to cause TSC. The c.3103G>A variant cosegregated with the pathogenic c.671T>G (p.M224R) variant and TSC in a single family.[24] We concluded that the p.G1035S substitution was a neutral variant, consistent with previous reports.[29,30] The c.3290G>A change was identified in a child with definite TSC and in one unaffected parent, and we concluded that it was also most likely a rare neutral variant.

Here we demonstrate that specific amino-acid substitutions close to the N-terminal of TSC1 (amino acids 117–

224) reduce the steady-state levels of TSC1. The location and the effects of these changes on TSC1 function are very similar to a small number of missense mutations described recently in some cases of bladder cancer,[31] suggesting that the pathogenetic mechanisms underlying TSC-associated lesions and tumours of the bladder may be related.

Several studies indicate that *TSC1* mutations are associated with a less severe clinical presentation in TSC patients.[9,12,13,15] The small number of patients that we identified with a *TSC1* missense mutation made it difficult to identify a specific phenotypic spectrum in this group. Nevertheless, the use of functional assays to differentiate between polymorphisms and pathogenic mutations, in TSC and other diseases, will not only facilitate the identification of pathogenic mutations but also help investigate possible genotype–phenotype correlations and provide insight into how specific amino-acid residues contribute to protein function.

Acknowledgements

Financial support was provided by the US Department of Defense Congressionally-Directed Medical Research Program (grant no. TS060052) and the Michelle Foundation. We thank the family members who contributed to this study. Dr N Migone is thanked for helpful comments on the paper. The authors report no conflicts of interest.

References

1 Gomez M, Sampson J, Whittemore V eds: *The Tuberous Sclerosis Complex*. Oxford, UK: Oxford University Press, 1999.
2 Roach ES, DiMario FJ, Kandt RS *et al*: Tuberous sclerosis consensus conference: recommendations for diagnostic evaluation. National Tuberous Sclerosis Association. *J Child Neurol* 1999; **14**: 401–407.
3 van Slegtenhorst M, de Hoogt R, Hermans C *et al*: Identification of the tuberous sclerosis gene *TSC1* on chromosome 9q34. *Science* 1997; **277**: 805–808.
4 The European Chromosome 16 Tuberous Sclerosis Consortium: Identification and characterization of the tuberous sclerosis gene on chromosome 16. *Cell* 1993; **75**: 1305–1315.
5 Li Y, Corradetti MN, Inoki K *et al*: TSC2: filling the GAP in the mTOR signaling pathway. *Trends Biochem Sci* 2003; **28**: 573–576.
6 Zhang H, Cicchetti G, Onda H *et al*: Loss of *Tsc1*/*Tsc2* activates mTOR and disrupts PI3K-Akt signaling through downregulation of PDGFR. *J Clin Invest* 2003; **112**: 1223–1233.
7 Kwiatkowski DJ, Zhang H, Bandura JL *et al*: A mouse model of TSC1 reveals sex-dependent lethality from liver hemangiomas, and up-regulation of p70S6 kinase activity in *Tsc1* null cells. *Hum Mol Genet* 2001; **11**: 525–534.
8 Nellist M, Sancak O, Goedbloed MA *et al*: Distinct effects of single amino acid changes to tuberin on the function of the tuberin–hamartin complex. *Eur J Hum Genet* 2005; **13**: 59–68.
9 Jones AC, Shyamsundar MM, Thomas MW *et al*: Comprehensive mutation analysis of *TSC1* and *TSC2*, and phenotypic correlations in 150 families with tuberous sclerosis. *Am J Hum Genet* 1999; **64**: 1305–1315.
10 van Slegtenhorst M, Verhoef S, Tempelaars A *et al*: Mutational spectrum of the *TSC1* gene in a cohort of 225 tuberous sclerosis complex patients: no evidence for genotype–phenotype correlation. *J Med Genet* 1999; **36**: 285–289.
11 Au KS, Rodriguez JA, Finch JL *et al*: Germ-line mutational analysis of the *TSC2* gene in 90 tuberous sclerosis patients. *Am J Hum Genet* 1998; **62**: 286–294.
12 Dabora SL, Jozwiak S, Franz DN *et al*: Mutational analysis in a cohort of 224 tuberous sclerosis patients indicates increased severity of *TSC2*, compared with *TSC1*, disease in multiple organs. *Am J Hum Genet* 2001; **68**: 64–80.
13 Sancak O, Nellist M, Goedbloed M *et al*: Mutational analysis of the *TSC1* and *TSC2* genes in a diagnostic setting: genotype–phenotype correlations and comparison of diagnostic DNA techniques in tuberous sclerosis complex. *Eur J Hum Genet* 2005; **13**: 731–741.
14 Niida Y, Lawrence-Smith N, Banwell A *et al*: Analysis of both *TSC1* and *TSC2* for germline mutations in 126 unrelated patients with tuberous sclerosis. *Hum Mutat* 1999; **14**: 412–422.
15 Au K-S, Williams AT, Roach ES *et al*: Genotype/phenotype correlation in 325 individuals referred for a diagnosis of tuberous sclerosis complex in the United States. *Genet Med* 2007; **9**: 88–100.
16 Tuberous sclerosis database – Leiden Open Variation Database. [www.chromium.liacs.nl/lovd/index.php?select_db=TSC2].
17 NetGene2 Server. [www.cbs.dtu.dk/services/NetGene2].
18 SpliceSiteFinder. [www.genet.sickkids.on.ca/~ali/splicesitefinder.html].
19 BDGP: Splice Site Prediction by Neural Network. [www.fruitfly.org/seq_tools/splice.html].
20 Nellist M, van Slegtenhorst MA, Goedbloed M *et al*: Characterization of the cytosolic tuberin–hamartin complex: tuberin is a cytosolic chaperone for hamartin. *J Biol Chem* 1999; **274**: 35647–35652.
21 van Slegtenhorst M, Nellist M, Nagelkerken B *et al*: Interaction between hamartin and tuberin, the *TSC1* and *TSC2* gene products. *Hum Mol Genet* 1998; **7**: 1053–1057.
22 Nellist M, Verhaaf B, Goedbloed MA *et al*: *TSC2* missense mutations inhibit tuberin phosphorylation and prevent formation of the tuberin-hamartin complex. *Hum Mol Genet* 2001; **10**: 2889–2898.
23 Jaeschke A, Hartkamp J, Saitoh M *et al*: Tuberous sclerosis complex tumor suppressor-mediated S6 kinase inhibition by phosphatidylinositide-3-OH kinase is mTOR independent. *J Cell Biol* 2002; **159**: 217–224.
24 Jansen FE, Braams O, Vincken KL *et al*: Overlapping neurologic and cognitive phenotypes in patients with *TSC1* or *TSC2* mutations. *Neurology* 2008; **70**: 908–915.
25 Lee-Jones L, Aligianis I, Davies PA *et al*: Sacrococcygeal chordomas in patients with tuberous sclerosis complex show somatic loss of *TSC1* or *TSC2*. *Genes Chromosomes Cancer* 2004; **41**: 80–85.
26 Goedbloed MA, Nellist M, Verhaaf B *et al*: Analysis of TSC2 stop codon variants found in tuberous sclerosis patients. *Eur J Hum Genet* 2001; **9**: 823–828.
27 Hodges AK, Li S, Maynard J *et al*: Pathological mutations in TSC1 and TSC2 disrupt the interaction between hamartin and tuberin. *Hum Mol Genet* 2001; **10**: 2899–2905.
28 Inoki K, Li Y, Zu T *et al*: TSC2 is phosphorylated and inhibited by Akt and suppresses mTOR signalling. *Nat Cell Biol* 2002; **4**: 648–657.
29 Young JM, Burley MW, Jeremiah SJ *et al*: A mutation screen of the TSC1 gene reveals 26 protein truncating and 1 splice site mutation in a panel of 79 tuberous sclerosis patients. *Ann Hum Genet* 1998; **62**: 203–213.
30 Dabora SL, Sigalas I, Hall F *et al*: Comprehensive mutation analysis of *TSC1* using two-dimensional electrophoresis with DGGE. *Ann Hum Genet* 1998; **62**: 491–504.
31 Pymar LS, Platt FM, Askham JM *et al*: Bladder tumour-derived somatic TSC1 missense mutations cause loss of function via distinct mechanisms. *Hum Mol Genet* 2008; **17**: 2006–2017.

Supplementary Information accompanies the paper on European Journal of Human Genetics website (http://www.nature.com/ejhg)

European Journal of Human Genetics (2009) 17, 301 – 310

www.nature.com/ejhg

ARTICLE

A reliable cell-based assay for testing unclassified *TSC2* gene variants

Ricardo Coevoets[1], Sermin Arican[1], Marianne Hoogeveen-Westerveld[1], Erik Simons[1], Ans van den Ouweland[1], Dicky Halley[1] and Mark Nellist*[,1]

[1]*Department of Clinical Genetics, Erasmus Medical Centre, Rotterdam, The Netherlands*

Tuberous sclerosis complex (TSC) is characterised by seizures, mental retardation and the development of hamartomas in a variety of organs and tissues. The disease is caused by mutations in either the *TSC1* gene or the *TSC2* gene. The *TSC1* and *TSC2* gene products, TSC1 and TSC2, form a protein complex that inhibits signal transduction to the downstream effectors of the mammalian target of rapamycin (mTOR). We have developed a straightforward, semiautomated in-cell western (ICW) assay to investigate the effects of amino acid changes on the TSC1–TSC2-dependent inhibition of mTOR activity. Using this assay, we have characterised 20 TSC2 variants identified in individuals with TSC or suspected of having the disease. In 12 cases, we concluded that the identified variant was pathogenic. The ICW is a rapid, reproducible assay, which can be applied to the characterisation of the effects of novel TSC2 variants on the activity of the TSC1–TSC2 complex.
European Journal of Human Genetics (2009) **17,** 301–310; doi:10.1038/ejhg.2008.184; published online 15 October 2008

Keywords: tuberous sclerosis complex; in-cell western; unclassified variants

Introduction

Tuberous sclerosis complex (TSC) is an autosomal dominant disorder characterised by seizures, mental retardation and the development of hamartomas in a variety of organs and tissues.[1] The disease is caused by mutations in either the *TSC1* gene on chromosome 9q34[2] or the *TSC2* gene on chromosome 16p13.3.[3] The *TSC1* and *TSC2* gene products, TSC1 and TSC2, form a protein complex that acts as a GTPase-activating protein (GAP) for the rheb GTPase, preventing the rheb-GTP-dependent stimulation of the mammalian target of rapamycin (mTOR).[4] In cells lacking either *TSC1* or *TSC2*, the downstream targets of mTOR, including p70 S6 kinase (S6K) and ribosomal protein S6, are constitutively phosphorylated.[5,6] The identification of the role of the TSC1–TSC2 complex in regulating mTOR has made it possible to compare the activity of different TSC1 and TSC2 variants. The effects of amino acid changes on TSC1–TSC2 complex formation, on the activation of rheb GTPase activity, and on the phosphorylation status of the downstream effectors of mTOR, can be determined.[7]

Comprehensive screens for mutations at the *TSC1* and *TSC2* loci have been performed in large cohorts of TSC patients.[8–11] In most studies ~20% of the identified mutations are either missense changes or small, in-frame insertions/deletions, predominantly in the *TSC2* gene. In some cases, when a missense change cosegregates with TSC, or when key relatives are not available for testing, it is difficult to establish whether the identified nucleotide change is a pathogenic mutation or a neutral variant. We identified a number of variants where it was not clear from the genetic data whether the identified variant was pathogenic or not.[10] To resolve some of these cases we tested the activity of the variant TSC1–TSC2 complexes using a variety of biochemical assays.[12]

To simplify and standardise the testing of TSC2 variants we have developed and tested an in-cell western (ICW) assay to determine whether specific *TSC2* sequence variants identified in individuals with, or suspected of having, TSC are disease

*Correspondence: Dr M Nellist, Department of Clinical Genetics, Erasmus Medical Centre, Dr Molewaterplein 50, 3015 GE Rotterdam, The Netherlands.
Tel: +31 10 7043357; Fax: +31 10 7049489;
E-mail: m.nellist@erasmusmc.nl
Received 15 April 2008; revised 9 July 2008; accepted 4 September 2008; published online 15 October 2008

causing. The ICW assay utilises secondary antibodies conjugated with near infrared fluorophores in combination with an infrared scanner enabling two distinct antibody signals to be detected simultaneously and quantified in fixed cells. The advantage of the ICW assay over immunoblot-based techniques is that no blotting step is required and the analysis and quantification can be performed directly in high-throughput multiwell plate formats. Therefore, the ICW assay streamlines both the experimental procedure and data analysis.

In-cell western assays to assess protein phosphorylation have been described previously.[13] However, in most reports, the effects of different pharmacological reagents have been monitored.[14] Here, we describe a transfection-based ICW assay to facilitate the characterisation of the effects of genetic changes in the *TSC2* gene on the activity of the TSC1–TSC2 complex and the mTOR signalling pathway. We have used this assay to characterise 20 TSC2 variants. Twelve variants (60%) did not inhibit mTOR activity in either the ICW assay or in a conventional immunoblot assay, and could therefore be classified as pathogenic mutations. Furthermore, we show that the ICW assay of TSC1–TSC2 function is amenable to the development of high-throughput, semiautomated protocols.

Materials and methods

Detection of TSC2 variants in TSC patients

Mutation analysis was performed as described previously[10] or by direct sequence analysis of all *TSC1* and *TSC2* coding exons and exon/intron boundaries. In addition, both genes were analysed using the multiplex ligation-dependent probe amplification assay (MRC Holland, Amsterdam, The Netherlands). Where possible, parental DNA was collected and tested for the presence of the identified variants and, in cases of *de novo* changes, paternity testing was performed. To investigate whether the identified sequence changes had an effect on splicing, three splice site prediction programs were used.[15–17]

Materials

Expression constructs encoding the 20 TSC2 variants (G62E, R98W, 275delN, Q373P, 580delASHATRVYEMLVSHIQLHYKHSYTLP (hereafter referred to as 580del26), A607E, T1068I, T1075I, T1075T, V1199G, P1292A, S1410L, G1416D, D1512A, G1544V, 1553delTGLGRLIELKDCQPDKVYL (hereafter referred to as 1553del19), H1617Y, V1623G, R1720Q and R1720W) were derived using the Stratagene QuikChange site-directed mutagenesis kit (Stratagene, La Jolla, CA, USA). Sequence changes were numbered according to the *TSC2* cDNA as originally published, as these corresponded to the cDNA used for the expression studies.[3] Nomenclature according to the *TSC2* mutation database[18] is given in Table 1.

All variants were verified by sequencing the complete *TSC2* cDNA open reading frame. All the other constructs used in this study have been described previously.[7,19,20] Polyclonal rabbit antisera specific for human TSC1 and TSC2 have been described previously.[19] Other antibodies were purchased from Cell Signaling Technology (Danvers, MA, USA) (1A5, anti-T389 phospho-S6K mouse monoclonal; 9B11, anti-myc tag mouse monoclonal; anti-myc tag

Table 1 Summary of the ICW-based functional characterisation of 20 TSC2 variants

Nucleotide change[a]	*Amino acid change*[a]	t-*test vs wild-type*[c]	t-*test vs control*[c]	*Pathogenicity*
203G>A (185G>A)	G62E	0.555398	**0.000106**	Unclassified
310C>T (292C>T)	R98W	**0.021536**	**0.013338**	Unclassified
842delACA (824delACA)	275delN	**0.001127**	0.475101	Pathogenic
1136A>C (1118A>C)	Q373P	0.278444	**0.000072**	Pathogenic[b]
1754del78 (1736del78)	580del26	**0.002041**	0.298704	Pathogenic
1838C>A (1820C>A)	A607E	**0.003675**	0.146591	Pathogenic
3221C>T (3203C>A)	T1068I	**0.000743**	0.622030	Pathogenic
3242C>T (3224C>T)	T1075I	0.658401	**0.000909**	Unclassified
3243C>T (3225C>T)	T1075T	0.184777	**0.000057**	Unclassified
3614T>G (3596T>G)	V1199G	**0.023734**	0.175070	Pathogenic
3892C>G (3943C>G)	P1292A (P1315A)	0.290908	**0.000063**	Unclassified
4247C>T (4298C>T)	S1410L (S1433L)	0.321151	**0.000192**	Unclassified
4265G>A (4316G>A)	G1416D (G1439D)	0.332362	**0.000246**	Unclassified
4553A>C (4604A>C)	D1512A (D1535A)	**0.000139**	0.811770	Pathogenic
4649G>T (4700G>T)	G1544V (G1567V)	**0.000316**	0.424123	Pathogenic
4675del57 (4726del57)	1553del19 (1576del19)	**0.032488**	0.641493	Pathogenic
4867C>T (4918C>T)	H1617Y (H1640Y)	**0.020428**	0.148090	Pathogenic
4886T>G (4937T>G)	V1623G (V1646G)	**0.039219**	0.347325	Pathogenic
5177G>A (5228G>A)	R1720Q (R1743Q)	**0.003169**	0.960154	Pathogenic
5176C>T (5227C>T)	R1720W (R1743W)	**0.017443**	0.521431	Pathogenic

[a]Nucleotide and amino acid numbering corresponding to reference.[3] Nucleotide and amino acid numbering corresponding to reference[18] are given in parentheses.
[b]Pathogenic *de novo* mutation, most likely causing aberrant splicing of the *TSC2* mRNA; the Q373P amino acid substitution did not affect TSC1–TSC2 complex function.
[c]*P*-values <0.05 are indicated in bold.

rabbit polyclonal), Zymed laboratories (San Francisco, CA, USA) (anti-TSC1 and anti-TSC2 mouse monoclonals) and Li-Cor Biosciences (Lincoln, NE, USA) (goat anti-rabbit 680 nm and goat anti-mouse 800 nm conjugates). Chemicals were from Merck (Darmstadt, Germany), unless specified otherwise.

Cell culture

Human embryonal kidney (HEK) 293T cells were grown in Dulbecco's modified Eagle's medium (DMEM) (Lonza, Verviers, Belgium) supplemented with 10% fetal bovine serum, 50 U/ml penicillin and 50 μg/ml streptomycin (DMEM+), in a 10% CO_2 humidified incubator.

Western blotting

Cells were seeded onto 24-well plates and transfected with 0.2 μg TSC2, 0.4 μg TSC1 and 0.1 μg S6Kmyc expression constructs using polyethyleneimine (PEI) (Polysciences Inc., Warrington, PA, USA). A 1:4 w/w mixture of plasmid DNA and PEI was incubated in 0.2 ml DMEM for 15 min at 20°C before adding to the cells. After 4 h, the DMEM/DNA/PEI was replaced with DMEM+. Twenty-four hours after transfection, the cells were transferred to ice, washed with phosphate-buffered saline (PBS) (4°C) and harvested in 50 μl lysis buffer (50 mM Tris-HCl pH 8.0, 150 mM NaCl, 50 mM NaF, 1% Triton X-100, protease inhibitor cocktail (Complete, Roche Molecular Biochemicals, Woerden, The Netherlands)). Cells were lysed for 10 min on ice before centrifugation (10 000 *g* for 10 min at 4°C). The supernatants were diluted in loading buffer, separated on 6% SDS-PAGE gels and transfered to nitrocellulose membranes, as described previously.[19] Membranes were blocked for 1 h at 20°C with 5% low-fat milk powder (Campina Melkunie, Eindhoven, The Netherlands) in PBS and incubated overnight at 4°C with the primary antibodies: 1/16 000 dilution of 1895 (rabbit polyclonal against TSC2[19]), 1/5000 dilution of 2197 (rabbit polyclonal against TSC1[19]), 1/5000 dilution of a rabbit polyclonal against the myc epitope tag and 1/2000 dilution of 1A5 (mouse monoclonal against p70 S6 kinase (S6K) phosphorylated at amino acid T389). Antibodies were diluted in blocking solution containing 0.1% Tween 20 (Sigma-Aldrich Fine Chemicals, Poole, UK). After washing 3× for 5 min in PBS containing 0.1% Tween 20 (PBST), the membranes were incubated for 1 h at 20°C in the dark in PBST containing 1/5000 dilutions of goat anti-rabbit 680 nm and goat anti-mouse 800 nm secondary antibodies. After washing (3× for 5 min in PBST, 1× in PBS) the membranes were scanned using the Odyssey™ Infrared Imager (169 μm resolution, medium quality with 0 mm focus offset) (Li-Cor Biosciences, Lincoln, NE, USA). The integrated intensities of the protein bands were determined using the Odyssey™ software (default settings with background correction; 3 pixel width border average method).

ICW assays

Cells were seeded onto 96-well plates coated with 0.1 mg/ml poly-L-lysine (Sigma-Aldrich Fine Chemicals). Cells at 85–95% confluency were transfected with 0.1 μg TSC2, 0.2 μg TSC1 and 0.05 μg S6Kmyc expression constructs using PEI, as before. Each transfection mix was divided equally between three wells. After 4 h, the DMEM/DNA/PEI mixtures were replaced with DMEM+. ICW assays were performed 24 h after transfection. Cells were rinsed with PBS, fixed with freshly prepared 4% paraformaldehyde for 20 min at 20°C, washed 3× for 5 min with PBS containing 0.1% Triton X-100 and incubated for 90 min in blocking solution before incubation overnight at 4°C with the primary antibodies. Three different primary antibody mixes were prepared: 1/200 dilution of mouse monoclonal anti-TSC2 antibody, 1/200 dilution of mouse monoclonal anti-TSC1 antibody and 1/200 dilution of 1A5 (S6K T389 phosphorylation-specific mouse monoclonal). The antibodies were diluted in blocking solution containing 0.1% Tween 20 and a 1/500 dilution of the rabbit polyclonal anti-myc antibody. Antibodies were diluted according to the manufacturer's recommendations and based on the results of calibration experiments (see Supplementary Figure 1).

After washing for 3× for 5 min in PBST, the cells were incubated for 1 h at 20°C in the dark with a 1/500 dilution of goat anti-rabbit 680 nm and 1/500 dilution of goat anti-mouse 800 nm in PBST. After washing (4× for 5 min in PBST) the plates were scanned using the Odyssey Infrared Imager (169 μm resolution, medium quality with 3 mm focus offset). The integrated intensities of the protein signals were determined using the Odyssey software (8.5 mm quantification grid with background correction; 3 pixel width border average method).

ICW assay automation

In-cell western assays were performed using a Tecan EVO200 liquid handling station (Tecan Benelux, Giessen, The Netherlands). Transfected cells were fixed as before, washed 3× for 5 min with PBS containing 0.1% Triton X-100 and placed in the station for the subsequent incubation and wash steps. After aspiration of the wash buffer, the cells were incubated with blocking solution for 90 min followed by the primary antibody mixes for 8.5 h. After washing (3× for 5 min with PBST), the cells were incubated for 5 h with the secondary antibodies and washed (3× for 5 min with PBST; 1× for 5 min with PBS). Finally the PBS was aspirated, and the plate removed for scanning on the Odyssey Infrared Imager, as before. All incubation steps were performed at 4°C in the dark.

Results

ICW assay for the analysis of TSC1-TSC2-mTOR signalling

To determine whether the ICW assay was suitable for the analysis of transfected HEK 293T cells, we compared S6K

T389 phosphorylation in cells expressing TSC1, S6K and either wild-type TSC2 or the TSC2 R611Q mutant. Control cells were transfected with the pcDNA3 expression vector alone (no *TSC2*, *TSC1* or *S6K* cDNA inserts) or were co-transfected with the TSC1 and S6K expression constructs only. A schematic of the 96-well plate is shown in Figure 1a, and the resulting scans are shown in Figure 1b. After subtraction of the background signals, the ratio of the TSC2, TSC1 or T389-phosphorylated S6K (T389) signal (green) to the total S6K signal (red) was determined (Figure 1c). S6K-T389 phosphorylation was reduced ~2-fold in cells expressing wild-type TSC2, compared to either cells expressing the R611Q mutant or to cells without TSC2 expression. A similar reduction in S6K-T389 phosphorylation was observed when the protocol was modified for the Tecan EVO200 liquid handling station (Figure 1d).

ICW analysis of TSC2 variants

Next, we tested 20 TSC2 variants identified in our patient cohort, including three in-frame deletions (275delN, 580del26 and 1553del19), 17 missense changes (G62E, R98W, Q373P, A607E, T1068I, T1075I, V1199G, P1292A, S1410L, G1416D, D1512A, G1544V, H1617Y, V1623G, R1720Q and R1720W) and one silent change (T1075T). Two of the variants, R1720Q and R1720W, had previously been shown to be *de novo* changes occurring in sporadic TSC patients and, on this basis, were assumed to be pathogenic mutations.[10,18] In the other 18 cases, essential genetic and/or clinical data were unavailable and the identified variants could not be classified as either pathogenic or non-pathogenic. The positions of the variant amino acids are indicated in Figure 2.

All variants were analysed using the ICW assay in three independent experiments. The integrated intensities of the fluorescent signals were quantified using the Odyssey software and the signals for each TSC2 variant, and for TSC1 and T389-phosphorylated S6K in the presence of the different variants were determined relative to the total S6K signal in the same well. Subsequently, the degree of S6K-T389 phosphorylation in the presence of the different TSC2 variants, relative to wild-type TSC2, was determined.

A representative scan is shown in Figure 3b. The total S6K signal was relatively constant across the different wells, indicating that inter-well differences in transfection efficiency and cell number were small. The signals for the different TSC2 variants were also relatively constant. None of the amino acid changes had a dramatic effect on the TSC2 signal, although a slight decrease was noted for the R611Q, 275delN, 580del26, A607E and V1623G variants. Similarly, the TSC1 signal was relatively constant, with only slight reductions in the presence of the TSC2 R611Q, 275delN, 580del26 and A607E variants. The T389 phosphorylation status of S6K was clearly dependent on the presence of the different TSC2 variants. TSC2-dependent inhibition of S6K-T389 phosphorylation was significantly reduced (ie, specific S6K T389 phosphorylation signal was increased compared to wild-type TSC2) in the presence of the R98W, 275delN, 580del26, A607E, T1068I, V1199G, D1512A, G1544V, 1553del19, H1617Y, V1623G, R1720Q and R1720W variants. As shown in Table 1, the T389/S6K ratio in the presence of these TSC2 variants was significantly different to the T389/S6K ratio in the presence of wild-type TSC2 (unpaired *t*-test $P<0.05$). Furthermore, in the presence of these variants, S6K T389 phosphorylation was comparable to T389 phosphorylation in the absence of TSC2 or in the presence of the TSC2 R611Q mutant (T389/S6K ratio was not significantly different from control: unpaired *t*-test $P>0.05$; Table 1). Only the R98W variant was significantly different from both the positive and negative controls (Figure 3 and Table 1). The G62E, Q373P, T1075I, T1075T, P1292A, S1410L and G1416D variants were as effective as wild-type TSC2 at inhibiting S6K T389 phosphorylation (T389/S6K ratio was not significantly different from wild-type TSC2: unpaired *t*-test $P>0.05$; T389/S6K ratio was significantly different from the T389/S6K ratio in the absence of TSC2: unpaired *t*-test $P<0.05$; Table 1).

Immunoblot analysis of the TSC2 variants

We analysed the effects of the TSC2 variants on mTOR activity by immunoblotting. In three independent experiments, the expression of TSC1 and the TSC2 variants, and the expression and T389 phosphorylation status of S6K

Figure 1 Optimisation of the ICW assay for analysis of TSC2 variants. (**a**) Schematic showing part of a 96-well cell culture plate. Cells in wells A1–A3 (row A) were transfected with expression constructs for wild-type TSC2, TSC1 and myc-tagged S6K (S6K); B1–B3 (row B) were transfected with expression constructs for the TSC2 R611Q variant, TSC1 and S6Kmyc; C1–C3 (row C) with vector only and D1–D3 (row D) with expression constructs for TSC1 and S6Kmyc only. A1–D1 (column 1) were probed with a monoclonal antibody specific for TSC2 (Zymed laboratories; green); A2–D2 (column 2) were probed with a monoclonal antibody specific for TSC1 (Zymed laboratories; green) and A3–D3 (column 3) were probed with a monoclonal antibody specific for T389-phosphorylated S6K (Cell Signaling Technology; green). All wells were probed with a polyclonal antibody specific for the S6K myc tag (Cell Signaling Technology; red). (**b**) Odyssey scans of the wells are shown in A, showing the 800 nm (green) channel (left), the 680 nm (red) channel (centre) and the merged image (right). The transfections in rows A, B and C are indicated on the right, the antibody signals revealed in columns 1, 2 and 3 are indicated below the scans. (**c**) Graphical representation of the scans is shown in B. The integrated intensities of the green and red fluorescent signals were determined using the Odyssey software. After subtraction of the background values (wells C1–C3; row C), the green:red ratio was calculated. (**d**) ICW assay using the Tecan EVO200 liquid handling station. Integrated intensities were determined and the green:red signal ratios calculated as in C for four separate transfection experiments. The mean TSC2/S6K, TSC1/S6K and T389/S6K ratios, and standard deviations are indicated. The mean T389/S6K ratio in the presence of wild-type TSC2 was significantly reduced compared to the TSC2 R611Q variant ($P=0.03$) and TSC1 only control ($P=0.004$).

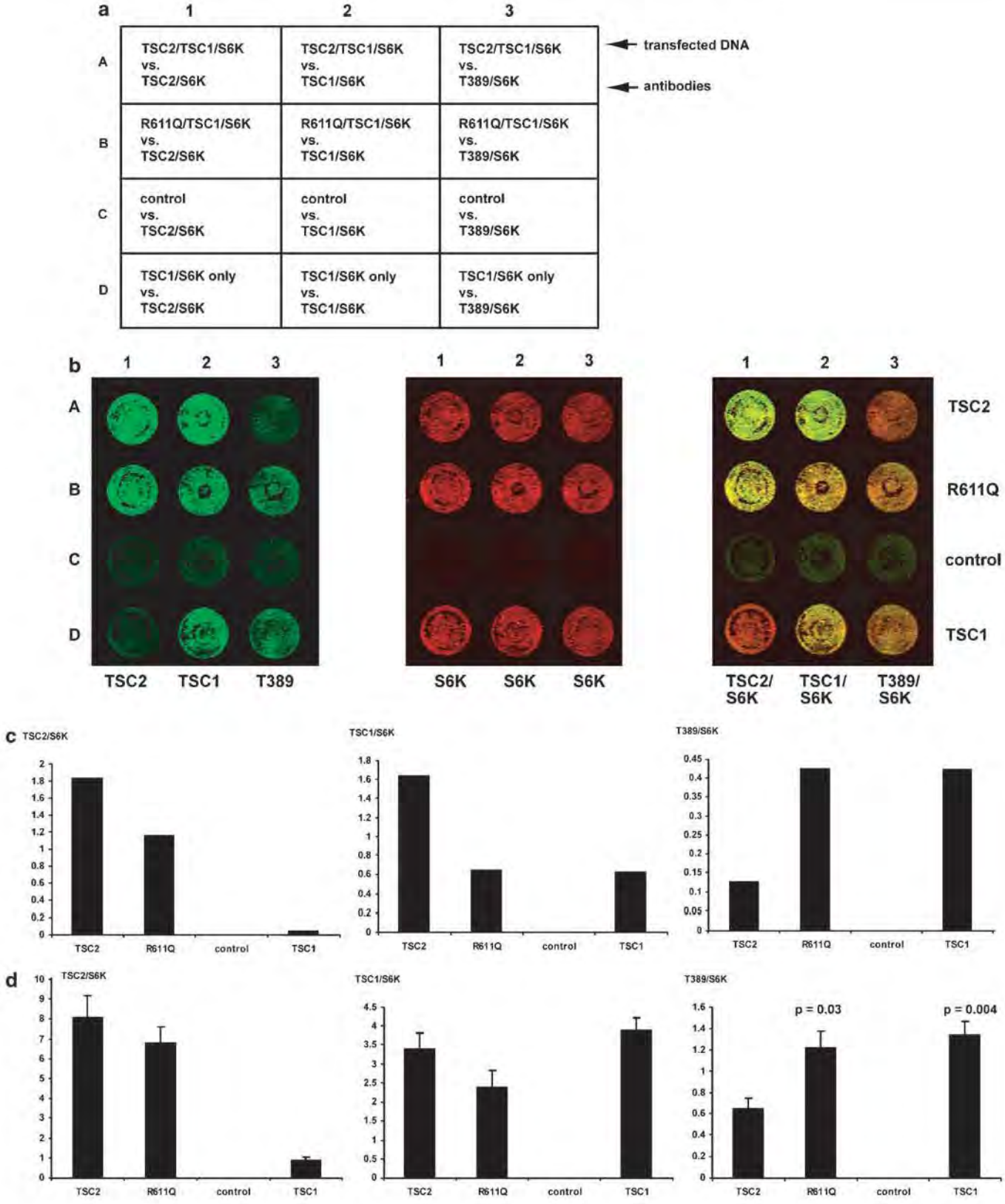
a
1
2
3
A
B
C
D
TSC2/TSC1/S6K vs. TSC2/S6K
TSC2/TSC1/S6K vs. TSC1/S6K
TSC2/TSC1/S6K vs. T389/S6K
R611Q/TSC1/S6K vs. TSC2/S6K
R611Q/TSC1/S6K vs. TSC1/S6K
R611Q/TSC1/S6K vs. T389/S6K
control vs. TSC2/S6K
control vs. TSC1/S6K
control vs. T389/S6K
TSC1/S6K only vs. TSC2/S6K
TSC1/S6K only vs. TSC1/S6K
TSC1/S6K only vs. T389/S6K
transfected DNA
antibodies
b
TSC2
TSC1
T389
S6K
S6K
S6K
TSC2/ S6K
TSC1/ S6K
T389/ S6K
TSC2
R611Q
control
TSC1
c
TSC2/S6K
TSC1/S6K
T389/S6K
TSC2
R611Q
control
TSC1
d
TSC2/S6K
TSC1/S6K
T389/S6K
p = 0.03
p = 0.004
TSC2
R611Q
control
TSC1

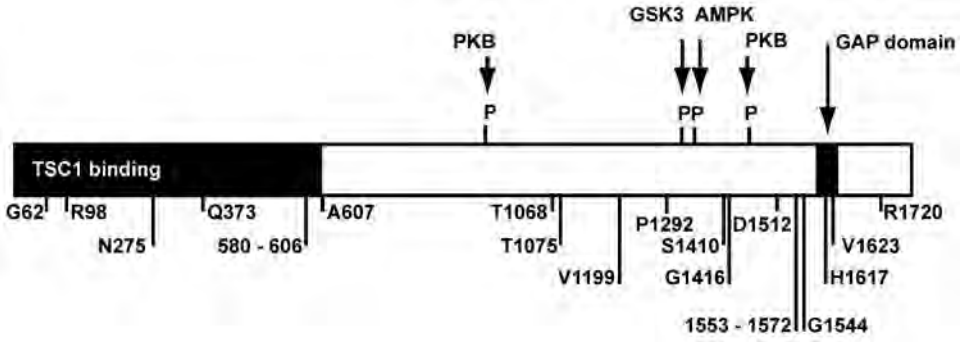

Figure 2 Schematic diagram of TSC2, showing the TSC1-binding and GAP domains, prominent sites of PKB, GSK3 and AMPK phosphorylation, and the positions of the variant amino acids tested in this study.

were determined (Figure 4). The results of the immunoblotting experiments were consistent with the ICW assays. Compared to wild-type TSC2 and the G62E, Q373P, T1075I, T1075T, P1292A, S1410L and G1416D variants, S6K T389 phosphorylation was increased in the presence of the R98W, 275delN, 580del26, A607E, T1068I, V1199G, D1512A, G1544V, 1553del19, H1617Y, V1623G, R1720Q and R1720W variants. The immunoblot data differed from the ICW data in that larger differences were detected in the signals of the different TSC2 variants, and in the TSC1 signal in the presence of the different TSC2 variants. The S6K signal was relatively constant, indicating that the observed differences were unlikely to be due to differences in cell number and transfection efficiency between the variants. Compared to wild-type TSC2, the signal for the R611Q variant was consistently reduced. In addition, the TSC1 signal was also reduced in the presence of the R611Q variant. Previous studies have demonstrated that the R611Q mutation disrupts the TSC1–TSC2 interaction, reducing the levels of TSC1 and TSC2 in cytosolic fractions.[20] A similar pattern was observed for the R98W, 275delN, 580del26 and A607E variants, indicating that these variants also have a reduced ability to interact with TSC1. The amino acids affected in these variants all map to regions of TSC2 that have previously been shown to be important for the TSC1–TSC2 interaction.[20–22]

Wild-type TSC2 was detected as a broad band on the immunoblots, consisting of 2–3 isoforms with slightly different migration characteristics. In contrast, some of the TSC2 variants appeared to migrate as a single band. This is most likely due to differences in the post-translational modification of the different variants.[7] We compared the phosphorylation status of the different variants using an antibody specific for TSC2 phosphorylated at the T1439 position. However, using this antibody, we did not observe any clear differences in TSC2-T1439 phosphorylation between wild-type TSC2 and the TSC2 variants (see Supplementary Figure 2).

Although the immunoblotting experiments supported the ICW data, the differences averaged over three independent experiments were not always significant (unpaired *t*-test; Figure 4). Therefore, the ICW gave more consistent and reproducible data, and allowed us to classify the 20 variants as pathogenic or not in a relatively short period of time. The ICW required fewer manipulations than the immunoblot analysis and was always performed using the same 96-well grid. Variables such as the cell harvest and fractionation steps and the gel and buffer characteristics most likely resulted in more inter-experiment differences in the immunoblot assays. A comparison of the steps involved in the two techniques is shown in Figure 5.

The ICW assay indicated that the TSC2 275delN, 580del26, A607E, T1068I, V1199G, D1512A, G1544V, 1553del19, H1617Y, V1623G, R1720Q and R1720W variants were likely to be pathogenic, as they all disrupted the ability of the TSC1–TSC2 complex to inhibit mTOR activity. Immunoblot analysis confirmed that these 12 variants are inactive and therefore disease causing.

The G62E, Q373P, T1075I, T1075T, P1292A, S1410L and G1416D variants were indistinguishable from wild-type TSC2 in both the ICW and immunoblot assays. However, it was possible that the corresponding nucleotide changes could still be pathogenic through effects on *TSC2* mRNA splicing. We analysed the nucleotide changes using three splice site prediction programs.[15–17] Only the 1136A>C (Q373P, *TSC2* exon 10) substitution was predicted to affect splicing. Codon 373 is encoded by the last three nucleotides of *TSC2* exon 10, and according to all three prediction programs, the 1136A>C substitution disrupts the exon 10 donor sequence, resulting in an aberrantly spliced *TSC2* mRNA. We concluded that the 1136A>C (Q373P) variant was a pathogenic splice site mutation, and not a missense mutation. Subsequent genetic analysis of the parents of the TSC patient with the *TSC2* 1136A>C (Q373P) variant demonstrated that this was a *de novo* change. Paternity was also confirmed in this case (data not shown).

In contrast to the TSC2 variants discussed above, the R98W variant could not be classified as either pathogenic or non-pathogenic. This variant was able to inhibit S6K T389 phosphorylation in both the ICW and immunoblot

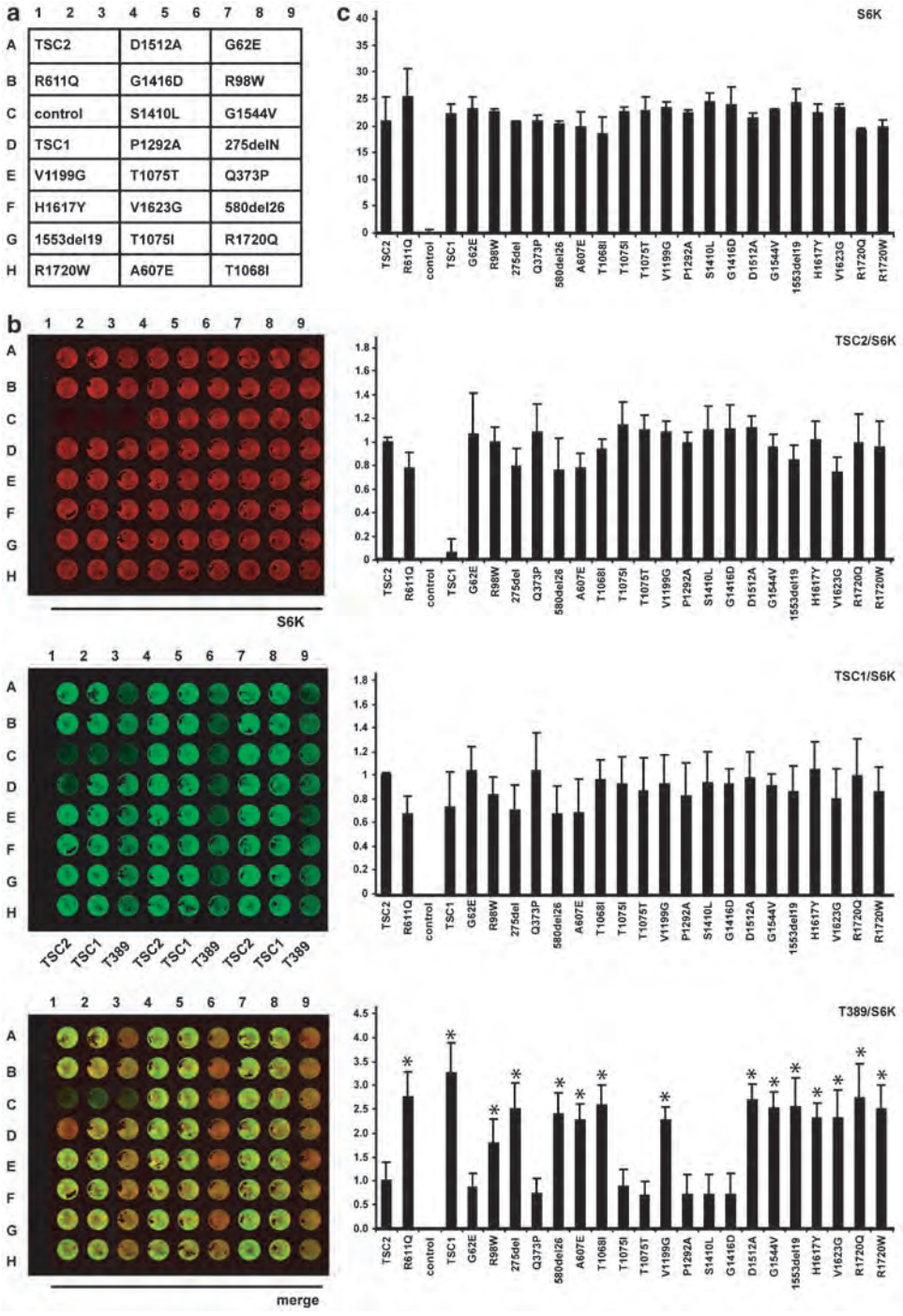

Figure 3 Characterisation of 20 TSC2 variants using the ICW assay. (**a**) Schematic showing part of a 96-well cell culture plate. Cells in wells A1–A3 (row A), B1–B3 (row B), C1–C3 (row C) and D1–D3 (row D) were transfected as before (see Figure 1). Cell in the remaining sets of three wells were transfected with expression constructs for the different TSC2 variants, TSC1 and S6Kmyc. All wells were probed with a polyclonal antibody specific for the S6K myc tag (red). Wells in columns 1, 4 and 7 were probed with a monoclonal antibody specific for TSC2 (green); wells in columns 2, 5 and 8 were probed with a monoclonal antibody specific for TSC1 (green) and wells in columns 3, 6 and 9 were probed with a monoclonal antibody specific for T389-phosphorylated S6K (green). (**b**) Odyssey scans of the wells are shown in (**a**). (**c**) Graphical representation of the results of three independent ICW assays. The integrated intensities of the green and red fluorescent signals were determined using the Odyssey software. In each case the background values, measured in wells C1–C3 (control), were subtracted from the integrated intensity. In the top graphic, the mean integrated intensity values for S6K are shown. In the three lower graphics, the expression of TSC2 and TSC1, and the T389 phosphorylation of S6K are indicated. To correct for inter-well differences in cell number and transfection efficiency, values are expressed relative to the total S6K signal. Standard deviations are indicated. TSC2 variants with a significantly different T389/S6K ratio than wild type ($P<0.05$) are indicated with an asterisk.

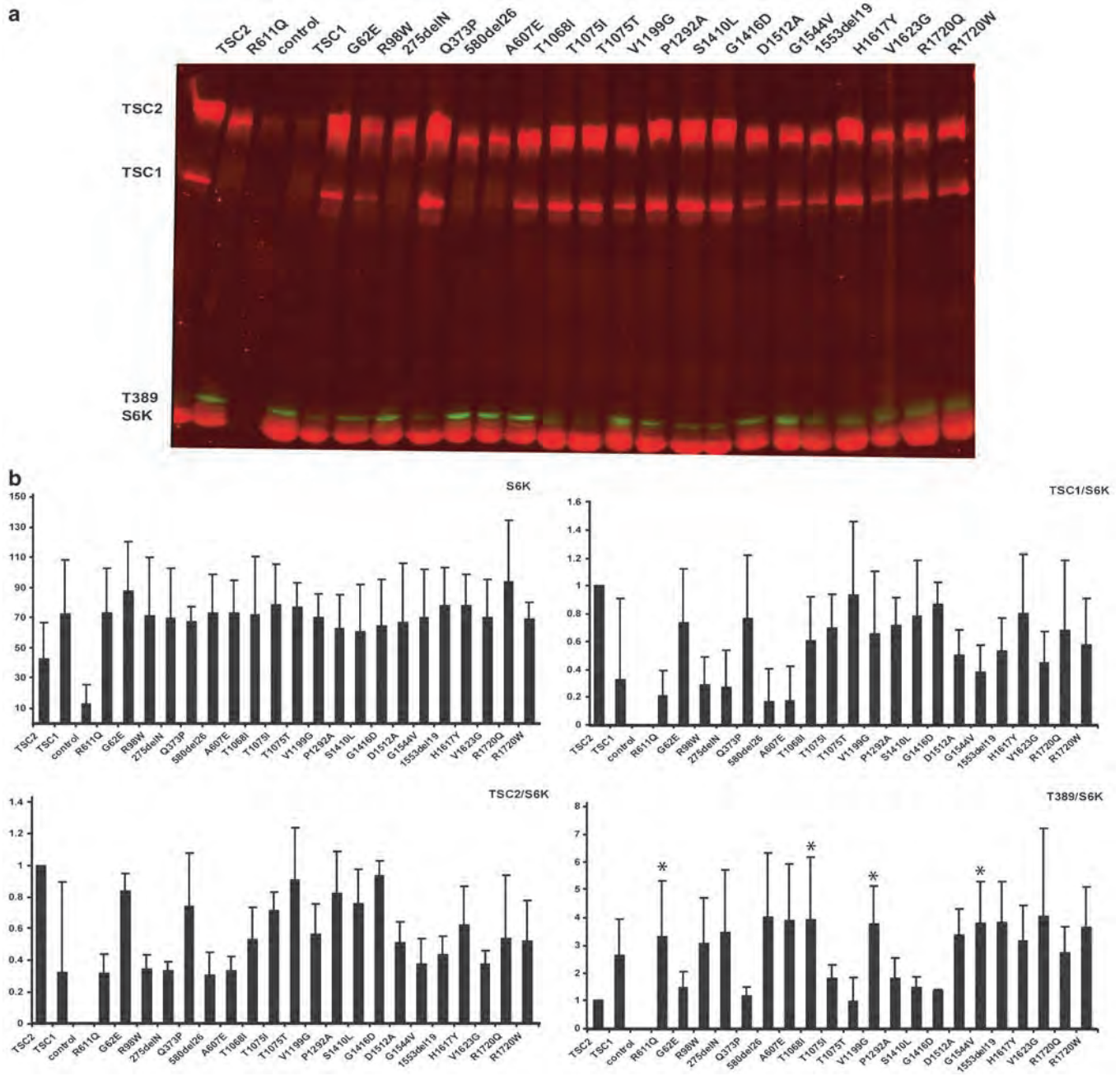

Figure 4 Characterisation of 20 TSC2 variants by immunoblot analysis. Cells co-transfected with expression constructs encoding TSC1, S6Kmyc and either wild-type TSC2 or one of the 20 TSC2 variants were harvested and cytosolic fractions separated on a 6% SDS-PAGE gel before transfer. Blots were probed with rabbit polyclonal antisera against TSC2, TSC1 and the myc epitope tag, and a mouse monoclonal against T389-phosphorylated S6K, followed by the Li-Cor goat anti-rabbit 800 and goat anti-mouse 680 secondary antibodies. (**a**) Representative scan of an immunoblot. Expression of the TSC2 variants, TSC1 and S6K (all red) and the T389 phosphorylation of S6K (green) are indicated. (**b**) Graphical representation of the results of three independent immunoblots. The integrated intensities of the green and red fluorescent signals were determined using the Odyssey software with background correction. In the top graphic, the mean values for S6K are shown. In the three lower graphics, the expression of TSC2 and TSC1, and the T389 phosphorylation of S6K are indicated. To correct for differences in cell number and transfection efficiency, values are expressed relative to the total S6K signal per lane. Standard deviations are indicated. TSC2 variants with a significantly different T389/S6K ratio than wild type ($P<0.05$) are indicated with an asterisk.

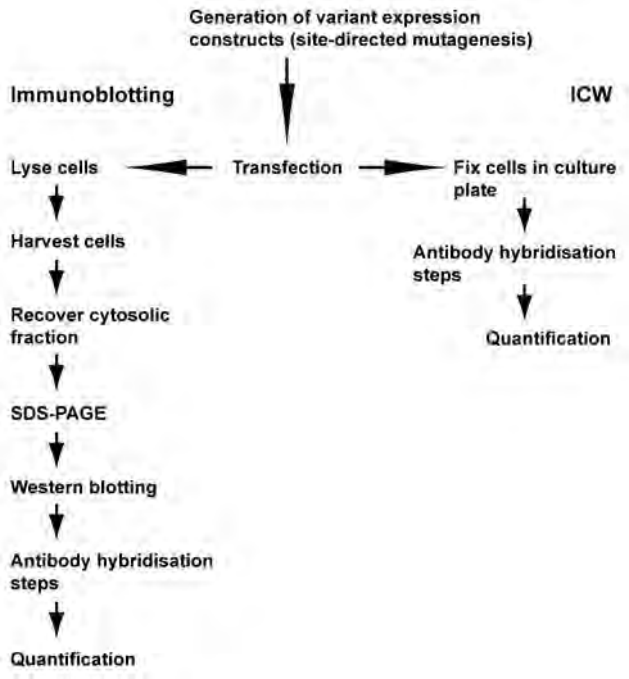

Figure 5 Flow diagram to show the steps involved in the ICW assay, compared to immunoblotting.

assays, but was less effective than wild-type TSC2. On the immunoblots, the expression of the R98W variant was reduced compared to wild-type TSC2, and the expression of TSC1 was also consistently reduced in the presence of this variant. This suggests that the R98W substitution affects the TSC1–TSC2 interaction, and therefore reduces the ability of the complex to inhibit mTOR signalling.

As shown in Figure 6, the *TSC2* 310C>T (R98W) substitution was detected in a mother and a fetus. The fetus did not survive to term and was diagnosed with TSC post-mortem. No signs of TSC were reported in either parent. The mother was heterozygous for the *TSC2* 310C>T (R98W) variant, whereas the fetus appeared to be hemizygous for this variant as the wild-type allele was not detected and MLPA analysis of the fetal DNA indicated that there was a deletion of *TSC2* exons 1–8. MLPA analysis of the *TSC1* locus in the fetus suggested that there was also a duplication of the entire *TSC1* coding region. However, due to a lack of material, we were unable to confirm the MLPA data. Therefore, the clinical, genetic and functional data for this variant were all problematic and we were unable to determine for certain whether the R98W substitution disrupts the TSC1–TSC2 complex sufficiently to cause TSC. *TSC2* missense mutations with apparently mild phenotypic effects have been described previously,[23–25] and have been shown to affect TSC1–TSC2 function *in vitro*.[24,25] In the family shown in Figure 6, it seems most likely that the deletion of exons 1–8 at the *TSC2* locus

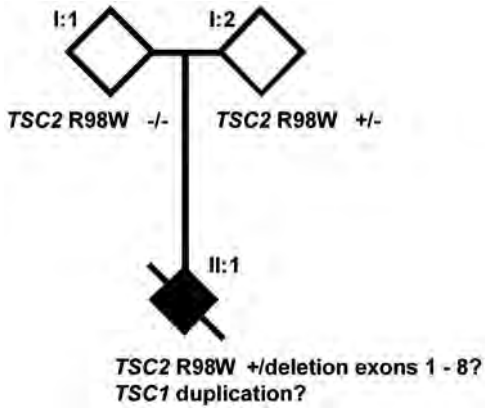

Figure 6 Pedigree showing inheritance of the TSC2 310 C>T (R98W) variant. Open symbols indicate no signs or symptoms of TSC; black symbol indicates definite TSC (diagnosed post-mortem). Genotypes, where known, are indicated.

caused TSC in the fetus. We could not rule out the possibility that the TSC2 R98W substitution modifies the phenotype in this family.

Discussion

Mutation analysis of individuals with, or suspected of having, a genetic disease facilitates the diagnosis, treatment and genetic counselling of those individuals and their families. However, in some cases, it is not possible to determine from the genetic data whether an identified nucleotide change is disease causing. Functional analysis of the predicted protein variants provides an additional method for determining whether specific changes are pathogenic. Here, we show that the ICW assay is a robust and reproducible assay for the analysis of unclassified TSC2 variants and can complement standard DNA-based molecular diagnostics. We tested the activity of 20 different TSC2 variants and identified 12 pathogenic changes (275delN, 580del26, A607E, T1068I, V1199G, D1512A, G1544V, 1553del19, H1617Y, V1623G, R1720Q and R1720W), 7 neutral variants (G62E, Q373P, T1075I, T1075T, P1292A, S1410L and G1416D), and one variant (R98W) where the functional significance of the substitution was not clear.

Characterisation of the effects of different TSC2 amino acid changes on the TSC1–TSC2 complex will help provide insight into the structure and function of the complex. The N-terminal 769 amino acids of TSC2 are important for the TSC1–TSC2 interaction.[19,22] Four changes mapping to this domain (R98W, 275delN, 580del26 and A607E) reduced the levels of both TSC1 and TSC2 in cytosolic fractions. We did not observe any effect of either the G62E or Q373P substitutions, indicating that these residues are not critical for the TSC1–TSC2 interaction. We analysed seven TSC2

variants affecting amino acids close to the TSC2 GAP domain (amino acids 1593–1631)[3] (Figure 2). All of these changes prevented the TSC1–TSC2-dependent inhibition of mTOR signaling, indicating that residues within and flanking the reported GAP domain are essential for TSC2 activity.

The TSC is one of several diseases that are caused by mutations in genes involved in the mTOR signalling pathway.[26] The application of similar ICW assays to analyse unclassified variants in individuals with these diseases may also prove to be a useful adjunct to standard molecular genetic analysis.

Acknowledgements

Financial support was provided by the US Department of Defense Congressionally-Directed Medical Research Program (grant no. TS060052), and the Michelle Foundation. The authors report no conflicts of interest.

References

1 Gomez M, Sampson J, Whittemore V (eds): *The Tuberous Sclerosis Complex*. Oxford, UK: Oxford University Press, 1999, pp 10–23.
2 van Slegtenhorst M, de Hoogt R, Hermans C *et al*: Identification of the tuberous sclerosis gene *TSC1* on chromosome 9q34. *Science* 1997; **277**: 805–808.
3 The European Chromosome 16 Tuberous Sclerosis Consortium: Identification and characterization of the tuberous sclerosis gene on chromosome 16. *Cell* 1993; **75**: 1305–1315.
4 Li Y, Corradetti MN, Inoki K, Guan K-L: TSC2: filling the GAP in the mTOR signaling pathway. *Trends Biochem Sci* 2004; **29**: 32–38.
5 Zhang H, Cicchetti G, Onda H *et al*: Loss of Tsc1/Tsc2 activates mTOR and disrupts PI3K-Akt signaling through downregulation of PDGFR. *J Clin Invest* 2003; **112**: 1223–1233.
6 Kwiatkowski DJ, Zhang H, Bandura JL *et al*: A mouse model of TSC1 reveals sex-dependent lethality from liver hemangiomas, and up-regulation of p70S6 kinase activity in *Tsc1* null cells. *Hum Mol Genet* 2001; **11**: 525–534.
7 Nellist M, Sancak O, Goedbloed MA *et al*: Distinct effects of single amino acid changes to tuberin on the function of the tuberin-hamartin complex. *Eur J Hum Genet* 2005; **13**: 59–68.
8 Jones AC, Shyamsundar MM, Thomas MW *et al*: Comprehensive mutation analysis of *TSC1* and *TSC2*, and phenotypic correlations in 150 families with tuberous sclerosis. *Am J Hum Genet* 1999; **64**: 1305–1315.
9 Dabora SL, Jozwiak S, Franz DN *et al*: Mutational analysis in a cohort of 224 tuberous sclerosis patients indicates increased severity of *TSC2*, compared with *TSC1*, disease in multiple organs. *Am J Hum Genet* 2001; **68**: 64–80.
10 Sancak O, Nellist M, Goedbloed M *et al*: Mutational analysis of the *TSC1* and *TSC2* genes in a diagnostic setting: genotype-phenotype correlations and comparison of diagnostic DNA techniques in tuberous sclerosis complex. *Eur J Hum Genet* 2005; **13**: 731–741.
11 Au K-S, Williams AT, Roach ES *et al*: Genotype/phenotype correlation in 325 individuals referred for a diagnosis of tuberous sclerosis complex in the United States. *Genet Med* 2007; **9**: 88–100.
12 Nellist M, Sancak O, Goedbloed M *et al*: Functional characterisation of the TSC1-TSC2 complex to assess multiple *TSC2* variants identified in single families affected by tuberous sclerosis complex. *BMC Med Genet* 2008; **9**: 10.
13 Wong SK: A 384-well cell-based phospho-ERK assay for dopamine D2 and D3 receptors. *Anal Biochem* 2004; **333**: 265–272.
14 Selkirk JV, Nottebaum LM, Ford IC *et al*: A novel cell-based assay for G-protein-coupled receptor-mediated cyclic adenosine monophosphate response element binding protein phosphorylation. *J Biomol Screen* 2006; **11**: 351–358.
15 NetGene2 Server. [www.cbs.dtu.dk/services/NetGene2].
16 SpliceSiteFinder. [www.genet.sickkids.on.ca/~ali/splicesitefinder.html].
17 BDGP. Splice Site Prediction by Neural Network [www.fruitfly.org/seq_tools/splice.html].
18 Tuberous sclerosis database—Leiden Open Variation Database. [www.chromium.liacs.nl/lovd/index.php?select_db=TSC2].
19 van Slegtenhorst M, Nellist M, Nagelkerken B *et al*: Interaction between hamartin and tuberin, the *TSC1* and *TSC2* gene products. *Hum Mol Genet* 1998; **7**: 1053–1057.
20 Nellist M, Verhaaf B, Goedbloed MA, Reuser AJJ, van den Ouweland AMW, Halley DJJ: *TSC2* missense mutations inhibit tuberin phosphorylation and prevent formation of the tuberin-hamartin complex. *Hum Mol Genet* 2001; **10**: 2889–2898.
21 Hodges A, Li S, Maynard J *et al*: Pathological mutations in TSC1 and TSC2 disrupt the interaction between hamartin and tuberin. *Hum Mol Genet* 2001; **10**: 2899–2905.
22 Li Y, Inoki K, Guan K-L: Biochemical and functional characterizations of small GTPase rheb and TSC2 GAP activity. *Mol Cell Biol* 2004; **24**: 7965–7975.
23 O'Conner SE, Kwiatkowski DJ, Roberts PS, Wollmann RL, Huttenlocher PR: A family with seizures and minor features of tuberous sclerosis and a novel TSC2 mutation. *Neurology* 2003; **61**: 409–412.
24 Mayer K, Goedbloed M, van Zijl K, Nellist M, Rott HD: Characterisation of a novel TSC2 missense mutation in the GAP related domain associated with minimal clinical manifestations of tuberous sclerosis. *J Med Genet* 2004; **41**: e64.
25 Jansen A, Sancak O, D'Agostino D *et al*: Mild form of tuberous sclerosis complex is associated with TSC2 R905Q mutation. *Ann Neurol* 2006; **60**: 528–539.
26 Inoki K, Corradetti MN, Guan K-L: Dysregulation of the TSC-mTOR pathway in human disease. *Nat Genet* 2005; **37**: 19–24.

Supplementary Information accompanies the paper on European Journal of Human Genetics website (http://www.nature.com/ejhg)

BMC Medical Genetics

BioMed Central

Research article

Open Access

Identification of a region required for TSC1 stability by functional analysis of *TSC1* missense mutations found in individuals with tuberous sclerosis complex

Melika Mozaffari[1], Marianne Hoogeveen-Westerveld[1], David Kwiatkowski[2], Julian Sampson[3], Rosemary Ekong[4], Sue Povey[4], Johan T den Dunnen[5], Ans van den Ouweland[1], Dicky Halley[1] and Mark Nellist*[1]

Address: [1]Department of Clinical Genetics, Erasmus Medical Centre, 3015 GE Rotterdam, The Netherlands, [2]Division of Experimental Medicine and Medical Oncology, Brigham and Womens Hospital, Boston MA 02115, USA, [3]Institute of Medical Genetics, University of Wales College of Medicine, Heath Park, Cardiff CF4 4XN, UK, [4]Research Department of Genetics, Evolution and Environment, University College London Wolfson House, 4 Stephenson Way, London, NW1 2HE, UK and [5]Department of Human and Clinical Genetics, Leiden University Medical Centre, 2333ZC Leiden, The Netherlands

Email: Melika Mozaffari - m.mozaffari@erasmusmc.nl; Marianne Hoogeveen-Westerveld - m.hoogeveen-westerveld@erasmusmc.nl; David Kwiatkowski - dk@rics.bwh.harvard.edu; Julian Sampson - Sampson@Cardiff.ac.uk; Rosemary Ekong - r.ekong@ucl.ac.uk; Sue Povey - s.povey@ucl.ac.uk; Johan T den Dunnen - dDunnen@HumGen.nl; Ans van den Ouweland - a.vandenouweland@erasmusmc.nl; Dicky Halley - d.halley@erasmusmc.nl; Mark Nellist* - m.nellist@erasmusmc.nl

* Corresponding author

Published: 11 September 2009

BMC Medical Genetics 2009, **10**:88 doi:10.1186/1471-2350-10-88

Received: 9 March 2009
Accepted: 11 September 2009

This article is available from: http://www.biomedcentral.com/1471-2350/10/88

Abstract

Background: Tuberous sclerosis complex (TSC) is an autosomal dominant disorder characterised by the development of hamartomas in a variety of organs and tissues. The disease is caused by mutations in either the *TSC1* gene on chromosome 9q34, or the *TSC2* gene on chromosome 16p13.3. The *TSC1* and *TSC2* gene products, TSC1 and TSC2, form a protein complex that inhibits signal transduction to the downstream effectors of the mammalian target of rapamycin (mTOR). Recently it has been shown that missense mutations to the *TSC1* gene can cause TSC.

Methods: We have used *in vitro* biochemical assays to investigate the effects on TSC1 function of *TSC1* missense variants submitted to the Leiden Open Variation Database.

Results: We identified specific substitutions between amino acids 50 and 190 in the N-terminal region of TSC1 that result in reduced steady state levels of the protein and lead to increased mTOR signalling.

Conclusion: Our results suggest that amino acid residues within the N-terminal region of TSC1 are important for TSC1 function and for maintaining the activity of the TSC1-TSC2 complex.

Background

Tuberous sclerosis complex (TSC) is an autosomal dominant disorder characterised by the development of hamartomas in a variety of organs and tissues, including the brain, skin and kidneys [1,2]. Mutations in either the *TSC1* gene on chromosome 9q34 [3], or the *TSC2* gene on

chromosome 16p13.3 [4] cause TSC. In most studies, 75 - 85% of individuals with TSC have been shown to carry a germ-line *TSC1* or *TSC2* mutation [5-9] and a further 5 - 10% carry *TSC1* or *TSC2* variants where it is not absolutely clear from the genetic data whether the change is disease-causing (a pathogenic variant), or not (a neutral variant). To determine whether these unclassified variants are disease-causing, the effect of the changes on protein function can be investigated [10,11].

The *TSC1* and *TSC2* gene products, TSC1 and TSC2, interact to form a protein complex [12]. TSC2 contains a GTPase activating protein (GAP) domain and acts on the rheb GTPase to inhibit rheb-GTP-dependent stimulation of the mammalian target of rapamycin (mTOR) [13]. The exact role of TSC1 in the TSC1-TSC2 complex is less clear, but it appears to be required for maintaining the stability, activity and correct intracellular localisation of the complex [14]. Inactivation of the TSC1-TSC2 complex results in activation of mTOR and phosphorylation of the mTOR targets p70 S6 kinase (S6K), ribosomal protein S6 and 4E-BP1 [15]. The effects of amino acid changes to TSC1 or TSC2 on TSC1-TSC2 complex formation, on the activation of rheb GTPase activity by the complex, and on the phosphorylation status of S6K and S6 can be determined [10,11,16]. Pathogenic missense changes towards the N-terminus of TSC2 prevent formation of the TSC1-TSC2 complex, while missense changes towards the C-terminus do not prevent TSC1-TSC2 binding but disrupt the rheb-GAP activity of TSC2 directly [10]. Pathogenic TSC1 missense changes are rare [5-9]. However, recent studies of TSC1 missense variants identified in bladder cancers [17] and in patients with TSC [11] have shown that TSC1 amino acid substitutions can be pathogenic, reducing steady state levels of TSC1 and leading to increased mTOR activity.

Here, we test 13 *TSC1* variants identified during mutation screening of individuals with TSC. Our analysis confirms that pathogenic *TSC1* missense mutations reduce steady state levels of TSC1, and result in increased mTOR signalling. Furthermore, we find that the intracellular localisation of pathogenic and neutral TSC1 variants is distinct. The pathogenic TSC1 amino acid substitutions are clustered within the conserved, hydrophobic N-terminal region of TSC1, indicating that this region plays an important role in TSC1 function.

Methods

Comparative analysis of TSC1 amino acid substitutions

TSC1 missense variants identified in individuals with TSC, or suspected of having TSC, and submitted to the LOVD *TSC1* mutation database [18,19] were chosen for analysis. To predict whether the variants were likely to be pathogenic, the amino acid substitutions were evaluated using the BLOSUM 62 and Grantham matrices [20,21], and a multiple sequence alignment analysis was performed using SIFT software [22,23]. Hydrophobicity plots and secondary structure predictions were generated using DNAMAN (Lynnon BioSoft), SABLE [24] and PSIPRED [25] software. To determine whether the identified changes were likely to have an effect on splicing, 3 different splice-site prediction programs were used [26-28].

Generation of constructs and antisera

Expression constructs encoding myc-tagged TSC1 variants were derived using the QuikChange site-directed mutagenesis kit (Stratagene, La Jolla, CA, U.S.A.). In each case the complete open reading frame of the mutated construct was verified by sequence analysis. Other constructs used in this study have been described previously [10,11]. Antibodies were described previously [12] or purchased from Cell Signaling Technology (Danvers, MA, U.S.A.), except for a mouse monoclonal antibody against TSC2 which was purchased from Zymed Laboratories (San Francisco, CA, U.S.A.) and a rabbit polyclonal antibody against ubiquitin which was purchased from DAKO (Glostrup, Denmark).

Effects of TSC1 variants on S6K T389 phosphorylation

Immunoblot analysis of S6K T389 phosphorylation in cells over-expressing TSC1 variants was performed as described previously [11]. Briefly, 80% confluent HEK 293T cells in 24-well cell culture dishes were transfected with a 4:2:1 mixture of the TSC1, TSC2 and S6K expression constructs (0.7 μg DNA total) in 50 μl Dulbecco's modified Eagle medium (DMEM) containing 2.1 μg polyethyleneimine (Polysciences, Warrington, PA, U.S.A.). Where necessary, an empty expression vector (pcDNA3; Invitrogen, Carlsbad, CA, U.S.A.) was added to make up the total amount of DNA. Twenty-four hours after transfection the cells were washed with cold PBS and lysed in 75 μl 50 mM Tris-HCl pH 8.0, 150 mM NaCl, 50 mM NaF and 1% Triton X100 containing protease inhibitors (Complete, Roche Molecular Biochemicals, Woerden, The Netherlands). After centrifugation (10 000 g, 10 minutes, 4°C), the supernatant and pellet fractions were recovered for immunoblot analysis. The pellet fractions were resuspended in 100 μl 62.5 mM Tris-HCl pH 6.8, 10% glycerol, 300 mM 2-mercaptoethanol, 2% SDS and sonicated (8 μm, 15 seconds, 4°C) prior to gel electrophoresis. Samples were run on 4-12% SDS-PAGE Criterion gradient gels (BioRad, Hercules, CA, U.S.A.) and blotted onto nitrocellulose. Blots were analysed using near infra-red fluorescent detection on an Odyssey™ Infrared Imager (169 μm resolution, medium quality with 0 mm focus offset) (Li-Cor Biosciences, Lincoln, NE, U.S.A.). The integrated intensities of the protein bands relative to the wild-type TSC1 values were determined in at least 3 separate experiments using the Odyssey™ software (default settings with

background correction; 3 pixel width border average method). Signal intensities were compared as described previously [29].

Proteosome-mediated degradation of TSC1 variants

HEK 293T cells were transfected with expression constructs encoding TSC2, S6K and the different TSC1 variants. Twenty-four hours after transfection the culture medium was replaced with DMEM containing either 42 μM MG-132 (Sigma-Aldrich, St. Louis, MO, U.S.A.) or vehicle control. After 4 hours, insulin (200 nM; Sigma-Aldrich) or vehicle control was added to the culture medium and, after a further 30 minute incubation, the cells were harvested and analysed by immunoblotting, as before.

Immunofluorescent detection of TSC1 variants

HEK 293T cells were seeded onto glass coverslips coated with poly-L-lysine (Sigma-Aldrich), transfected with expression constructs encoding the TSC1 variants and processed for immunofluorescent microscopy as described previously [12]. Fixed, permeabilised cells were incubated with a rabbit polyclonal antibody specific for TSC2 [12] and a mouse monoclonal antibody specific for the TSC1 C-terminal myc epitope tag (9B11, Cell Signaling Technology), followed by fluorescein isothiocyanate- and Cy3-coupled secondary antibodies against mouse and rabbit immunoglobulins (DAKO) respectively. Cells were studied using a Leica DM RXA microscope and Image Pro-Plus version 6 image analysis software.

Results

Comparative analysis of TSC1 amino acid substitutions

We selected 13 TSC1 amino acid substitutions (*TSC1* c.149T>C (p.L50P), c.153A>C (p.E51D), c.182T>C (p.L61P), c.278T>G (p.L93R), c.397G>T (p.V133F), c.568C>T (p.R190C), c.569G>C (p.R190P), c.1001C>T (p.S334L), c.1433A>G (p.E478G), c.1648C>G (p.Q550E), c.1974C>G (p.D658E), c.1976C>T (p.A659V) and c.2420T>C (p.I807T)) that were either possible pathogenic changes, or could not be excluded as neutral variants [18] (Table 1). In this group there was one confirmed *de novo* change, *TSC1* c.182T>C (p.L61P), that was very likely to be pathogenic. In one individual with TSC, 2 *TSC1* missense changes, c.149T>C (p.L50P) and c.2420T>C (p.I807T), were reported. To establish whether either of these changes was responsible for TSC, or whether the combination of both changes was required to inactivate TSC1, we tested a L50P-I807T double variant as well as the L50P and I807T single variants.

To predict whether the amino acid substitutions were likely to be pathogenic, we determined the scores of the BLOSUM 62 [20] and Grantham [21] amino acid substitution matrices for all the missense variants in the LOVD *TSC1* database (Figure 1A and 1B). These scores give an indication of the differences between amino acid pairs based on amino acid composition, polarity and molecular volume, as well as substitution frequencies. Both matrices indicated that the amino acid substitutions listed in the LOVD *TSC1* database in general become more conservative towards the C-terminal of TSC1. We also performed a SIFT analysis [23] using a multiple sequence alignment of TSC1 derived from 14 different species (human, chimpanzee, maccaca, cow, dog, horse, mouse, rat, chicken, pufferfish, honey bee, fruitfly, mosquito and fission yeast). The SIFT algorithm combines information from both the chemical structure of the individual amino acids and the evolutionary conservation of the protein to predict for each amino acid residue which substitutions can be tolerated by the protein. The results of the SIFT analysis are shown in Figure 1C and Table 1. Overall, the N-terminal (amino acids 1 - 270) and C-terminal (amino acids 680 - 1164) regions of TSC1 did not tolerate amino acid substitutions while the central region (amino acids 270 - 680) was predicted to be more tolerant (Figure 1C). Of the 13

Table 1: Summary of the functional analysis of TSC1 missense variants from the LOVD *TSC1* mutation database

Nucleotide change	Exon	Amino acid substitution	SIFT prediction	Effect on TSC1 function? (t-test)	Conclusion
c.149T>C	4	p.L50P	not tolerated	yes (p = 0.03)	pathogenic
c.153A>C	4	p.E51D	tolerated	no (p = 0.3)	neutral variant
c.182T>C	4	p.L61P	not tolerated	yes (p = 0.002)	pathogenic
c.278T>G	5	p.L93R	not tolerated	yes (p = 0.03)	pathogenic
c.397G>T	6	p.V133F	not tolerated	yes (p = 0.005)	pathogenic
c.569G>C	7	p.R190P	not tolerated	yes (p = 0.004)	pathogenic
c.568C>T	7	p.R190C	not tolerated	no (p = 0.19)	neutral variant
c.1001C>T	10	p.S334L	tolerated	no (p = 0.19)	neutral variant
c.1433A>G	14	p.E478G	tolerated	no (p = 0.6)	possible splice mutation
c.1648C>G	15	p.Q550E	tolerated	no (p = 0.9)	neutral variant
c.1974C>G	15	p.D658E	tolerated	no (p = 0.13)	neutral variant
c.1976C>T	15	p.A659V	tolerated	no (p = 0.1)	neutral variant
c.2420T>C	19	p.I807T	tolerated	no (p = 0.18)	neutral variant

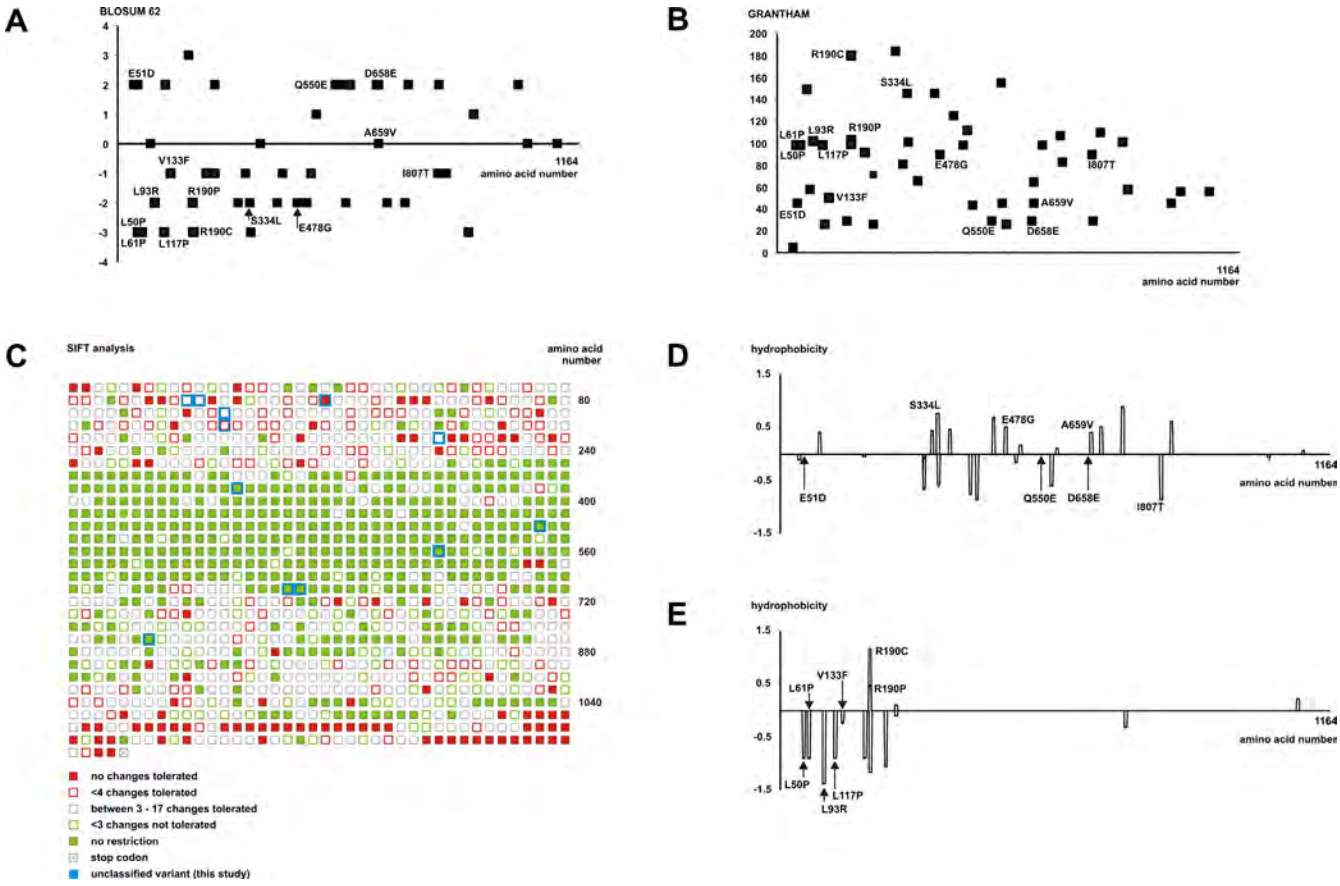

Figure 1

Predicted effects of amino acid substitutions on TSC1. (A) Plot of BLOSUM 62 scores for substitutions in the LOVD *TSC1* mutation database. Positive values represent conservative substitutions, negative values represent non-conservative substitutions. Substitutions investigated in this study are indicated. (B) Plot of Grantham scores for substitutions in the LOVD *TSC1* mutation database. The higher the Grantham score, the less conservative the substitution. Substitutions investigated in this study are indicated. (C) SIFT analysis of TSC1. Each amino acid is represented by a box. Solid green boxes represent positions that are completely tolerant (all substitutions possible); open green boxes represent positions where 1 or 2 substitutions are not tolerated. Solid red boxes represent intolerant positions (no substitutions tolerated); open red boxes represent positions where 3 or fewer substitutions are tolerated. Empty boxes represent positions where between 3 and 17 substitutions are tolerated. The positions of substitutions tested in this study are indicated in blue. (D) Comparative hydrophobicity profile of wild-type TSC1 with variants predicted by SIFT analysis to be tolerated. Hydrophobicity values were calculated for each amino acid using DNAMAN software (default parameters). Differences in the predicted hydrophobicity per amino acid were plotted. Values > 0 indicate an increase in hydrophobicity of the variant relative to wild-type; values < 0 indicate a decrease. Variants analysed as part of this study are indicated. (E). Comparative hydrophobicity profile of wild-type TSC1 with variants predicted by SIFT analysis not to be tolerated.

substitutions selected for this study, 7 were predicted to be tolerated and therefore unlikely to be pathogenic (Table 1). Of these, 5 were located in the central, substitution-tolerant region of TSC1 (amino acids 270 - 680). Six substitutions were predicted not to be tolerated and therefore likely to be pathogenic. All of these changes were located in the substitution-intolerant N-terminal region (amino acids 1 - 270). Finally, we investigated the effect of the substitutions on the hydrophobicity of TSC1 (Figure 1D and 1E). Three substitutions, p.E51D, p.Q550E and p.D658E, had no significant effect. These were all predicted by the SIFT algorithm to be tolerated changes. Of the remaining tolerated changes, p.S334L, p.E478G and p.A659V increased the hydrophobicity, while the p.I807T substitution had the opposite effect (Figure 1D). In the group of changes not tolerated by the SIFT analysis, the p.L50P, p.L61P, p.L93R and p.V133F substitutions decreased the hydrophobicity while the p.R190C and p.R190P substitutions increased the hydrophobicity (Figure 1E).

Splice site prediction analysis of the *TSC1* nucleotide changes was performed using 3 independent splice site prediction programs. Neither NetGene2 [26] nor Human Splicing Finder [28] predicted any splicing defects for any of the 13 changes. In contrast, NNSPLICE 0.9 [27] predicted that the *TSC1* c.1433A>G (p.E478G) change would result in the creation of an alternative splice donor site 6 nucleotides downstream of the wild-type exon 14 donor site. Furthermore, the wild-type site was no longer recognised as a splice donor site by the NNSPLICE 0.9 algorithm. If this prediction is correct, the new splice donor site created by the *TSC1* c.1433A>G change would result in the insertion of 2 extra codons (encoding amino acids GN) between codons 479 and 480, in addition to the p.E478G substitution.

Functional analysis of TSC1 amino acid substitutions

We characterised the effects of the 13 TSC1 single missense variants and the L50P/I807T double variant on the activity of the TSC1-TSC2 complex. We compared the 14 variants to wild-type TSC1 and the TSC1-L117P pathogenic variant [11]. As shown in Figure 2, the L50P, L61P, L93R, V133F and R190P amino acid substitutions all resulted in reduced levels of TSC1 (Figure 2A and 2B) and increased mTOR activity, as estimated by the T389 phosphorylation status of S6K (Figure 2A and 2D). These substitutions all had the same effect on TSC1 as the previously-characterised L117P substitution [11]. In each case, the T389/S6K ratio was significantly different from wild-type TSC1 (unpaired t-test p values all < 0.05; Table 1). We did not observe any differences between the L50P variant and the L50P/I807T double variant. Both variants were detected at low levels and did not inhibit S6K phosphorylation as effectively as wild-type TSC1.

The E51D, R190C, S334L, E478G, Q550E, D658E, A659V and I807T variants were detected at comparable levels to wild-type TSC1 (Figure 2A and 2B) and S6K T389 phosphorylation was reduced to the same levels as in the presence of wild-type TSC1 (Figure 2A and 2D). In each case, there was no significance difference in the T389/S6K ratio compared to wild-type TSC1 (unpaired t-test p values > 0.05; Table 1).

TSC1 variants are degraded by the proteosome

We considered two possible reasons for why the TSC1 L50P, L61P, L93R, V133F, R190P and L50P/I807T variants were detected at low levels. One possibility was that the variants were insoluble and therefore not present in the cell lysate fraction analysed by immunoblotting. We analysed the insoluble post cell lysis pellet fractions, but did not detect any of the TSC1 variants in these fractions (data not shown).

The second possibility was that the L50P, L61P, L93R, V133F, R190P and L50P/I807T variants were subject to rapid turn-over and degradation. Therefore, we treated cells expressing wild-type TSC1 or the L50P, L61P, L93R, V133F, R190P, L50P/I807T or L117P variants with the proteosome-inhibitor MG-132 [30]. After 4 hours treatment we observed an increase in the L50P, L61P, L93R, V133F, R190P, L50P/I807T and L117P signals when cells were treated with MG-132 (Figure 3A).

We estimated mTOR activity in MG-132-treated cells by measuring the T389 phosphorylation status of S6K in cells expressing the L50P or L117P variants and treated with MG-132 and/or insulin (Figure 3B-3D). The L50P and L117P signals were increased relative to the TSC1 wild-type signals in unstimulated cells treated with MG-132 as well as in cells treated with MG-132 and stimulated with 200 nM insulin for 30 minutes (Figure 3B and 3C). In (unstimulated and insulin stimulated) cells not treated with MG-132, wild-type TSC1 was detected at higher levels than the L50P and L117P variants, consistent with the analysis shown in Figure 2. In untreated cells, S6K T389 phosphorylation was increased in cells expressing the L50P and L117P variants, compared to cells expressing wild-type TSC1, consistent with the analysis shown in Figure 2. MG-132 treatment did not affect the detected levels of total S6K (Figure 3A), but in cells expressing the L50P and L117P variants, S6K T389 phosphorylation was increased compared to cells expressing wild-type TSC1, in both insulin-stimulated and unstimulated cells (Figure 3B and 3D).

Intracellular localisation of the TSC1 variants

Exogenous expression of the TSC1 E51D variant resulted in the formation of large, cytoplasmic TSC1 protein aggregates (Figure 4A), consistent with previous results with wild-type TSC1 [31]. Coexpression of TSC2 resulted in a dramatic reduction in the number of aggregates, and both TSC2 and the TSC1 E51D variant were detected throughout the cytoplasm (Figure 4C and 4D). We observed the same expression pattern for the TSC1 R190C, S334L, E478G, Q550E, D658E, A659V and I807T variants (data not shown).

In contrast to wild-type TSC1 and the E51D, R190C, S334L, E478G, Q550E, D658E, A659V and I807T variants, the L50P variant did not form large cytoplasmic aggregates when over-expressed in HEK 293T cells. Instead, the variant was expressed relatively uniformly throughout the cytoplasm (Figure 4F). This localisation was unaffected by coexpression of TSC2 (Figure 4H and 4I) or by MG-132 treatment (Figure 4K). The intracellular localisation patterns of the L61P, L93R, V133F and R190P variants were indistinguishable from the L50P variant (data not shown).

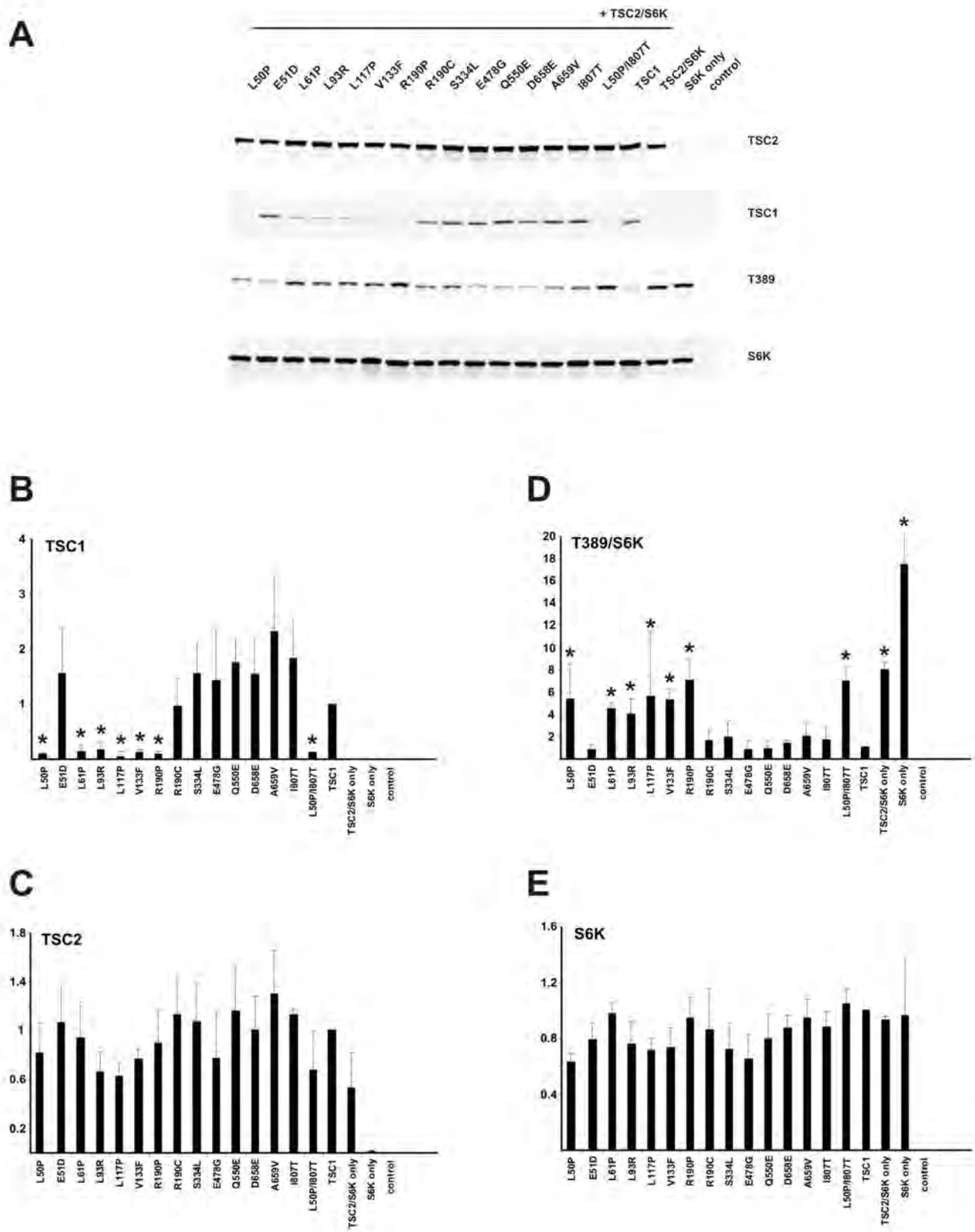

Figure 2 *(see legend on next page)*

Figure 2 *(see previous page)*
Immunoblot analysis of TSC1 variants. (A) Cells expressing the TSC1 variants and control cells expressing wild-type TSC1 and S6K only (TSC1/S6K), TSC2 and S6K only (TSC2/S6K), S6K only (S6K) or empty vector only (control) were analysed by immunoblotting. (B) Quantification of the immunoblot signals for the TSC1 variants. The integrated intensities of the signals for each variant, relative to wild-type TSC1, were determined in 3 independent experiments. Standard deviations are indicated. Signals significantly reduced compared to wild-type (unpaired t-test, p values < 0.05) are indicated with asterisks. (C) Quantification of the TSC2 signals. The TSC2 signals in the presence of the different TSC1 variants were not significantly different from the signal in the presence of wild-type TSC1 (unpaired t-test, p values >0.05). (D) Inhibition of S6K T389 phosphorylation in the presence of the TSC1 variants. The ratio of the S6K T389 phosphorylation signal to the total S6K signal (T389/S6K) was determined relative to wild-type TSC1 (wild-type TSC1 T389/S6K ratio = 1). Standard deviations are indicated. Variants with a significantly increased T389/S6K ratio (unpaired t-test p values < 0.05) are indicated with asterisks. (E) Quantification of the total S6K signals. The total S6K signals in the presence of the different variants were not significantly different to wild-type TSC1 (unpaired t-test, p values >0.05).

Discussion

We investigated the effects of 13 putative pathogenic amino acid substitutions on TSC1 function. Our findings are summarised in Table 1. The *TSC1* c.149T>C (p.L50P), c.182T>C (p.L61P), c.278T>G (p.L93R), c.397G>T (p.V133F) and c.569G>C (p.R190P) changes resulted in reduced levels of TSC1, a reduction in the TSC1-TSC2-dependent inhibition of mTOR activity and a distinct intracellular expression pattern compared to wild-type TSC1. We conclude that these changes are pathogenic. According to the LOVD *TSC1* mutation database the p.L61P and p.L93R substitutions are probably pathogenic [18]. Our functional analysis supports this conclusion. The p.L50P, p.V133F and p.R190P substitutions are classified as being of unknown pathogenicity in the database. Our data indicates that these changes are pathogenic.

Several studies indicate that *TSC1* mutations are associated with a less severe clinical presentation in TSC patients [7-9] and further study is required to determine whether patients with a *TSC1* missense mutation follow this pattern, or have a distinct phenotypic spectrum compared to other TSC patient groups.

The c.153A>C (p.E51D), c.568C>T (p.R190C), c.1001C>T (p.S334L), c.1648C>G (p.Q550E), c.1974C>G (p.D658E), c.1976C>T (p.A659V) and c.2420T>C (p.I807T) substitutions did not affect TSC1 in our assays and were predicted to have no effect on *TSC1* mRNA splicing. The LOVD *TSC1* mutation database lists the c.153A>C (p.E51D), c.568C>T (p.R190C) and c.1001C>T (p.S334L) variants as probably not pathogenic, and our functional analysis indicates that they are neutral variants. Furthermore, mutation screening in additional individuals with TSC resulted in the identification of definite pathogenic *TSC2* mutations in patients carrying the c.153A>C (p.E51D), c.568C>T (p.R190C) and c.1001C>T (p.S334L) substitutions, confirming the classification of these variants as non-pathogenic (data not shown). The LOVD *TSC1* mutation database lists the c.1648C>G (p.Q550E) and c.2420T>C (p.I807T) variants as being of unknown pathogenicity. Our analysis indicates that these variants are not pathogenic, although we could not confirm experimentally that they do not affect *TSC1* mRNA splicing.

The c.1433A>G (E478G) substitution is listed as being of unknown pathogenicity and did not affect TSC1 function in our assays. However, one of three splice site prediction programs identified a potential effect of this substitution on splicing. We did not have access to RNA from this particular individual so we compared the activity of the protein product of the predicted splice isoform to wild-type TSC1, the E478G variant and the L117P pathogenic variant. We did not observe any differences between the predicted TSC1 E478GinsGN variant and either wild-type TSC1 or the E478G [see Additional Files 1 and 2]. Therefore, we did not find any evidence that the c.1433A>G substitution was pathogenic.

All of the amino acid substitutions that affected TSC1 function in our assays were in the N-terminal region of TSC1 that was shown by our SIFT analysis to be relatively intolerant of amino acid changes (amino acids 1 - 270; see Figure 1). Two amino acid substitutions from this region, p.E51D and p.R190C, did not affect TSC1 function in our assays. Aspartate (E) and glutamate (D) are acidic amino acids. The BLOSUM 62 and Grantham matrices classify this substitution as conservative (Figure 1A and 1B) and our SIFT analysis predicted that the p.E51D substitution should be tolerated (Table 1). Therefore, in this case, the experimental data were in agreement with the *in silico* predictions. In contrast, the p.R190C substitution was non-conservative according to the BLOSUM 62 and Grantham matrices and was not tolerated according to our SIFT analysis. The predictions were therefore inaccurate for this particular amino acid substitution since the functional analysis did not reveal an effect on TSC1 function, and genetic analysis indicated that the substitution was not pathogenic. This result demonstrates that a conclusion

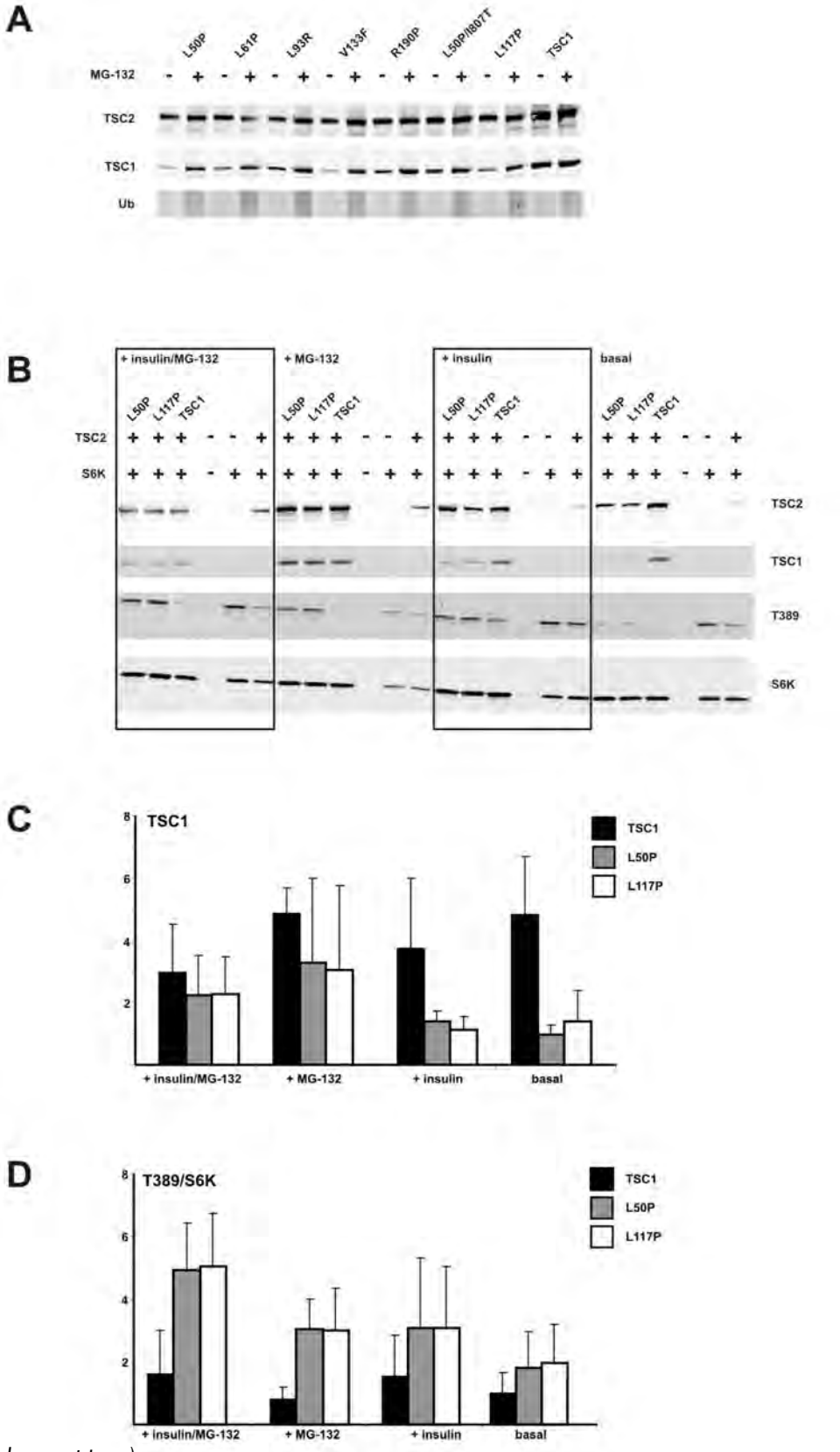

Figure 3 *(see legend on next page)*

Figure 3 *(see previous page)*
Proteosome-mediated degradation of pathogenic TSC1 variants. (A) Immunoblot showing levels of TSC2, wild-type TSC1 and pathogenic TSC1 variants in cells treated with 42 μM MG-132 for 4 hours, or left untreated. The blot was incubated with an antibody against ubiquitin (Ub) to show the effect of the MG-132 treatment. (B) Immunoblot showing levels of TSC2, wild-type TSC1 and the L50P and L117P variants, S6K and T389-phosphorylated S6K (T389) in cells treated with 42 μM MG-132 and 200 nM insulin (+ insulin/MG-132), 42 μM MG-132 only (+ MG-132), 200 nM insulin only (+ insulin), or left untreated (basal). (C) Quantification of the immunoblot signals, showing MG-132-dependent inhibition of proteosome-mediated degradation of the TSC1 L50P and L117P variants. The mean integrated intensities (arbitrary units) of the signals for wild-type TSC1 (black), and the L50P (grey) and L117P (white) variants are shown. MG-132 treatment resulted in a relative increase in the signals for the L50P and L117P variants compared to wild-type TSC1 in both insulin stimulated and unstimulated cells. (D) Quantification of the immunoblot signals showing increased S6K T389 phosphorylation in MG-132 treated cells expressing the L50P or L117P variants. S6K T389 phosphorylation was determined as in Figure 2. (T389/S6K ratio). Compared to MG-132-treated cells expressing wild-type TSC1, MG-132 treatment of cells expressing the L50P and L117P variants increased the T389/S6K ratio.

with respect to pathogenicity based on *in silico* analysis only should be made with caution.

To provide clinicians and researchers with the maximum amount of information, gene variant databases should move towards incorporating both *in vitro* and *in silico* data [32]. We will add the functional and *in silico* results on the variants described here to the LOVD *TSC1* database as part of the individual entries. We will include the BLOSUM 62, Grantham and SIFT scores as well as the potential splice effects of the different variants. However, for all apparent missense variants, conclusions with regard to pathogenicity will continue to rely on clinical, family and functional data. As the above example shows, although *in silico* analysis is a valuable research tool, it is not yet reliable enough to inform clinical decisions.

All the pathogenic TSC1 amino acid substitutions identified to date map between residues 50 and 224 (this study and [11]). One explanation for the apparent clustering of pathogenic amino acid substitutions to this region is that it is critical for TSC1 function. Alternatively, these substitutions may simply be less conservative than the neutral variants we tested. Although the pathogenic substitutions between amino acids 50 and 190 identified in this study were not conservative, there was no clear distinction between these changes and other neutral substitutions. For example, as shown in Figure 1, the neutral p.R190C variant is a non-conservative, non-tolerated substitution that is predicted to have a large effect on TSC1 hydrophobicity, while the pathogenic p.R190P variant is a more conservative substitution and has a less dramatic effect on TSC1 hydrophobicity. Similarly, the p.V133F substitution is more conservative than the p.R190C substitution and has a relatively mild effect on TSC1 hydrophobicity, yet still has a dramatic effect on TSC1 function in our assays. In addition to the p.E51D and p.R190C substitutions, 6 other TSC1 amino acid substitutions did not affect TSC1 function in our assays. The neutral p.S334L and p.E478G substitutions are non-conservative changes located within the substitution-tolerant central region of TSC1 defined by the SIFT analysis (amino acids 270 - 680; see Figure 1). The neutral, non-conservative p.I807T substitution lies outside this central region, but was also predicted by the SIFT algorithm to be tolerated (Table 1). The neutral p.Q550E, p.A659V and p.D658E substitutions are all conservative, tolerated changes. The results of the *in silico* and functional analyses are consistent with the N-terminal of TSC1 being a conserved, substitution-intolerant region that has an important role in maintaining TSC1 expression and activity in the cell.

The L50P, L61P, L93R, V133F and R190P variants were detected at lower levels compared to wild-type TSC1 and the E51D, R190C, S334L, Q550E, D658E, A659V and I807T variants. Inhibition of proteosome-mediated degradation resulted in increased levels of the L50P and L117P variants, indicating that the pathogenic TSC1 variants are normally rapidly degraded by the proteosome. Interestingly, increasing the levels of the TSC1 L50P and L117P variants by inhibiting proteosome activity resulted in an increase in mTOR activity, as estimated by the extent of S6K T389 phosphorylation. Therefore, increased expression of the L50P and L117P variants had a dominant negative effect on mTOR signalling. One possible explanation for this effect is that the mutant variants sequester TSC2 in inactive TSC1-TSC2 complexes, thereby reducing the capacity of the cells to inhibit mTOR activity. Therefore, MG-132 treatment may help distinguish more clearly between pathogenic and non-pathogenic TSC1 variants.

It is unlikely that this dominant negative effect is significant *in vivo* in TSC patients because, as our studies indicate, the L50P and L117P variants are rapidly degraded compared to wild-type TSC1 (Figure 2A). However, it could provide an explanation for the relative scarcity of *TSC1* missense mutations. It is possible that other missense variants are stable and do have a dominant negative

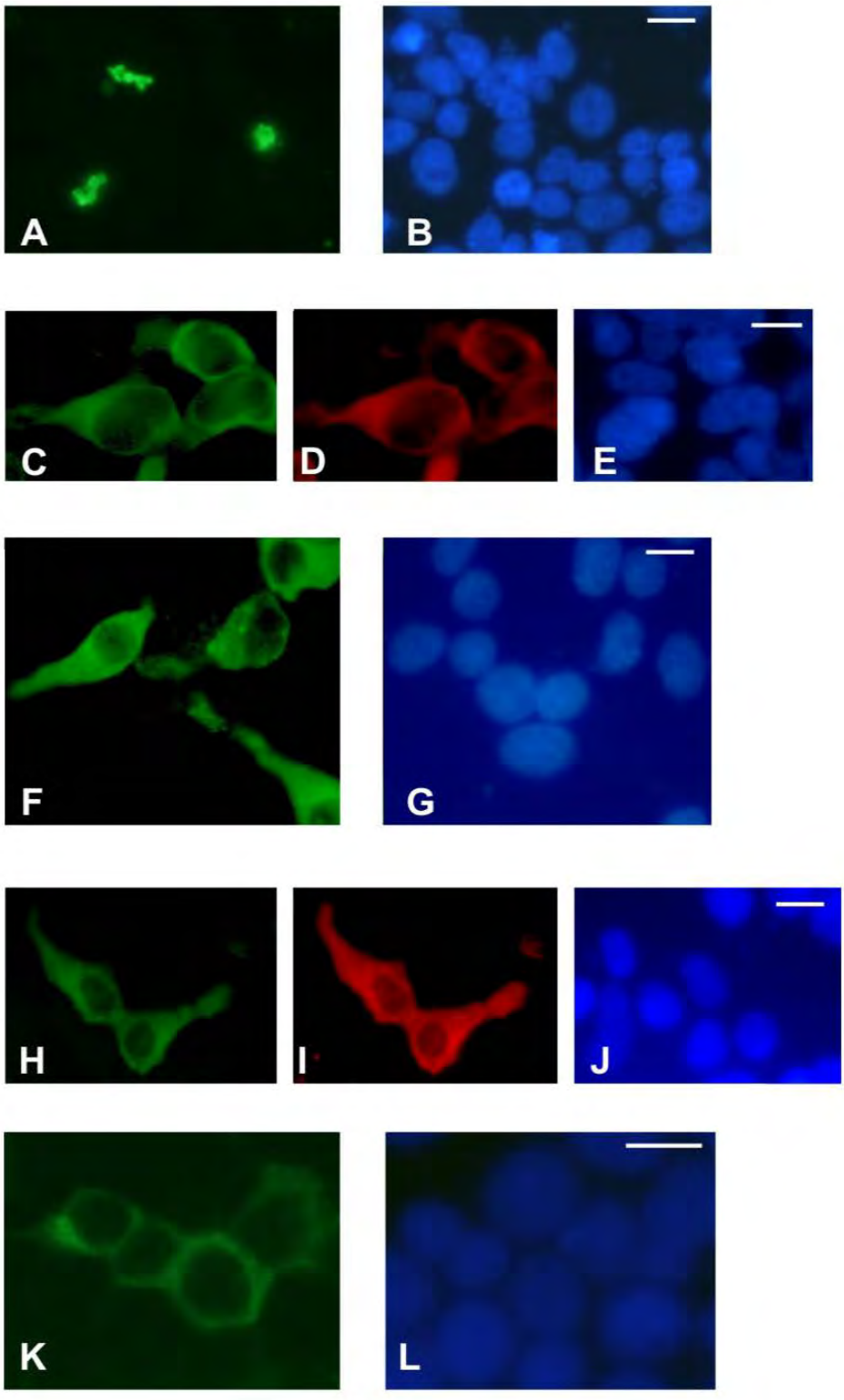

Figure 4 *(see legend on next page)*

Figure 4 *(see previous page)*
Intracellular localisation of TSC1 variants detected by immunofluorescence microscopy. (A - B) Immunofluorescence microscopy of cells expressing the TSC1 E51D variant. (A) Punctate cytoplasmic localisation of the E51D variant; (B) DAPI nuclear stain. White scale bar: 5 μm.(C - E) Immunofluorescence microscopy of cells coexpressing TSC2 and the E51D variant. (C) Diffuse cytoplasmic localisation of the E51D variant in the presence of TSC2; (D) Diffuse cytoplasmic localisation of TSC2; (E) DAPI nuclear stain. White scale bar: 5 μm. (F - G) Immunofluorescence microscopy of cells expressing the TSC1 L50P variant. (F) Diffuse cytoplasmic localisation of the L50P variant; (G) DAPI nuclear stain. White scale bar: 5 μm. (H - J) Immunofluorescence microscopy of cells coexpressing TSC2 and the L50P variant. (H) Diffuse cytoplasmic localisation of the L50P variant in the presence of TSC2; (I) Diffuse cytoplasmic localisation of TSC2; (J) DAPI nuclear stain. White scale bar: 5 μm. (K - L) Immunofluorescence microscopy of cells expressing the TSC1 L50P variant and treated with MG-132. (K) Diffuse cytoplasmic localisation of the L50P variant after MG-132 treatment; (L) DAPI nuclear stain. White scale bar: 5 μm

effect on TSC1-TSC2 function *in vivo* that is incompatible with embryonic survival.

Further study is required to explore in more detail how amino acids close to the N-terminal (residues 50 - 224) are important for TSC1 function. One possibility is that they are necessary for the proposed membrane localisation of TSC1 [33]. Alternatively, they may mediate other inter- or intramolecular interactions. Our observation that pathogenic amino acid substitutions prevent the formation of large TSC1-containing aggregate structures suggests that amino acids 50 - 224 may help mediate TSC1 homodimerisation.

Conclusion

We have analysed 13 *TSC1* variants identified in TSC patients that cause missense changes to the TSC1 protein, and identified 5 pathogenic substitutions. Our data confirm that functional assays can be used to differentiate between neutral and pathogenic variants, facilitating the identification of pathogenic mutations in individuals with TSC and providing insight into how specific amino acid residues contribute to protein function.

Amino acids close to the N-terminal of TSC1 (amino acids 50 - 190) are essential for TSC1 function. Amino acid changes to this region prevent the formation of large TSC1 aggregates and promote proteosome-mediated degradation of the protein, thereby reducing steady state levels of TSC1 and resulting in increased signalling through mTOR. Rapid degradation of the mutant TSC1 isoforms *in vivo* most likely prevents the possible dominant negative effects of these variants on TSC1-TSC2-dependent inhibition of mTOR signalling.

Abbreviations

TSC: tuberous sclerosis complex; GAP: GTPase activating protein; mTOR: mammalian target of rapamycin; S6K: p70 S6 kinase.

Competing interests

The authors declare that they have no competing interests.

Authors' contributions

MM, MHW and MN performed the practical work; mutation information was provided by DK, JS, AvdO and DH; RE, SP and JdD are responsible for curation of the LOVD *TSC1* mutation database. The manuscript was drafted by MN and read and approved by all authors.

Additional material

Additional file 1

Additional Figure 1: Inhibition of S6K-T389 phosphorylation by the TSC1 E478GinsGN variant. *Figure showing the inhibition of S6K-T389 phosphorylation by the TSC1. E478GinsGN predicted splice variant*
Click here for file
[http://www.biomedcentral.com/content/supplementary/1471-2350-10-88-S1.jpeg]

Additional file 2

Figure Legend Additional Figure 1: Inhibition of S6K-T389 phosphorylation by the TSC1 E478GinsGN variant. *Figure legend to Additional Figure 1.*
Click here for file
[http://www.biomedcentral.com/content/supplementary/1471-2350-10-88-S2.doc]

Acknowledgements

Financial support was provided by the U.S. Department of Defense Congressionally-Directed Medical Research Program (grant #TS060052), NIH NINDS NS31535 and the Tuberous Sclerosis Alliance. The authors report no conflicts of interest.

References

1. Gomez M, Sampson J, Whittemore V, eds: *The tuberous sclerosis complex* Oxford, UK: Oxford University Press; 1999.
2. Roach ES, DiMario FJ, Kandt RS: **Tuberous sclerosis consensus conference: recommendations for diagnostic evaluation. National Tuberous Sclerosis Association.** *J Child Neurol* 1999, **14:**401-407.
3. van Slegtenhorst M, de Hoogt R, Hermans C: **Identification of the tuberous sclerosis gene *TSC1* on chromosome 9q34.** *Science* 1997, **277:**805-808.
4. The European Chromosome 16 Tuberous Sclerosis Consortium: **Identification and characterization of the tuberous sclerosis gene on chromosome 16.** *Cell* 1993, **75:**1305-1315.
5. Jones AC, Shyamsundar MM, Thomas MW: **Comprehensive mutation analysis of *TSC1* and *TSC2*, and phenotypic correlations**

in 150 families with tuberous sclerosis. *Am J Hum Genet* 1999, **64:**1305-1315.
6. Dabora SL, Jozwiak S, Franz DN: **Mutational analysis in a cohort of 224 tuberous sclerosis patients indicates increased severity of *TSC2*, compared with *TSC1*, disease in multiple organs.** *Am J Hum Genet* 2001, **68:**64-80.
7. Sancak O, Nellist M, Goedbloed M: **Mutational analysis of the *TSC1* and *TSC2* genes in a diagnostic setting: genotype-phenotype correlations and comparison of diagnostic DNA techniques in tuberous sclerosis complex.** *Eur J Hum Genet* 2005, **13:**731-741.
8. Niida Y, Lawrence-Smith N, Banwell A: **Analysis of both *TSC1* and *TSC2* for germline mutations in 126 unrelated patients with tuberous sclerosis.** *Hum Mutat* 1999, **14:**412-422.
9. Au K-S, Williams AT, Roach ES: **Genotype/phenotype correlation in 325 individuals referred for a diagnosis of tuberous sclerosis complex in the United States.** *Genet Med* 2007, **9:**88-100.
10. Nellist M, Sancak O, Goedbloed MA: **Distinct effects of single amino acid changes to tuberin on the function of the tuberin-hamartin complex.** *Eur J Hum Genet* 2005, **13:**59-68.
11. Nellist M, Heuvel D van den, Schluep D: **Missense mutations to the *TSC1* gene cause tuberous sclerosis complex.** *Eur J Hum Genet* 2009, **17:**319-328.
12. van Slegtenhorst M, Nellist M, Nagelkerken B: **Interaction between hamartin and tuberin, the *TSC1* and *TSC2* gene products.** *Hum Mol Genet* 1998, **7:**1053-1057.
13. Li Y, Corradetti MN, Inoki K: **TSC2: filling the GAP in the mTOR signaling pathway.** *Trends Biochem Sci* 2003, **29:**32-38.
14. Rosner M, Hanneder M, Siegel N: **The tuberous sclerosis gene products hamartin and tuberin are multifunctional proteins with a wide spectrum of interacting partners.** *Mut Res* 2008, **658:**234-246.
15. Huang J, Manning BD: **The TSC1-TSC2 complex: a molecular switchboard controlling cell growth.** *Biochem J* 2008, **412:**179-90.
16. Nellist M, Sancak O, Goedbloed MA: **Functional characterisation of the TSC1-TSC2 complex to assess multiple TSC2 variants identified in single families affected by tuberous sclerosis complex.** *BMC Med Genet* 2008, **9:**10.
17. Pymar LS, Platt FM, Askham JM: **Bladder tumour-derived somatic TSC1 missense mutations cause loss of function via distinct mechanisms.** *Hum Mol Genet* 2008, **17:**2006-2017.
18. **Tuberous sclerosis database - Leiden Open Variation Database** [http://www.LOVD.nl/TSC1]
19. Fokkema IF, den Dunnen JT, Taschner PE: **LOVD: easy creation of a locus-specific sequence variation database using an "LSDB-in-a-box" approach.** *Hum Mutat* 2005, **26:**63-68.
20. Henikoff S, Henikoff JG: **Amino acid substitution matrices from protein blocks.** *Proc Natl Acad Sci USA* 1992, **89:**10915-10919.
21. Grantham R: **Amino acid difference formula to help explain protein evolution.** *Science* 1973, **185:**862-864.
22. Ng PC, Henikoff S: **Predicting the effects of amino acid substitutions on protein function.** *Annu Rev Genomics Hum Genet* 2006, **7:**61-80.
23. Ng PC, Henikoff S: **Accounting for human polymorphisms predicted to affect protein function.** *Genome Res* 2002, **12:**436-446.
24. Adamczak R, Porollo A, Meller J: **Accurate Prediction of Solvent Accessibility Using Neural Networks Based Regression.** *Proteins: Structure, Function and Bioinformatics* 2004, **56:**753-767.
25. Jones DT: **Protein secondary structure prediction based on position-specific scoring matrices.** *J Mol Biol* 1999, **292:**195-202.
26. **NetGene2 Server** [http://www.cbs.dtu.dk/services/NetGene2]
27. **BDGP: Splice Site Prediction by Neural Network** [http://www.fruitfly.org/seq_tools/splice.html]
28. **Human Splicing Finder** [http://www.umd.be/HSF/HSF.html]
29. Coevoets R, Arican S, Hoogeveen-Westerveld M: **A reliable cell-based assay for testing unclassified *TSC2* gene variants.** *Eur J Hum Genet* 2009, **17(3):**301-310.
30. Lee DH, Goldberg AL: **Proteasome inhibitors: valuable new tools for cell biologists.** *Trends Cell Biol* 1998, **8:**397-403.
31. Nellist M, van Slegtenhorst MA, Goedbloed M: **Characterization of the cytosolic tuberin-hamartin complex: tuberin is a cytosolic chaperone for hamartin.** *J Biol Chem* 1999, **274:**35647-35652.
32. Cotton RG, Auerbach AD, Axton M: **Genetics. The Human Variome Project.** *Science* 2008, **322:**861-862.
33. Cai SL, Tee AR, Short D: **Activity of TSC2 is inhibited by AKT-mediated phosphorylation and membrane partitioning.** *J Cell Biol* 2006, **173:**279-89.

Pre-publication history

The pre-publication history for this paper can be accessed here:

http://www.biomedcentral.com/1471-2350/10/88/prepub

J Neuropathol Exp Neurol
Vol. 68, No. 10
October 2009
pp. 1136–1146

ORIGINAL ARTICLE

Hamartin Variants That Are Frequent in Focal Dysplasias and Cortical Tubers Have Reduced Tuberin Binding and Aberrant Subcellular Distribution In Vitro

Céline Lugnier, MS, Michael Majores, MD, Jana Fassunke, PhD, Katharina Pernhorst, MSc, Pitt Niehusmann, MD, Matthias Simon, MD, Mark Nellist, PhD, Susanne Schoch, PhD, and Albert Becker, MD

Abstract

Focal cortical dysplasia type IIb is characterized by epilepsy-associated malformations that are often composed of balloon cells and dysplastic neurons. There are many histopathologic similarities between focal cortical dysplasia type IIb and cortical tubers in tuberous sclerosis complex (TSC), an autosomal-dominant phakomatosis caused by mutations in the *TSC1* or *TSC2* genes that encode hamartin and tuberin. We previously found that an allelic variant of *TSC1* (hamartin^{H732Y}) is increased in focal cortical dysplasia type IIb. Here, we investigated the subcellular localization of hamartin^{H732Y} and its interaction with tuberin in vitro. Coimmunoprecipitation assays with tuberin revealed reduced tuberin binding of hamartin^{H732Y} compared with wild-type hamartin. Tuberin binding was also reduced for 2 *TSC1* stop mutants (hamartin^{R692X} and hamartin^{R786X}) that are present in brain lesions of TSC patients. Colocalization assays of hamartin and tuberin were performed in HEK293T cells, and the subcellular localization of the hamartin variants were studied using immunocytochemistry. There was an impairment of tuberin binding of hamartin^{H732Y} and aberrant nuclear distribution of hamartin^{H732Y} in these cells, whereas hamartin^{R692X} and hamartin^{R786X} were, like wild-type tuberin, localized in the cytoplasm. These data suggest a fundamental functional impairment of hamartin^{H732Y} and the 2 *TSC1* stop mutants hamartin^{R692X} and hamartin^{R786X} in vitro. Future studies will be needed to characterize the roles of these *TSC1* sequence variants in the genesis of dysplastic epileptogenic developmental brain lesions.

Key Words: Amino acid exchange, Hamartin, Insulin receptor signaling pathway, mTOR, Subcellular distribution, Tuberin.

INTRODUCTION

Tuberous sclerosis complex (TSC) is an autosomal-dominant multiorgan disorder characterized by benign tumors and dysplastic lesions in many organs, including skin, kidney, lungs, heart, and brain (1, 2). Cerebral cortical tubers are frequently composed of large dysmorphic neurons and giant cells. Cortical dysplasias associated with focal epilepsies consist of dysplastic cytomegalic neurons and balloon cells (focal cortical dysplasia type IIb [FCD_{IIb}] according to the so-called Palmini classification [3]; Fig. 1). Thus, they resemble cortical tubers. Patients with FCD_{IIb} generally lack additional features of a neurocutaneous phakomatosis (4).

Tuberous sclerosis complex is caused by mutations in *TSC1* on chromosome 9q34 (5) or *TSC2* on chromosome 16p13.3 (6, 7). Remarkably, *TSC1*/*TSC2* mutations are only detected in approximately 85% of TSC patients (8). Hamartin and tuberin, the corresponding gene products, form a heterodimer operating as a tumor suppressor in the phosphatidylinositol 3-kinase pathway (5, 9, 10). Consistent with the Knudson 2-hit hypothesis, extracerebral neoplasms in TSC patients frequently harbor loss of heterozygosity (11). In contrast, loss of heterozygosity has been rarely found in TSC brain lesions (12).

Recent data suggest that the TSC pathway in neurons is highly sensitive to gene dosage effects, including the observation that *TSC1* haploinsufficiency impairs neuronal morphology (13). Furthermore, only little is known about a potentially impaired subcellular distribution of *TSC1* sequence variants, that is, aberrant nuclear localization of hamartin in a tuber was demonstrated in a case study (14). It has also been shown that oligomerization of the hamartin carboxyl-terminal coiled coil domain was inhibited in the presence of tuberin (15). The presence of hamartin aggregates in FCD_{IIb} components (Fig. 1) may suggest that aberrant

From the Departments of Neuropathology (CL, MM, JF, KP, PN, SS, AB), Pathology (MM, JF), Epileptology (PN), and Neurosurgery (MS), University of Bonn Medical Center, Bonn, Germany; and Department of Clinical Genetics, Erasmus Medical Centre, Rotterdam, The Netherlands (MN).

Send correspondence and reprint requests to: Albert J. Becker, MD, Department of Neuropathology, University of Bonn Medical Center, Sigmund-Freud-Str. 25, D-53105 Bonn, Germany; E-mail: albert_becker@uni-bonn.de

Céline Lugnier and Michael Majores contributed equally to the work.

This work is supported by Deutsche Forschungsgemeinschaft (SFB TR3, C6, B8, Albert Becker, Susanne Schoch; KForG "Innate Immunity" TP2, Albert Becker; Emmy Noether program: Susanne Schoch; SFB-645: Susanne Schoch), Deutsche Krebshilfe (Jana Fassunke, Michael Majores, Albert Becker), Bundesministerium für Bildung und Forschung (NGFNplus, 01GS08122; Albert Becker, Susanne Schoch), European Union EPICURE (Albert Becker), and the BONFOR program of the University of Bonn Medical Center (Albert Becker, Michael Majores, Susanne Schoch).

Online-only color figures are available at http://www.jneuropath.com.

interactions between hamartin and tuberin also occur in these epilepsy-associated lesions.

Here, we used in vitro approaches to analyze whether *TSC1* coding allele variants in the predicted tuberin-binding domain of hamartin (5) impair this interaction and lead to aberrant subcellular distribution of the resulting hamartin protein variants. Therefore, we focused on the allelic variant known to be increased in FCD_{IIb} patients, that is, a base exchange from C to G in exon 17 of *TSC1* at nucleotide 2415 that results in an amino acid exchange from the basic histidine to the neutral tyrosine at codon 732 ($hamartin^{H732Y}$ [16]). This variant is also present at lower frequencies in TSC patients and unaffected individuals (17–19). We also analyzed $hamartin^{R692X}$ and $hamartin^{R786X}$, that is, truncations in the hamartin-tuberin interaction domain that are frequently observed in TSC-associated cortical tubers (18–20). Our data suggest strikingly impaired tuberin binding as well as divergent subcellular distribution patterns of these hamartin variants and provide novel insights into their pathogenetic role in FCD and TSC.

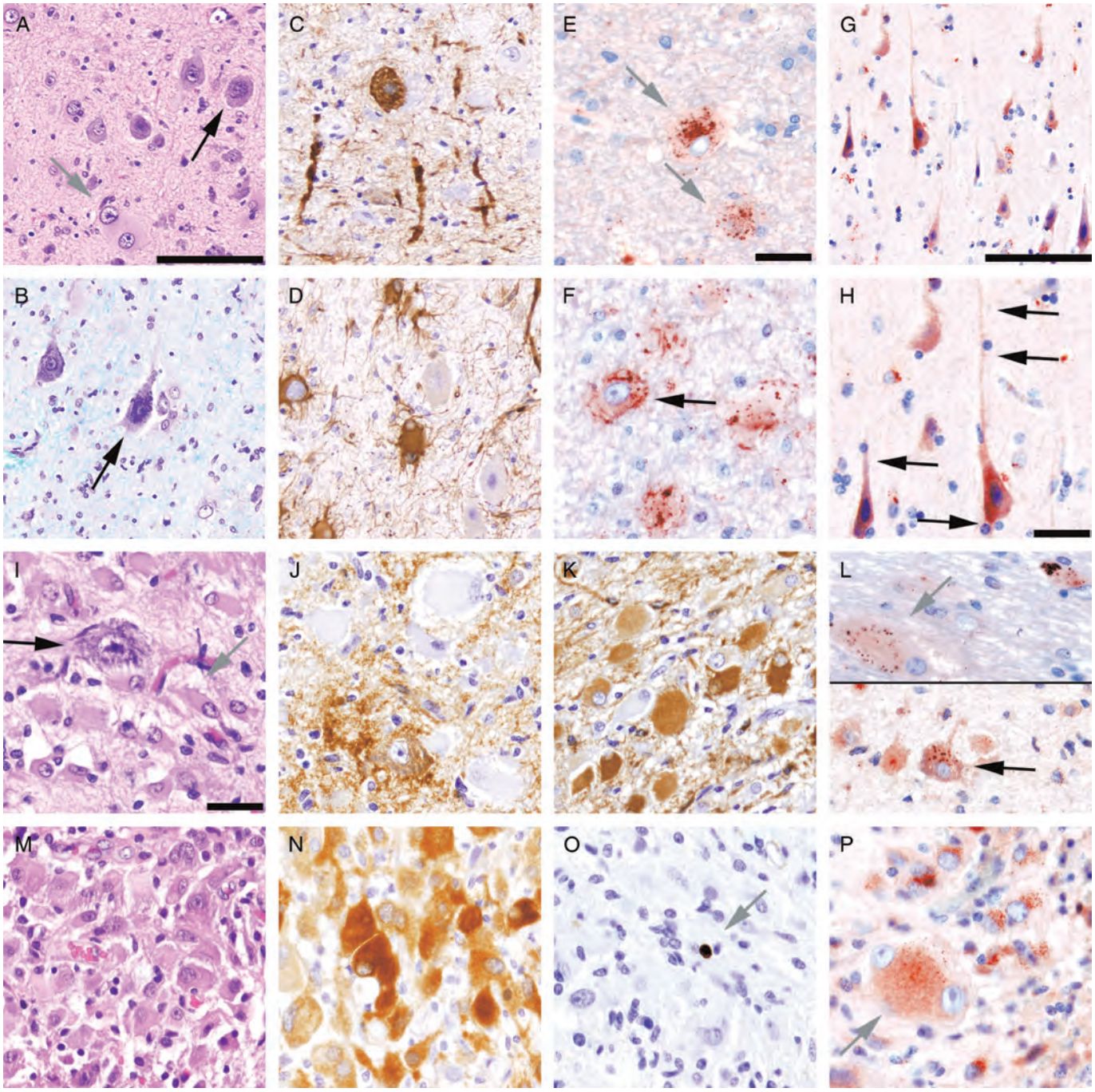

MATERIALS AND METHODS

Surgical Specimens and Immunohistochemistry

Tissue specimens were obtained from FCD_{IIb} (n = 12 patients), cortical tubers (n = 2 patients), and subependymal giant cell astrocytomas (SEGAs, n = 3 patients) (Table). Biopsy samples were collected from patients with chronic pharmacoresistent focal epilepsies in the Epilepsy Surgery Program at the University of Bonn. One patient with SEGA did not have epilepsy. In all epileptic patients (n = 16), surgical removal of the lesion was necessary to achieve seizure control after presurgical evaluation, as previously described (21). Only patients with cortical tubers and SEGAs had additional features characteristic of TSC (5, 8). In a patient with a SEGA (ID 17), neurosurgical intervention was carried out under tumor-surgical considerations. The clinical characteristics of the patients are summarized in the Table. Written informed consent was obtained from all patients concerning the use of brain tissue. All procedures were conducted in accordance with the Declaration of Helsinki and approved by the ethics committee of the University of Bonn Medical Center. Surgical specimens were fixed in formaldehyde overnight and embedded in paraffin. The FCD_{IIb} specimens were reviewed by experienced neuropathologists and classified according to international classification schemes (3). Hematoxylin and eosin (H&E) and Nissl–Luxol fast blue stains and immunohistochemistry with antibodies against vimentin and neurofilament protein were carried out according to standard procedures (22). Immunohistochemical staining of hamartin in paraffin sections was performed using a monoclonal antibody (Cell Signaling, Frankfurt, Germany; Clone 1B2, diluted 1:200) according standard procedures (22). Negative control reactions replacing the primary specific antibody by nonspecific immunoglobulin were performed to assure specific binding affinity (data not shown).

Generation of Plasmid Constructs

To generate pmCherry-TSC1, we first amplified the human TSC1 cDNA coding sequence from pcDNA3.1mycA-TSC1 and subcloned the amplicon into the pCDNA3.1 V5 HIS TOPO vector (Invitrogen, Munich, Germany) using the primer pair TSC1 forward (5′-GCG GCT AGC ATG GCC CAA CAA GCA AAT G-3′) and TSC1 reverse (5′-GCG GGT ACC TTA GCT GTG TTC ATG AGT CTC-3′). Subsequently, an mCherry tag was inserted N-terminally in pcDNA3.1-TSC1 to generate pmCherry-TSC1. Therefore, mCherry was amplified from the pBKS-mCherry plasmid (a generous gift from Dr T. Südhof, Stanford, CA) using the primer pair mCherry forward (5′-GCG TCT AGA ACC ATG GTG AGC AAG GGC GA-3′) and mCherry reverse (5′-GCG GCT AGC CTT GTA CAG CTC GTC CAT GCC-3′). The resulting polymerase chain reaction product was digested with NheI and XbaI (Fermentas, Burlington, Canada) and pCDNA3.1-TSC1 with NheI. DNA sequencing was performed to verify that all sequences were correct (BigDye Terminator v3.1 Cycle Sequencing Kit; Applied Biosystems, Foster City, CA). Truncated and mutated hamartin proteins were generated by site-directed mutagenesis of the pCDNA-mcherry-TSC1 plasmids (QuickChange II Site–directed mutagenesis kit, Stratagene, Cedar Creek, TX) following the manufacturer's manual with the following primers: $TSC1^{R786X}$ forward: 5′-CAG ATC AGA CAG CTA CAG CAT GAC TGA GAG GAG TTC TAC-3′; $TSC1^{R786X}$ reverse: 5′-GTA GAA TTC CTC TCA GTC ATG CTG TAG CTG TCT GAT CTG-3′. By base exchange from C to T in codon 786 of *TSC1*, a stop codon is created, resulting in a truncated TSC1 protein. For rapid screening of mutant clones, a silent base exchange from G to A was generated, which resulted in the deletion of a PstI restriction site (CTGCA/G). For another truncated *TSC1* variant, we used the primers: $TSC1^{R692X}$ forward: 5′-GAT GAG ATC CGC ACC CTC TGA GAC CAG CTG CTT TTA CTG CAC AAC-3′; $TSC1^{R692X}$ reverse: 5′-GTT GTG CAG TAA AAG CAG CTG GTC TCA GAG GGT GCG GAT CTC ATC-3′. The base exchange from C to T creates a stop codon at position 692 of *TSC1*, whereas the silent mutation from T to C resulted in the creation of a new PvuII restriction site (CAG/CTG). We further used the primers: $TSC1^{H732Y}$ forward: 5′-GTG ATC AAA GCA GCA GCT CTC GAG GAA TAT AAT GCT GCC ATG-3′; $TSC1^{H732Y}$ reverse: 5′-CAT GGC AGC ATT ATA TTC CTC GAG AGC TGC

FIGURE 1. Neuropathologic and immunohistochemical characteristics of focal cortical dysplasia type IIb (FCD_{IIb}), cortical tubers, and subependymal giant cell astrocytoma (SEGA). **(A, B)** The co-occurrence of large dysplastic neurons (black arrow) with aggregates of Nissl substance (**A**, H&E; **B**, Nissl–Luxol fast blue) and Taylor-type balloon cells (gray arrow) are typical neuropathologic findings in FCD_{IIb}. **(C–H)** Immunohistochemical (IHC) characteristics of FCD_{IIb} include expression of neurofilament in dysmorphic neurons and axonal congestion **(C)** and prominent expression of vimentin in balloon cells **(D)**. IHC with an antibody against hamartin reveals granular aggregates of hamartin in the cytoplasm of balloon cells that are characterized by a round eccentric nucleus (**E**, gray arrows) and dysmorphic neurons with a central nucleus and prominent nucleolus **([F]** black arrow). In contrast, regularly oriented neurons in normal cerebral cortex show homogeneous cytoplasmic distribution of hamartin; astroglia are devoid of hamartin expression **(G)**. In a higher magnification of the field in **(G)**, there is homogeneous expression of hamartin in the somata, axons, and dendrites of regularly shaped neurons **([H]** black arrows). **(I–L)** Cortical tubers. Similar to FCD_{IIb}, cortical tubers are characterized by an admixture of large dysmorphic neurons (black arrow) and giant cells (gray arrow **[I]**). Dysmorphic neurons show perisomatic strong expression of synaptophysin, whereas giant cells contrast negative **(J)**. Glial fibrillary acidic protein is present in giant cells **(K)**. Granular aggregates of hamartin are present in the cytoplasm of giant cells **([L]** upper part, gray arrow) and in dysmorphic neurons **([L]** lower part, black arrow). **(M–P)** SEGA. These lesions are composed of densely packed giant cells **([M]** H&E) that have substantial expression of neuronal specific enolase **(N)** and low proliferative activity **([O]** gray arrow, IHC with an antibody against Ki67 [MiB1]). Giant cells such as the binucleated example (gray arrow) show distinct cytoplasmic granular aggregation of hamartin **(P)**. Scale bars = **(A–D, G)** 100 μm; **(E, F,** and **H–P)** 50 μm.

TABLE. Clinical Features and Diagnoses of Patients

Case No.	Neuropathologic Diagnosis	Main Clinical Features	Age at Surgery, years, Sex	Age at Epilepsy Onset, years	Seizure Frequency†	Medication at the Time of Surgery
1	FCD_{IIb}	CPS, sGTCS	23, F	14	4/month	LTG, PGB
2	FCD_{IIb}	CPS	9, M	<1	15/day	LTG, PB
3	FCD_{IIb}	SPS, CPS, sGTCS	28, F	2	7/day	PHT, LTG
4	FCD_{IIb}	SPS, CPS, sGTCS	18, F	3	6/day	OXC, LEV
5	FCD_{IIb}	SPS	21, M	7	ND	PHT, LEV, ZON
6	FCD_{IIb}	SPS, CPS, sGTCS	29, F	3	10/day	LTG
7	FCD_{IIb}	SPS, CPS, sGTCS	34, F	3	5/month	LEV, LTG, CBZ
8	FCD_{IIb}	SPS, sGTCS	28, M	2	ND	CBZ, LEV
9	FCD_{IIb}	SPS, CPS	2, F	2	3/day	OXC
10	FCD_{IIb}	SPS, CPS, sGTCS	24, M	3	11/month	LEV, OXC, PGB, PHT
11	FCD_{IIb}	CPS	36, M	26	6/day	ZON, PB, LEV, OXC
12	FCD_{IIb}	CPS, sGTCS	20, M	4	2/month	OXC, PHT
13*	Cortical tuber	SPS, CPS, sGTCS	12, M	2	1/day	PHT, VPA
14*	Cortical tuber	SPS, CPS	0.8, F	0.5	5/day	OXC, VPA
15*	SEGA	CPS	8, M	<1	7/day	TPM, VPA
16*	SEGA	Hydrocephalus occlusus, CPS, sGTCS	38, M	ND	ND	CBZ
17*	SEGA	Intraventricular tumor	21, F	—	—	—

*Cases with tuberous sclerosis complex.

†Seizure frequency, events per month or day.

CBZ, carbamazepine; CPS, complex partial seizure; F, female; FCD, focal cortical dysplasia of indicated types; LEV, levetiracetam; LTG, lamotrigine; M, male; ND, not determined (the age at onset of epileptic seizures of Patient 16 and the exact seizure frequency of Patients 5, 8, and 16 are not known. Patient 17 did not have clinically apparent seizures); OXC, oxcarbazepine; PB, phenobarbital; PGB, pregabalin; PHT, phenytoin; SEGA, subependymal giant cell astrocytoma; sGTCS, secondary generalized tonic clonic seizures; SPS, simple partial seizure; TPM, topiramate; VPA, valproate; ZON, zonisamide.

TGC TTT GAT CAC-3′. This base exchange from C to T results in an amino acid exchange from histidine to tyrosine, screened by the detection of an additional restriction site of XhoI (C/TCGAG) generated by a silent base exchange from G to C. Mutagenesis was verified by restriction digest and sequencing.

Cell Culture and Transfection Procedures

HEK293T cells were cultured in Dulbecco modified Eagle medium (Invitrogen, Carlsbad, CA) supplemented with 10% fetal calf serum and 1% penicillin/streptomycin at 37°C in 5% carbon dioxide. Transfection of HEK293T cells was performed using Lipofectamine 2000 (Invitrogen) following the manufacturer's protocol.

Colocalization Assay

HEK293T cells were cultured on coverslips and transfected with TSC2-enhanced green fluorescence protein and the different mCherry-TSC1 expression plasmids, at a confluence of approximately 25%, as previously described. After 48 hours, cells were fixed in 4% paraformaldehyde and analyzed by confocal fluorescence microscopy (Olympus, Munich, Germany). Micrographs were examined using a colocalization assay plug-in on ImageJ.

Western Blot Analysis

For Western blot experiments, HEKT293 cells were transfected with the mCherry-TSC1 plasmid at about 80% confluence and cultured for 2 more days. Cell pellets were resuspended in PBS and 6× loading dye (4× Tris-Cl/sodium dodecyl sulfate [SDS] pH 6.8, 30% glycerol, 10% SDS, 5%-mercaptoethanol, 0.012% bromphenol blue) and then lysed by sonification. Equal amounts of cell lysate were separated by electrophoresis on an 8% SDS–polyacrylamide gel and transferred to nitrocellulose membranes (Protran Whatman, Kent, UK) overnight at 4°C. After blocking the membrane for 1 hour with PBS/1% cold water fish gelatin (Sigma-Aldrich, St Louis, MO), it was incubated overnight with a monoclonal hamartin antibody (dilution 1:1000) (Hamartin 1B2 Mouse mAB, Cell Signaling, Boston, MA) in PBS, 0.1% TWEEN. IrDye fluorescent secondary antibodies (LI-COR, Lincoln, NE) were diluted 1:20,000 in PBS, 0.1% TWEEN, 0.01% SDS, and incubated for 1 hour. Immunoblots were visualized using the LI-COR Odyssey system (LI-COR).

Immunoprecipitation Assays

For immunoprecipitation analyses, HEK293T cells were harvested 2 days after cotransfection with the various cherry-tagged TSC1 expression plasmids and the green fluorescence protein-tagged TSC2 expression plasmid. Cell pellets were resuspended in lysis buffer (150 mmol/L NaCl, 40 mmol/L Tris-HCl pH 7.4, 1 mmol/L EDTA, 0.5% Nonidet P-40, 1 mmol/L phenylmethanesulfonyl fluoride, protease inhibitor cocktail; Roche, Indianapolis, IN) and incubated for 1 hour at 4°C. Meanwhile, 30 μL of protein A/G plus agarose (Santa Cruz Biotechnology, Santa Cruz, CA) slurry were conjugated with 1 μg of an antibody against hamartin (sc-12082) or tuberin (sc-893) (both from Santa

Cruz Biotechnology) in 500 μL lysis buffer at 4°C. After centrifugation of the cell lysate for 10 minutes at 14,000 rpm at 4°C, the supernatant was precleared with 50 μL of protein A/G plus agarose slurry and 1 μg of normal mouse IgG (Santa Cruz Biotechnology) for 1 hour at 4°C. Subsequently, the lysate was added to the conjugated primary antibodies and incubated for 2 hours, rotating at 4°C. The immunoprecipitated complexes were washed 5 times with lysis buffer and analyzed by electrophoresis on a 6% SDS polyacrylamide gel followed by immunoblotting, as previously described.

Immunocytochemistry and Phase-Contrast Microscopy

For immunofluorescence analysis, HEK293T cells were cultured on coverslips for 2 days after transfection and then fixed in 4% paraformaldehyde for 15 minutes at room temperature. After 3 rounds of washing with ice-cold PBS, cells were permeabilized with 0.1% Triton X-100/PBS for 15 minutes and then blocked for 1 hour at room temperature (blocking buffer: 10% normal goat serum, 1% bovine serum albumin in PBS). Cells were incubated overnight with primary antibodies anti-LAMP1 and anti-ERGIC-53/p58 (Sigma-Aldrich) at 4°C and diluted in blocking buffer to a concentration of 1:200. After washing with PBS, secondary antibody was added in a dilution of 1:400 in blocking buffer for 1 hour. The labeling was analyzed by confocal fluorescence microscopy as previously described. Cultured cells were photographed by phase-contrast microscopy (Observer A1; Zeiss, Jena, Germany) in the culture plate.

Statistical Analysis

Two-sided Student *t*-test was used for statistical analysis of the data.

RESULTS

We have observed that the lesions of FCD_{IIb}, that is, common epilepsy-associated malformations that resemble cortical tubers in TSC (Figs. 1A–D, I–K), show strikingly aberrant cytoplasmic granular aggregation of hamartin in balloon cells and in dysmorphic neurons (Figs. 1E, F). By contrast, regularly shaped neurons in normal cerebral cortex have a homogeneous cytoplasmic distribution of hamartin (Figs. 1G, H). Moreover, aberrant hamartin aggregation in FCD_{IIb} is also observed in dysmorphic neuronal and giant cell elements of cortical tubers (Figs. 1L) and in highly differentiated subependymal SEGAs (Figs. 1M–P). Both cortical tubers and SEGAs are frequently associated with TSC. These observations prompted us to determine whether sequence variants of *TSC1* that are frequent in FCD_{IIb} and TSC-associated brain lesions are associated with aberrant subcellular distribution or impaired tuberin binding of the resulting hamartin variants. Because numerous components of the phosphatidylinositol 3-kinase cascade operate abnormally in FCD_{IIb} and cortical tubers (23), we used a highly controlled in vitro approach for this analysis.

We first generated various plasmids that express *TSC1* fused to the fluorescent reporter mCherry. In addition to wild-type (WT) *TSC1*, we derived *TSC1* constructs carrying the amino acid exchanges H732Y, R786X, and R692X (Fig. 2). Mutations in codons 786 and 692 result in truncated hamartin variants that are frequently detected in TSC patients (18–20) and are localized at different sites within the tuberin interaction domain of hamartin (Fig. 2). Next, we tested for protein expression and stability of the *TSC1* fusion proteins by transfection of HEK293T cells and immunoblotting. HEK293T cells are a widely used cell line for protein interaction experiments. All proteins were expressed at high levels and migrated at the expected calculated molecular weights (Fig. 3).

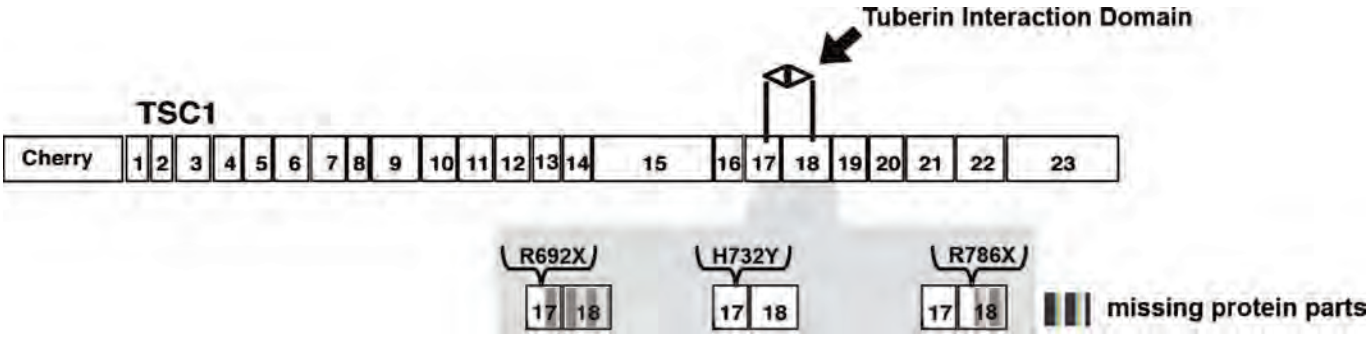

FIGURE 2. Generation of mutant hamartin proteins. A Cherry tag was inserted N-terminally to the tuberous sclerosis complex (*TSC1*) cDNA (numbered boxes indicating exons); 3 different mutations were introduced into the coding sequence of *TSC1* by site-directed mutagenesis (highlighted on gray background); 2 of the sequence alterations resulted in truncating mutations, the generation of stop codons at positions R786X and R692X. The resulting proteins are referred to as hamartin^{R786X} and hamartin^{R692X}. Hamartin^{R692X} terminates in the beginning of exon 17; hamartin^{R786X} comprises the amino acids encoded by the entire exon 17 and terminates in the middle of exon 18. The protein parts that are missing as result of introducing the truncating mutations are indicated. A third sequence alteration in the *TSC1* cDNA (i.e. a C to G base exchange in exon 17 of *TSC1*) results in an amino acid exchange at codon 732 of hamartin, from the basic histidine to neutral tyrosine (hamartin^{H732Y}). Importantly, this latter alteration does not result in a truncated hamartin protein variant.

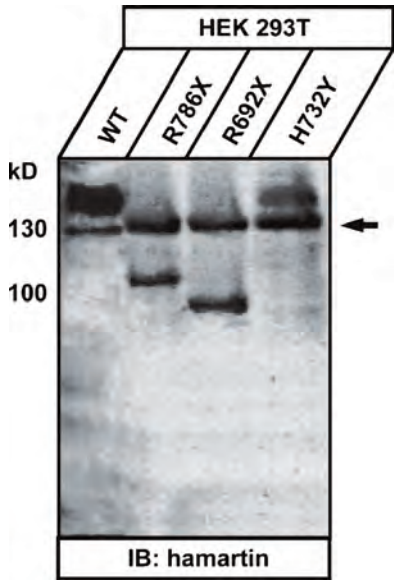

FIGURE 3. Hamartin cherry fusion proteins are expressed in HEK293T cells. To analyze the subcellular distribution of the various hamartin variants, plasmids coding for fusion proteins of hamartin with the fluorescent marker mCherry were generated. The sizes of the fusion proteins were determined by immunoblotting of transfected HEK293T whole cell lysates. As expected, wild-type (WT) hamartin fused to cherry is detected at approximately 158 kd (endogenous tuberous sclerosis complex (*TSC1*) 130 kd, cherry 28 kd). Hamartin^{H732Y} fused to cherry is the same size as hamartin^{WT} fused to cherry. Hamartin^{R692X} fused to cherry represents the smallest protein (100 kd); hamartin^{R786X} fused to cherry is of intermediate size (110 kd). The arrow marks the HEK293T-endogenous hamartin at 130 kd.

To assess the binding efficiency of WT and mutant TSC1 proteins to tuberin in vitro, we performed immunoprecipitation experiments from extracts of transiently transfected HEK293T cells using an antibody directed against an epitope present in all mutant hamartin protein variants and then probed the precipitates with an antibody against tuberin. As shown in Figures 4A and B, tuberin was efficiently precipitated when coexpressed with hamartin^{WT}, but there was reduction in tuberin-binding affinity for hamartin^{R692X}. Because this protein variant contains an aberrant stop codon positioned most N-terminal in the tuberin interaction domain, the resulting hamartin product lacks large portions of the coiled-coil domain responsible for tuberin binding (Figs. 4A, B); 5.1-fold binding reduction, for hamartin^{R692X} n = 3 replicates, hamartin^{WT} for all n = 9 replicates, *t*-test, $p < 0.05$. Correspondingly, the hamartin^{R786X} variant also showed a significantly reduced binding affinity to tuberin (Figs. 4A, B); 3.3-fold binding reduction, for hamartin^{R786X} n = 4 replicates, *t*-test, $p < 0.05$. In the hamartin^{R786X} protein, however, a larger part of the tuberin binding coiled-coil domain is present than in hamartin^{R692X}. Strikingly, also a hamartin protein variant (hamartin^{H732Y}), which is found in normal individuals, TSC patients with cortical tubers, as well as in FCD_{IIb}, and in which the tuberin binding domain only exhibits a single amino acid exchange, showed a significant reduction in tuberin binding (Figs. 4A, B); 2.3-fold binding reduction, for hamartin^{H732Y} n = 9 replicates, *t*-test, $p < 0.05$. Identical results were obtained if the immunoprecipitations were performed vice versa using an antibody against tuberin (data not shown). Together, these experiments show that mutations found in the tuberin-binding domain of hamartin in cortical tubers and in FCD_{IIb} directly affect the interaction of these 2 proteins.

We next characterized the subcellular distribution of the different hamartin protein variants. Hamartin^{WT} showed a cytoplasmic localization mostly concentrated in close vicinity to the cellular membrane (Fig. 5). The expression pattern of hamartin^{WT} seemed homogeneous. Hamartin^{R692X} and hamartin^{R768X} were more dispersed in the cytoplasm and accumulated in granular-like patterns that are distinct from that of hamartin^{WT} (white arrows, Fig. 5). The granular masses of hamartin^{R692X} and hamartin^{R768X} suggest self-aggregation, a phenomenon that has been previously described (15). Intriguingly, hamartin^{H732Y} revealed a completely different subcellular distribution as it was almost completely localized in the nucleus without any significant cytoplasmic expression. This observation was confirmed by 4′,6-diamidino-2-phenylindole, dihydrochloride (DAPI) staining (Fig. 5).

We next examined the consequences of the H732Y allelic variant on the interaction of hamartin and tuberin in live cells. We overexpressed both proteins in HEK293T cells

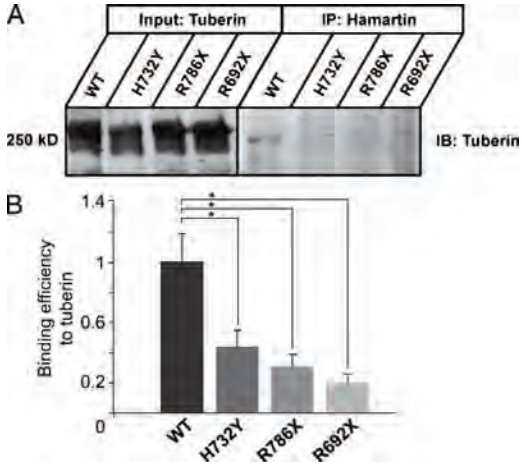

FIGURE 4. Immunoprecipitation of hamartin and tuberin. **(A)** Hamartin-cherry variants were immunoprecipitated using a hamartin antibody. Subsequently, immunoblots were probed with an antibody against tuberin. The probes were normalized to the whole lysates. Only the tuberin band of the wild-type (WT) hamartin probe can be detected with certainty. This assay was also performed in the reverse order with identical results (data not shown). **(B)** To examine the binding efficiency between hamartin, WT, and mutant variants and tuberin in vitro, the amount of tuberin that was immunoprecipitated by the different hamartin variants was quantitated after immunoblotting using AIDA software. All 3 hamartin variants show a substantially decreased binding to tuberin compared with that of hamartin^{WT}. Hamartin^{WT}, n = 9; hamartin^{H732Y}, n = 9; hamartin^{R786X}, n = 4; hamartin^{R692X}, n = 3; *t*-test, $*p \leq 0.05$.

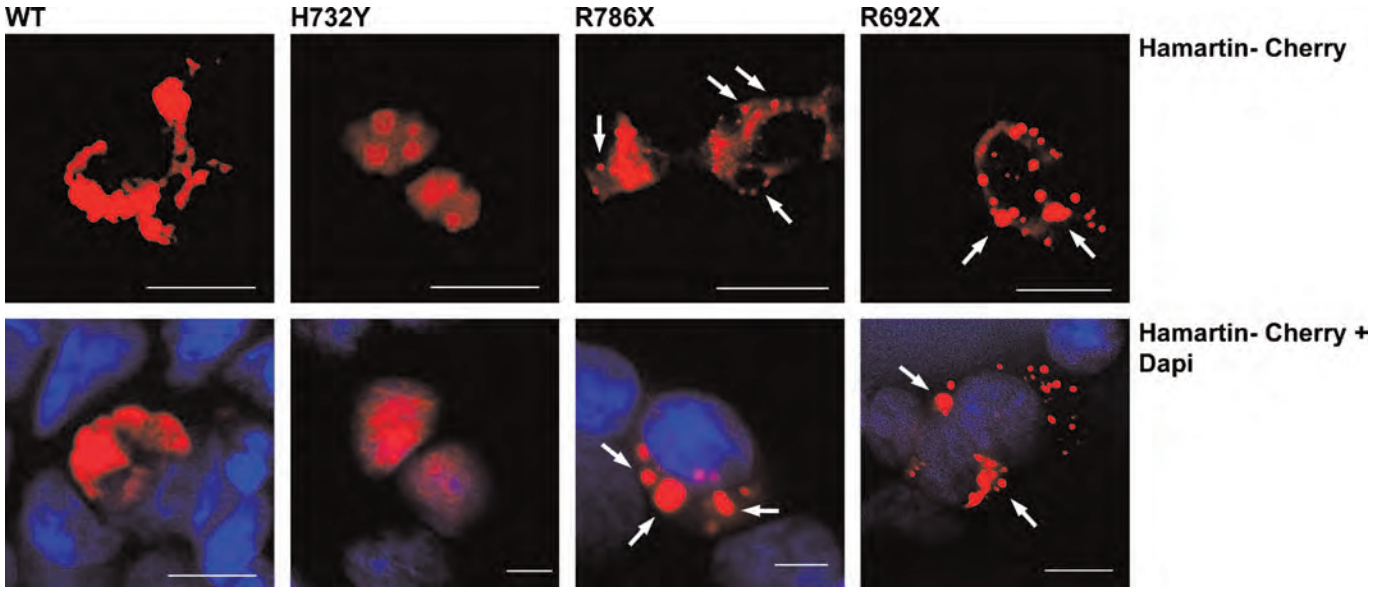

FIGURE 5. Subcellular distribution of hamartin variants in HEK293T cells. HEK293T cells were transfected with tuberous sclerosis complex (TSC1)–mCherry expression plasmids (red – view figure in color online-only); nuclei were labeled with DAPI (blue – view figure in color online-only). Cells only stained with DAPI are nontransfected cells. The different hamartin mutants and the wild-type (WT) were analyzed by confocal fluorescence microscopy. Hamartin^{WT} showed cytoplasmic localization mostly concentrated near the cellular membrane. In contrast, the hamartin^{R786X} and hamartin^{R692X} variants were more disseminated throughout the cytoplasm and accumulated in granular aggregates (white arrows). Hamartin^{H732Y} exhibited a completely different subcellular distribution compared with that of the other proteins as it was almost completely transferred to the nucleus. The exclusively nuclear localization of hamartin^{H732Y} was confirmed by colocalization with DAPI staining. Scale bars = 10 μm.

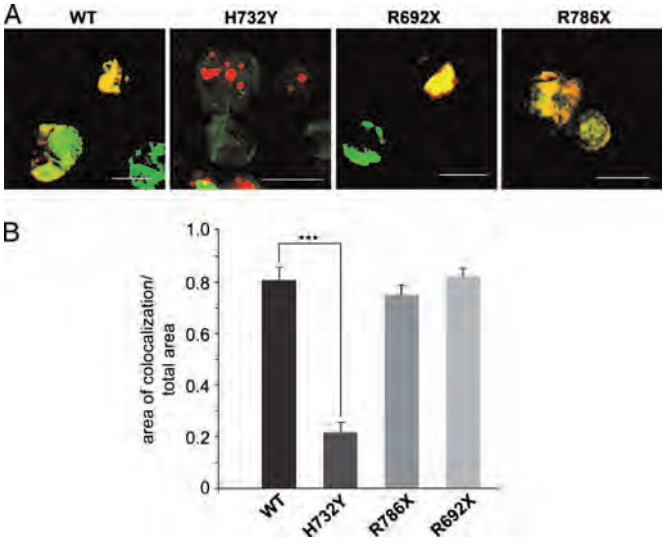

FIGURE 6. Colocalization assay of tuberin and hamartin in HEK293T cells. **(A)** HEK293T cells were cotransfected with plasmids coding for mCherry-hamartin (red – view figure in color online-only) and enhanced green fluorescence protein–tuberin (green – view figure in color online-only) fusion proteins. Cells were analyzed by confocal fluorescence microscopy. Wild-type (WT) hamartin shows nearly 100% colocalization with tuberin. Cotransfection of hamartin^{H786X} and tuberin and of hamartin^{R692X} and tuberin, respectively, resulted in a redistribution of the granular pattern observed for hamartin^{WT} into a diffuse pattern, which colocalized with tuberin. Hamartin^{H732Y} showed no redistribution when cotransfected with tuberin but stayed strictly in the nucleus indicating reduced colocalization with tuberin (red, cherry fluorescent protein; blue, DAPI; Scale bars = 10 μm. View figure in color online-only). **(B)** Semiquantitative analysis of the colocalized area of hamartin and tuberin in relation to the entire area of single cells by an ImageJ plug-in developed for the examination of colocalization assays (*t*-test, $p < 0.001$; for hamartin^{H732Y}, n = 48 cells counted; for hamartin^{WT}, n = 46 cells counted; for hamartin^{R786Y}, n = 50 cells counted; for hamartin^{R692X}, n = 45 cells counted).

and analyzed their colocalization pattern by confocal fluorescence microscopy. The data corroborated the observation that hamartin^{H732Y} was translocated to the nucleus even in the presence of increased levels of tuberin. Interestingly, tuberin showed a diffuse cytoplasmic distribution pattern (Fig. 6A). Using the ImagJ plug-in, we analyzed the colocalization of hamartin and tuberin semiquantitatively and detected significantly reduced colocalization of hamartin^{H732Y} with tuberin compared with that of WT (*t*-test, $p < 0.001$; for hamartin^{H732Y}, n = 48 cells counted; for hamartin^{WT}, n = 46 cells counted; for hamartin^{R786Y}, n = 50 cells counted; for hamartin^{R692X}, n = 45 cells counted; Fig. 6B). Hamartin^{WT} showed colocalization with tuberin in a largely cytoplasmic distribution (Figs. 6A, B). Interestingly, in these experiments, both truncation mutants exhibited a strong cytoplasmic colocalization with tuberin highly similar

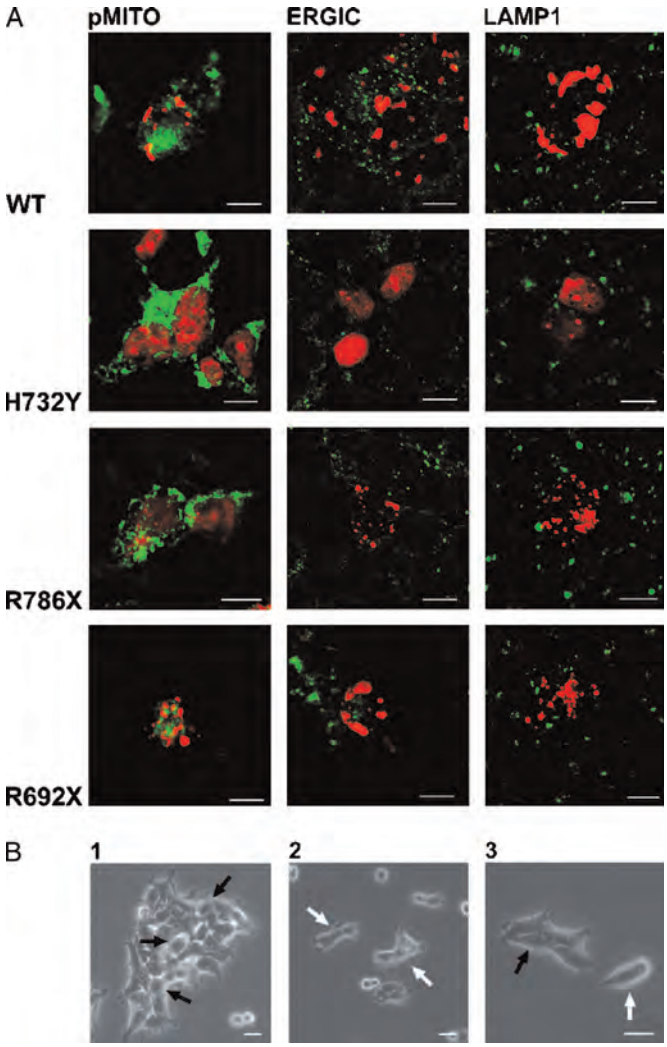

FIGURE 7. Analysis of potential colocalization of hamartin in different subcellular compartments. **(A)** Cells were transfected with various mCherry-hamartin fusion proteins. Immunocytochemistry was performed with anti-LAMP1, which marks lysosomes, and anti-ERGIC-53/p58, which marks endoplasmic reticulum and Golgi apparatus components. These primary antibodies were detected with a green fluorescent secondary antibody. For colocalization of hamartin with mitochondria, HEK293T cells were cotransfected with the hamartin variants fused to mCherry and a plasmid exclusively expressed in mitochondria, pmito–green fluorescence protein (a generous gift from W. Altrock; IFN, Magdeburg, Germany). Results were analyzed by confocal fluorescence microscopy. Hamartin^{R692X} was present in nuclei; the other variants were located in the cytoplasm in different distribution patterns. There was no reproducible or substantial colocalization of hamartin with any of these compartment-specific markers. **(B)** Different growth patterns of untransfected HEK293T cells were visualized by phase-contrast microscopy. The panels demonstrate the high degree of density-dependent diversity of sizes and shapes of the HEK293T cells grown in culture. Cell contacts were associated with more rounded shapes (black arrows **[B1]**), whereas isolated cells exhibit a more spindle-like morphology (white arrows **[B2]**). At higher magnification, clustered HEK293T cells (black arrow **[B3]**) reveal round to ovoid shapes, whereas isolated cellular components seem more elongated with the formation of small processes (white arrow **[B3]**). Scale bars = **(A)** 10 μm; **(B)** 100 μm. WT, wild-type.

to the distribution pattern of hamartin^{WT} (Figs. 6A, B). None of the cotransfected hamartin protein variants resulted in an altered distribution of tuberin in the cells.

We performed further immunocytochemistry of transfected HEK293T cells with probes of proteins localized specifically at the Golgi apparatus, the endoplasmic reticulum and lysosomes, and mitochondria to determine whether the individual hamartin variants had different colocalization patterns within these subcellular compartments (Fig. 7A). We did not observe distinct or specific colocalization patterns of the individual hamartin protein variants with these compartments, however. Importantly, the distribution patterns of the distinct hamartin variants were independent of the variable morphology of the HEK293T cells (Fig. 7B). Generally, clustered cells in close contact exhibit a round to ovoid appearance (Figs. 7B1, B3). In contrast, individual cells in more isolated localization reveal a rather spindle-like shape (Figs. 7B2, B3). The variability of HEK293T cellular shape distribution was independent of transfection of cells with the different TSC1 variants.

DISCUSSION

We observed strikingly aberrant subcellular distribution patterns of hamartin in various epilepsy- and TSC-associated lesions. In contrast to neurons in normal cortex that have diffuse cytoplasmic expression of hamartin FCD_{IIb}, cortical tubers and SEGAs exhibit cytoplasmic granular aggregates of hamartin (Fig. 1); these are similar to previously reported findings (24). Our present in vitro results also reveal striking differences in tuberin binding and subcellular distribution among hamartin variants that are frequently observed in epilepsy-associated cortical dysplasias and cortical tubers (17–20). Both hamartin variants with a truncated tuberin-binding domain exhibited significantly reduced binding affinity to tuberin. This observation is surprising for hamartin^{R786X}, which still encompasses a substantial part of this domain. Interestingly, hamartin^{H732Y}, an allelic variant of *TSC1* present in healthy individuals (17), is highly abundant in FCD_{IIb} (16) and is present in TSC patients who lack pathogenic *TSC1*, and *TSC2* mutations (18) also showed a substantially reduced ability to interact with tuberin. Indeed, the affinities of hamartin^{H732Y} and hamartin^{R786X} to tuberin were similar (Fig. 3). This result was rather surprising because 1) in contrast to hamartin^{H732Y}, the hamartin^{R786X} variant has been reported to cause manifest TSC and 2) the hamartin^{H732Y} variant differs from hamartin^{WT} by only a single amino acid exchange from the basic amino acid histidine to the neutral tyrosine within the interaction domain to tuberin. This sequence alteration at codon 732 may alter the 3-dimensional structure of hamartin at the predicted binding domain with tuberin (5). Aberrant interaction of hamartin^{H732Y} with tuberin is compatible with downstream activation of the phosphatidylinositol 3-kinase cascade recently described in FCD_{IIb} (9, 25, 26).

An important aspect for understanding the pathophysiological relevance of *TSC1* allelic variants relates to potentially aberrant subcellular localization of the corresponding hamartin variants compared with tuberin. Factors such as cell type-specific differences and low abundance or antibody limitations may account for previous findings that hamartin and tuberin are localized to different cellular compartments (10, 15, 27–29). It has been demonstrated, however, that tuberin and hamartin associate physically in vivo (10, 30); all of these studies provide evidence for a cytosolic tuberin-hamartin complex. Hamartin has been localized to the membrane/particulate (P100) fraction of cultured cells (30, 31). Recently, nuclear localization of hamartin in pancreatic acinar tissues and individual cell components in the cerebellar granular layer of the cerebellum were also reported (32).

Because of its subcellular localization, hamartin may transmit information about changes in cell adhesion to the nucleus; its involvement in normal cell death may accompany cell detachment or provide an additional potential indirect mechanism through which the cell cycle could be affected. Indeed, it has been suggested that hamartin is a nuclear shuttling protein that accumulates in the nucleus upon inhibition of nuclear export with leptomycin B, which itself inhibits Exportin 1, a protein required for nuclear export of proteins containing a nuclear export sequence (1). Intriguingly, our finding of hamartin^{H732Y} accumulation in the nucleus (in contrast to hamartin^{WT}, hamartin^{R786X}, and hamartin^{R692X}, which are cytoplasmic) implies the following scenarios for allelic variants in contrast to hamartin^{WT}, which is tightly bound to tuberin in a protein complex. Because of the conserved nuclear localization sequence ("RQQHALRNRR" sequence at 708 of hamartin), hamartin^{H732Y} has a reduced binding affinity to tuberin and is shuttled into the nucleus. In view of the relevance of hamartin for cell cycle regulation, this aberrant cytoplasmic-nuclear shuttling of hamartin disrupts the cycling of affected cells. In contrast, hamartin^{R786X} and hamartin^{R692X} are not transported to the nucleus. Accordingly, hamartin^{R692X} lacks the nuclear localization sequence at 708, whereas for hamartin^{R786X}, another mechanism, such as protein misfolding of the truncated protein, may account for its localization. Aberrant nuclear accumulation of hamartin^{H732Y} might impair cell cycling, although the specific effects of this phenomenon were not addressed by the experimental approaches of the present study. It has been shown, however, that hamartin and tuberin influence the activity of molecules critically involved in cell cycle regulation such as CDK1 (33). On the other hand, this aberrant protein variant might also perturb regular nuclear functions in a manner similar to what is known for aberrant protein aggregates in neurodegenerative conditions such as spinocerebellar ataxia type 3 (34). Recent data demonstrated that appropriate phosphorylation, sequestration, and turnover of the TSC protein complex represent critical issues for proper cellular function (35–37). Particularly, the aberrant cytoplasmic aggregates of hamartin we demonstrated in FCD_{IIb}, cortical tuber and SEGA patient tissues, as well as our in vitro findings for the hamartin stop variants may imply impairment of protein sequestration. However, we did not observe increased association of the hamartin stop variants, such as with lysosomes (Fig. 7).

The hamartin^{H732Y} allele is also detected in the normal population, with a frequency of 0.5%. Therefore, this sequence alteration cannot be sufficient to cause TSC or FCD. Intriguingly, it has been recently shown that the TSC pathway is sensitive to gene dosage effects, such that loss of a single copy of *TSC1*, as it is manifest in all neurons of TSC patients, is sufficient to disturb dendritic spine structure (13). Furthermore, loss of heterozygosity has been shown in FCD_{IIb} components of individuals carrying the hamartin^{H732Y} allele (16). Our present data suggest that hamartin^{H732Y} may constitute a predisposing germline variant with low penetrance and a strongly restricted manifestation pattern, which only in individual cells (or e.g. restricted neural precursor clones) overcomes a virtual pathological threshold. This concept is compatible with the remarkable notion that surgical resection of FCD_{IIb} is curative with respect to seizure events in most patients (38), whereas TSC patients with cortical tubers frequently develop secondary seizure foci after removal of epileptogenic tubers/foci.

It was suggested recently that hamartin could have discrete and specialized functions besides its role in the TSC1/TSC2 complex because of its nuclear localization (39). In line with this idea, hamartin is capable of attenuating the proliferation of mammalian cells (40). Aberrant cellular accumulation of hamartin allelic variants may therefore account for reduced proliferation and cellular densities in cortical dysplasias (41) and the characteristic enlarged and dysplastic cellular phenotype of FCD_{IIb} elements. Based on these considerations, our data suggest that hamartin, which has mainly been regarded as an interaction partner in the tumor suppressor complex with tuberin, has a pronounced independent functional relevance in the pathogenetic context of TSC and cortical dysplasias.

ACKNOWLEDGMENT

The authors thank Christiane Esch for valuable technical support.

REFERENCES

1. Hengstschlager M, Rodman DM, Miloloza A, et al. Tuberous sclerosis gene products in proliferation control. Mutat Res 2001;488:233–39
2. Gomez MR. Varieties of expression of tuberous sclerosis. Neurofibromatosis 1988;1:330–38
3. Palmini A, Najm I, Avanzini G, et al. Terminology and classification of the cortical dysplasias. Neurology 2004;62:S2–S8
4. Taylor DC, Falconer MA, Bruton CJ, et al. Focal dysplasia of the cerebral cortex in epilepsy. J Neurol Neurosurg Psychiatry 1971;34: 369–87
5. van Slegtenhorst M, de Hoogt R, Hermans C, et al. Identification of the tuberous sclerosis gene *TSC1* on chromosome 9q34. Science 1997;277: 805–8
6. Sampson JR, Harris PC. The molecular genetics of tuberous sclerosis. Hum Mol Genet 1994;3:1477–80
7. Carbonara C, Longa L, Grosso E, et al. 9q34 loss of heterozygosity in a tuberous sclerosis astrocytoma suggests a growth suppressor-like activity also for the *TSC1* gene. Hum Mol Genet 1994;3:1829–32
8. Kwiatkowski DJ. Tuberous sclerosis: From tubers to mTOR. Ann Hum Genet 2003;67:87–96
9. Baybis M, Yu J, Lee A, et al. mTOR cascade activation distinguishes tubers from focal cortical dysplasia. Ann Neurol 2004;56:478–87
10. van Slegtenhorst M, Nellist M, Nagelkerken B, et al. Interaction between hamartin and tuberin, the *TSC1* and *TSC2* gene products. Hum Mol Genet 1998;7:1053–57
11. Green AJ, Johnson PH, Yates JR. The tuberous sclerosis gene on chromosome 9q34 acts as a growth suppressor. Hum Mol Genet 1994;3: 1833–34
12. Henske EP, Scheithauer BW, Short MP, et al. Allelic loss is frequent in tuberous sclerosis kidney lesions but rare in brain lesions. Am J Hum Genet 1996;59:400–6
13. Tavazoie SF, Alvarez VA, Ridenour DA, et al. Regulation of neuronal morphology and function by the tumor suppressors Tsc1 and Tsc2. Nat Neurosci 2005;8:1727–34
14. Jansen FE, Notenboom RG, Nellist M, et al. Differential localization of hamartin and tuberin and increased S6 phosphorylation in a tuber. Neurology 2004;63:1293–95
15. Nellist M, van Slegtenhorst MA, Goedbloed M, et al. Characterization of the cytosolic tuberin-hamartin complex. Tuberin is a cytosolic chaperone for hamartin. J Biol Chem 1999;274:35647–52
16. Becker AJ, Urbach H, Scheffler B, et al. Focal cortical dysplasia of Taylor's balloon cell type: Mutational analysis of the *TSC1* gene indicates a pathogenic relationship to tuberous sclerosis. Ann Neurol 2002;52:29–37
17. Jones AC, Daniells CE, Snell RG, et al. Molecular genetic and phenotypic analysis reveals differences between TSC1 and TSC2 associated familial and sporadic tuberous sclerosis. Hum Mol Genet 1997;6:2155–61
18. van Slegtenhorst M, Verhoef S, Tempelaars A, et al. Mutational spectrum of the *TSC1* gene in a cohort of 225 tuberous sclerosis complex patients: No evidence for genotype-phenotype correlation. J Med Genet 1999;36:285–89
19. Dabora SL, Jozwiak S, Franz DN, et al. Mutational analysis in a cohort of 224 tuberous sclerosis patients indicates increased severity of TSC2, compared with TSC1, disease in multiple organs. Am J Hum Genet 2001;68:64–80
20. Hung CC, Su YN, Chien SC, et al. Molecular and clinical analyses of 84 patients with tuberous sclerosis complex. BMC Med Genet 2006;7:72
21. Kral T, Clusmann H, Urbach J, et al. Preoperative evaluation for epilepsy surgery (Bonn Algorithm). Zentralbl Neurochir 2002;63: 106–10
22. Fassunke J, Majores M, Tresch A, et al. Array analysis of epilepsy-associated gangliogliomas reveals expression patterns related to aberrant development of neuronal precursors. Brain 2008;131:3034–50
23. Becker AJ, Blümcke I, Urbach H, et al. Molecular neuropathology of epilepsy-associated glioneuronal malformations. J Neuropathol Exp Neurol 2006;65:99–108
24. Gutmann DH, Zhang Y, Hasbani MJ, et al. Expression of the tuberous sclerosis complex gene products, hamartin and tuberin, in central nervous system tissues. Acta Neuropathol 2000;99:223–30
25. Schick V, Majores M, Engels G, et al. Differential Pi3K-pathway activation in cortical tubers and focal cortical dysplasias with balloon cells. Brain Pathol 2007;17:165–73
26. Miyata H, Chiang AC, Vinters HV. Insulin signaling pathways in cortical dysplasia and TSC-tubers: Tissue microarray analysis. Ann Neurol 2004;56:510–19
27. Lamb RF, Roy C, Diefenbach TJ, et al. The TSC1 tumour suppressor hamartin regulates cell adhesion through ERM proteins and the GTPase Rho. Nat Cell Biol 2000;2:281–87
28. Wienecke R, Maize JC Jr, Shoarinejad F, et al. Co-localization of the TSC2 product tuberin with its target Rap1 in the Golgi apparatus. Oncogene 1996;13:913–23
29. Murthy V, Haddad LA, Smith N, et al. Similarities and differences in the subcellular localization of hamartin and tuberin in the kidney. Am J Physiol Renal Physiol 2000;278:F737–46
30. Plank TL, Yeung RS, Henske EP. Hamartin, the product of the tuberous sclerosis 1 (*TSC1*) gene, interacts with tuberin and appears to be localized to cytoplasmic vesicles. Cancer Res 1998;58:4766–70
31. Yamamoto Y, Jones KA, Mak BC, et al. Multicompartmental distribution of the tuberous sclerosis gene products, hamartin and tuberin. Arch Biochem Biophys 2002;404:210–17
32. Fukuda T, Kobayashi T, Momose S, et al. Distribution of Tsc1 protein detected by immunohistochemistry in various normal rat tissues and the renal carcinomas of Eker rat: Detection of limited colocalization with *Tsc1* and *Tsc2* gene products in vivo. Lab Invest 2000;80:1347–59
33. Catania MG, Mischel PS, Vinters HV. Hamartin and tuberin interaction with the G2/M cyclin-dependent kinase CDK1 and its regulatory cyclins A and B. J Neuropathol Exp Neurol 2001;60:711–23

34. Bichelmeier U, Schmidt T, Hubener J, et al. Nuclear localization of ataxin-3 is required for the manifestation of symptoms in SCA3: In vivo evidence. J Neurosci 2007;27:7418–28
35. Habib SL, Michel D, Masliah E, et al. Role of tuberin in neuronal degeneration. Neurochem Res 2008;33:1113–16
36. Chong-Kopera H, Inoki K, Li Y, et al. TSC1 stabilizes TSC2 by inhibiting the interaction between TSC2 and the HERC1 ubiquitin ligase. J Biol Chem 2006;281:8313–16
37. Hu J, Zacharek S, He YJ, et al. WD40 protein FBW5 promotes ubiquitination of tumor suppressor TSC2 by DDB1-CUL4-ROC1 ligase. Genes Dev 2008;22:866–71
38. Becker AJ, Klein H, Baden T, et al. Mutational and expression analysis of the reelin pathway components CDK5 and doublecortin in gangliogliomas. Acta Neuropathol 2002;104:403–8
39. Johnson MW, Kerfoot C, Bushnell T, et al. Hamartin and tuberin expression in human tissues. Mod Pathol 2001;14:202–10
40. Miloloza A, Rosner M, Nellist M, et al. The *TSC1* gene product, hamartin, negatively regulates cell proliferation. Hum Mol Genet 2000; 9:1721–27
41. Thom M, Martinian L, Sen A, et al. Cortical neuronal densities and lamination in focal cortical dysplasia. Acta Neuropathol (Berl) 2005;110: 383–92

Biochimica et Biophysica Acta 1802 (2010) 774–781

Contents lists available at ScienceDirect

Biochimica et Biophysica Acta

journal homepage: www.elsevier.com/locate/bbadis

Analysis of TSC1 truncations defines regions involved in TSC1 stability, aggregation and interaction

Marianne Hoogeveen-Westerveld, Carla Exalto, Anneke Maat-Kievit, Ans van den Ouweland, Dicky Halley, Mark Nellist *

Department of Clinical Genetics, Erasmus Medical Centre, Dr. Molewaterplein 50, 3015 GE Rotterdam, The Netherlands

ARTICLE INFO

Article history:
Received 4 May 2010
Received in revised form 7 June 2010
Accepted 8 June 2010
Available online 12 June 2010

Keywords:
Tuberous sclerosis complex
TSC1
TSC2
TORC1

ABSTRACT

Tuberous sclerosis complex (TSC) is an autosomal dominant disorder characterised by the development of hamartomas in a variety of organs and tissues. The disease is caused by mutations in either the *TSC1* gene on chromosome 9q34, or the *TSC2* gene on chromosome 16p13.3. The *TSC1* and *TSC2* gene products, TSC1 and TSC2, interact to form a protein complex that inhibits signal transduction to the downstream effectors of the target of rapamycin complex 1 (TORC1). Here we investigate TSC1 structure and function by analysing a series of truncated TSC1 proteins. We identify specific regions of the protein that are important for TSC1 stability, localisation, interactions and function.

1. Introduction

Tuberous sclerosis complex (TSC) is an autosomal dominant disorder characterised by the development of hamartomas in a variety of organs and tissues, including the brain, skin and kidneys [1]. Mutations in either the *TSC1* gene on chromosome 9q34 [2], or the *TSC2* gene on chromosome 16p13.3 [3] cause TSC.

The *TSC1* and *TSC2* gene products, TSC1 and TSC2, interact to form a protein complex [4]. TSC2 contains a GTPase activating protein (GAP) domain, and the TSC1–TSC2 complex has been shown to have GAP activity for a GTPase called ras homolog expressed in brain (RHEB). The TSC1–TSC2 complex stimulates the hydrolysis of RHEB-bound GTP to GDP, thereby inhibiting the RHEB-GTP-dependent stimulation of the target of rapamycin complex 1 (TORC1) [5]. TORC1 regulates a wide array of cellular processes, including transcription, translation and autophagy [6]. Inactivation of the TSC1–TSC2 complex results in the phosphorylation of TORC1 targets, including p70 S6 kinase (S6K) and elongation factor 4E binding protein 1 and, consequently, increased protein synthesis and cell growth [6]. TSC1 has limited homology with other proteins [2] and the exact role of TSC1 in the TSC1–TSC2 complex is not completely clear. Some studies have shown that TSC1 is required for TSC2 GAP activity [7–9], while others suggest that TSC1 is not essential for GAP activity but is necessary to maintain the stability, activity and correct intracellular localisation of the TSC1–TSC2 complex [10,11]. TSC1 has been shown to be involved in recruitment of the TSC1–TSC2 complex to cell membranes [12] and may integrate multiple inputs to help regulate TORC1 activity, or perform other, independent functions [13].

In the absence of TSC2, over-expressed TSC1 forms Triton X100-insoluble aggregates or inclusions due to interactions between the coiled coil regions (amino acids 719–998) of different TSC1 molecules [14]. Coexpression of TSC2 prevents the formation of these inclusions, resulting in a shift of TSC1 to Triton X100-soluble cell lysate fractions [15]. Stable TSC1–TSC2 complexes can be immunoprecipitated from these cell fractions, demonstrating that TSC2 acts as a molecular chaperone, maintaining TSC1 in a stable cytosolic form [14]. Recently, we identified TSC1 amino acid substitutions in TSC patients that prevented TSC1 inclusion formation *in vitro* [16,17]. Surprisingly, none of these changes mapped to the coiled coil region, indicating that other regions of TSC1 are also important for the expression and localisation of the protein.

To gain additional insight into the structure and function of TSC1, we compared full-length TSC1 to a series of TSC1 N- and C-terminal truncation proteins. Our *in vitro* analysis demonstrates that the N-terminal region is important for TSC1 stability and that both the N-terminal and coiled coil regions are required for TSC1 aggregation. Furthermore, we show that multiple regions of TSC1 are required for binding TSC2 and that some TSC1 truncations can co-operate with TSC2 to inhibit TORC1 activity. This information will be useful for the functional characterisation of unclassified *TSC1* variants identified in individuals with TSC.

Abbreviations: TSC, tuberous sclerosis complex; RHEB, ras homolog expressed in brain; TORC1, target of rapamycin complex 1; S6K, p70 S6 kinase; GAP, GTPase activating protein

* Corresponding author. Tel.: +31 10 7044628; fax: +31 10 7044736.
E-mail address: m.nellist@erasmusmc.nl (M. Nellist).

0925-4439/$ – see front matter © 2010 Elsevier B.V. All rights reserved.
doi:10.1016/j.bbadis.2010.06.004

2. Materials and methods

2.1. Generation of constructs and antisera

To derive expression constructs encoding myc-tagged TSC1 C-terminal truncations a KpnI site was introduced into a full-length myc-tagged TSC1 expression construct by site-directed mutagenesis (QuikChange, Stratagene, La Jolla, CA, U.S.A.). After digestion with KpnI to excise the 3′ portion of the *TSC1* open reading frame (ORF), the vector and remaining ORF was re-circularised so that the epitope tag remained in-frame with the last codon of the truncated *TSC1* ORF. N-terminal truncations were derived in a similar way. A NheI site was introduced to allow excision of the 5′ portion of the *TSC1* ORF. In each case the complete open reading frame of the new construct was verified by sequence analysis. Expression constructs were derived for 4 C-terminal truncation proteins: Q900 (TSC1 amino acids 1–900, molecular mass 100 kDa), R692 (amino acids 1–692, 80 kDa), R509 (amino acids 1–509, 60 kDa) and T339 (amino acids 1–339, 35 kDa); one N-terminal truncation protein, M351 (amino acids 351–1164, 100 kDa), and one truncation protein, M351-Q900, lacking both termini (amino acids 351–900, 65 kDa). The pathogenic L117P and M224R missense changes were introduced by site-directed mutagenesis, as described previously [15]. An overview of the expressed TSC1 truncation proteins is shown in Fig. 1. Other constructs used in this study have been described elsewhere [4,15,18].

Antibodies were purchased from Cell Signaling Technology (Danvers, MA, U.S.A.), except for a mouse monoclonal antibody against TSC2 which was purchased from Zymed Laboratories (San Francisco, CA, U.S.A.), or were described previously [4]. Secondary antibodies for infra-red detection proteins on immunoblots were obtained from Li-Cor Biosciences (Lincoln, NE, U.S.A.).

2.2. Immunoblot analysis of cells over-expressing TSC1 truncations

HEK 293T cells in 3.5 cm dishes were transfected with expression constructs using polyethylenimine (Polysciences Inc., Warrington, PA, U.S.A.)[19]. Twenty-four hours after transfection the cells were washed with cold phosphate buffered saline (PBS) and lysed in 0.15 ml lysis buffer (50 mM Tris–HCl (pH 7.5), 100 mM NaCl, 50 mM NaF, 1% Triton X100 and a protease inhibitor cocktail (Complete, Roche Molecular Biochemicals)) for 10 min on ice. The cell lysates were cleared by centrifugation (10,000 *g* for 10 min at 4 °C) and the supernatant (Triton X100-soluble) and pellet (Triton X100-insoluble) fractions were recovered. The pellet fractions were resuspended in 0.15 ml lysis buffer and sonicated at 12 μm for 15 s prior to immunoblot analysis using the Criterion SDS-PAGE system (BioRad, Hercules, CA, U.S.A.). Protein expression levels were estimated by near infra-red detection and quantification of the blotted proteins on an Odyssey™ scanner (Li-Cor Biosciences).

To estimate the effect of the TSC1 truncation proteins on S6K T389 phosphorylation HEK 293T cells were transfected with a 4:2:1 mixture of the TSC1, TSC2 and S6K expression constructs and harvested as above. The Triton X100-soluble fractions were analysed by immunoblotting, as described previously [16,17].

2.3. Immunofluorescent detection of TSC1 truncations

HEK 293T cells were seeded onto glass cover slides coated with poly-L-lysine (Sigma-Aldrich, Carlsbad, CA, U.S.A.), transfected and processed for immunofluorescent microscopy as described previously [16]. Fixed, permeabilised cells were incubated with a primary mouse monoclonal antibody specific for the myc epitope tag, followed by a cyanine (Cy2)-coupled secondary antibody (DAKO,

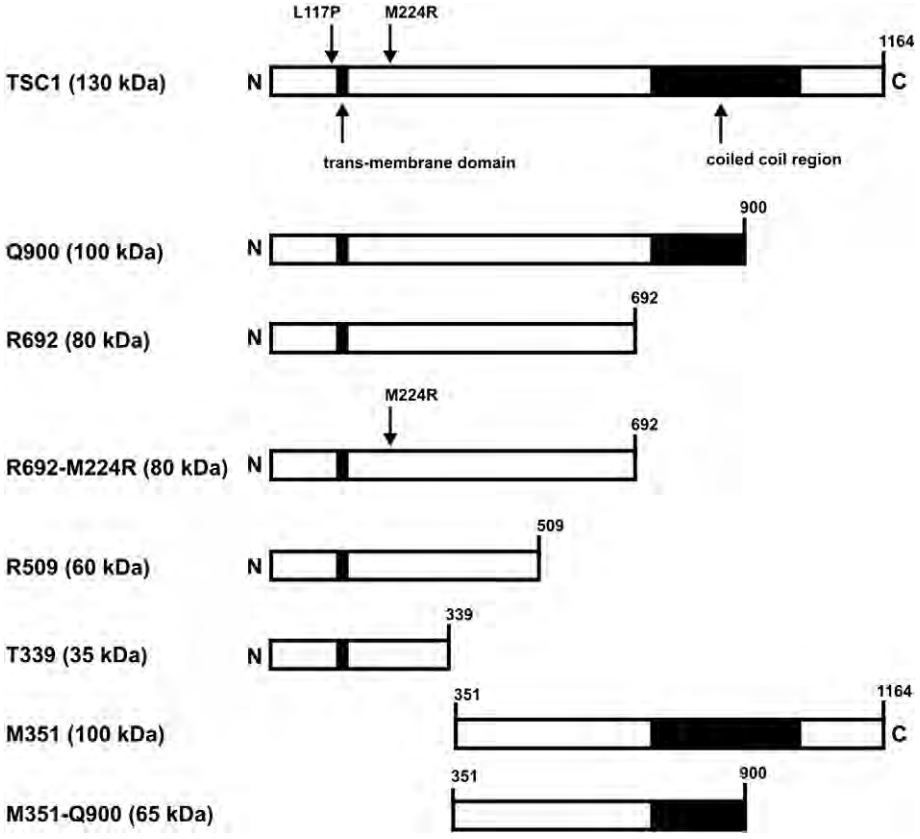

Fig. 1. TSC1 truncation proteins. Schematic diagram illustrating the TSC1 truncation proteins used as part of this study. The positions of the predicted transmembrane domain (amino acids 127–144), coiled coil region (amino acids 719–998), and the L117P and M224R missense mutations identified in individuals with TSC are indicated. Numbers indicate the positions of the first and last amino acids, relative to the full-length protein (top).

Carpinteria, CA, U.S.A.). Cells were mounted in Mowiol (Calbiochem, La Jolla, CA, U.S.A.) and studied using a Leica DM RXA microscope and Image Pro-Plus version 6 image analysis software.

2.4. Coimmunoprecipitation of TSC2 with the TSC1 truncations

Immunoprecipitations were performed using the Triton X100-soluble cell lysate fractions. EZ Red anti-myc affinity beads (Sigma-Aldrich) were pre-equilibrated in lysis buffer prior to incubation with the cell lysates for 3 h at 4 °C with gentle rotation. The beads were washed at least 3 times with >20-fold excess of lysis buffer per wash step. Beads were recovered by gentle centrifugation (1000 *g* for 15 s at 4 °C) between each wash step, and resuspended in sample buffer prior to immunoblot analysis.

3. Results

3.1. TSC1 truncation proteins

We derived expression constructs for 4 C-terminal TSC1 truncations that we called: Q900, R692, R509 and T339. The Q900 truncation consists of TSC1 amino acids 1–900 and corresponds to a *TSC1* c.2919C>T (p.Q900X) mutation, the most distal *TSC1* mutation identified in our patient cohort [20]. We identified this mutation in 2 unrelated cases of TSC. Clinical data was available for one of these individuals (Table 1). The R692 and R509 truncations consist of amino acids 1–692 and 1–509 respectively, and correspond to the *TSC1* c.2295C>T and c.1746C>T mutations. Together these 2 mutations account for >5% of the *TSC1* variants listed in the Leiden Open Tuberous Sclerosis Complex Variation Database [21]. We identified the *TSC1* c.2295C>T mutation in 6 families in our cohort, and in 5 cases had clinical data on one or more individuals (Table 1). We identified 6 cases with the *TSC1* c.1746C>T mutation in our cohort. Clinical data was available for one individual (Table 1). The T339 truncation corresponds to a *TSC1* c.1015dupA mutation identified in an individual with very mild peripheral features of TSC, epilepsy and cognitive disturbances (Table 1) (P. de Vries, personal communication).

In addition to the C-terminal truncations, we expressed 2 proteins lacking 350 amino acids from the N-terminus of TSC1. Truncation protein M351 consisted of TSC1 amino acids 351–1164, and truncation protein M351-Q900 consisted of amino acids 351–900. A schematic overview of the truncation proteins is shown in Fig. 1.

Full-length TSC1 and the TSC1 truncation proteins were expressed as fusion proteins containing a C-terminal myc epitope tag. This tag did not interfere with either the TSC1–TSC2 interaction, or with the function of the TSC1–TSC2 complex [15–19]. We compared the relative expression levels of the truncation proteins in the Triton X100-soluble and -insoluble fractions by immunoblotting. Full-length TSC1 and the Q900 truncation were detected predominantly in the Triton X100-insoluble fraction, while the remaining truncation proteins were detected predominantly in the soluble fraction (Fig. 2A,C).

Table 1
Clinical findings in individuals with the *TSC1* c.2919C>T (p.Q900X), *TSC1* c.2295C>T (p.R692X) and *TSC1* c.1015dupA (p.T339X) mutations.

Case	Mutation	Renal	Other	Skin	Neurological	Brain
1	c.2919C>T	RC	–	HM, FA, SP	E, MR, BD	SEN, CT
2	c.2295C>T	–	CR	HM	E, MR	SEN, CT
3	c.2295C>T	–	–	HM	E	SEN, CT
4.1	c.2295C>T	–	–	FA, HM	E	SEGA
4.2	c.2295C>T	–	–	UF	E	SEN
5	c.2295C>T	–	CR	HM, SP	E, BD	–
6	c.2295C>T	–	DP, RP	FA, UF	E, BD	SEN, CT
7	c.1746C>T	RC	CR	–	–	SEN, CT
8	c.1015dupA	–	WPW	HM	E, BD	–

Key: –, not present, or not recorded; RC, renal cysts; CR, cardiac rhabdomyoma; DP, dental pit; RP, retinal phakoma; WPW, Wolff–Parkinson–White syndrome; HM, hypomelanotic macule; SP, shagreen patch; UF, ungual fibroma; FA, facial angiofibroma; E, epilepsy; MR, mental retardation; BD, behavioural disturbance; SEN, subependymal nodule; CT, cortical tuber; and SEGA, subependymal giant cell astrocytoma.

3.2. TSC1 truncation prevents aggregate formation

The Q900 truncation protein localised to cytoplasmic punctate inclusions or aggregates in HEK 293 T cells (Fig. 3A) and was detected predominantly in Triton X100-insoluble cell lysate fractions, similar to full-length TSC1 (Fig. 2A,C). In contrast, truncation proteins R692, R509 and T339 that lack the entire coiled coil region, and the M351 truncation protein, that contains the coiled coil region but lacks the TSC1 N-terminal, were detected predominantly in Triton X100-soluble cell lysate fractions (Fig. 2A,C) and did not form cytoplasmic inclusions (Fig. 3C,D, and data not shown) We concluded that the coiled coil region was necessary but not sufficient for aggregate formation.

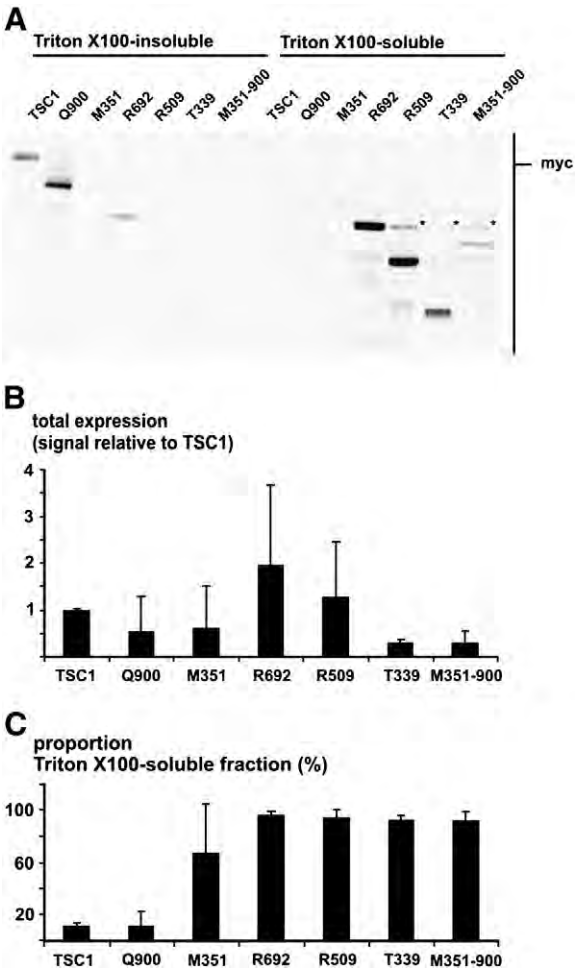

Fig. 2. Immunoblot analysis of TSC1 truncation proteins. Wild-type myc-tagged TSC1 (TSC1) and the myc-tagged truncations were over-expressed in HEK 293T cells. Triton X100-soluble and -insoluble cell lysate fractions were separated on 4–12% gradient SDS-PAGE gels, blotted and incubated with a monoclonal mouse antibody against the myc epitope tag. (A) Immunoblot of Triton X100-soluble and -insoluble cell lysate fractions. Bands marked with an asterisk (*) are due to leakage of the signal from the R692 truncation. (B) Total expression of the TSC1 truncation proteins. Truncation protein levels were quantified in at least 3 separate experiments, and the mean expression levels, relative to full-length myc-tagged TSC1, were derived. Standard deviations are indicated. (C) Relative expression of the TSC1 truncations in Triton X100-soluble and -insoluble cell lysate fractions. The signal detected in the soluble fraction was divided by the total signal (soluble + insoluble) for each protein in at least 3 separate experiments. Standard deviations are indicated.

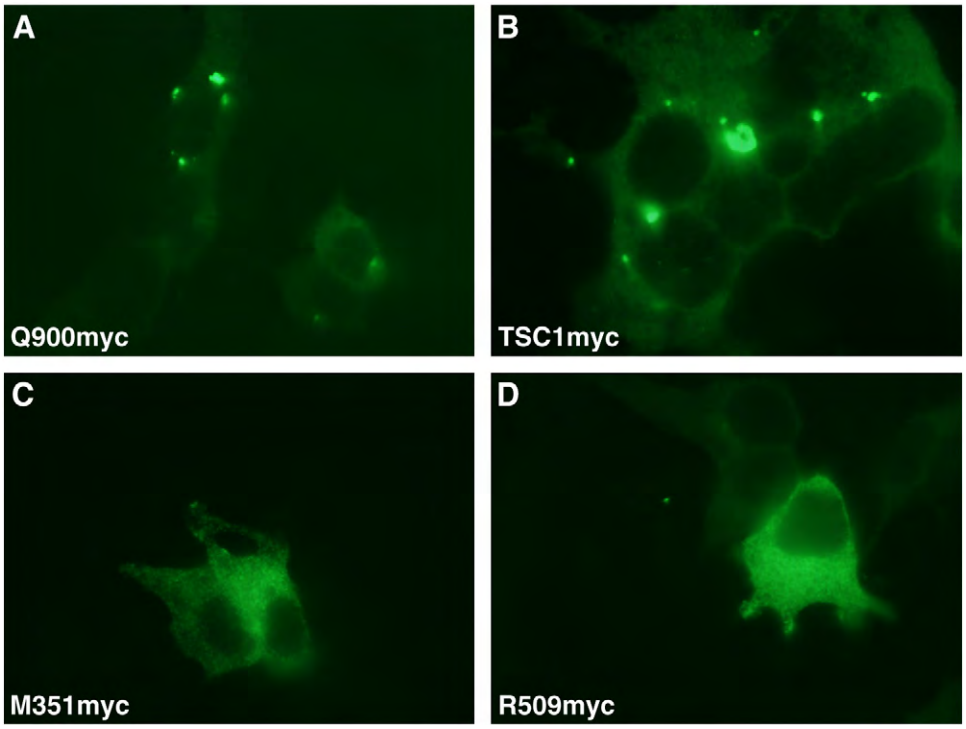

Fig. 3. Immunofluorescence analysis of TSC1 truncation protein expression. Transfected HEK 293T cells expressing the different truncation proteins were fixed and incubated with an antibody against the myc epitope tag. (A) Punctate, cytoplasmic localisation of truncation protein Q900. (B) Punctate, cytoplasmic localisation of full-length TSC1. (C) Diffuse, cytoplasmic localisation of truncation protein M351. (D) Diffuse, cytoplasmic localisation of truncation protein R509.

3.3. The N-terminal region is required for TSC1 stability

Pathogenic amino acid substitutions in the N-terminal region of TSC1 prevent TSC1 aggregation and reduce expression levels *in vitro* [16,17]. To determine whether this destabilisation is due to effects on local protein folding, or due to long-range interactions between the N- and C-terminal regions of TSC1, a pathogenic N-terminal amino acid substitution (M224R) [17] was introduced into the R692 truncation protein. that lacks the C-terminal region (amino acids 693–1164). As shown in Fig. 4, the M224R substitution reduced the amount of both full-length TSC1 and the R692 truncation detected in the Triton X100 soluble fraction, demonstrating that the M224R substitution had the same effect irrespective of the presence or absence of amino acids 693–1164. We concluded that the low expression levels of TSC1 missense mutants [16,17,22] are more likely due to autonomous effects on the N-terminal region than disruption of long-range interactions with the TSC1 C-terminal, containing the predicted coiled coil regions.

3.4. TSC1 truncation reduces the stability of the TSC1–TSC2 complex

The formation of stable, Triton X100-soluble TSC1–TSC2 complexes prevents TSC1 aggregation [14]. We coexpressed TSC2 with the TSC1 truncations in HEK 293T cells and estimated the proportions of the expressed proteins in the Triton X100-soluble fractions (Fig. 5A,C). As expected, the proportion of full-length TSC1 detected in the Triton X100-soluble fraction was increased by coexpression of TSC2, as estimated by immunoblotting (compare Figs. 2C and 5C). TSC2 coexpression had a similar effect on the Q900 truncation, increasing the proportion detected in the soluble fraction (compare Figs. 2C and 5C).

To investigate whether the TSC1 truncation proteins interacted directly with TSC2, we coexpressed TSC2 with the different TSC1 truncations and immunoprecipitated the truncation proteins from the Triton X100-soluble cell lysate fractions. We determined whether TSC2 was coimmunoprecipitated by immunoblotting. As shown in Fig. 6, all the TSC1 truncation proteins were immunoprecipitated efficiently, even those that were expressed at low levels. TSC2 coimmunoprecipitated with TSC1 and with the M351 and Q900 truncations, and to a lesser extent with the R692 and R509 truncations. TSC2 was not coimmunoprecipitated with the M351-Q900 or T339 truncations or with a control protein (myc-tagged β-lactamase).

The interaction detected between the Q900 truncation and TSC2 was consistent with the observed shift of the Q900 truncation from the insoluble to the soluble fraction (compare Figs. 2 and 5). However, the TSC2–Q900 interaction appeared weaker than that between TSC2 and full-length TSC1 (Fig. 6D). Similarly, TSC2 was coimmunoprecipitated with the M351 truncation, but less efficiently than with full-length TSC1 (Fig. 6D). Therefore, we concluded that multiple regions of TSC1 are necessary for the interaction with TSC2 and to form a stable TSC1–TSC2 complex.

3.5. The central region of TSC1 is involved in TSC1–TSC1 interactions

Interactions between the TSC1 coiled coil regions cause TSC1 aggregation [14]. We sought additional evidence for TSC1–TSC1 interactions by coimmunoprecipitation. As shown in Fig. 7, the myc-tagged TSC1 truncations were immunoprecipitated from Triton X100-soluble fractions. Coimmunoprecipitated full-length (untagged) TSC1 was detected by immunoblotting. TSC1 was coimmunoprecipitated with the M351 and M351-Q900 truncations that contain part or all of the coiled coil region, and, to a lesser extent, by the R509 and R692 truncations, that do not (Fig. 7A,C). TSC1 was not detected in the T339 and Q900 immunoprecipitates, or in the control immunoprecipitate. We were unable to detect stable TSC1–Q900 complexes by coimmunoprecipitation because both full-length TSC1 and the Q900 truncation localised predominantly to the Triton X100-insoluble cell lysate fractions. We concluded that in addition to the coiled coil region, the central region of TSC1 (amino acids 351–509) is involved in the TSC1–TSC1 interaction.

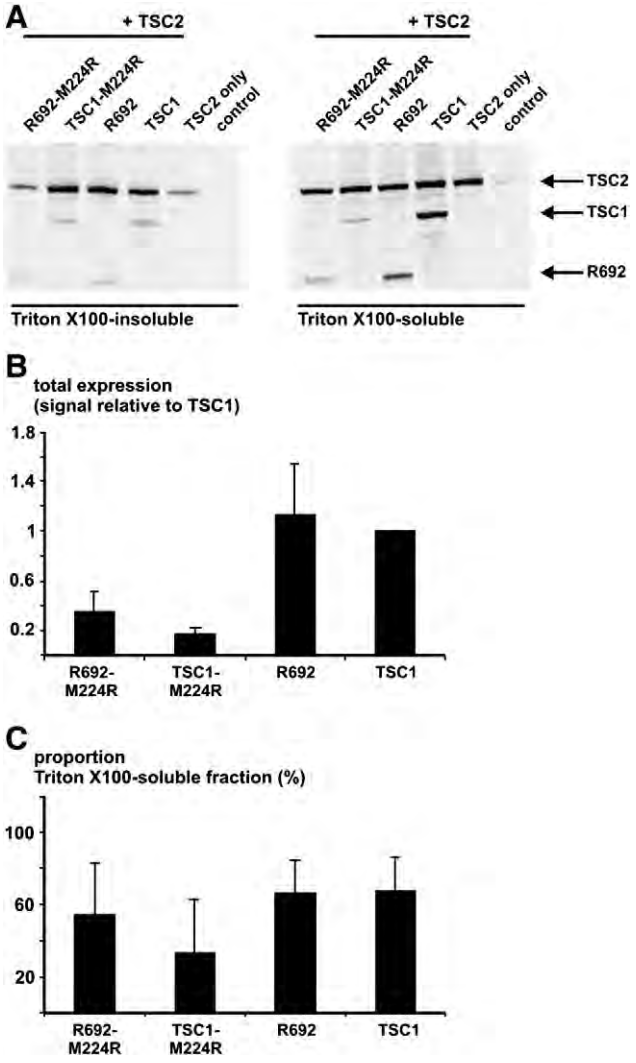

Fig. 4. Effect of the pathogenic M224R amino acid substitution on expression of the R692 truncation protein. Wild-type myc-tagged TSC1 (TSC1), the TSC1-M224R mutant, the R692 truncation protein, and the R692-M224R mutant truncation were coexpressed with TSC2 in HEK 293T cells. Triton X100-soluble and -insoluble cell lysate fractions were separated on 4–12% gradient SDS-PAGE gels, blotted and incubated with antibodies specific for TSC2 and the myc epitope tag. (A) Immunoblot showing expression of full-length TSC1 and the R692 truncation protein compared to the TSC1-M224R and R692-M224R mutants. The levels of the TSC1-M224R and R692-M224R mutants detected in the Triton X100 soluble fraction is reduced compared to wild-type TSC1 and the R692 truncation. Coexpressed TSC2 is shown as a control for transfection efficiency. (B) Total expression of the TSC1-M224R and R692-M224R mutants. Protein levels in the Triton X100 soluble and insoluble fractions were quantified and summed in at least 3 separate experiments, and the mean expression levels, relative to full-length myc-tagged TSC1, were calculated. Standard deviations are indicated. (C) Relative expression of the TSC1-M224R and R692-M224R mutants in Triton X100-soluble and -insoluble cell lysate fractions. The signal detected in the soluble fraction was divided by the total signal (soluble + insoluble) for each protein in at least 3 separate experiments. Standard deviations are indicated.

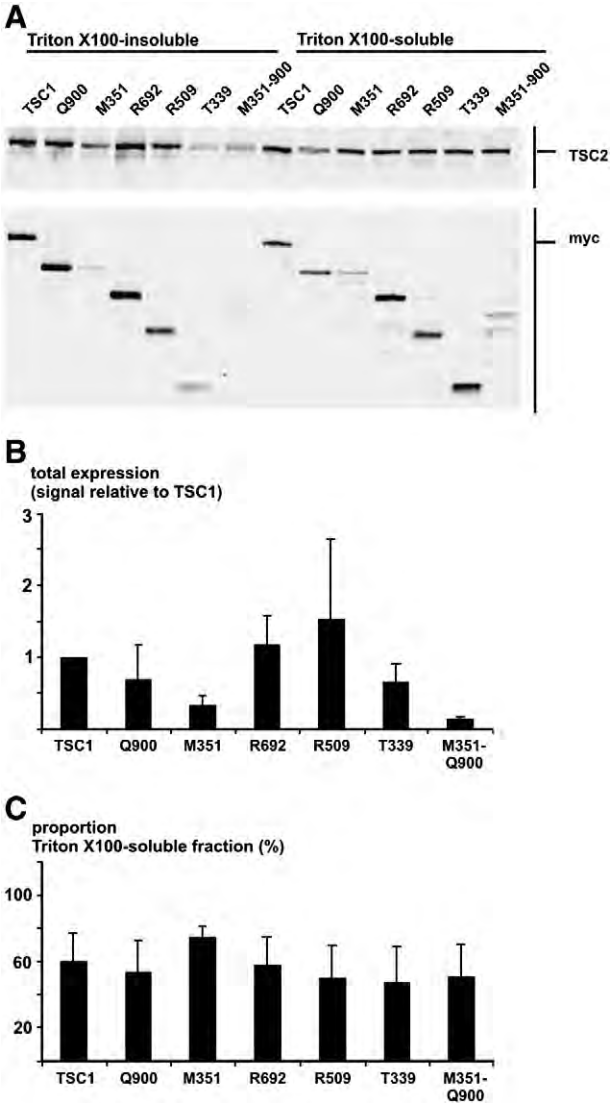

Fig. 5. Immunoblot analysis of coexpression of TSC2 and the TSC1 truncation proteins. Wild-type myc-tagged TSC1 (TSC1) and the myc-tagged truncations were coexpressed with TSC2 in HEK 293T cells. Triton X100-soluble and -insoluble cell lysate fractions were separated on 4–12% gradient SDS-PAGE gels, blotted and incubated with antibodies specific for TSC2 and the myc epitope tag. (A) Immunoblot of Triton X100-soluble and -insoluble cell lysate fractions prepared from cells coexpressing TSC2 and the TSC1 truncation proteins. (B) Effect of TSC2 coexpression on expression levels of the TSC1 truncation proteins. Protein levels were quantified as in Fig. 2B. Standard deviations are indicated. (C) Effect of TSC2 coexpression on the relative expression levels of the TSC1 truncation proteins in Triton X100-soluble and -insoluble cell lysate fractions. Expression levels were quantified as in Fig. 2C. Standard deviations are indicated.

3.6. TSC1 truncation proteins help TSC2 suppress TORC1 activity

To determine whether the TSC1 truncations could affect the TSC2-dependent inhibition of S6K-T389 phosphorylation, TSC2, S6K and the TSC1 truncations, were expressed in HEK 293T cells and the T389 phosphorylation status of S6K was estimated by immunoblotting, as shown in Fig. 8. The R509 truncation was not included in this analysis as it comigrated with S6K, making it difficult to detect and quantify separate R509 and S6K signals.

Although the expression levels of the different TSC1 truncation proteins were variable (Fig. 8B), the expression levels of TSC2 (Fig. 8C) and S6K (Fig. 8E) were relatively constant. This indicated that coexpression of the different TSC1 truncations did not affect TSC2 expression levels. In cells coexpressing TSC2 and full-length TSC1, S6K-T389 phosphorylation was reduced approximately 7-fold compared to cells expressing neither protein, or to cells expressing TSC1 only (Fig. 8D). Expression of TSC2 only (without TSC1) was less effective than coexpression of TSC1 and TSC2: S6K-T389 phosphorylation was approximately 5-fold higher in TSC2 expressing cells, than in TSC1–TSC2 expressing cells. Coexpression of the TSC1 T339 and M351-Q900 truncations did not affect the ability of TSC2 to reduce S6K-T389 phosphorylation (Fig. 8D). In contrast, coexpression of TSC2 with the pathogenic TSC1-L117P variant [17] reduced S6K-T389 phosphorylation to a level approximately 3-fold higher than in the TSC1-TSC2 expressing cells, indicating that this variant can partially

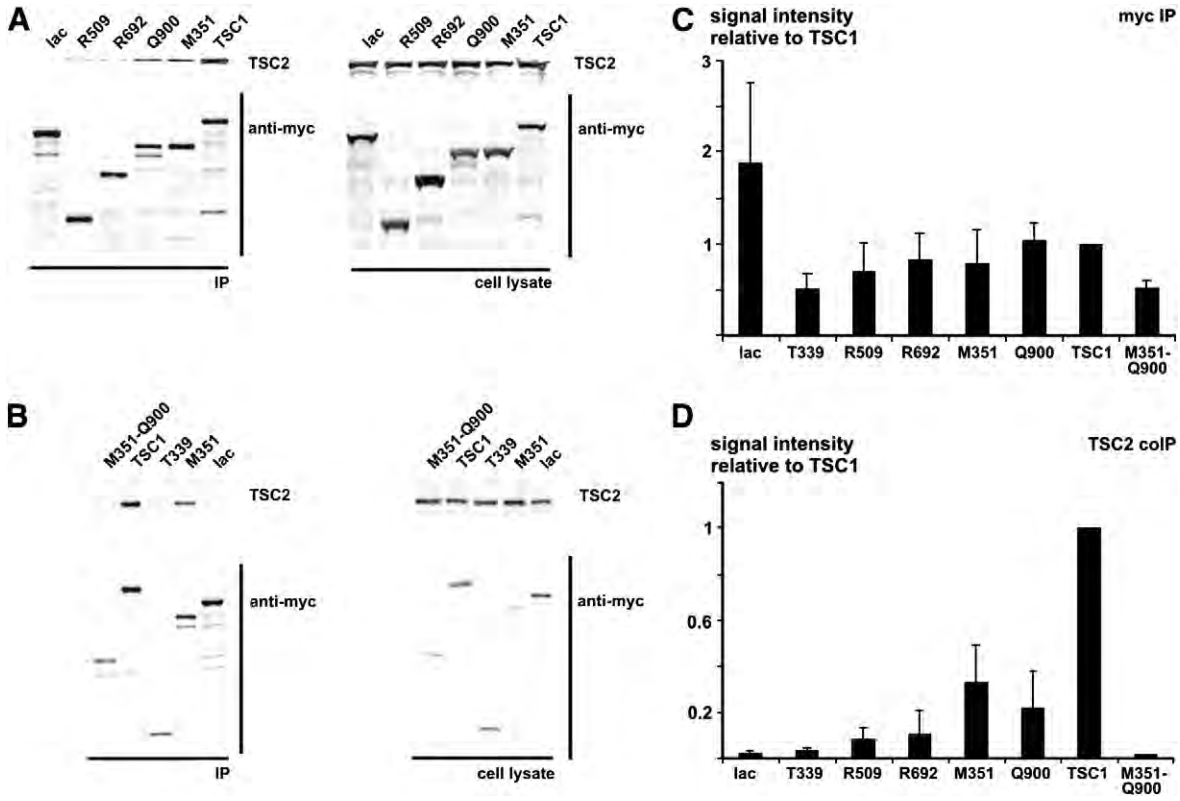

Fig. 6. Immunoblot analysis of TSC1–TSC2 interactions. TSC1 truncation proteins were coexpressed with TSC2 in HEK 293T cells. The truncation proteins were immunoprecipitated from Triton X100-soluble cell lysate fractions using an anti-myc epitope affinity matrix, and coimmunoprecipitated TSC2 was detected by immunoblotting. Each interaction was tested at least 3 times. (A and B) Immunoblots showing coimmunoprecipitation of TSC2 with full-length TSC1 and the M351, Q900, R692 and R509 truncations, but not with the M351-Q900 or T339 truncations, or the myc-tagged β-lactamase control protein (lac). (C) Mean total signal intensity of the immunoprecipitated truncations, relative to full-length TSC1. Standard deviations are indicated. (D) Mean total signal intensity of coimmunoprecipitated TSC2, relative to the TSC2 signal detected after coimmunoprecipitation with full-length TSC1. Standard deviations are indicated.

inhibit TORC1 activity *in vitro*. Interestingly, the M351, Q900 and R692 truncations had a similar effect. In each case, S6K-T389 phosphorylation was increased approximately 3-fold with respect to the TSC1–TSC2 expressing cells, but reduced with respect to cells expressing TSC2 only. Therefore, in this *in vitro* assay, the TSC1 R692, M351 and Q900 truncation proteins all increased the TSC2-dependent inhibition of S6K-T389 phosphorylation, albeit not as effectively as full-length TSC1.

4. Discussion

TSC1 and *TSC2* encode the TSC1–TSC2 protein complex, an essential regulator of TORC1 [23]. TSC2 contains the active site of the TSC1–TSC2 complex and therefore has a clearly defined functional role. In contrast, the role of TSC1 is less clear. Some studies suggest that TSC1 is required for TSC2 GAP activity, while others indicate that TSC1 does not affect the catalytic activity of the TSC1–TSC2 complex, but prevents the degradation of the complex [7–11]. To gain more insight into the structure and function of TSC1, we compared the characteristics of a series of TSC1 truncation proteins with full-length, wild-type TSC1.

We found that deletion of the complete TSC1 coiled coil region (amino acids 719–998) prevented TSC1 aggregation and that sequences close to the N-terminal were required for both stability and aggregate formation. Deletion of amino acids 901–1164, containing the C-terminal part of the coiled coil region, did not prevent aggregate formation but did reduce the strength of the TSC1–TSC2 interaction and the activity of the TSC1–TSC2 complex, consistent with the identification of truncating mutations in this region of the *TSC1* gene in TSC patients [20,21].

Deletion of the N-terminal region (amino acids 1–350) had the same effect on TSC1 expression levels as pathogenic missense changes to this region [16,17,22]. When one of these mutations (M224R) [17] was introduced into the R692 truncation protein, the expression level of the truncation protein was reduced, indicating that the N-terminal region has an autonomous effect on TSC1 stability. It has been suggested that a putative transmembrane domain in the N-terminal region of TSC1 (amino acids 127–144) may be important for the correct localisation of the TSC1–TSC2 complex [12]. One possibility is that recruitment of TSC1 to membranes might help stabilise the TSC1–TSC2 complex. Mutant TSC1–TSC2 complexes, that are unable to be recruited to the membrane, might therefore be degraded more rapidly.

To investigate the interactions between TSC2 and the TSC1 truncation proteins we performed coimmunoprecipitation experiments. Together, deletion of the N- and C-terminal regions of TSC1 (amino acids 1–350 and 901–1164) prevented TSC2 binding, while truncation at either terminal only reduced the interaction, indicating that both the N- and C-terminal regions of TSC1 are necessary for the formation of stable TSC1–TSC2 complexes. The M351 and Q900 truncations that were able to bind TSC2, were also able to promote the TSC2-mediated inhibition of TORC1 activity, as assayed by the phosphorylation status of the TORC1 substrate, S6K.

Full-length TSC1 coimmunoprecipitated with the R509 and M351-Q900 truncations, confirming that TSC1 interacts with itself [14], and indicating that the central region of the protein (amino acids 351–509) is required for this interaction. In these experiments we only overexpressed TSC1 and the TSC1 truncations, not TSC2. Furthermore, the M351-Q900 truncation did not interact with TSC2. Therefore, it is unlikely that the detected TSC1–TSC1 interactions are a consequence of

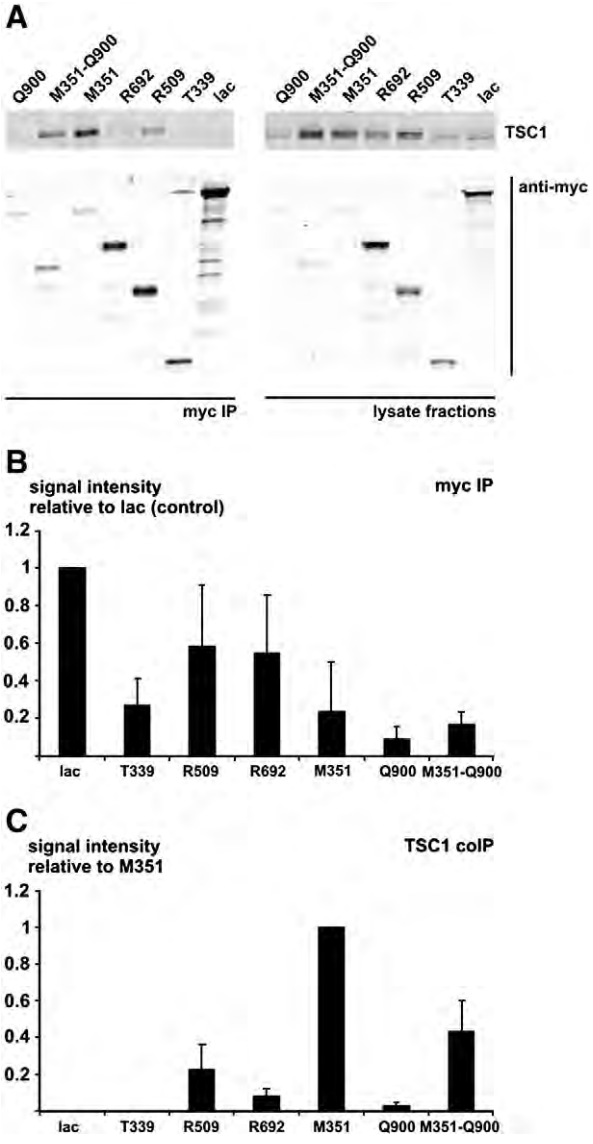

Fig. 7. Immunoblot analysis of TSC1–TSC1 interactions. The myc-tagged TSC1 truncations were coexpressed with full-length TSC1 (untagged) in HEK 293T cells. The truncations were immunoprecipitated from Triton X100-soluble cell lysate fractions using an anti-myc epitope affinity matrix. Coimmunoprecipitated, untagged TSC1 was detected by immunoblotting. Each interaction was tested at least 3 times. (A) Immunoblot showing coimmunoprecipitation of full-length TSC1 with the M351-Q900, M351, R692 and R509 truncations, but not with the Q900 or T339 truncations, or the myc-tagged β-lactamase control protein (lac). (B) Mean total signal intensity of the immunoprecipitated truncations, relative to the β-lactamase control protein (lac). Standard deviations are indicated. (C) Mean total signal intensity of coimmunoprecipitated TSC1, relative to the signal detected after coimmunoprecipitation with the M351 truncation. Standard deviations are indicated.

the formation of TSC1–TSC2 complexes containing multiple TSC1 and TSC2 subunits. Nevertheless, the TSC1–TSC1 interaction indicates that it is possible that TSC1–TSC2 complexes consist of multiple TSC1 and TSC2 subunits *in vivo*. It will be interesting to investigate whether substitutions in the central region of TSC1 (amino acids 351–900) disrupt TSC1–TSC1 binding, and whether such changes can cause the TSC phenotype.

Recently it has been proposed that different *TSC1* and *TSC2* mutations may result in different neurocognitive manifestations of TSC, depending on the exact effects of the mutations on the regulation of signaling by the TSC1–TSC2 complex [24]. One requirement of this hypothesis is that mutant TSC1 and TSC2 isoforms are expressed. Although all our experiments were performed *in vitro* on over-expressed proteins, our data suggest that if truncated TSC1 isoforms are expressed, then they may indeed have distinct effects on TSC1–TSC2 function *in vivo*. Only limited clinical data were available for the individuals with mutations corresponding to the truncation proteins analysed. However, we did not observe any obvious differences between the individuals with a *TSC1* c.2295C>T (p.R692X), *TSC1* c.2919C>T (p.Q900X) or *TSC1* c.1015dupA (p.T339X) mutation. More work is required to establish whether the distinct functional characteristics of truncated TSC1 isoforms influence the (neurocognitive) phenotype in TSC.

5. Conclusions

The N-terminal region of TSC1 (amino acids 1–350) is required to stabilise TSC1 and maintain expression levels in the cell. The central (amino acids 351–509) and C-terminal (amino acids 693–1164) regions are required for TSC1–TSC1 interactions.

Multiple regions of TSC1, including the N- and C-terminal regions, are required for binding TSC2, and the binding between truncated TSC1 proteins and TSC2 is sufficient to promote the ability of TSC2 to inhibit TORC1 activity *in vitro*. This information will be useful for the detailed functional characterisation of unclassified *TSC1* missense variants identified in individuals with TSC.

Acknowledgements

P. de Vries (University of Cambridge, U.K.) is thanked for providing information on the *TSC1* c.1015dupA (p.T339X) mutation, and for useful comments on the manuscript.

Financial support was provided by the U.S. Department of Defense Congressionally-Directed Medical Research Program (grant #TS060052). The authors report no conflicts of interest. The funding source had no role in the project.

References

[1] M. Gomez, J. Sampson, V. Whittemore (Eds.), The Tuberous Sclerosis Complex, Oxford University Press, Oxford, UK, 1999.
[2] M. van Slegtenhorst, R. de Hoogt, C. Hermans, M. Nellist, L.A.J. Janssen, S. Verhoef, D. Lindhout, A.M.W. van den Ouweland, D.J.J. Halley, J. Young, M. Burley, S. Jeremiah, K. Woodward, J. Nahmias, M. Fox, R. Ekong, J. Wolfe, S. Povey, J. Osborne, R.G. Snell, J.P. Cheadle, A.C. Jones, M. Tachataki, D. Ravine, J.R. Sampson, M.P. Reeve, P. Richardson, F. Wilmer, C. Munro, T.L. Hawkins, T. Sepp, J.B.M. Ali, S. Ward, A.J. Green, J.R.W. Yates, M.P. Short, J.H. Haines, S. Jozwiak, J. Kwiatkowska, E.P. Henske, D.J. Kwiatkowski, Identification of the tuberous sclerosis gene *TSC1* on chromosome 9q34, Science 277 (1997) 805–808.
[3] The European Chromosome 16 Tuberous Sclerosis Consortium, Identification and characterization of the tuberous sclerosis gene on chromosome 16, Cell 75 (1993) 1305–1315.
[4] M. van Slegtenhorst, M. Nellist, B. Nagelkerken, J. Cheadle, R. Snell, A. van den Ouweland, A. Reuser, J.R. Sampson, D. Halley, P. van der Sluijs, Interaction between hamartin and tuberin, the *TSC1* and *TSC2* gene products, Hum. Mol. Genet. 7 (1998) 1053–1057.
[5] Y. Li, M.N. Corradetti, K. Inoki, K.-L. Guan, TSC2: filling the GAP in the mTOR signaling pathway, Trends Biochem. Sci. 28 (2003) 573–576.
[6] D.A. Guertin, D.M. Sabatini, Defining the role of mTOR in cancer, Cancer Cell 12 (2007) 9–22.
[7] Y. Zhang, X. Gao, L.J. Saucedo, B. Ru, B.A. Edgar, D. Pan, Rheb is a direct target of the tuberous sclerosis tumour suppressor proteins, Nat. Cell Biol. 5 (2003) 578–581.
[8] A. Garami, F.J. Zwartkruis, T. Nobukuni, M. Joaquin, M. Roccio, H. Stocker, S.C. Kozma, E. Hafen, J.L. Bos, G. Thomas, Insulin activation of Rheb, a mediator of mTOR/S6K/4E-BP signaling, is inhibited by TSC1 and 2, Mol. Cell 11 (2003) 1457–1466.
[9] A.R. Tee, B.D. Manning, P.P. Roux, L.C. Cantley, J. Blenis, Tuberous sclerosis complex gene products, tuberin and hamartin, control mTOR signaling by acting as a GTPase-activating protein complex toward Rheb, Curr. Biol. 13 (2003) 1259–1268.
[10] A.F. Castro, J.F. Rebhun, G.J. Clark, L.A. Quilliam, Rheb binds tuberous sclerosis complex 2 (TSC2) and promotes S6 kinase activation in a rapamycin- and farnesylation-dependent manner, J. Biol. Chem. 278 (2003) 32493–32496.
[11] K. Inoki, Y. Li, T. Xu, K.-L. Guan, Rheb GTPase is a direct target of TSC2 GAP activity and regulates mTOR signaling, Genes Dev. 17 (2003) 1829–1834.
[12] S.L. Cai, A.R. Tee, J.D. Short, J.M. Bergeron, J. Kim, J. Shen, R. Guo, C.L. Johnson, K. Kiguchi, C.L. Walker, Activity of TSC2 is inhibited by AKT-mediated phosphorylation and membrane partitioning, J. Cell Biol. 173 (2006) 279–289.
[13] M. Rosner, M. Hanneder, N. Siegel, N. Valli, M. Hengstschlager, The tuberous sclerosis gene products hamartin and tuberin are multifunctional proteins with a wide spectrum of interacting partners, Mutat. Res. 658 (2008) 234–246.
[14] M. Nellist, M.A. van Slegtenhorst, M. Goedbloed, A.M.W. van den Ouweland, D.J.J. Halley, P. van der Sluijs, Characterization of the cytosolic tuberin-hamartin

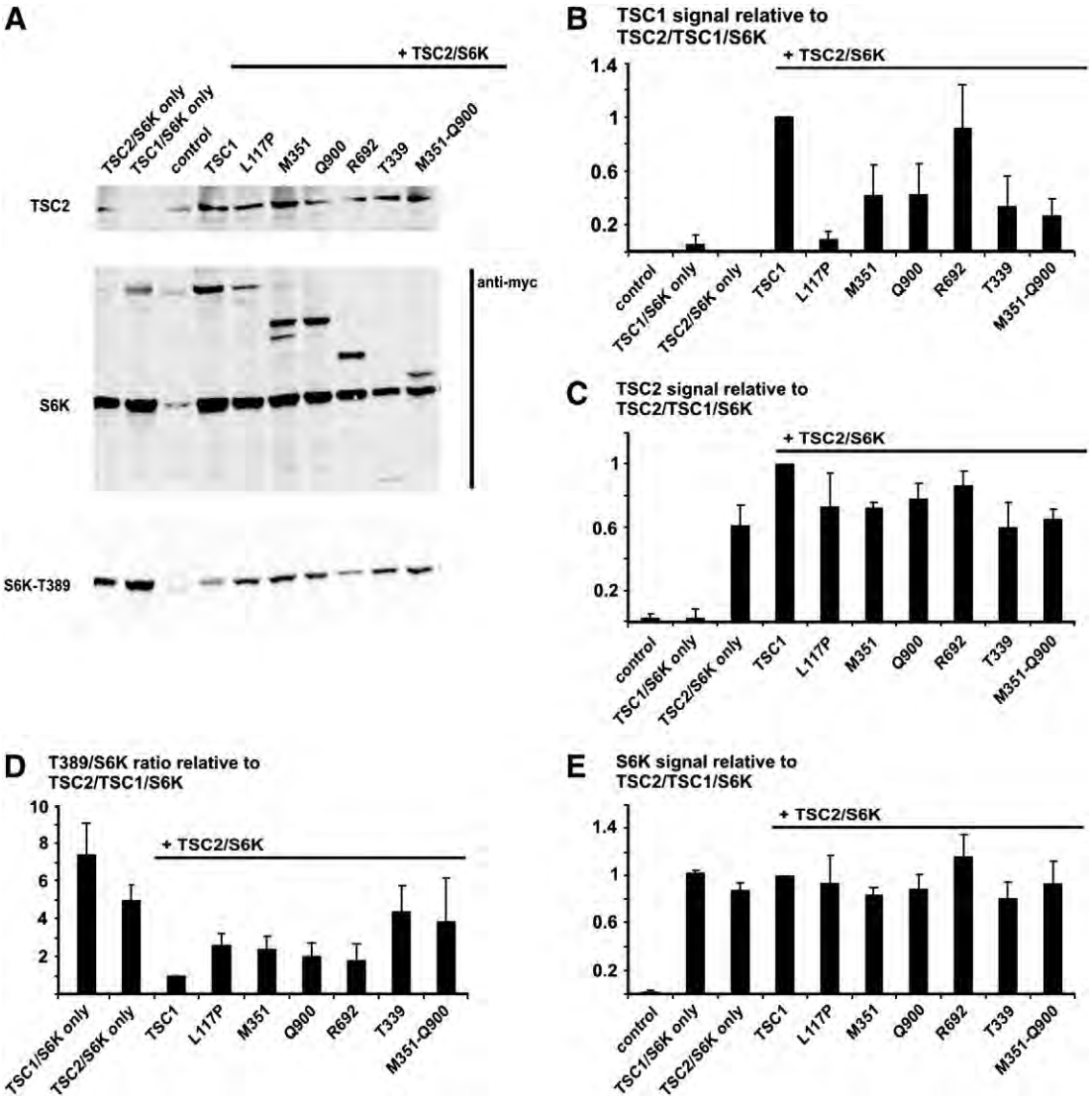

Fig. 8. Inhibition of S6K-T389 phosphorylation by the TSC1 proteins truncations. (A) Immunoblot analysis of cells expressing S6K, TSC2 and either wild-type TSC1 (TSC1), mutant TSC1 (L117P), or the TSC1 truncation proteins (Q900, M351, R692, T339 and M351-Q900). Cells transfected with vector only were included as a control (control). (B) Expression of the TSC1 truncation proteins. The signals for each truncation protein, relative to wild-type TSC1, were determined in 3 independent experiments. Standard deviations are indicated. (C) Expression of TSC2 in the presence of the TSC1 truncation proteins. The TSC2 signals in the presence of the different TSC1 truncations, relative to the TSC2 signal in the presence of wild-type TSC1 were compared. No large differences were observed. (D) Inhibition of S6K T389 phosphorylation in the presence of different TSC1 truncations. The ratio of the T389 S6K phosphorylation signal intensity to the total S6K signal intensity (T389/S6K), relative to the wild-type TSC1 (wild-type TSC1 T389/S6K ratio = 1) was determined for each truncation. Standard deviations are indicated. (E) Expression of S6K in the presence of the TSC1 truncations. The total S6K signal in the presence of each of the different truncations, relative to the signal in the presence of wild-type TSC1 (TSC1), was determined for each truncation. Standard deviations are indicated. The total S6K signals in the presence of the different truncations were similar, indicating that transfection efficiency and gel-loading were consistent between samples.

complex: tuberin is a cytosolic chaperone for hamartin, J. Biol. Chem. 274 (1999) 35647–35652.
[15] M. Nellist, B. Verhaaf, M.A. Goedbloed, A.J.J. Reuser, A.M.W. van den Ouweland, D.J.J. Halley, *TSC2* missense mutations inhibit tuberin phosphorylation and prevent formation of the tuberin–hamartin complex, Hum. Mol. Genet. 10 (2001) 2889–2898.
[16] M. Mozaffari, M. Hoogeveen-Westerveld, D. Kwiatkowski, J. Sampson, R. Ekong, S. Povey, J.T. den Dunnen, A. van den Ouweland, D. Halley, M. Nellist, Identification of a region required for TSC1 stability by functional analysis of TSC1 missense mutations found in individuals with tuberous sclerosis complex, BMC Med. Genet. 10 (2009) e88.
[17] M. Nellist, D. van den Heuvel, D. Schluep, C. Exalto, M. Goedbloed, A. Maat-Kievit, T. van Essen, K. van Spaendonck-Zwarts, F. Jansen, P. Helderman, G. Bartalini, O. Vierimaa, M. Penttinen, J. van den Ende, A. van den Ouweland, D. Halley, Missense mutations to the *TSC1* gene cause tuberous sclerosis complex, Eur. J. Hum. Genet. 17 (2009) 319–328.
[18] M. Nellist, O. Sancak, M.A. Goedbloed, C. Rohe, D. van Netten, K. Mayer, A. Tucker-Williams, A.M.W. van den Ouweland, D.J.J. Halley, Distinct effects of single amino acid changes to tuberin on the function of the tuberin–hamartin complex, Eur. J. Hum. Genet. 13 (2005) 59–68.
[19] R. Coevoets, S. Arican, M. Hoogeveen-Westerveld, E. Simons, A. van den Ouweland, D. Halley, M. Nellist, A reliable cell-based assay for testing unclassified *TSC2* gene variants, Eur. J. Hum. Genet. 17 (2009) 301–310.
[20] O. Sancak, M. Nellist, M. Goedbloed, P. Elfferich, C. Wouters, A. Maat-Kievit, B. Zonnenberg, S. Verhoef, D. Halley, A. van den Ouweland, Mutational analysis of the TSC1 and TSC2 genes in a diagnostic setting: genotype–phenotype correlations and comparison of diagnostic DNA techniques in tuberous sclerosis complex, Eur. J. Hum. Genet. 13 (2005) 731–741.
[21] Tuberous sclerosis database — Leiden Open Variation Database [http://www.chromium.liacs.nl/lovd/index.php?select_db=TSC1].
[22] L.S. Pymar, F.M. Platt, J.M. Askham, E.E. Morrison, M.A. Knowles, Bladder tumour-derived somatic TSC1 missense mutations cause loss of function via distinct mechanisms, Hum. Mol. Genet. 17 (2008) 2006–2017.
[23] K. Inoki, K.-L. Guan, Tuberous sclerosis complex, implication from a rare genetic disease to common cancer treatment, Hum. Mol. Genet. 18 (2009) 94–100.
[24] P. de Vries, C.J. Howe, The tuberous sclerosis complex proteins — a GRIPP on cognition and neurodevelopment, Trends Mol. Med. 13 (2007) 319–326.